Stony Brook University

Evolution of the Cardiac Electrophysiological System and Regulation of Ion Channel Gene Expression

A Dissertation Presented

by

Qinghong Yan

to

The Graduate School

in Partial Fulfillment of the

Requirements

for the Degree of

Doctor of Philosophy

in

Neuroscience

Department of Neurobiology and Behavior

Stony Brook University

December 2012

Stony Brook University

The Graduate School

Qinghong Yan

We, the dissertation committee for the above candidate for the

Doctor of Philosophy degree, hereby recommend

acceptance of this dissertation.

David McKinnon - Dissertation Advisor
Professor, Department of Neurobiology and Behavior

David Talmage - Chairperson of Defense
Associate Professor, Department of Pharmacological Sciences

Paul Adams
Professor, Department of Neurobiology and Behavior

Howard Sirotkin
Associate Professor, Department of Neurobiology and Behavior

J. Peter Gergen
Professor, Department of Biochemistry and Cell Biology

This dissertation is accepted by the Graduate School

Charles Taber
Interim Dean of the Graduate School

Abstract of the Dissertation

Evolution of the Cardiac Electrophysiological System and Regulation of Ion Channel Gene Expression

by

Qinghong Yan

Doctor of Philosophy

in

Neuroscience

Department of Neurobiology and Behavior

Stony Brook University

2012

There are two basic ways by which biological systems can evolve, either by changes in the sequence of protein coding regions (structural evolution) or by changes in gene regulatory function (regulatory evolution). The relative importance of regulatory versus structural evolution for the evolution of different biological systems is a subject of controversy. The primacy of

regulatory evolution in the diversification of morphological traits has been promoted by many evolutionary developmental biologists. For physiological traits, however, the role of regulatory evolution has received less attention or has been considered to be relatively unimportant. To address this issue for electrophysiological systems, I examined the importance of regulatory and structural evolution in the evolution of the electrophysiological function of cardiac myocytes in mammals.

The enormous variation in mammalian body size is an important factor in the evolutionary success of this class of animals and appropriate scaling of cardiovascular system function is critical in supporting this morphological diversity. Scaling of cardiac electrophysiology with body mass requires large changes in the ventricular action potential duration and heart rate in mammals. These changes in cellular electrophysiological function are produced by systematic and coordinated changes in the expression of multiple ion channel and transporter genes.

Two related phenomena were first studied: the change in action potential morphology in small mammals and the scaling of action potential duration across mammalian phylogeny. In general, the functional properties of the ion channels involved in ventricular action potential repolarization were found to be relatively invariant. In contrast, there were large changes in the expression levels of multiple ion channel and transporter genes. For the Kv2.1 and Kv4.2 potassium channel genes, which are primary determinants of the action potential morphology in small mammals, the functional properties of the proximal promoter regions were found to vary in concordance with species dependent differences in mRNA expression, suggesting that evolution of *cis*-regulatory elements is the primary determinant of this trait. Scaling of action potential duration was found to be a complex phenomenon, involving changes in the expression of a large

number of channels and transporters. Given the static nature of mammalian ion channel coding sequences and gene number, regulatory evolution is concluded as the primary mechanisms for the evolution of most mammalian electrophysiological systems.

Expression of one important potassium current, the transient outward current (I_{to}), changes significantly during mammalian evolution. Changes in I_{to} expression are determined, in part, by variation in the expression of an obligatory auxiliary subunit encoded by the KChIP2 gene. Expression of the KChIP2 gene is restricted to electrically excitable cells, primarily cardiac myocytes and a subset of neurons. Transcription in both heart and brain is initiated from the same CpG island promoter, which belongs to a large and poorly understood class of promoters in mammals. Species-dependent variation of KChIP2 expression in heart is mediated by the evolution of the *cis*-regulatory function of this gene. Surprisingly, the major locus of evolutionary change for KChIP2 gene expression in heart lies within the CpG island core promoter. It was demonstrated that CpG island promoters are not simply permissive for gene expression but can also contribute to tissue-selective expression and, as such, can function as an important locus for the evolution of *cis*-regulatory function. More generally, evolution of the *cis*-regulatory function of voltage-gated ion channel genes appears to be an effective and efficient way to modify channel expression levels in order to optimize electrophysiological function.

In addition, appropriate regulation of ion channel expression is critical for the maintenance of both electrical stability and normal contractile function in the heart. Mechanisms that contribute to maintaining expression of functional ion channels at relatively constant levels following perturbations of channel biosynthesis are likely to contribute significantly to the stability of electrophysiological systems in some pathological conditions. In order to examine the robustness of L-type calcium current expression, the response to changes in Ca^{2+} channel Cav1.2

gene dosage was studied in adult mice. Using a cardiac-specific inducible Cre recombinase system, Cav1.2 mRNA was reduced to 11 ± 1% of control values in homozygous floxed mice and the mice died rapidly (11.9 ± 3 days) after induction of gene deletion. For these mice, no effective compensatory changes in ion channel gene expression were triggered following deletion of both Cav1.2 alleles, despite the dramatic decay in cardiac function. In contrast to the homozygote knockout mice, following knockout of only one Cav1.2 allele, cardiac function remained unchanged, as did survival. Cav1.2 mRNA expression in the left ventricle of heterozygous knockout mice was reduced to 58 ± 3% of control values and there was a 21 ± 2% reduction in Cav1.2 protein expression. There was no significant reduction in L-type Ca^{2+} current density in these mice. The results are consistent with a model of L-type calcium channel biosynthesis in which there are one or more saturated steps, which act to buffer changes in both total Cav1.2 protein and L-type current expression.

Table of Contents

List of Figures

Chapter 1: Introduction

Chapter 2: Evolution of Ventricular Myocyte Electrophysiology

Chapter 3: Evolution of CpG Island Promoter Function Underlies Changes in KChIP2 Potassium Channel Subunit Gene Expression in Mammalian Heart

Preface

I started my graduate school in the Stony Brook University Neuroscience program in 2006 and decided to join Dr. David McKinnon's laboratory for my dissertation research. In McKinnon lab, I worked on two related projects for my thesis study: the evolution of electrophysiological systems and the regulation of ion channel expression.

The evolution project aimed to understand how cellular electrophysiological function (action potential duration and action potential morphology) are scaled to match the evolution of body mass in mammals. We examined the *cis*-regulatory function of proximal promoter regions of several ion channel genes that are important in scaling cellular electrophysiological function to body mass. We found that regulatory evolution (changes in regulatory function) rather than structural evolution (changes in protein function) underlies the evolution of cardiac electrophysiological function. In particular, *cis*-regulatory elements are the primary determinants of the changes in ventricular action potential morphology. This study provides an important parallel to the much more common studies on the evolution of development.

In a continuation of this evolution study, I began a more specific study on the KChIP2 gene, which encodes an auxiliary subunit that is an absolute requirement for the expression of the transient outward potassium current (I_{to}). The function of the I_{to} current has changed significantly during mammalian evolution. Species-dependent variation in the expression of this current underlies much of the difference in action potential morphology between mammalian species and changes in KChIP2 gene expression are a major contributor to the differences in expression. This study revealed that species-

dependent variations in KChIP2 expression are mediated by *cis*-regulatory evolution, confirming that evolution of *cis*-regulatory function of voltage-gated ion channel genes is an effective and efficient way to modify channel expression levels and optimize electrophysiological function. Surprisingly, the 450bp CpG island core promoter region was found to be the primary locus of evolution mediated changes. This was the first study to show that CpG island promoters are not simply permissive for gene expression but can also contribute to tissue-selective expression and, as such, can function as an important locus for the evolution of *cis*-regulatory function. These results were published in PNAS.

In addition to these molecular genetics studies, I spent a considerable amount of time developing and characterizing transgenic mice lines in the lab. I participated in the creation of two floxed mice lines and developed cardiac and brain-specific KChIP2, Kv2.1 and L-type calcium channel inducible (modified-Cre) knockout lines. I have been managing the mouse colony of ~300 mice and created a comprehensive record system for these mice. Part of these studies have resulted in one paper characterizing the L-type calcium channel knockout in heart. It was of interest to understand the mechanisms that maintain a relatively constant level of ion channel gene expression and functional stability of the calcium channel, especially in some pathological diseases. This published study examined the robustness of ion channel expression in response to changes in gene dosage and it was found that L-type calcium channel biosynthesis involves one or more saturated steps, which act to buffer changes in both total Cav1.2 protein and L-type current expression.

* This dissertation contains work by others. *Chapters 2, 3 and 6* are published work with multiple authors. David McKinnon contributes to the design of experiments and writing of the published results. Most of the electrophysiology, mRNA and protein chemistry experiments are done by Barbara Rosati.

My contributions in the published work: Figures 2, 3 and 8 for *Chapter 2*; all figures for *Chapter 3*; Figures 1, 2, 4 and 5 for *Chapter 6*.

Acknowledgments

First, I would like to deeply thank my advisor Dr. David McKinnon, for his generous support and guidance. I am very fortunate to have him as my advisor. I respect him as a knowledgeable and intelligent scientist and an honest, rigorous and thoughtful researcher. I learned a lot while working with him. He is also an original thinker and is pursuing basic science problems with great enthusiasm, both of which are rare in the current scientific community. As a mentor, he has wisely pointed out and patiently corrected many of my shortcomings. I greatly appreciate everything he has done for me. I cherish the memory of the fun times in the lab when the two of us are fighting unseriously. He is not only an advisor, but also a father and friend, as he is extremely sweet and friendly, and deserves the love and respect.

The second person I have tons of "thank you" to say is Dr. Barbara Rosati. She is a very careful, organized and rigorous scientist. She is a great teacher and has taught me a lot of things in and outside the lab. She always gives the clearest explanation and she is so knowledgeable that she always has an answer to almost any questions in science and everyday life. She has been extremely patient in helping me improving my writing and dealing with my sometimes tough personalities. She is also my psychologist and helped me solving a lot of problems in my real life. She is a dear friend to me and I thank her for sharing all the deepest feelings and for her help all along.

I want to sincerely thank my committee members, Drs. David Talmage, Paul Adams, Peter Gergen and Howard Sirotkin, for their understanding, support and criticism, and the program director Mary Kritzer, for her help in the graduation process.

I also want to sincerely thank Dr. Shian-Ren Liou, who taught me BAC library screening and making of transgenic mice. She is my closest companion for the first few years in the lab and an angel in my life. She is the most selfless person I have ever known. She is the person that I can always trust and feel home to talk to. Life has been hard on her and I wish her to recover from the stroke as much as possible.

I would like to thank Min Kim and Maria Pritz, who are our current and past graduate students in the lab. I enjoyed doing experiments with them and especially appreciate their company in the lab. I also learned a lot from them as my peers, because they are both people with great personalities.

I also want to thank my team - all the undergraduates that have worked with me, especially Rajeev Masson, Yi Ren, Sruti Akella, Candice Maietti and Rabia Nauman. They allow me to improve my teaching and teamwork skills. Thank them for being so helpful.

I would also like to thank my parents, sister and friends. In particular, I am deeply in debt to my fiancé, Jie Wu, who has selflessly loved me more than anyone else in the world. I thank him for being with me all the time, through happiness and difficulties. Because of him, I can be worry-free and focus on pursuing my career and doing things that I enjoy doing. He made me the luckiest person in the world.

In the end, I would like to dedicate everything to the beautiful village (江西省上高县上甘山乡黄家村茜陂坑) where I grew up. This is a place that lies in the bottom of my heart and occurs in my dreams every night. It is disappearing in the wild and being forgotten by the world. I want people to know its existence.

Chapter 1

Introduction

The heart is a major organ responsible for maintaining blood perfusion throughout the body. The rhythmic pumping maintained by the heart is driven by its electrical activity, which triggers and coordinates contraction and relaxation of the heart cells (or cardiac myocytes). Because of the highly connected nature of the cardiac tissue, or myocardium (functional syncytium), the heart is prone to electrical instabilities, known collectively as cardiac arrhythmias. Given its importance in heart function, a deep understanding of the cardiac electrophysiological system is crucial for clinical diagnosis and treatment of cardiac disease, which is the leading cause of death in the U.S. and worldwide (Hoyert and Xu 2012).

The electrophysiology of the heart has been studied for over a century and the mechanisms underlying the genesis and propagation of the cardiac rhythm are very well understood. Mammals encompass a broad range of body sizes and this imposes a strong constraint on the evolution of cardiac function. The consequent scaling of cardiac electrophysiological function provides an ideal system in which to study how gene regulation changes amongst relatively closely related species. The relatively simple and well understood physiology of the heart makes it feasible to gain a relatively complete understanding of how this system has evolved.

The electrical activity in the heart is produced by flow of charged ions through various ion channels in the myocytes cell membrane. Ion channels are a large family of membrane proteins with a total of 143 members in vertebrates (Yu et al. 2005). Many of the ion channels are expressed in multiple tissues and a subset of them are expressed in the heart. Expression of ion channels can be regulated at multiple levels, although the expression level of most cardiac channels seems to be hardwired in the genome (Rosati and McKinnon, 2004). Because of the importance of transcriptional regulation, mutations in ion channel gene regulatory regions are

likely to underlie many genetically determined cardiac electrical disorders (Bezzina et al. 2006). With the aim of understanding the evolution of the cardiac electrophysiological system, my dissertation primarily focuses on the cardiac ion channel gene regulatory function, which is likely to be an important locus of genetic variation affecting cardiac ion channel expression and the susceptibility to arrhythmias in human populations.

MOLECULAR MECHANISMS OF EVOLUTION

Evolution can proceed in two ways at the molecular level: either by changing the protein function ("structural evolution") or by changing the regulation of the gene ("regulatory evolution"). The recognition of the key role that the evolution of gene regulation plays in the evolution of animal form and function is relatively recent (King and Wilson 1975; Jacob 1977). Subsequent progress has been slow because of the difficulty in studying gene regulatory systems. In recent years, however, a body of work in evolutionary developmental biology ("evo-devo") has accumulated on this topic (Davison 2001; Carroll et al. 2001; Carroll 2005; Wray 2007) that has resulted in the development of three key concepts:

1. Evolution of gene regulation is more flexible and more common than the evolution of protein coding regions because it limits the problem of pleiotropy.

2. The molecular changes that produce regulatory evolution are more likely to be changes in *cis*-regulatory regions rather than the reorganization of transcription factor networks, again because this tends to limit pleiotropy.

3. *Cis*-regulatory regions are organized into discrete functional modules that can evolve independently.

None of these concepts are inviolate laws but instead should be viewed as statistical tendencies. They are thought to reflect the most common solution to problems regarding the evolution of gene regulation.

Regulatory Evolution versus Structural Evolution

In multi-cellular animals, the majority of proteins have key functions in multiple different cell types. This fact greatly increases the constraints on protein sequence and function and is likely to make an important contribution to the relative stability of many gene coding sequences during the course of evolution. Most genes, including ion channel genes, are expressed in multiple cell types. For example, the ion channels that are expressed in ventricular myocytes are also expressed in a wide range of other cell types where they often have quite different functions. A specific example is the KCNQ1 channel which is involved in cardiac action potential repolarization and fluid transport in the inner ear (Nicolas et al. 2001; Rivas and Francis 2005).

A broad distribution pattern in different cell types creates a considerable constraint on evolutionarily mediated changes in protein function. For a specific mutation to be fixed in the population, it has to have either neutral or advantageous effects in multiple cell types. This constraint will increase with increasing morphological and physiological complexity of the animal. It is likely that the highly conserved nature of most ion channels is due, in part, to their broad patterns of distribution throughout the body, which creates a complex web of dependencies on the function of that particular channel.

Since the evolution of gene coding regions would easily be problematic for pleiotropy, as a result, it has been proposed that evolution of gene regulation, as opposed to protein structure, is of primary importance in the evolution of animal morphology (Davison 2001; Carroll et al. 2001; Carroll 2005; Wray 2007).

Cis-Regulation versus Regulation of Transcription Factor Networks and the Modular Organization of *Cis*-Regulatory Regions

A second key idea is that regulatory evolution is primarily mediated by evolution of *cis*-regulatory elements rather than by rearrangement of transcription factor networks. An example of this is the remarkable conservation of the roles of genes involved in cardiac or eye specification such as tinman/Nkx2.5 and Pax6 (Wawersik and Maas 2000; Bishopric 2005). This theory proposes that the arrangement of networks of transcription factors remains highly stable over long periods of evolutionary history and that most of the evolutionary changes in animal development and morphology occur at the level of the *cis*-regulatory elements. A third, related idea is that *cis*-regulatory regions are organized in a modular fashion, with different elements mediating specific cell-type or temporal patterns of gene expression (Davison 2001).

Both of these ideas can be illustrated by examples from the developmental literature (Fig. 1). Changes in morphology can be produced either by gaining of a new modular *cis*-regulatory element or following the loss of a *cis*-regulatory element, without involving any changes in the coding region or protein function. For example, the gaining of wing pigmentation spot in *Drosophila biarmipes* is produced by selective expression of the *yellow* gene product on the wing and such a change in evolution is driven by mutations in the *cis*-regulatory elements upstream of this gene that resulted in gaining of a wing-spot specific element (Fig. 1A) (Gompel et al. 2005). Another example is the reduction of pelvic spine in the freshwater population of the threespine stickleback fish, which is produced by the loss of Pitx1 expression in the pelvic region as a result of the selective loss of activity of the hind-limb *cis*-regulatory element (Fig. 1B) (Shapiro et al. 2004).

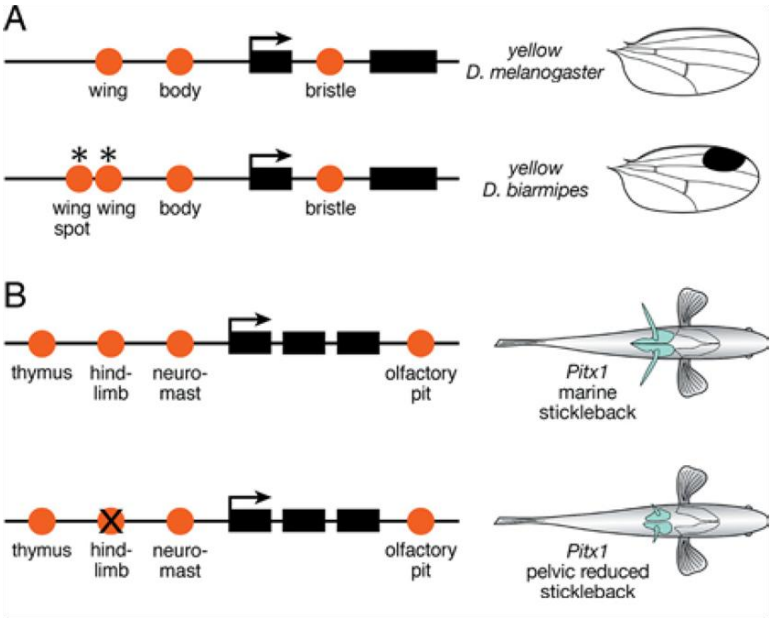

Figure 1. Evolution of modular *cis*-regulatory elements

(A) Gain of a *cis*-regulatory element (red circle) controlling wing expression of the *yellow* gene underlies the shift in wing pigmentation pattern between *Drosophila biarmipes* and *Drosophila melanogaster*. (B) Inactivation of hind limb specific *cis*-regulatory element in the Pitx1 gene underlies the reduction in pelvic spine length in stickleback fish. Figure from Carroll (2005).

AN IMPORTANT *CIS*-REGULATORY REGION: THE CPG ISLAND PROMOTER

Protein-coding regions, which turned out to represent only 1.5% of the mammalian genome (Mouse Genome Sequencing et al. 2002), have been studied extensively as the most important genetic loci for evolution and biological function. The remaining 98.5% of the genome, initially designated dismissively as "junk DNA" (Cowan et al. 2002), has been re-evaluated in recent years after the discovery that it contains important *cis*-regulatory elements or RNA-coding regions. A protein-coding region itself is in vain if not flanked by appropriate *cis*-regulatory regions. By interacting with RNA polymerase and transcription factors, these *cis*-regulatory regions trigger and regulate transcription of the protein-coding region, determining when, where and to what extent that gene product is expressed.

Transcription initiates at gene sites known as promoters, which contain one or multiple recurrent and well characterized elements: TATA box, initiator element, downstream promoter element (DPE), TFIIB recognition element (BRE) and CpG islands (Butler and Kadonaga 2002; Saxonov et al. 2006; Sandelin et al. 2007). To briefly describe these elements (reviewed in detail by Butler and Kadonaga, Smale and Kadonaga and Sandelin et al.): TATA box has a core consensus sequence "TATAAA" and is usually located 25-34bp upstream of the transcription start site (TSS); The initiator element encompasses the TSS and has a consensus sequence of YYANWYY where A is the start site; The DPE locates 28-32bp downstream of TSS, has a consensus of RGWYV and generally occurs together with initiator element; The BRE occurs in some TATA box promoters by being located immediately upstream of the TATA sequence and has a consensus of SSRCGCC; CpG islands are stretches of genomic DNA that are rich in CpG

dinucleotides and usually lack methylation. Out of all these promoter elements, the TATA box is the most studied and was initially thought to be ubiquitous for eukaryotic genes (Weinmann 1992; Butler and Kadonaga 2002). With the progress of large scale sequencing and characterization of non-coding regions, only a small fraction (10-20%) of all mammalian genes were found to have a TATA box promoter (Ohler 2006). In contrast, the CpG island promoters turned out to be driving expression for more than half of the mammalian genes. Recent studies showed that as many as 72% of the human genes have a CpG island promoter (Saxonov et al. 2006). Despite the fact that the CpG island promoters are found in the majority of the mammalian genes, the mechanisms of transcription initiation from this class of promoter and their regulation are poorly, if at all, characterized.

In order to understand how regulation of gene expression evolves, it is of uttermost importance to gain insight on how this most prevalent class of promoters in higher species – the CpG island promoters – work.

CpG Deficiency and CpG Islands

In higher vertebrates, including mammals, the cytosine residue at CpG dinucleotides is the substrate for DNA methylation which occurs globally in the genome. The methylated cytosine can be spontaneously deaminated into thymine, a phenomenon that was first described in the lacI gene of Escherichia coli (Coulondre et al. 1978). The cytosine residue is chemically unstable and can be subjected to hydrolytic deamination. Deamination converts the unmethylated cytosine into uracil, which can be efficiently recognized and repaired by the cell as uracil is not normally found in DNA. For methylated cytosine, however, the conversion to thymine by the

hydrolytic deamination is not efficiently recognized and repaired, as thymine is a normal component of DNA. Eventually, the mutation can be fixed in the genome after the next round of duplication and as a result, CpG dinucleotides are generally depleted in the genome, due to accumulation of this spontaneous mutation (Duncan and Miller 1980). However, in the 'sea' of CpG-deficient and highly methylated vertebrate genome sequences, there exist these stretches of DNA with overly enriched, non-methylated CpG dinucleotides called 'CpG islands'. Striking as their sequence composition, their position seem to globally overlap with gene transcription start sites, revealing that a possible, most common function of CpG islands is to act as gene promoters, or their regulators. Because of their location, early, large scale genome studies have used CpG islands as landmarks to search for genes (Bird 1987; Larsen et al. 1992; Ioshikhes and Zhang 2000).

Computationally, CpG islands were initially defined as DNA regions longer than 200bp, with a G+C content greater than 50% and an observed/expected CpG ratio (O/E) greater than 0.6 (Gardiner-Garden and Frommer 1987). There had been tremendous improvements in the computational annotation of CpG islands since this initial standard was proposed. In order to better associate CpG islands to annotated genes in the genome, Takai and Jones (2002) later proposed more stringent criteria for defining CpG islands (longer than 500bp in length, with G+C content greater than 55% and O/E greater than 0.65) that filtered out most of the Alu repeats and unknown sequences. This definition of CpG islands is now widely recognized and used in most recent studies (Fazzari and Greally 2004; Rach et al. 2011). However, relatively recently, a totally different CpG identification method was proposed, named "CpG clustering", which makes calls based on CpG density (Hackenberg et al. 2006; Glass et al. 2007). This method does not reply on the G+C content, O/E ratio or length and allows detecting CpG islands

at AT-rich regions. Despite the relative homogeneity in the definition of CpG islands, the computational methods for detecting CpG islands are still very variable in the literature (Saxonov et al. 2006; Sharif et al. 2010; Wu et al. 2010).

However, while the computational annotation of CpG islands is improving and becoming more standardized, there are more pressing issues to be addressed on the biology of CpG islands. In particular, how are CpG islands recognized by nuclear factors and what are the criteria of recognition used by the cell? Other than their high content of CpG dinucleotides, what other structural features do CpG islands carry and what functions do these features have? Or, rather than being recognized by specific factors and carrying any special functions, are CpG islands simply the footprint of some biological processes that protect them from methylation and mutation?

Distribution of CpG Island Promoters

The computational analysis of CpG islands gives a general overview about the distribution of CpG island promoters in the genome. Different CpG island annotation algorithms result in minor differences in the proportions of genes that are associated CpG islands and proportion of CpG islands that are associated with genes. Figure 2 shows a comparison of two different computation algorithms (Gardiner-Garden and Frommer 1987; Hackenberg et al. 2006; Glass et al. 2007). Not all gene promoters are associated with CpG islands and not all CpG islands are associated with gene promoters. About 60-70% annotated gene promoters are associated with CpG islands (40-50% of the tissue-specific genes and 80-90% of the house-keeping genes, Fig. 2A), while more than half of the CpG islands are associated with annotated

gene promoters after elimination of the repetitive sequences (Fig. 2B). For CpG islands that are not associated with annotated promoters, studies have shown evidence of promoter function and they may therefore represent alternative promoters inside a gene or sites for initiating the transcription of non-coding RNAs that regulate gene expression (Illingworth et al. 2010; Maunakea et al. 2010; Deaton and Bird 2011).

CpG island promoters seem to be especially common for genes in the cardiac electrophysiological system. As shown in Table 1, more than 90% of the important cardiac ion channel and transporter genes (53 out 57 in human and 51 out of 56 in mouse) are associated with a CpG island promoter.

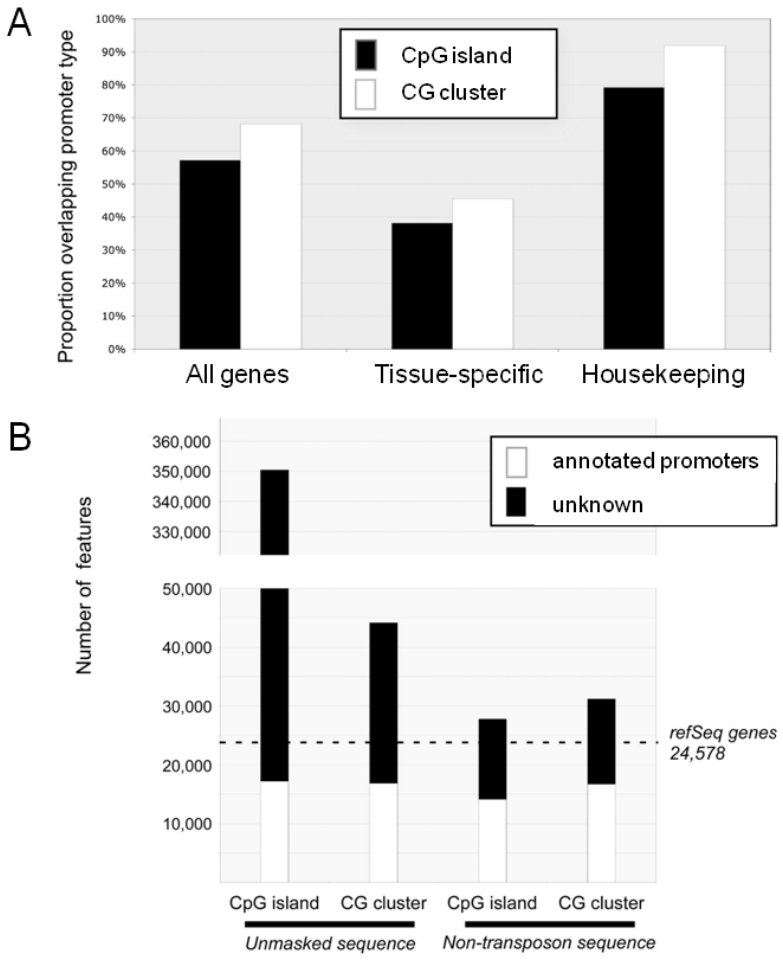

Figure 2. Distribution of CpG island promoters in the genome

(A) Percentage of genes that are associated with CpG island promoters. All genes are further divided into two categories: tissue-specific and housekeeping. Two computational methods are compared ("CpG island" versus "CG cluster"), represented by black and white bars respectively. (B) Number of CpG islands that are associated with promoters. The two computational methods are labeled on the x-axis. Although the absolute number does not change much, the percentage of CpG islands that are associated promoters increases after filtering out repetitive sequences ("non-transposon sequence"). Figure adapted from Glass et al. 2007.

Table 1. Analysis of the presence of CpG island promoters in all the important cardiac ion channel and transporter genes in mouse and human.

Index	Gene Name	CpG island promoter?		Chromosome location in human
		Human	Mouse	
1	SCN5a (Nav1.5)	Y	Y	chr3:38,565,044-38,742,634
2	SCN1b (Navβ1)	Y	Y	chr19:35,516,828-35,532,409
3	SCN3b (Navβ3)	Y	Y	chr11:123,492,339-123,598,861
4	SCN4b (Navβ4)	Y	Y	chr11:117,994,682-118,036,535
5	Cacna1C (Cav1.2)	Y	Y	chr12:2,111,258-2,887,373
6	Cacnb2 (Cavβ2)	Y	Y	chr10:18,322,179-18,882,282
7	Cacna2d1 (Cavα2δ-1)	Y	Y	chr7:81,392,844-82,406,167
8	Cacna2d2 (Cavα2δ-2)	Y	Y	chr3:50,391,275-50,601,004
9	Cacna1G (Cav3.1)	Y	Y	chr17:48,626,860-48,714,791
10	Cacna1H (Cav3.2)	Y	Y	chr16:1,136,882-1,273,342
11	HCN2	Y	Y	chr19:581,855-619,933
12	HCN4	Y	Y	chr15:73,595,864-73,737,036
13	KCNA2 (Kv1.2)	Y	Y	chr1:111,057,775-111,222,201
14	KCNA4 (Kv1.4)	Y	Y	chr11:28,275,181-30,327,589
15	KCNA5 (Kv1.5)	Y	Y	chr12:5,021,439-5,362,344
16	KCNB1 (Kv2.1)	Y	Y	chr20:47,962,894-48,133,045
17	KCND2 (Kv4.2)	Y	Y	chr7:117,803,620-120,497,515
18	KCND3 (Kv4.3)	Y	Y	chr1:112,298,804-112,545,959
19	KCNH2 (erg1)	Y	Y	chr7:150,555,422-150,696,575
20	KCNQ1 (KVLQT1)	Y	Y	chr11:2,436,252-2,919,041
21	KCNJ2 (Kir2.1)	Y	Y	chr17:68,162,681-68,176,992
22	KCNJ12 (Kir2.2)	Y	Y	chr17:21,194,491-21,459,764
23	KCNJ4 (Kir2.3)	Y	Y	chr22:38,792,722-38,869,452
24	KCNJ3 (Kir3.1)	Y	Y	chr2:155,298,787-156,932,224
25	KCNJ5 (Kir3.4)	Y	Y	chr11:128,736,914-128,805,917
26	KCNJ8 (Kir6.1)	Y	Y	chr12:21,808,129-21,957,838
27	KCNJ11 (Kir6.2)	Y	Y	chr11:17,398,340-17,414,929
28	KCNK1 (TWIK1)	Y	Y	chr1:233,515,714-234,042,294
29	KCNK6 (TWIK2)	Y	Y	chr19:38,805,924-38,826,962
30	KCNK3 (TASK1)	Y	Y	chr2:26,862,391-26,991,581
31	KCNK2 (TREK1)	Y	Y	chr1:214,832,396-215,765,826
32	KCNK4 (TRAAK1)	Y	Y	chr11:64,056,669-64,069,192
33	KCNK12 (THIK1)	Y	Y	chr2:47,703,868-48,016,267
34	KCNAB1 (Kvβ1)	Y	Y	chr3:155,568,180-156,430,348
35	KCNAB2 (Kvβ2)	Y	Y	chr1:6,050,730-6,168,093
36	KCNE3 (MiRP3)	Y	Y	chr11:74,107,555-74,207,875
37	KCNIP2 (KChIP2)	Y	Y	chr10:103,577,410-103,606,729
38	PIAS3 (KChAP)	Y	Y	chr1:145,568,274-145,587,067
39	FREQ (NCS1)	Y	Y	chr9:132,893,468-133,276,698
40	ABCC8 (SUR1)	Y	Y	chr11:17,406,807-17,518,214

41	ABCC9 (SUR2)	Y	Y	chr12:21,924,794-22,204,632
42	SERCA2a (ATP2A2)	Y	Y	chr12:110,649,045-110,823,731
43	ATP1A1	Y	Y	chr1:116,659,170-117,085,217
44	ATP1B1	Y	Y	chr1:169,055,070-169,120,133
45	GLUT1 (SLC2A1)	Y	Y	chr1:43,349,685-43,431,321
46	GLUT4 (SLC2A4)	Y	Y	chr17:7,164,359-7,199,224
47	SGLT1 (SLC5A1)	Y	Y	chr22:32,347,168-32,528,339
48	Cx43 (Gja1)	Y	Y	chr6:121,622,062-122,761,944
49	Cx45 (Gja7) (GLC1)	Y	Y	chr17:42,855,813-42,930,142
50	Cx30 (Gjb6)	Y	Y	chr13:20,753,020-20,991,016
52	KCNK17 (TALK2)	Y	-	chr6:39,195,511-39,285,212
53	KCNE1 (MinK)	Y	N	chr21:35,774,080-35,895,347
54	NCX1 (SLC8A1)	Y	N	chr2:40,654,404-40,685,196
51	Cx30.2 (Gjd3)	N	Y	chr17:38,516,744-38,521,090
55	KCNE2 (MiRP1)	N	N	chr21:35,537,671-35,803,697
56	ATP1A2	N	N	chr1:160,067,918-160,123,980
57	Cx40 (Gja5)	N	N	chr1:147,134,619-147,389,758

The presence of a CpG island promoter is determined by whether there is a CpG island (annotated using the HMM model developed by Wu et al. 2010) overlapping with a transcription start site of the gene (Y: overlap, N: no overlap). Genes are randomly listed except for the last seven genes, which either are not consistent between mouse and human or do not have a CpG island promoter in both species. These seven genes are listed at the bottom of the table. Alternative gene names are indicated in parenthesis.

Mechanisms of Transcription from CpG Island Promoters

For TATA box promoters, TATA binding proteins specifically recognize the TATA box and direct RNA polymerase II (PolII) binding (Berk 2000). However, unlike the TATA box, CpG island promoters lack specific sequence elements. It was suggested that the GC richness of CpG islands increases the probability of transcription factor binding, since mammalian transcription factor binding sites are generally more GC-rich than the bulk genome and many contain CpG in their DNA recognition sequence (Deaton and Bird 2011). Sp1 is a transcription factors that has a GC-rich DNA recognition site and can also recruit TATA-binding proteins (Wierstra 2008) and CpG island promoters were indeed shown to bind to TATA-binding proteins as well (Ramirez-Carrozzi et al. 2009). Consistent with these findings, Hargreaves et al. (2009) observed high levels of Sp1 binding to CpG island promoters but not to non-CpG island ones and found that Sp1 is required for PolII recruitment to CpG island promoters. Putting these evidences together, it seems CpG island promoters can use Sp1 to attract TATA-binding protein and initiate transcription similarly to the TATA box promoters.

In addition to Sp1, Deaton and Bird (2011) listed a few other transcription factors such as Nrf-1, E2F, ETS, CRE, E-box motifs and others that are enriched at CpG islands. Nozaki et al. (2011) found two transcription factors, MAZ and PU.1, whose binding sites were associated with dispersed promoters, which were named by having multiple, dispersed TSSs and were mostly CpG island promoters, but not with focused promoters, which were named by having a single, focused TSS and were generally non-CpG island promoters.

Furthermore, Deaton and Bird (2011) suggested that CpG island promoters have a transcriptionally permissive state that allows initiation to occur loosely at a number of locations (hence determining a dispersed TSS distribution pattern). Although only less than half of the

genes in the genome are expressed in a typical cell, as many as 75%, including some inactive genes, are bound by PolII and marked by the permissive chromatin modifications H3K4me3, K3K9ac and H3K14ac (Guenther et al. 2007). Those inactive genes do experience transcription initiation but not productive elongation, which correlates with the presence of the initiating form of PolII but absence of the elongating form (Hargreaves et al. 2009).

Consistent with the transcriptionally permissive state in CpG islands, bidirectional, short transcription occurs regularly at CpG island promoter, as detected by global nuclear run-on assays (Core et al. 2008). Two independent studies found that primary response genes with CpG island promoters are bound by Sp1 and PolII, carry constitutively active chromatin features (reduced nucleosome occupancy, marked by H3K4me3 and H3Ac modifications), and allow rapid induction of gene expression to occur without the presence of SWI/SNF nucleosome remodeling complex; while genes lack a CpG island promoter are assembled into stable nucleosomes and their activiation is dependent on nucleosome remodeling (Hargreaves et al. 2009; Ramirez-Carrozzi et al. 2009). It seems this active but futile transcription by the constitutively bound PolII is required to maintain the open chromatin states at CpG island promoters, as inactivation of transcription resulted in loss of marks such as H3K4me3, H3K9Ac in addition to the loss of PolII binding at CpG island promoters (Hargreaves et al. 2009).

The transcriptionally permissive state of CpG island suggests that the regulation of CpG island promoter probably takes place after the step of transcription initiation (Deaton and Bird 2011), although studies have been exclusively focusing on the mechanism of PolII recruitment. As a result, PolII pausing, which is found by recent studies to occur frequently in metazoan genes (Gilchrist et al. 2012), might be an important regulatory step especially for transcription of genes with CpG island promoters.

Evolution of CpG Island Promoters

How do CpGs accumulate into islands in the genome during evolution? As the rest of the genome is actively undergoing depletion of CpGs, the "accumulation" step in the formation of CpG islands is likely to be a passive step.

A study by Glass et al. (2007) suggests an interesting hypothesis on the evolution of CpG islands (Fig. 3). Once a DNA sequence is long enough, a CpG-dense region can occur simply by chance. As a result, at the beginning, when there is not yet any selection on CpG islands and methylation-caused depletion of CpG dinucleotides is not yet involved, the distribution of the likelihood to find a certain number of CpGs along the DNA sequence will be a normal one, as shown in yeast by Glass and colleagues (Fig. 3). However, for species that evolved after yeast, this distribution starts to drift slightly towards the left, that is, it becomes easier to find a CpG-dense region. This suggests that evolution started to favor accumulation of CpG dinucleotides since the appearance of multicellular organisms. This observation is supported by Irizarry et al., who were able to find the presence of CpG islands in all 28 multicellular species examined, including plants and animals, but not in unicellular organisms (Irizarry et al. 2009).

Global genomic DNA methylation starts to occur in vertebrates (Tweedie et al. 1997). This is accompanied with dramatic depletion, suppression or decay of CpG dinucleotides, indicated by stepwise decrease of the average O/E value shown on the top right corner of each panel in Figure 3: 0.801-0.994 in invertebrates to 0.5-0.6 in cold-blooded vertebrates, and ultimately down to around 0.2 in warm-blooded vertebrates. Similarly, starting from Fugu, the distribution of the likelihood to find CpGs not only drifts towards the left, but also has a long tail on the right. This distribution tail, which is a result of CpG decay, becomes more and more prominent in the following higher organisms. However, emergence of CpG islands, shown as the

first small peak before the major second peak in the distribution, occurred later than methylation, not until sometime around the existence of zebrafish (the authors suggested that methylation is not enough to account for the rise of CpG islands) and CpG islands become prominent only in birds and mammals.

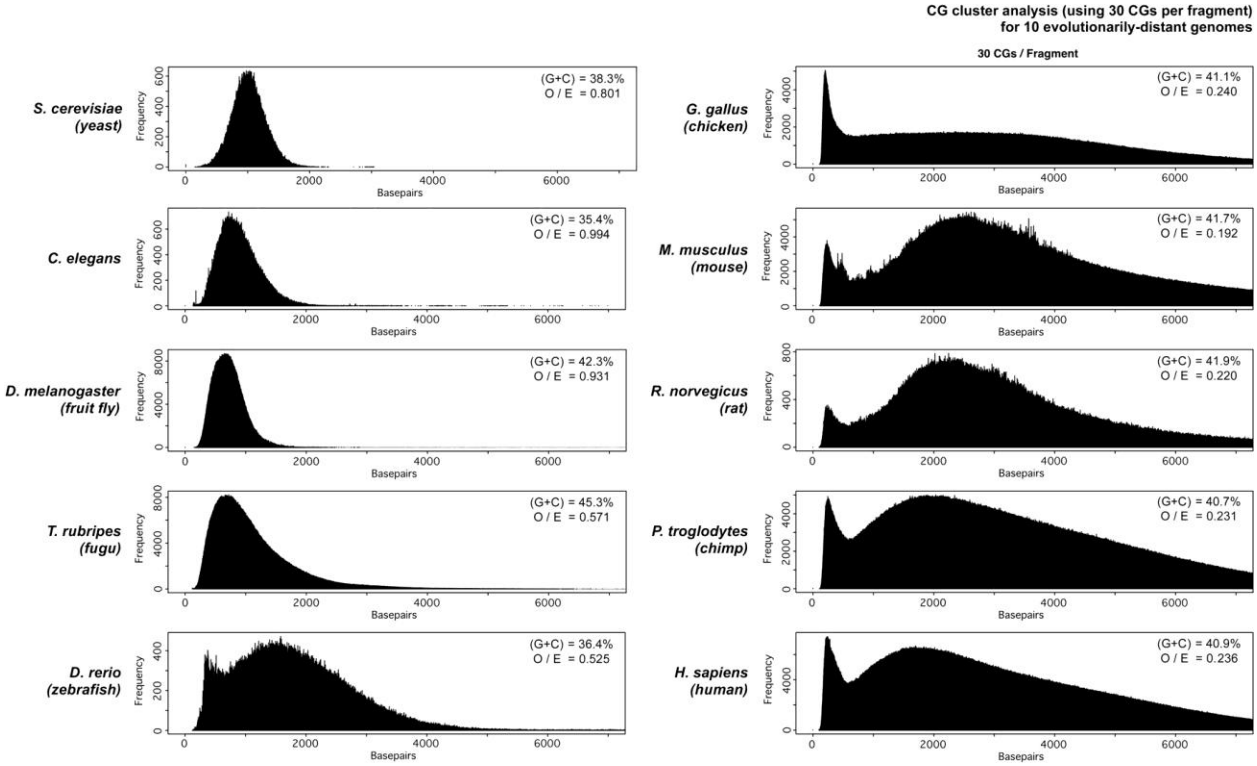

Figure 3. CpG densities in ten eukaryotic genomes

This figure is plotting the density of CpGs in the genome different species (the denser the smaller the x-axis). The x-axis represents the length of a genomic DNA fragment that contains 30 CpGs. The y-axis represents the frequency of fragment length (x-axis). Figure from Glass et al. 2007.

Unfortunately the two representative invertebrate species in this study, Caernohabditis elegans and Drosophila melanogaster, are exceptional cases, in which the genome is predominantly unmethylated. Studies by the Bird lab showed that all the other invertebrates analyzed have partially methylated (10-40%) genomes (Bird et al. 1979; Bird and Taggart 1980; Suzuki et al. 2007) and this pattern of compartmental methylation is probably widespread in

multicellular organisms including plants, multicellular fungi and the slime mold (Antequera et al. 1984; Tweedie et al. 1997). These results support the hypothesis proposed by Irizarry et al. (2009) that CpG islands are present in all multicellular organisms.

Takai and Jones pushed the boundary of methylated species even further. By checking the frequency of all 16 dinucleotides, they suggested that CpG suppression/methylation occurred in every eukaryotes including yeast, but not in the prokaryote E.coli. This is worth noticing but the conclusion is drawn too fast. Unlike the human, the lower level of dinucleotides frequency in other species including yeast is not unique to CpG dinucleotides, but also occurs to other dinucleotides such as CpC, GpC and GpG (Takai and Jones 2002). As a result, this phenomenon is probably caused by some other factors rather than spontaneous mutation of methylated CpG.

Association of CpG islands with transcription start sites seem to co-occur with the emergence of CpG islands as an independent function group as shown in Fig. 3. Another study by Sharif et al. (2010), which used a completely different method to annotate CpG islands, made an analogous finding. They found that CpG island promoters start to exist in zebrafish and became prominent in both birds and mammals (warm-blooded vertebrates) (Fig. 4), similar to the occurrence of CpG islands found by Glass et al.. Association of CpG islands to transcription initiation seem to be the reason why CpG islands are kept in evolution, as Sharif et al. did not find enrichments at other regions such as the transcription termination site. This indicates that the function of CpG islands as promoters is a positive feature that has been selected for during evolution.

In conclusion, existence of CpG islands is a feature accompanied by genome methylation. CpG islands are prominent in warm blood vertebrates, possibly because of their important

function as promoters, but the rise of CpG islands during evolution does not occur suddenly and these regions can be found already in invertebrates and other multicellular organisms.

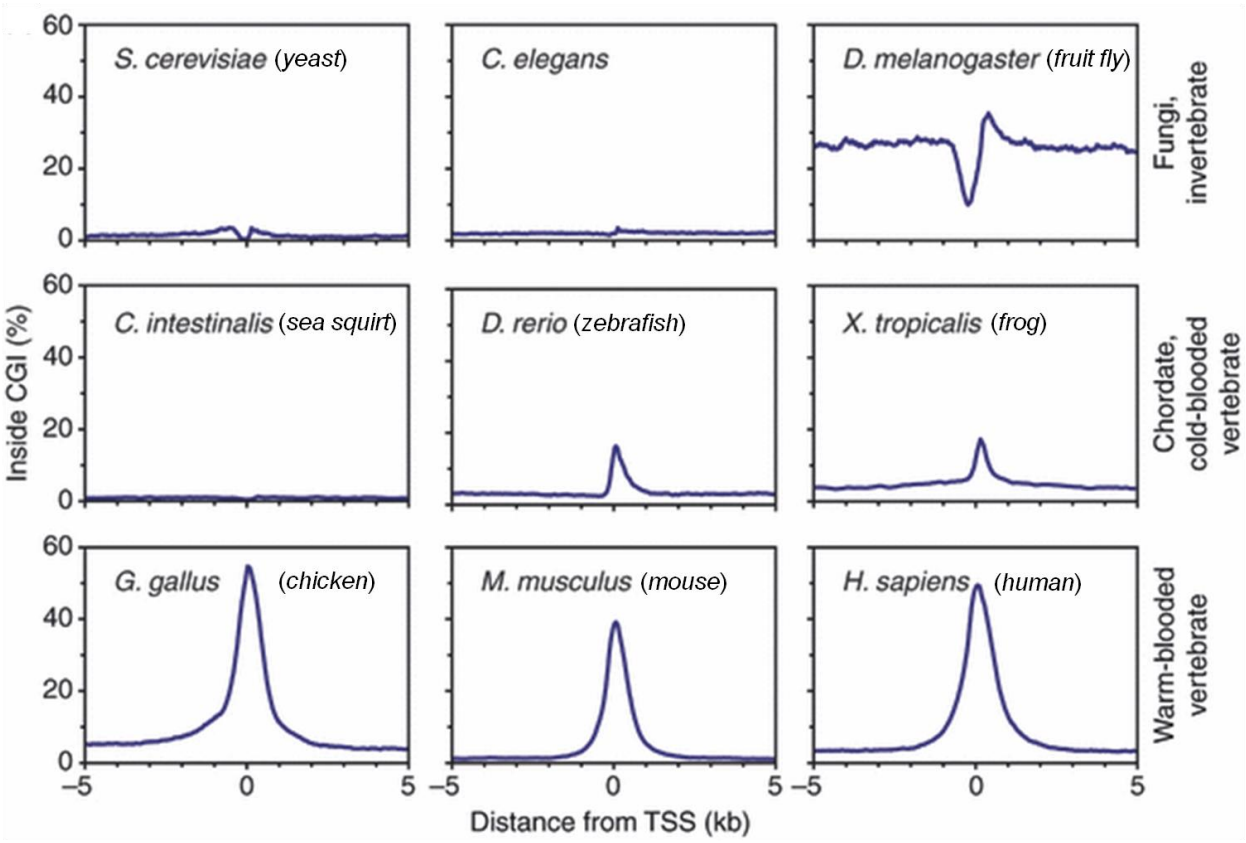

Figure 4. Enrichment of CpG islands at the transcription start sites (TSS)

This shows the distributions of CpG islands around the TSS in 9 species. The x-axis indicates the relative position to the TSS (-5 kb to +5 kb) and the y-axis represents the CpG island frequency at the respective position. Figure adapted from Sharif et al. 2010.

CARDIAC MYOCYTE – AN IDEAL SYSTEM TO STUDY THE EVOLUTION OF CELLULAR ELECTROPHYSIOLOGICAL FUNCTION

The ability of mammals to occupy an unusually wide range of ecological niches depends in part on the enormous range of body sizes within this class of animals (Schmidt-Nielsen 1984). The largest living land animal (elephant) weighs 100,000 times more than a mouse and a million times more than the smallest land mammal (Etruscan Shrew). This wide variation in body size is, in turn, dependent on appropriate scaling of the cardiovascular system function. Heart weight itself scales directly with body weight and there are no significant changes among species in the morphology of either the heart or of the cardiac myocytes (Prothero 1979; Loughrey et al. 2004).

Due to body size dependent changes in the physical properties of the arterial tree, it is necessary to scale the heart rate (HR) and, hence, the ventricular action potential duration (APD) systematically with body mass in order to maintain a minimum diastolic pressure independent of body size (Holt et al. 1968; Elzinga and Westerhof 1991). In particular, as the body size decreases, the size of the arterial network and therefore its overall compliance decreases. Since arterial compliance is one of the major factors determining blood pressure, in small mammals (Fig. 5B) the decrease in blood pressure after a cardiac contraction (systole) is much faster than in larger mammals (Fig. 5A), with a larger arterial compliance. This means that, in smaller animals, the average blood pressure would fall under a minimum threshold if the cardiac function was not adjusted. Therefore, in small mammals, a much faster heart rate is required in order to maintain diastolic blood pressure above a constant minimum value, which is determined by the perfusion requirements of critical organs such as the brain and the kidney. This value

turns out to be essentially invariant in terrestrial mammals and this key constraint, i.e. the requirement for adequate tissue perfusion, means that the heart rate and, consequently, the action potential duration have to scale in a predictable fashion with body mass (Fig.5 and *Chapter 2*, Fig. 1).

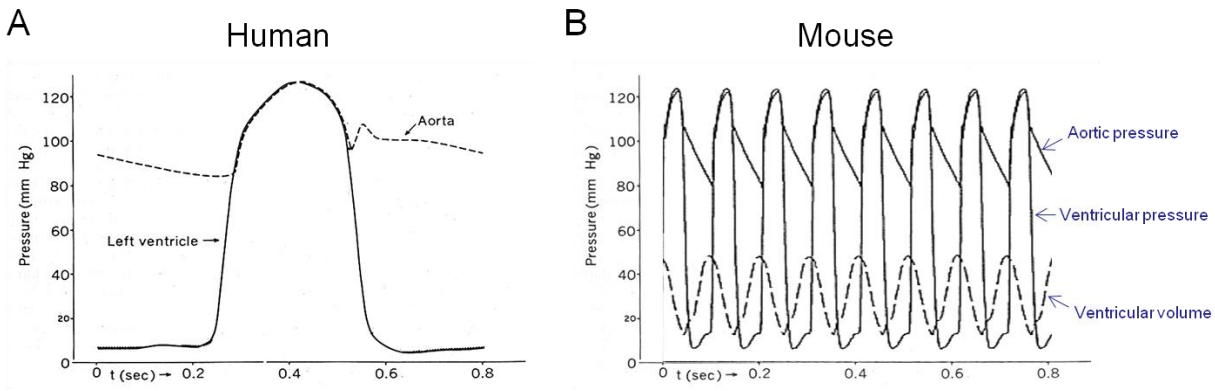

Figure 5. Comparison of mouse and human blood pressure

(A) Aorta and left ventricular pressure in human. (B) Aortic and ventricular pressure and ventricular volume in mouse. Figure adapted from Mountcastle 1980 and Segers et al. 2005.

Limited Effect of Phylogeny to the Evolution of Cardiac Electrophysiology

The constraint imposed by body weight on cardiac function is so strong that it overrides even the effect of phylogeny. The limited effect of phylogeny on scaling of cardiac function in mammals appears evident if we compare cardiac electrophysiology of two commonly used experimental species, dog and mouse, to the human heart electrophysiology. Despite the fact that the canine is phylogenetically more distant from human with respect to the mouse (Fig. 6), the similar body sizes of the two species requires similar heart rates and action potential durations and this is achieved by similar molecular mechanisms that were presumably shared by a most recent common ancestor.

In contrast, the small rodents (mouse, rat and hamster), which are more closely related to primates than dogs, have more divergent cardiac electrophysiological properties from humans, including most notably the expression of ion channel genes that are not expressed in the hearts of larger animals.

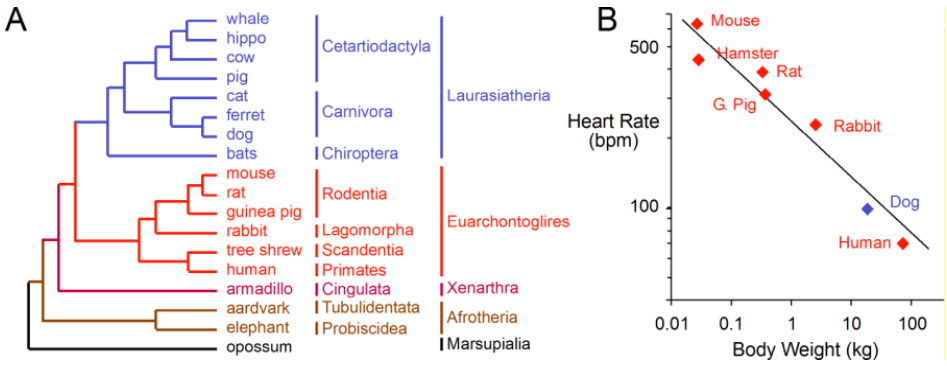

Figure 6. Mammalian phylogeny and the evolution of cardiac electrophysiology

(A) Phylogeny of extant placental mammals and one outgroup (adapted from Murphy et al (2001)). (B) Scaling of resting heart rate with body weight of animals to be used in the proposed study. Colors correspond to the four major mammalian clades identified by sequence homology.

Regulatory Evolution in the Physiological System

The ideas developed from the study of the evolution of development have been relatively slow to influence understanding of how physiological systems, such as cellular electrophysiology, evolve. This is due in most part to the difficulty of finding model physiological systems that are amenable to the study of regulatory evolution.

The scaling of cardiac electrical function is an ideal model in which to study the role of regulatory evolution in a physiological system. Cellular electrophysiology is essentially computational in nature and changes in levels of ion channel expression can fundamentally modify the output of this system (Rosati and McKinnon 2009). In such a computational system, the output (i.e. a change in membrane voltage, *dV/dt*) is produced by the summation of sodium (I_{Na}), calcium (I_{Ca}) and potassium (I_K) currents:

$$-C_m \, dV/dt = I_{Na} + I_{Ca} + I_K$$

The size of these currents (I_{Na}, I_{Ca}, I_K) is directly proportional to the number of ion channels in the cell membrane, which is generally determined by the level of transcriptional activity of different ion channel genes (Rosati and McKinnon 2004; Chandler et al. 2009). As a consequence, the relative level of expression of different ion channel genes has a direct effect on system function. In addition, ion fluxes are among the most metabolically expensive functions of electrically excitable cells (Attwell and Laughlin 2001) and there is a strong constraint to minimize overall channel expression levels. These two factors mean that cellular electrophysiological function will generally be strongly dependent on channel expression levels. One indicator of this is that these systems are prone to haploinsufficiencies (Table 2), a situation

which reduced dosage of genes resulted in insufficient expression and an abnormal phenotype (Deutschbauer et al. 2005; Veitia and Birchler 2010).

For a system like cellular electrophysiology, it is more likely that regulatory evolution will predominate because of its computational nature. This is at difference with other physiological systems, such as sensory and metabolic systems that perform specific physical tasks and do not have computational functions. For example, the sensitivity of a retinal photoreceptor cell to different wavelengths of light is absolutely dependent on the structure and function of opsin. This protein performs a key physical task, transduction of physical energy, and no conceivable form of regulatory evolution can change a yellow-green sensitive photoreceptor cell into a blue-violet sensitive cell (assuming that there is no gene for blue-violet opsin in the genome). For the wavelength sensitivity of this system to evolve there has to be structural evolution of the opsin gene. Similar arguments apply to many proteins that function in physiological systems that interface with the physical world and must perform specific physical tasks, such as sensory transduction, motor function, digestive enzymes or the enzymes in most metabolic pathways.

In the majority of the electrophysiological systems, however, computational function predominates. In particular, the cellular electrophysiology of the heart, at its simplest, functions as a square pulse generator that controls a pump. The cardiac cycle has two phases, the contraction phase (systole) and the relaxation phase (diastole) (Fig. 7A). This contraction-relaxation cycle has two key parameters: the period or cycle time (T) and the pulse duration (τ). The period (T) is determined by the heart rate. The pulse duration (τ) corresponds to the period of ventricular contraction.

At the level of cellular electrophysiology these two parameters are produced by two key computations. One computation produces a timing cycle that sets the basal heart rate. This is performed by sinoatrial node (SAN) cells and is the sum of the duration of the diastolic depolarization phase and the action potential duration of these cells. The second computation produces the depolarization-repolarization cycle that underlies the ventricular action potential duration and is performed by the bulk ventricular myocytes.

It is this computational function that evolves (Fig. 7B). There appears to be minimal changes in the structure of the molecular components that underlie this computation (Rosati and McKinnon, 2009; Rosati et al, 2008). It is the weights of the parameters in the computation, the basal current levels, that appear to evolve.

There are many other predominantly computational physiological systems. The nervous system, for example, is almost entirely computational. In this system, computational function depends on three properties: the neural circuitry, the strength of the synaptic connections between cells and the intrinsic electrophysiology of the neurons, all of which can evolve somewhat independently. The specific advantage of the cardiac system is that it provides insight into the evolution of one of these functions (intrinsic electrophysiology), in relative isolation.

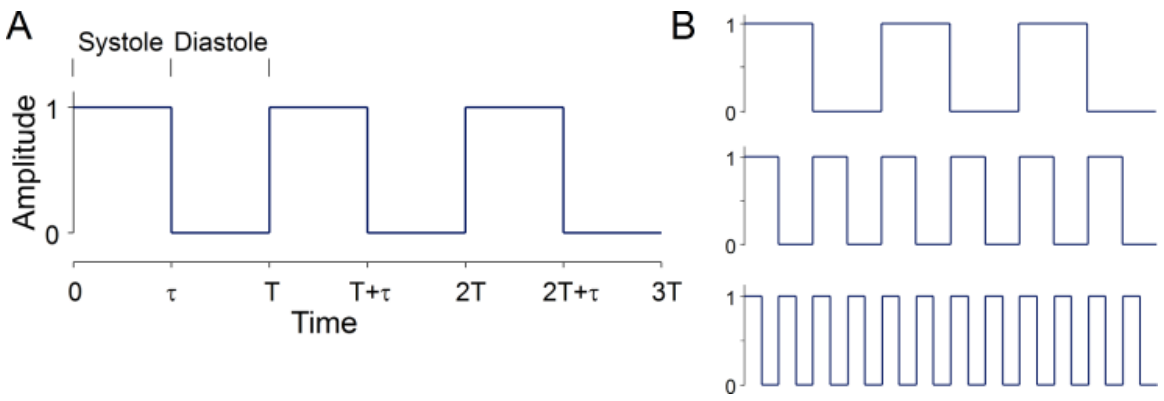

Figure 7. Evolution of the cardiac cycle

(A) The cardiac cycle time (T) equals 1/(heart rate). The period of contraction, systole, (τ) is followed by a period of relaxation, diastole. (B) The parameters of this cycle scale with body weight and it is this computational function that evolves to match body weight.

REGULATION OF ION CHANNEL GENE EXPRESSION

In order for ion channel genes to be expressed in a specific cellular electrophysiological phenotype, several processes are involved, from gene transcription, mRNA processing, translation and protein processing to assembly of subunits, transportation to the cell membrane and, finally, assembly into a functional channel complex (Fig. 8) (Deutsch 2003; Rosati and McKinnon 2004). The initial gene transcription step is critical and it is the target of *cis*-regulatory evolution. In addition, the channel protein is subjected to degradation and cell signaling molecules can produce covalent or allosteric modification of channel function (Fig. 8B). These modifications are generally reversible, resulting in transient changes in the level of functional channel expression.

When considering the regulation of ion channel expression in the adult heart, there are two extremes (Fig. 8). One is that ion channel expression is under homeostatic regulatory control. This regulation would be dynamic throughout the life of the adult, subtly adjusting the expression levels to optimize cellular physiological function. In this case, the system will be extremely tolerant to perturbations and the cellular physiological phenotype will tend to remain constant despite deficiency in some steps of the biosynthesis pathway. This possibility should be rare, as it would be relatively resistant to transcriptional regulation and evolutionary control.

The other extreme is that there is a vector of ion channel expression levels that is hardwired into the genome during the course of evolution, which largely determines the expression level and physiological function throughout the course of adult life. Because of the lack of feedback regulation, the initial step of gene transcription would determine the final output

of the biosynthesis pathway. As a result, genes with a "hardwired" regulation would be very sensitive to transcriptional regulation and *cis*-regulatory evolution control.

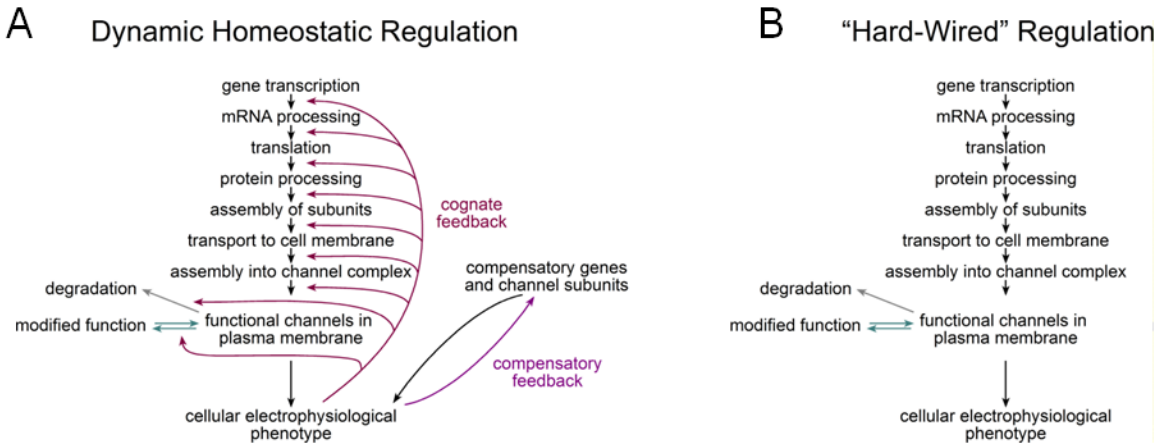

Figure 8. Comparison of two extreme possibilities of cardiac ion channel regulation

(A) An idealized model of dynamic homeostatic regulation of ion channel expression. Black arrows represent the biosynthesis pathway of the regulatory circuit. Colored arrows represent the feedback arm of the circuit. The feedback pathway has two components. The cognate feedback pathway (crimson) regulates expression within the biosynthetic pathway of a single gene. The compensatory feedback pathway (purple) regulates the expression of complementary or antagonistic genes. The modulatory pathway (teal) represents all the ways in which cell signaling molecules can produce covalent or allosteric modification of channel function.

(B) Biosynthetic pathway without feedback. Expression levels are largely dependent on the rate of gene transcription, although absolute channel expression levels will be determined by the efficiency of subsequent steps.

Figure adapted from Rosati and McKinnon 2004.

In principle, different ion channels may lie at different points along a continuum between these two possibilities. However, genetic studies in both humans and mice provide strong evidence that the expression levels of many channels in cardiac myocytes are largely hardwired. As described by Rosati and McKinnon (2004), haploinsufficiencies are particularly revealing regarding the presence or absence of homeostatic regulation of ion channel expression in the heart. If a haploinsufficiency occurs in response to a null mutation in an ion channel gene, it implies either that there is a complete absence of any feedback pathway from the electrophysiological phenotype or that the feedback is ineffective.

Haploinsufficiencies have been observed in multiple ion channel genes in both human and mouse. Mutations in four genes affecting four major cardiac currents (I_{Ks} I_{Kr} I_{K1} I_{Na}) have been shown to produce haploinsufficiencies in humans (Table 2). In mice, heterozygous knockout of two ion channel genes (SCN5A and KChIP2) produced an approximately 50% reduction in ion current expression, the functional equivalent of a haploinsufficiency (Table 2).

Table 2. Haploinsufficiency Mutations Affecting Cardiac Ion Channel Genes

Human Cardiac Ion Channel Genes:

Current	Gene	Phenotype	Reference
I_{Ks}	KCNQ1 (Kv7.1)	Long QT syndrome	Wang et al. 1999
I_{Kr}	KCNH2 (Kv11.1)	Long QT syndrome	Sanguinetti et al. 1996
I_{K1}	KCNJ2 (Kir2.1)	Long QT syndrome	Fodstad et al. 2004
I_{Na}	SCN5A (Nav1.5)	Idiopathic ventricular fibrillation	Chen et al. 1998

Heterozygous Knockouts in Mouse:

Current	Gene	Phenotype	Reference
I_{to}	KChIP2	KChIP2 expression and I_{to} current reduced to 50%	Kuo et al. 2001
I_{Na}	SCN5A	Impaired conduction, ventricular tachycardia	Papadatos et al. 2002

In total, five ion currents, comprising a majority of the major voltage-gated ion currents in the heart, have been shown to lack effective feedback mechanisms regulating their expression in the adult. This may be true for most of the other ion channels expressed in the heart, since there is very little compelling evidence for homeostatic feedback regulating the expression of any other major ion current in the adult heart (Rosati and McKinnon 2004). One major focus of my dissertation work is on the evolution of the KChIP2 gene, which is a necessary component for the I_{to} channel and a typical hardwired gene in the cardiac electrophysiological system.

In contrast to the ion currents mentioned above, the Cav1.2 channel, which underlies L-type calcium current ($I_{Ca,L}$), seems to undergo robust regulation, at least seen under pathophysiological conditions (Beuckelmann et al., 1991; Schroder et al, 1998; He et al, 2001; Chen et al, 2002; Piacentino et al, 2003; Tomaselli and Marban, 1999; Pitt et al, 2006). One of the topics of my study is to elucidate the regulation of the Cav1.2 gene in a conditional heterozygous knockout system.

KChIP2 and the I_{to} Current

KChIPs (Voltage-gated Potassium (Kv) Channel Interacting Proteins) are small calcium binding proteins that function as auxiliary subunits for the transient outward potassium current (I_{to} in the heart or I_A in the brain). A total of four KChIP genes (KChIP1-4) have been identified to date. All of them are expressed abundantly in the brain with distinct expression patterns (Rhodes et al. 2004; Xiong et al. 2004), while KChIP2 is the only isoform expressed in the heart (Rosati et al, 2001).

In the mammalian heart, the transient outward potassium current (I_{to}) plays a key role in action potential repolarization and in shaping the action potential morphology (Nerbonne 2000). Due to its rapid activation and inactivation properties, I_{to} regulates the size of the initial influx of Ca^{2+} ions into the cell, thereby affecting myocyte contraction (Sah et al. 2003). In small rodents, I_{to} plays a critical role in controlling ventricular action potential duration. In larger mammals, such as canine and human, I_{to} underlies phase 1 repolarization and plays a role in setting the level of the plateau phase (van der Heyden et al. 2006). This current contributes to create the characteristic spike-and-dome morphology of the ventricular action potential in these species being responsible for a 'notch' in the action potential waveform (see *Chapter 2*, Fig 2A).

There is significant species dependent variation in the expression of I_{to}'s underlying molecular components, the level of expression and the spatial distribution of gene expression. I_{to} has two phenotypes, a fast and a slow one segregated by their kinetics of recovery from inactivation. The fast I_{to} ($I_{to,f}$) is expressed in most mammalian species except for the guinea pig and pig (Findlay 2003; Li et al. 2003; Zhabyeyev et al. 2004; Patel and Campbell 2005). The slow I_{to} is found in some species and its primary subunit is encoded by the Kv1.4 gene. Table 3 is a summary of the expression of $I_{to,f}$ and its molecular components in different species.

Table 3. Species Variation in the Expression of $I_{to,f}$ Genes*

Species	$I_{to,f}$	Kv4.2	Kv4.3	KChIP2
Human	Y	N	Y	Y
Dog	Y	N	Y	Y
Ferret	Y	N	Y	Y
Rabbit	Y	N	low	Y
Guinea Pig	N	N	N	N
Rat	Y	Y	Y	Y
Mouse	Y	Y	Y	Y

* Data taken from (Dixon and McKinnon 1994; Dixon et al. 1996; Oudit et al. 2001; Rosati et al. 2001; Rosati et al. 2003; Patel and Campbell 2005; Rosati et al. 2006; van der Heyden et al. 2006). Y, present at moderate to high levels in the ventricle, low, present at low levels, N, either not present or present at very low levels.

Even though there are species-dependent variations, Kv4.2, Kv4.3 and KChIP2 are the main molecular components of $I_{to,f}$ in all mammals in which this current is expressed (Table 2). Kv4.2 gene encodes the primary subunit of I_{to} in the heart of small rodents (Dixon and McKinnon 1994) and Kv4.3 encodes the primary α-subunit of the I_{to} current in canine and human heart (Dixon et al. 1996). Kv4.3 is also expressed in the hearts of small rodents, but its contribution to the I_{to} current in these species is negligible, as shown in the knockout of this gene in mouse (Niwa et al. 2008). As the only KChIP expressed in the heart, KChIP2 is essential for the expression of the I_{to} current (Kuo et al. 2001, Rosati et al. 2001). Knockout of KChIP2 resulted in complete loss of the I_{to} current in mouse and the variation of KChIP2 expression determines the regional variation of this current in large mammals, as described in detail below.

In addition to the species-dependent differences in subunit composition, there is regional variation of I_{to} expression across the ventricular walls of all species that express this current

(Patel and Campbell 2005). I_{to} shows a gradient expression of highest to lowest from the epicardium to the endocardium (Fig. 9A, using the canine as an example). The molecular determinants for the regional variation of I_{to} vary in a species-dependent manner. In large mammals like the human and canine, the spatial distribution of I_{to} is determined by the auxiliary subunit KChIP2 (Fig. 9B) (Rosati et al. 2001; Rosati et al. 2003; Rosati et al. 2006). In small rodents like the mouse and rat, regional variation of the primary subunit Kv4.2 determines the gradient of I_{to} expression (Fig. 9C) (Dixon and McKinnon 1994, Rosati et al. 2001). The gradient expression of I_{to} plays a critical role in producing transmural variation of the duration of action potential (longer in the endocardium than the epicardium), which in turn, allows repolarization in the heart to occur in an orderly manner.

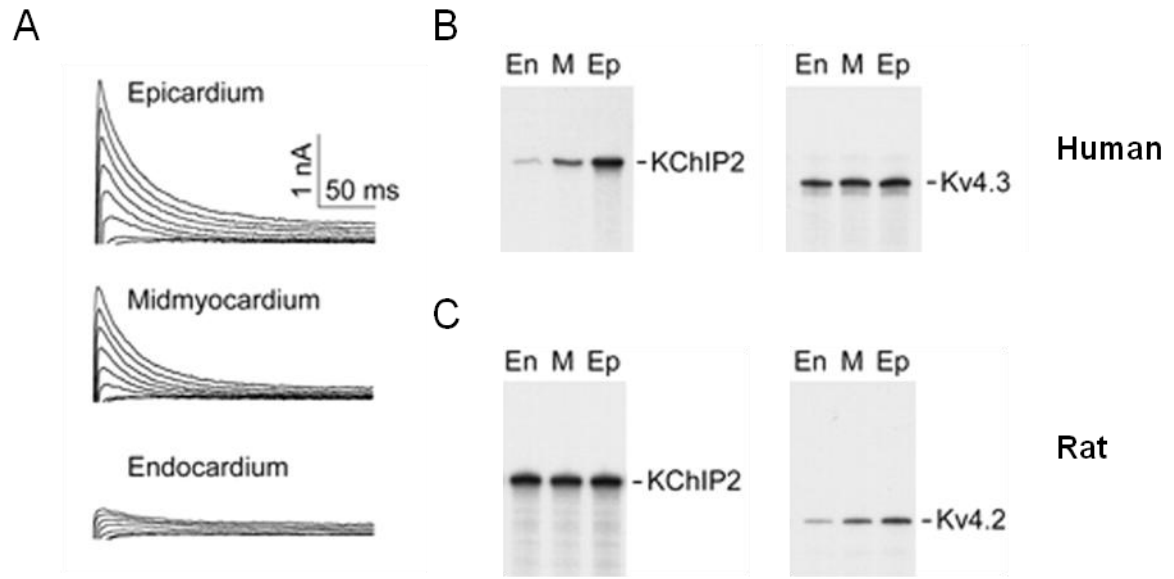

Figure 9. Expression of I_{to} and its molecular components across the left ventricular free wall

(A) I_{to} current recorded from the epicardial, midmyocardial and endocardial myocytes isolated from canine left ventricular free wall. (B-C) mRNA expression of the molecular components of I_{to} across the ventricular free wall of human and rat determined by RNA protection analysis. (B) In human, there is a correlating gradient expression in the auxiliary subunit KChIP2 but not the primary subunit Kv4.3. En, endocardium. M, midmyocardium. Ep, epicardium. (C) In rat, the I_{to} gradient is matched by regional variation of the primary subunit Kv4.2 but not the auxiliary subunit KChIP2. Figure adapted from Rosati et al. 2001.

Cav1.2 and the L-type Calcium Current

Ca^{2+} is the most versatile ion in the cell by being both a charged ion that can change membrane potential when flowing through membranes and a ubiquitous second messenger involved in several essential cellular processes (Clapham 2007). In the heart and muscle tissue, Ca^{2+} has a third role providing a link between electrical excitation and cell contraction (excitation and contraction coupling, ECC). A key element for ECC in cardiac myocytes is the voltage-gated L-type calcium channels located on the plasma membrane and in specialized membrane structures known as the T-tubules (Orchard et al. 2009; Hong et al. 2010). These channels open in response to a cell depolarization during the action potential, allowing Ca^{2+} influx to the cell. The Ca^{2+} entry through L-type calcium channels further triggers Ca^{2+} release through ryanodine receptors located on the membranes of the sarcoplasmic reticulum (SR). This release causes a dramatic increase of the cytosolic Ca^{2+} concentration, which switches on the contractile machinery in cardiac myocytes (Bers 2002).

The L-type calcium channel is a complex of proteins made up by the pore-forming subunit (α_1 subunit) and a few regulatory/ auxiliary subunits (β, α2/δ, and γ) (Catterall 2000; Bodi et al. 2005). The α_1 subunit is a large protein consists of four homologous domains (I to IV), each containing six transmembrane segments (S1 to S6) linked by a cytoplasmic loop between segments S5 and S6 (Takahashi and Catterall 1987). In ventricular myocytes, the α_1 subunit is encoded by the Cav1.2 gene and the γ subunit is not expressed (Bodi et al. 2005). The α2δ and β auxiliary subunits are required for the channel function, playing a role of modulating the biophysical properties and trafficking of the α_1 subunit to the membrane (Varadi et al. 1991; Hofmann et al. 1994; Yamaguchi et al. 1998).

Due to the unusually complex role of calcium in the physiology of the myocyte, there are multiple constraints on the function of the L-type calcium channel. At a minimum, the calcium current produced by the channel has to meet two criteria: be large enough to maintain excitation-contraction coupling but not so large as to result in calcium overload. Violating either of these conditions can, in principle, provide a feedback signal to homeostatically regulate calcium channel expression (Sadoshima and Izumo 1997; Tarone and Lembo 2003). Although expression of most ion channels is transcriptionally regulated (Table 1), the Cav1.2 channel might be an exception, suggested by pathological studies where little or no change in the L-type calcium current was observed despite a decrease in Cav1.2 mRNA during heart failure (Beuckelmann et al., 1991; Schroder et al, 1998; Chen et al, 2002; Piacentino et al, 2003; Tomaselli and Marban, 1999; Pitt et al, 2006).

Chapter 2

Evolution of Ventricular Myocyte Electrophysiology

INTRODUCTION

Studies in evolutionary developmental biology ("evo-devo") (Carroll 2005; Carroll et al. 2005; Wray 2007) have suggested regulatory evolution, especially cis-regulatory evolution as the primary molecular mechanisms underlying the evolution of developmental systems. The applicability of these ideas to the evolution of physiological systems has either been brought into question (Hoekstra and Coyne 2007) or has been uncertain (Carroll 2005). There is, in principle, no reason why these same concepts should not apply to the evolution of physiological systems and it is chosen to address this issue by studying the evolution of the electrophysiological properties of mammalian cardiac ventricular myocytes in this chapter.

A primary constraint on the electrophysiological properties of the mammalian heart is the scaling of body weight. Heart weight scales directly with body weight and there are no significant changes in the morphology of either the heart or of the cardiac myocytes (Prothero 1979; Loughrey et al. 2004). Similarly, several fundamental physiological properties of the cardiovascular system, including mean arterial pressure and minimum diastolic pressure (Holt et al. 1968; Elzinga and Westerhof 1991), are highly constrained and remain relatively invariant across mammalian phylogeny. These constrained physiological properties reflect the core function of the system: to maintain arterial blood pressure at a level sufficient to ensure adequate organ perfusion, particularly for critical organs such as the brain.

In contrast, many of the electrophysiological properties of the heart show systematic changes with body weight. These include heart rate (Stahl 1967; Holt et al. 1968; Schmidt-Nielsen 1984), action potential duration (the rate of action potential repolarization), action potential morphology and the rate of calcium ion reuptake (Bers 2002). The electrophysiological

properties of the heart vary in a systematic fashion in order to compensate for the changes in the physical properties of the vasculature and heart produced by scaling of body and heart weight. These concerted changes in electrophysiological function act to maintain the constrained physiological properties, such as mean arterial blood pressure, largely unchanged across mammalian phylogeny and are a critical factor in the ability of mammals to assume such a large range of body sizes (Holt et al. 1968; Westerhof and Elzinga 1991).

This chapter focuses on the electrophysiological properties of left ventricular myocytes, the primary function of which is the maintenance of arterial blood pressure. This function is both relatively simple and well understood within the context of the whole animal physiology. Ventricular myocytes are also one of the most intensively studied and best understood systems at the level of cellular physiology, with a correspondingly detailed knowledge of the molecular biology of ion channel and transport function (Bers 2002; Nerbonne and Kass 2005) and, as such, they provide an unparalleled system in which to study the evolution of electrophysiological traits. In this chapter, the mechanisms that produce changes in one specific trait, action potential morphology, are described and the relative importance of regulatory and structural evolution in the scaling of action potential duration and calcium reuptake is examined.

MATERIALS AND METHODS

Choice of Species

Mammalian species that are common experimental models for cardiac electrophysiological studies were chosen for study. The eight species used in the study encompass a broad range of body weights and show the typical allometric relationship between body size and heart rate or action potential duration observed for most terrestrial mammals (Fig. 1A and B). These species were: human (*Homo sapiens*), canine (*Canis familiaris*), ferret (*Mustela putorius furo*), rabbit (*Oryctolagus cuniculus*), guinea pig (*Cavia porcellus*), rat (*Rattus norvegicus*), Chinese hamster (*Cricetus griseus*) and mouse (*Mus musculus*).

Analysis of mRNA Expression

Animals were euthanized either with halothane or sodium pentobarbital (100 mg/kg, IV or IP), depending upon the species. The hearts were quickly removed and the left ventricular free wall was dissected. Total RNA was prepared using Qiagen RNeasy columns. Human RNA samples were obtained from independent commercial suppliers (Ambion or BioChain).

Complementary DNAs were prepared as previously described (Rosati et al, 2004). Three independent primer pairs for each gene were used for mRNA quantitation by real-time PCR, which was performed using the SYBR Green QuantiTect PCR Kit (Qiagen). Experimental samples were analyzed in triplicate. Expression values for a given gene were the average of results from three independent sets of eight RNA samples. Real-time PCR products were sequenced to confirm that the amplicons were from the mRNA of interest.

Isolation and Sequencing of Genomic DNA Regions from Hamster and Guinea Pig

BAC clones encompassing the Kv2.1 proximal promoter regions were identified in BAC libraries (CHORI) using a non-radioactive probe labeled with Digoxigenin-11-dUTP (DIG-11-dUTP alkali-labile, Roche). Probe sequences were based on cDNA sequences or conserved regions from multiple species and positive clones were detected using anti-DIG-AP, Fab fragments (Roche) and CDP-Star (Roche). Specific DNA fragments of interest were isolated from positive BAC clones (BACPAC Resources Center) by a combination of restriction mapping and southern blotting and subfragments were subcloned into pBluescript for sequencing. DNA sequences were submitted to Genbank (accession numbers EU643795 and EU643796).

Subcloning of Proximal Promoter Regions

Comparisons of Kv2.1 and Kv4.2 proximal promoter sequences were performed using the Vista alignment program (Frazer et al. 2004) and conserved regions were used as landmarks to select orthologous sequences from the two genes, although these were not identical in length (see Supplemental Material). For both genes the selected sequences terminated immediately before the initiator methionine in the first exon. DNA fragments for the Kv2.1 (mouse 1,601 bp, hamster 1,680 bp, guinea pig 1,786 bp, human 1,891 bp) and Kv4.2 (mouse 2,590 bp, human 2,567 bp) genes were subcloned from BAC clones into a luciferase reporter plasmid (pGL2, Promega).

Rat Neonatal Myocyte Transfection, Culture and Luciferase Assay

Neonatal rat cardiomyocytes were isolated and cultured as described (Yin et al. 2004). Transfection was performed using the Rat Cardiomyocyte Nucleofector Kit (Amaxa) in a Nucleofector I device (Amaxa). Each sample included an internal control Renilla luciferase plasmid (phRL-SV40, 1000-fold lower concentration than the test plasmids). Negative (pGL2-basic) and positive (pGL2-control) controls were also included in each experiment. After electroporation the cells were plated onto fibronectin-coated 12-well plates and cultured at 37 ℃ in 5% CO_2 for 48 hours. Cell survival was approximately 35%. Luciferase Assays were performed using the Dual Luciferase Reporter Assay Kit (Promega). Firefly and Renilla luciferase activities were measured using a Lumat luminometer (Berthold).

Myocyte Electrophysiology

Preparation of guinea pig and canine myocytes was performed as described previously (Sun and Wang 2005; Dong et al. 2006) and mouse ventricular myocytes were isolated using the same method as that used for guinea pig. For the recording of Ca^{2+} currents, isolated ventricular myocytes were maintained at room temperature and perfused with a Na^{+}- and K^{+}-free solution that contained (in mM) TEA-Cl 137, CsCl 5.4, $CaCl_2$ 2, $MgCl_2$ 1, HEPES 5, glucose 10, and 4-aminopyridine 3 (pH = 7.4). Glass pipettes were filled with solution containing (in mM) Cs-aspartate 115, CsCl 20, EGTA 11, HEPES 10, $MgCl_2$ 2.5, and Mg-ATP 2 (pH = 7.2), and had a resistance of 1.5–2.5 MΩ. After the membrane was ruptured, cells were clamped at –60 mV for 10 minutes to allow dialysis of the intracellular solution and stabilization of the Ca^{2+} currents before measurement of Ca^{2+} currents began.

Perforated patch-clamp recordings were used for action potential recordings and the dynamic clamp studies. Glass pipettes were back-filled with a pipette solution containing (in mM): K-aspartate 110, KCl 20, NaCl 8, HEPES 10, $MgCl_2$ 2.5, $CaCl_2$ 0.1, and 240 mg/ml amphotericin B (pH adjusted to 7.2 with KOH). Cells were studied once stable series resistances <7 MΩ were achieved. All action potential and contraction experiments were performed at 34 ℃.

Dynamic clamp experiments were performed as previously described (Sun and Wang 2005; Dong et al. 2006). A modified version of the Windows-based DynClamp software was used in the dynamic clamp studies (Pinto et al. 2001). Voltage sampling of the dynamic clamp software and output of the current injection command were through an Axon Digidata 2100 A/D board. I_{to} was defined as a rapidly and fully inactivating outward current, formulated as described previously (Dong et al. 2006).

Myocyte contraction was imaged using a CCD camera and cell length and shortening were measured using a video edge detector (Crescent Electronics).

Expression of Kv1.5, KCNH2 and KCNQ1 Channels

The mouse and human Kv1.5 cDNA were obtained commercially (Open Biosystems). The human KCNH2 and KCNQ1 cDNA clones have been described previously (Sanguinetti et al. 1995; Sanguinetti et al. 1996). Full-length guinea pig cDNA clones were derived using a combination of RACE and standard PCR as described previously (Shi et al. 1997) (accession numbers EF204534 and EF204535). Channel expression and recording using *Xenopus* oocytes were performed as described previously (Sanguinetti et al. 1995; Sanguinetti et al. 1996). The decaying phase of tail current traces was fitted to one (KCNH2 or I_{Ks}) or two (KCNQ1)

exponential functions. Peak tail current amplitudes were normalized to the maximum value and the resulting data were fitted to a Boltzmann function.

RESULTS

Scaling of Ventricular Action Potential Duration

The relationship between body weight and the resting heart rate of terrestrial mammals was fitted using an allometric equation with a scaling coefficient of -0.25 ± 0.02 (Fig. 1A), similar to values obtained in earlier studies using independent data sets (Stahl 1967; Holt et al. 1968). Ventricular action potential durations for a range of terrestrial mammals were estimated from QT intervals obtained from electrocardiogram studies (Fig. 1B). The inverse action potential duration, which corresponds approximately to the overall rate of repolarization following the upstroke of the action potential, scales continuously over a wide range of body sizes and has a scaling coefficient of -0.22 ± 0.02.

The scaling of heart rate and APD are similar but not perfectly matched. There is a modest increase in the fraction of the cardiac cycle taken up by the action potential in smaller mammals, so that this value displays a weak dependence on body mass (Fig. 1C). This is consistent with the observation that the diastolic interval decreases as a fraction of the cardiac cycle in smaller mammals (Popovic et al. 2006). Because the coronary blood supply to the left ventricle is only active during diastole, there is a strong constraint on the minimum fraction of the cardiac cycle that must be devoted to diastole in order to ensure adequate perfusion of the myocardium, which must be one important factor maintaining the relatively tight linkage between heart rate and action potential duration.

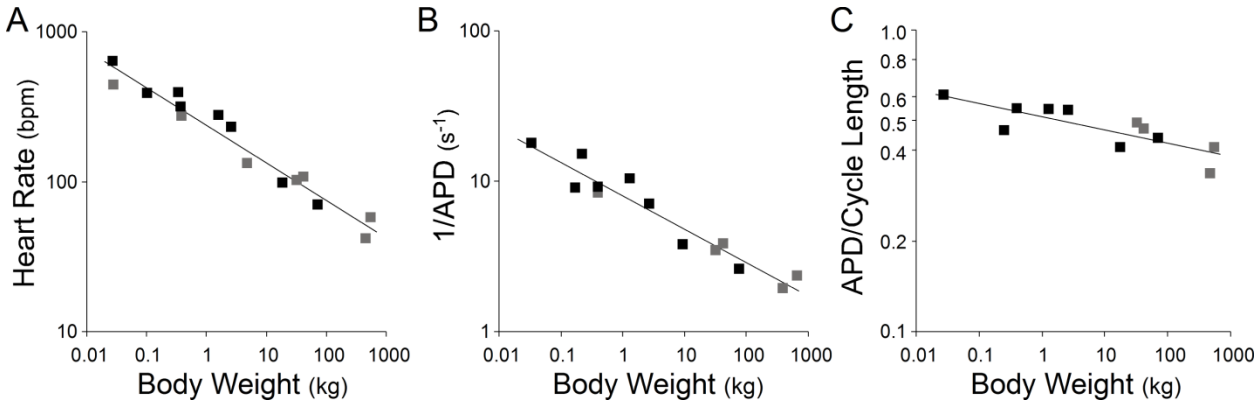

Figure 1. Scaling of action potential duration.

(A) Relationship between resting heart rate and body weight for terrestrial mammals. Data were fitted with the allometric equation: $y = a\ M^{b}$, where a is constant, M is the body weight, and b is the scaling coefficient ($b = -0.25 \pm 0.02$). The species used in the current study are represented by black squares: other species are represented with gray squares. Data were obtained from a survey of the literature. (B) Relationship between the inverse ventricular action potential duration (s^{-1}) and body weight for terrestrial mammals (scaling coefficient $b = -0.22 \pm 0.02$). Ventricular action potential duration was estimated from uncorrected QT intervals obtained from electrocardiogram studies using conscious resting animals. (C) Relationship between the fraction of the cardiac cycle taken up by the action potential and body weight (scaling coefficient $b = -0.04 \pm 0.01$). Data points were calculated from those studies in which both the heart rate and the QT interval were recorded from the same animals.

Discontinuities in Scaling of Ventricular Action Potential Morphology

Although ventricular APD scales over a large range of mammalian body weights without any obvious discontinuities (Fig. 1B), at the cellular level there are marked discontinuities in the electrophysiological mechanisms underlying action potential repolarization in the ventricles of mammals of different weights. In species the size of guinea pig and larger, action potential repolarization depends primarily on three potassium currents: the I_{Ks} and I_{Kr}, which have relatively slow kinetics of activation, and the inward rectifier current I_{K1} (Nerbonne and Kass 2005). In smaller species, repolarization is primarily dependent on two relatively large and rapidly activating potassium currents, I_{to} and I_{Kur}. These differences in repolarization mechanism are reflected in the morphology of the ventricular action potential.

In large and intermediate sized mammals, such as canine and guinea pig, action potentials have a 'spike and dome' morphology, whereas action potentials in small mammals, such as the mouse, have a 'triangular' morphology, which is distinguished by the lack of a prominent plateau phase (Fig. 2A). The presence of a large I_{to} in the myocytes of small mammals precludes the development of the high plateau phase observed in larger animals. The critical role of I_{to} expression levels in determining action potential morphology can be shown experimentally by adding a large I_{to} to either the guinea pig or canine myocytes using dynamic clamp (gray traces in Fig. 2A). Following addition of this current, the action potential assumes a morphology that is similar to that of the mouse action potential.

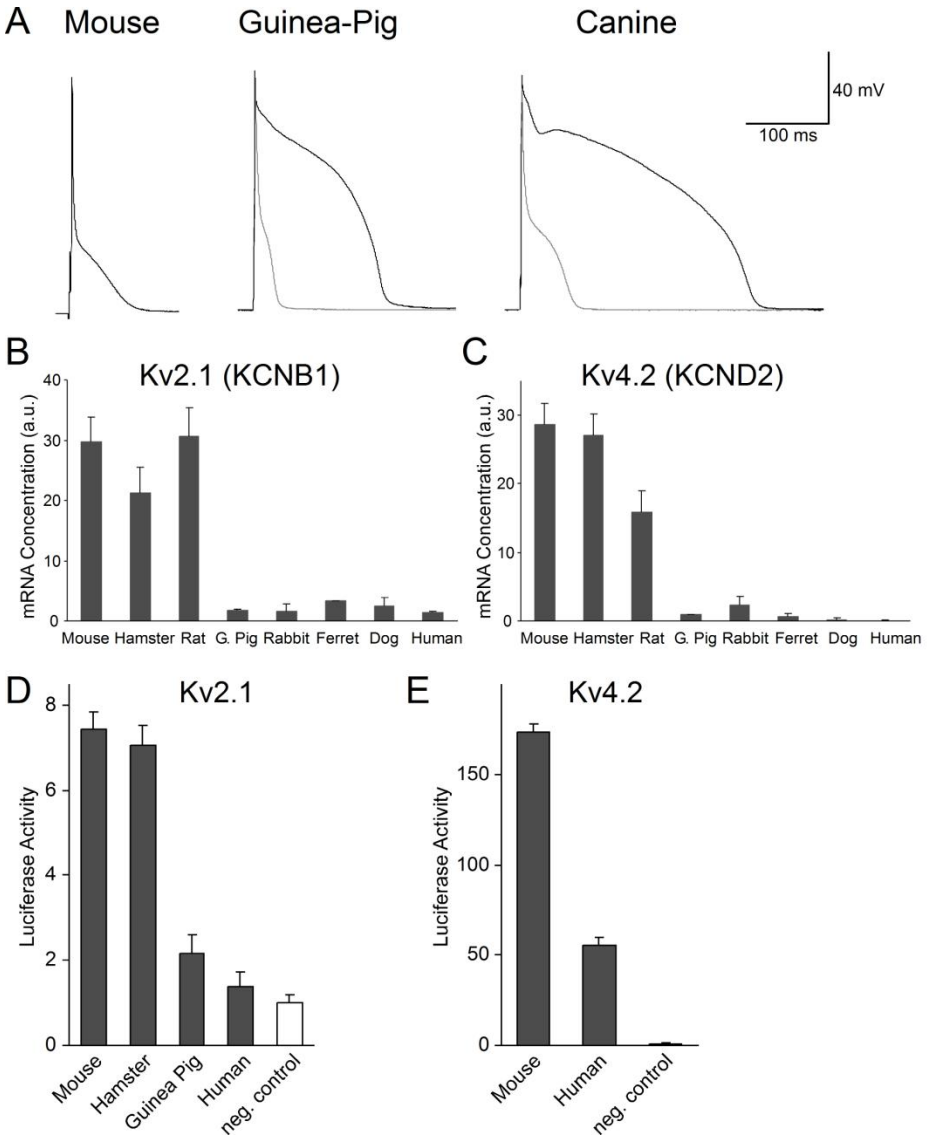

Figure 2. Discontinuities in scaling of ventricular action potential morphology

(A) Comparison of ventricular action potentials recorded from mouse, guinea pig and canine ventricular myocytes. For the guinea pig and canine cells the waveform following the addition of a mathematically modeled I_{to} current (≈50 pA/pF) using dynamic clamp is shown in gray. Comparison of (B) Kv2.1 (*KCNB1*) and (C) Kv4.2 (*KCND2*) mRNA expression in the left ventricular wall of eight mammalian species. Histograms show means ± S.D. (n = 3). (D) Comparison of the functional properties of mouse, hamster, guinea pig and human Kv2.1 proximal promoter regions. (E) Comparison of the functional properties of mouse and human Kv4.2 proximal promoter regions. For promoter analysis, orthologous regions of genomic DNA (see Methods) were subcloned into a luciferase reporter gene construct and gene activity was determined by assaying luciferase activity following transfection into cultured rat neonatal cardiac myocytes. Data values are expressed relative to the background level of luciferase activity following transfection of the control plasmid (pGL2-basic). Histograms show means ± S.D. (n = 3-6).

Regulation of Rapidly Activating Repolarizing Currents

The discontinuity in action potential repolarization mechanism is produced by abrupt changes in the level of expression of the I_{to} and I_{Kur} channels and this is reflected in the expression of two genes that encode these channels (Fig. 2B and C). The species-dependent expression pattern of the genes underlying the main component of the I_{to} channel (Kv4.2) and one component of the rapidly activating potassium channel delayed rectifier channel I_{Kur} (Kv2.1) resemble a step function, with both Kv2.1 and Kv4.2 mRNA being abundantly expressed in mouse, hamster and rat ventricles but uniformly low in all larger species (Fig. 2B and C).

A second channel type that also contributes to I_{Kur}, the Kv1.5 channel, was tested but expression of Kv1.5 mRNA was poorly correlated with expression of the channel, suggesting that regulation of this channel is either post-transcriptional, dependent on a yet-to-be identified accessory subunit or the mRNA is expressed at significant levels in cells other than myocytes in the ventricle wall (Wang et al. 1999; Bru-Mercier et al. 2003). The function of this channel is conserved, as shown in the comparison of human and mouse Kv1.5 channel in a heterologous expression system (Fig. 3). The Kv4.2 alpha subunit makes the primary contribution to I_{to} expression in small rodents (Guo et al. 2005). In larger animals expression of I_{to} is highly variable, relatively small when present (Rosati et al. 2003) and has little or no effect on action potential duration in these species (Sun and Wang 2005). The small I_{to} found in these species is encoded by the Kv4.3 gene (Dixon et al. 1996), which displays highly variable species dependent expression patterns, with no correlation to body size (*Chapter 5*, Fig. 2).

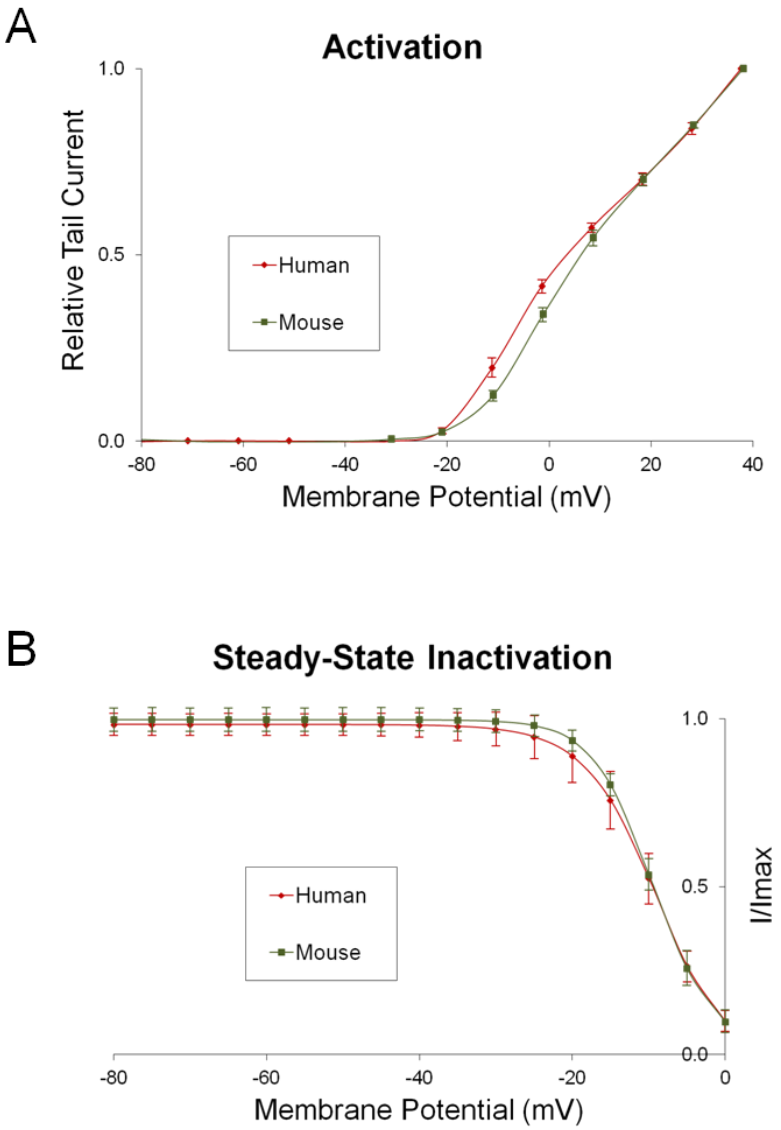

Figure 3. Comparison of human and mouse Kv1.5 channel function in Xenopus Oocytes

(A) Activation curve determined from tail currents for human and mouse Kv1.5 current. (B) steady-state inactivation for human and mouse Kv1.5 current. (n=6 for both mouse and human, error bars are standard deviation.)

Comparison of Mouse, Hamster, Guinea Pig and Human Kv2.1 Proximal Promoter Function

In principle, the changes in Kv2.1 mRNA expression in different species (Fig. 2B) can be produced by changes in either the *cis*- or trans-regulatory elements controlling gene expression. To address this issue the transcriptional activity of the proximal promoter regions of the mouse, hamster, guinea pig and human Kv2.1 genes were compared in cultured rat myocytes.

There are clear differences in the transcriptional activity of the Kv2.1 proximal promoters from different species that closely reflect the differences in mRNA expression (Fig. 2D). This result suggests that the differences in Kv2.1 mRNA expression observed *in vivo* are mediated by changes in the functional properties of *cis*-regulatory elements found in the Kv2.1 gene.

Given the highly distributed nature of mammalian gene regulation, it is notable how well the different *in vivo* expression patterns of the Kv2.1 gene are retained by the proximal promoter regions when expressed *in vitro*. In addition to the large difference between the mouse/hamster and guinea pig/human expression levels, the guinea pig/human promoters are essentially turned "off" in cardiac myocytes *in vitro*, as they are *in vivo*.

Comparison of Mouse and Human Kv4.2 Proximal Promoter Function

There were also clear differences in the transcriptional activity of the mouse and human Kv4.2 proximal promoter regions (Fig. 2E). For the Kv4.2 gene, although there are large differences between the mouse and human constructs, expression of the human promoter is significantly above the background levels seen *in vivo* and expression relative to the Kv2.1

constructs was also anomalously high. Both results suggest that the Kv4.2 promoter construct lacks one or more repressor elements found in the native gene.

Function and Regulation of Slowly Activating Repolarizing Currents

The changes in I_{to} and I_{Kur} expression are clear examples of regulatory evolution. The scaling of action potential duration in larger species could, however, involve structural evolution modifying the function of one or more of the other currents that are required for action potential generation in these animals. Guinea pig and larger species depend predominantly on two voltage-gated potassium currents, I_{Ks} and I_{Kr}, for action potential repolarization. Therefore, of all the channels involved in this process, these channels would seem to be the most obvious candidates for structural evolution. The α subunits of the I_{Ks} and I_{Kr} channels are encoded by the KCNQ1 and KCNH2 genes, respectively. If, for example, the activation rate of the KCNQ1 channel scaled between human and guinea pig, this change in channel function could contribute significantly to the decrease in action potential duration observed in guinea pigs.

Because it is difficult to accurately record the kinetic properties of I_{Ks} and I_{Kr} in large mammals, due to the relatively small size of the currents, the properties of the guinea pig and human KCNQ1 and KCNH2 channels were compared using a heterologous expression system. No significant difference in either the rate or voltage dependence of KCNQ1 channel activation was observed, either when the channel was co-expressed with its normal auxiliary subunit, KCNE1 (Fig. 4A and B), or when expressed alone (data not shown). The only detectable difference between the channels from the two species was an approximately 20% slower deactivation rate for the guinea pig channel compared to human. This small difference was

observed when the channels were expressed alone or when coexpressed with KCNE1. For the I_{Kr} current, no detectable differences were found in comparisons of the kinetic properties of human and guinea pig KCNH2 channels, and the two currents were indistinguishable (Fig. 4C, D and E).

In contrast to the conserved channel function, it is known that guinea pig myocytes express significantly higher levels of the I_{Ks} and I_{Kr} currents than do larger species (Lu et al. 2001) and this is likely to be one important factor contributing to the decreased action potential duration in these species. Both KCNQ1 and KCNH2 gene expression was found to be significantly ($P<0.01$) increased in guinea pig compared to larger species (Fig. 4F&G) suggesting that regulatory evolution of KCNQ1 and KCNH2 gene expression may contribute to the scaling of action potential duration. Regulation of these currents is complex, however, and it has been shown previously that KCNH2 mRNA and protein are expressed at high levels in small rodents (Wymore et al. 1997; Pond and Nerbonne 2001) whereas the I_{Kr} is very small, so other factors in addition to expression of the α subunits are likely to contribute to the regulation of these currents.

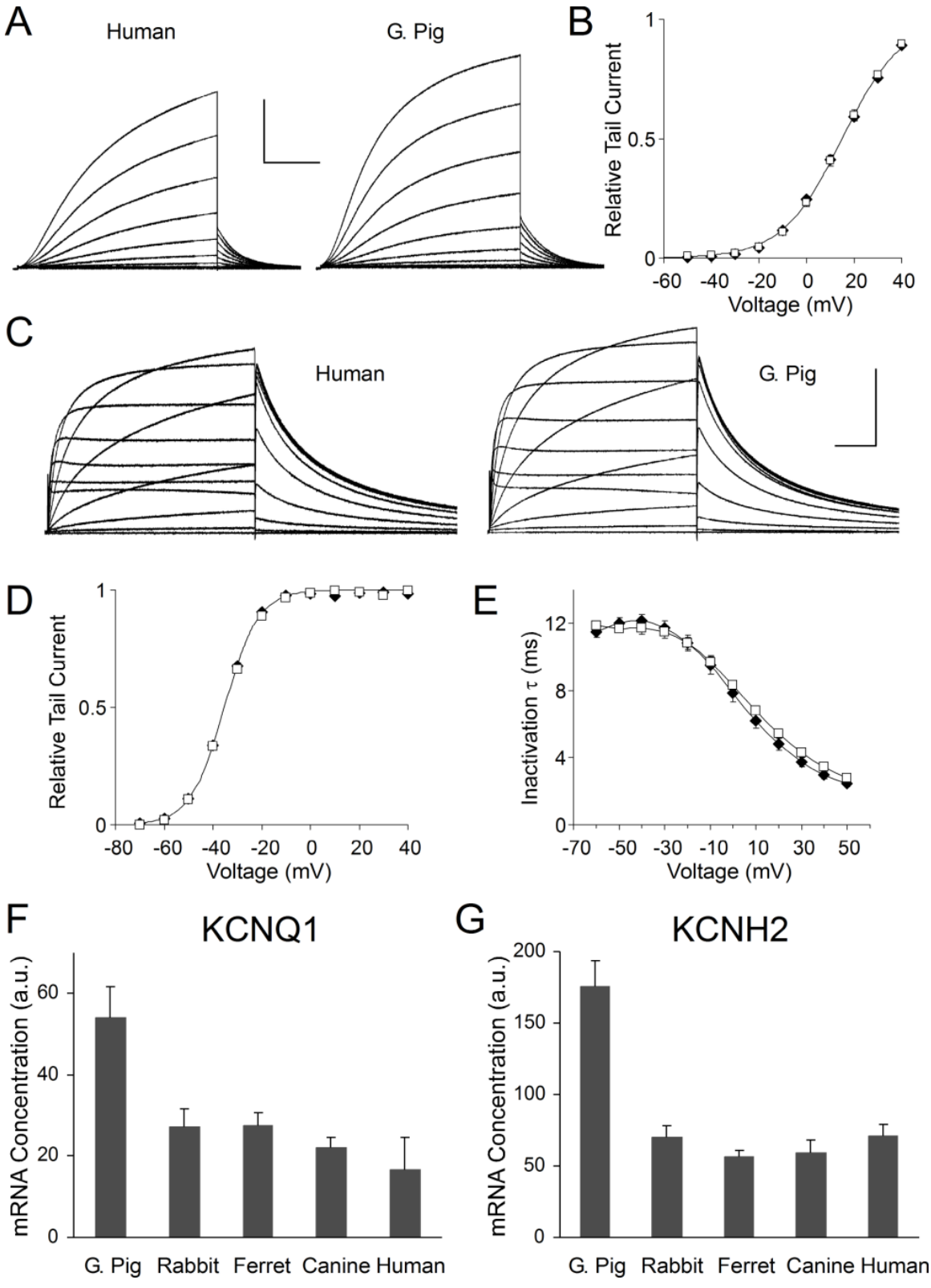
A
Human
G. Pig
B
Relative Tail Current
1
0.5
0
-60 -40 -20 0 20 40
Voltage (mV)
C
Human
G. Pig
D
Relative Tail Current
1
0.5
0
-80 -60 -40 -20 0 20 40
Voltage (mV)
E
Inactivation τ (ms)
12
8
4
0
-70 -50 -30 -10 10 30 50
Voltage (mV)
F
KCNQ1
mRNA Concentration (a.u.)
60
40
20
0
G. Pig Rabbit Ferret Canine Human
G
KCNH2
mRNA Concentration (a.u.)
200
150
100
50
0
G. Pig Rabbit Ferret Canine Human

Figure 4. KCNQ1 and KCNH2 function and expression.

(A) Current traces of human (left) and guinea pig (right) KCNQ1 channels co-expressed with KCNE1 in *Xenopus* oocytes. (current scale: 4 or 2.5 μA respectively, time scale: 2 seconds). (B) Activation curve determined from tail currents for human and guinea pig KCNQ1 (n = 10). Data were fitted with Boltzmann curves ($V_{1/2}$ = 14.9 ± 0.2 and 15.0 ± 0.3 mV, k = -12.2 ± 0.2 and -12.6 ± 0.3, respectively). (C) Current traces of human (left) and guinea pig (right) KCNH2 channels expressed in *Xenopus* oocytes (current scale 0.4 μA, time scale 1 second). (D) Activation curves (determined from tail currents) and inactivation time constants for human and guinea pig KCNH2 channels expressed in *Xenopus* oocytes (n = 14 and 21 respectively). Data were fitted with Boltzmann curves ($V_{1/2}$ = -34.9 ± 0.3 and -35.3 ± 0.3 mV, k = -7.2 ± 0.2 and -7.0 ± 0.2, respectively). (E) Inactivation time constants for human and guinea pig KCNH2 channels. For (B), (D) and (E), data points show means±SEM and symbols are human (open square) and guinea pig (black diamond). Comparison of *KCNQ1* (F) and *KCNH2* (G) gene expression in the left ventricular free wall of guinea pig and larger species. Histograms show means ± S.D. (n = 3).

Function and Regulation of the L-type Calcium Current

One other channel for which changes in kinetic properties could have an impact on action potential duration, particularly in species with a spike and dome action potential morphology, is the L-type calcium current ($I_{Ca,L}$). The kinetic properties of $I_{Ca,L}$ were determined using voltage-clamp recordings in three species, mouse, guinea pig and canine and the biophysical properties of the currents were found to be quite similar (Fig. 5A). The normalized I-V curves for the three species were very similar (Fig. 5B). The steady-state inactivation curves were also similar, although the mouse curve was shifted 4 mV more negative relative to the guinea pig, which overlapped with canine (Fig. 5C). The rate of inactivation for the mouse and guinea pig currents was best described by two time constants, which were indistinguishable for the two species (Fig. 5D). The relatively small canine current could not be reliably fitted with two time constants. In this case, the single fitted time constant was intermediate between those of mouse and guinea pig. Qualitatively, there is very little difference in the inactivation properties of these currents.

In contrast to the relatively constant biophysical properties, there were significant changes in peak calcium current expression levels. In this case, however, the change in expression level is unrelated to regulation of action potential duration because there was a significant increase in calcium current density with decreasing body weight for the three species tested (Fig. 5E). If scaling of action potential duration was the sole determinant of $I_{Ca,L}$ expression levels, it would be expected that the calcium current would either remain constant or decline in smaller species, because this current will generally act to lengthen action potential duration.

Expression of *$Ca_v1.2$* (CACNA1C) mRNA, which encodes the α subunit of the predominant L-type calcium channel in ventricular myocytes (Striessnig 1999; Rosati et al.

2007), was relatively constant (Fig. 5F), with the changes between species being significantly less than was seen for $I_{Ca,L}$ density. Expression of several cardiac calcium channel auxiliary subunit genes, β_2, $\alpha_2\delta$-1 and $\alpha_2\delta$-2, which have been shown to affect calcium current expression (Striessnig 1999; Arikkath and Campbell 2003), showed no consistent dependence on body weight for the species tested (data not shown). The mechanism by which $I_{Ca,L}$ expression is modified between different species remains uncertain, therefore, and it may involve post-transcriptional mechanisms regulating the expression of functional channels rather than transcriptional regulation.

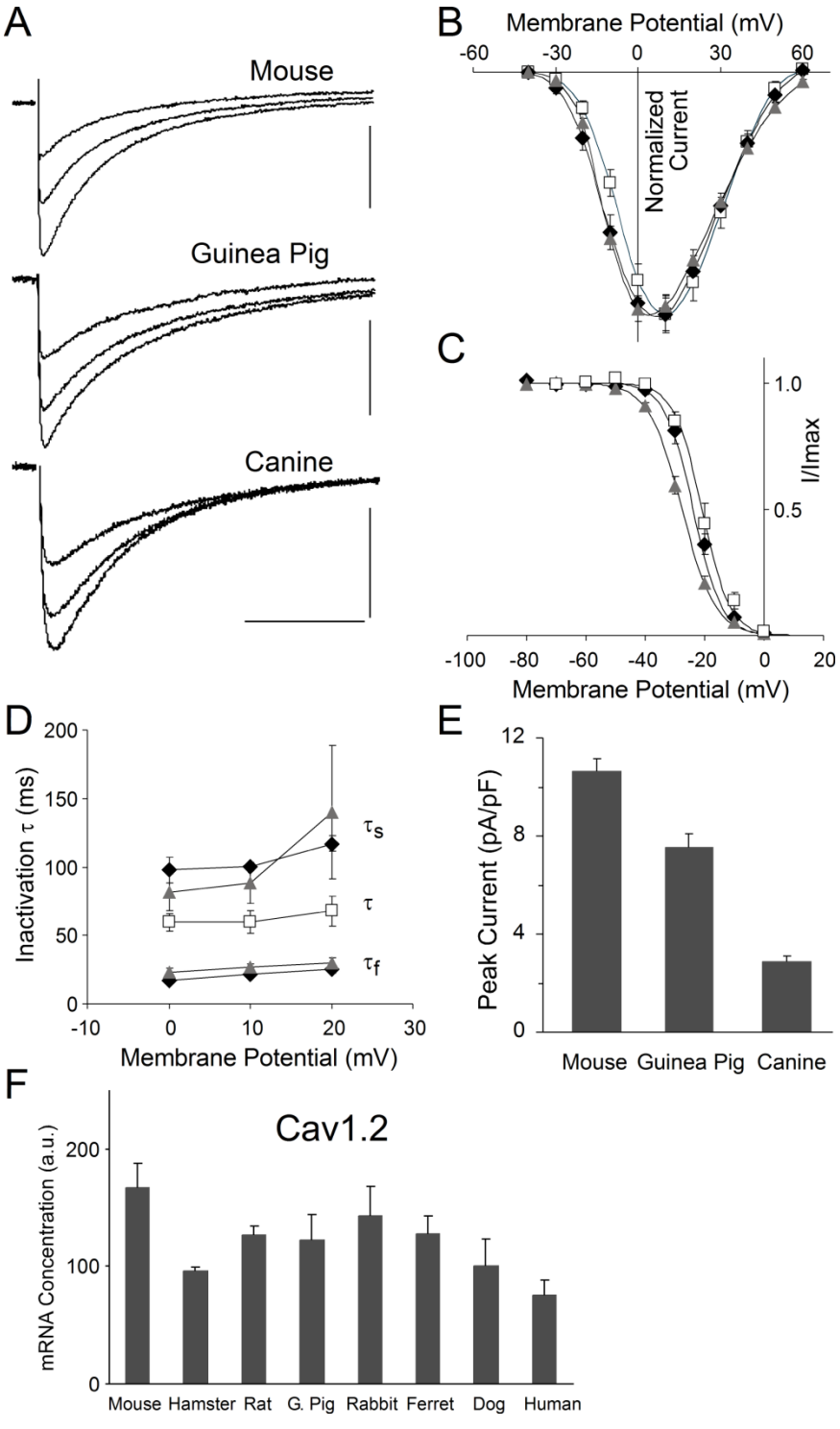
A
Mouse
Guinea Pig
Canine
B
Membrane Potential (mV)
-60
-30
0
30
60
Normalized Current
C
1.0
0.5
I/Imax
-100
-80
-60
-40
-20
0
20
Membrane Potential (mV)
D
Inactivation τ (ms)
200
150
100
50
0
τs
τ
τf
-10
0
10
20
30
Membrane Potential (mV)
E
Peak Current (pA/pF)
12
8
4
0
Mouse
Guinea Pig
Canine
F
Cav1.2
mRNA Concentration (a.u.)
200
100
0
Mouse
Hamster
Rat
G. Pig
Rabbit
Ferret
Dog
Human

Figure 5. Calcium current function and expression in ventricular myocytes.

(A) L-type calcium current traces recorded from mouse, guinea pig and canine myocytes (current scale 5, 4 and 2 pA/pF respectively, time scale 80 ms). Holding potential was -50 mV, and currents were elicited by voltage steps to 20, 30 and 40 mV. (B) Normalized I-V relations for mouse, guinea pig and canine $I_{Ca,L}$ in ventricular myocytes. (C) Steady-state inactivation for $I_{Ca,L}$. Data were fitted with Boltzmann curves ($V_{1/2}$ = -27.7 ± 0.9, -23.9 ± 1.4, -20.9 ± 1.6 mV, k = 5.6 ± 0.1, 4.7 ± 0.2, 4.7 ± 0.1, n = 7, 14, 8, respectively). (D) Inactivation time constant (τ) for $I_{Ca,L}$. For mouse and guinea pig the data were fitted with a biexponential curve with two time constants (τ_f and τ_s), whereas for canine an exponential curve with a single time constant (τ) was fitted (n = 5, 5 and 6, respectively). For (B), (C) and (D) data points are means ± S.D., and symbols are mouse (gray triangle), guinea pig (black diamond) and canine (open square). (E) Comparison of peak calcium current density in mouse, guinea pig and canine ventricular myocytes. Histogram shows means ± SEM, for mouse, guinea pig, and canine (n = 31, 14 and 19, respectively). (F) Comparison of Cav1.2 (CACNA1C) mRNA expression in the left ventricular wall of eight mammalian species. Histogram shows means ± S.D. (n = 3).

Interactions Between $I_{Ca,L}$ Density and the Maintenance of Excitation-Contraction Coupling

Given that $I_{Ca,L}$ shows systematic changes in magnitude with body size that cannot be explained by regulation of action potential duration, it is likely that the changes in $I_{Ca,L}$ magnitude reflects constraints imposed by the maintenance of excitation-contraction coupling. This possibility was examined in canine ventricular myocytes using action potential clamp (Fig. 6). A normal canine action potential waveform elicits a robust contraction in canine myocytes, as expected. In contrast, a mouse action potential waveform fails to elicit a contraction in these cells. To determine whether the failure of the mouse action potential to elicit a contraction in canine myocytes was due simply to the smaller size of $I_{Ca,L}$ in canine myocytes, $I_{Ca,L}$ was increased by one of two independent methods: an increase in external calcium concentration or treatment with the calcium channel activator BAY-K 8644 (BayK). In both cases, the increased magnitude of $I_{Ca,L}$ restored excitation-contraction coupling, suggesting that constraints related to the maintenance of excitation-contraction coupling drive the increased $I_{Ca,L}$ density in mouse myocytes.

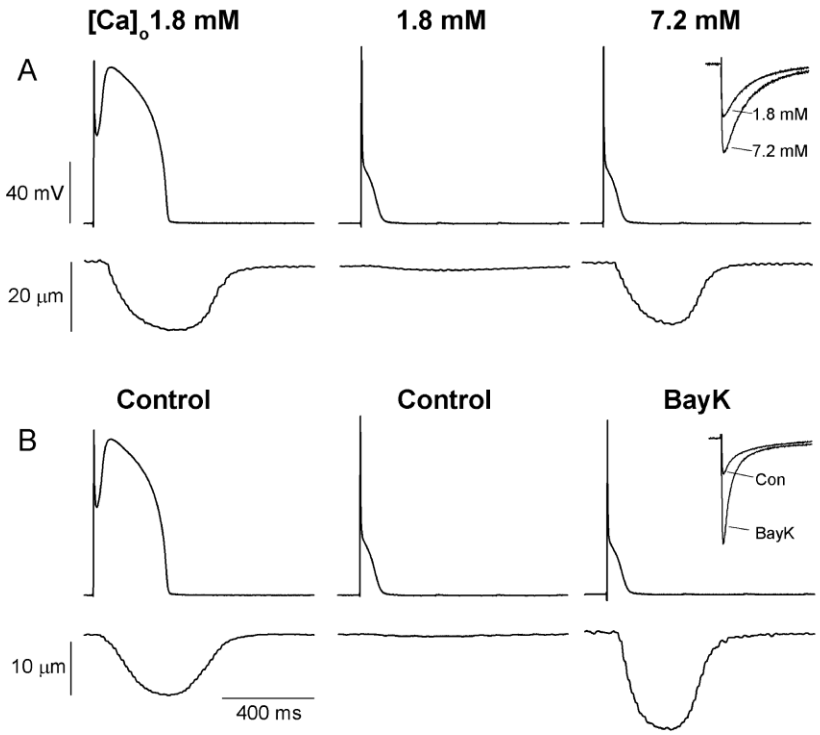

Figure 6. Action potential clamp recordings from canine myocytes and corresponding unloaded contraction.

Top panels show imposed action potential voltage-clamp waveform, and bottom panels show unloaded cell shortening. (A) Canine action potential waveform in the presence of normal external calcium (left panel). Mouse action potential waveform in the presence of normal external calcium (center panel). Note the failure to initiate a contraction. Mouse action potential waveform in the presence of 7.2 mM external calcium (right panel) restores the contraction (inset shows a comparison of peak calcium current recorded under voltage clamp in the control and 7.2 mM external calcium solutions). (B) Similar experimental design to that shown in panel (A) using 0.5 μM BayK to increase calcium current (inset). Again, note the recovery of contraction with the mouse action potential waveform when the calcium current is experimentally enhanced.

Scaling of Calcium Reuptake

There is a tight linkage between the duration of the calcium transient triggered by an action potential and the duration of myocyte contraction (Bers 2002). As a consequence, one important constraint on the scaling of cardiac electrophysiological function is that the duration of the calcium transient must also decrease with decreasing body size. There are two transporter systems responsible for the rapid uptake of calcium ions from the cytosol, the sarcoplasmic reticulum (SR) Ca^{2+}-ATPase pump and the Na^{+}/Ca^{2+} exchanger (Bers 2002). The primary change with body weight is seen in the activity of the Ca^{2+}-ATPase pump and this also appears to be an example of regulatory evolution. The activity of the SR Ca^{2+}-ATPase pump increases significantly with decreasing body size due to an increase in the density of Ca^{2+}-ATPase pump proteins, rather than to a change in the specific activity of the pump (Hamilton and Ianuzzo 1991; Hove-Madsen and Bers 1993; Su et al. 2003; Vangheluwe et al. 2005). Due to this increase in Ca^{2+}-ATPase pump activity, the relative activity of the two transport systems changes significantly with body size. In small mammals the Ca^{2+} uptake process is dominated by the Ca^{2+}-ATPase pump, whereas in larger mammals there is a greater role for the Na^{+}/Ca^{2+} exchanger, although the Ca^{2+}-ATPase pump is still the dominant uptake mechanism (Bassani et al. 1994; Bers 2002).

These body mass-dependent changes in calcium handling appear to be determined at the level of transcription. Expression of SERCA2 (ATP2A2) mRNA, which encodes the SR Ca^{2+}-ATPase pump, scales steeply with body weight, with a similar scaling factor to that of inverse action potential duration (Fig. 7A). Expression of the NCX1 gene, which encodes the Na^{+}/Ca^{2+} exchanger, is essentially independent of body size although there is some species-dependent variation in expression levels (Fig. 7B). This result is consistent with the observation that the

level of Na^+/Ca^{2+} exchanger activity does not vary systematically with body mass (Sham et al. 1995).

Unlike the action potential, there are no discontinuities in the scaling of the calcium reuptake transporters. This most likely reflects the fact that the rate of calcium uptake can scale in a simple linear way in proportion to the abundance of the molecular components that underlie the process. Calcium ion pumping obeys the law of mass action and linear scaling of the concentration of one of the key reactants, the Ca^{2+}-ATPase pump, produces an appropriate effect, an increased rate of Ca^{2+} uptake.

Regulation of the Sodium Channel

There is a modest dependence of *SCN5A* (*$Na_v1.5$*) mRNA expression on body weight (Fig. 7C) and there is a significant difference in the average expression values for the three smallest species, which express large I_{to} and I_{Kur} currents, compared to the five largest species ($P<0.01$). Because sodium channel expression appears to be predominantly mediated by transcriptional regulation (Papadatos et al. 2002; Bezzina et al. 2006), this may produce an increase in sodium current expression in these smaller species. The relatively fast activation times of the large I_{to} and I_{Kur} result in partial overlap of these currents with the activation period of the sodium current, and the increased *SCN5A* expression may represent a compensatory mechanism, possibly to maintain action potential peak height (Pandit et al. 2001).

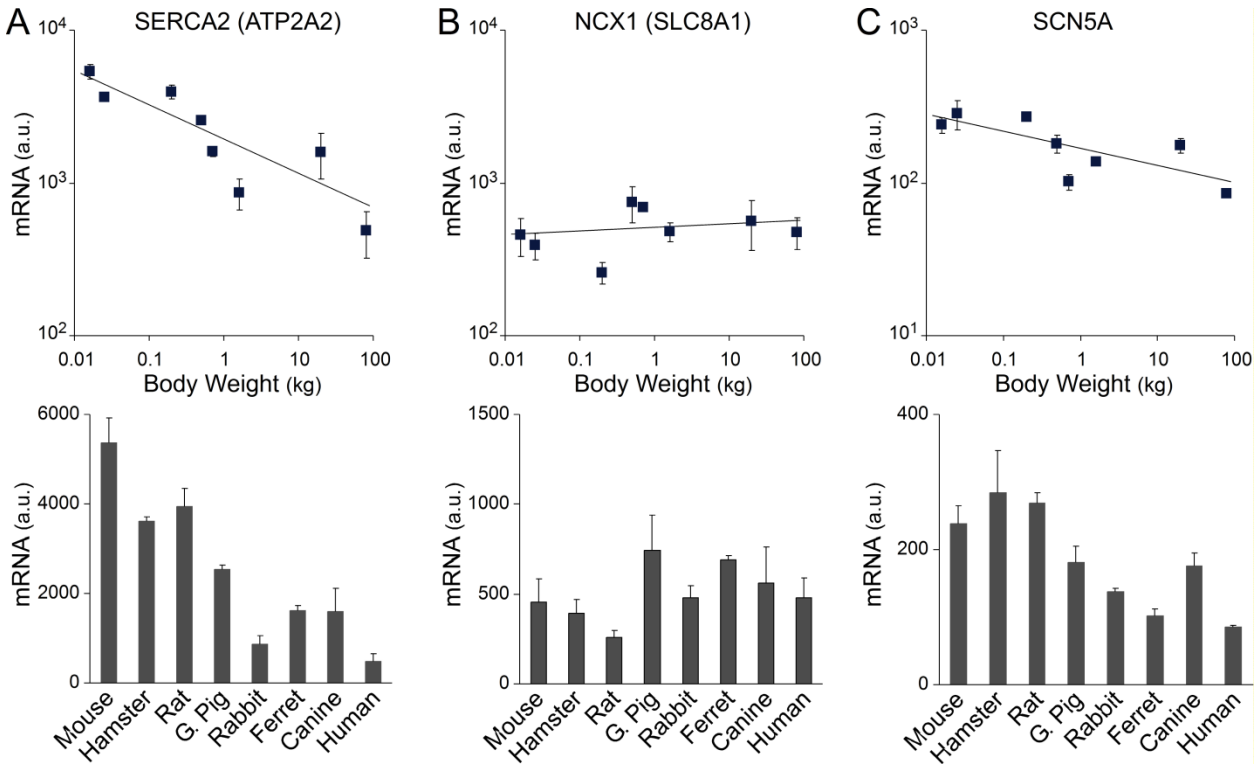

Figure 7. Comparison of SERCA2, NCX1 and SCN5A mRNA expression in the left ventricular wall of eight mammalian species.

Upper panel shows dependence on body weight and lower panel shows the same data replotted as histograms (means ± S.D., n = 3). (A) Dependence of SERCA2 (*ATP2A2*) mRNA expression levels on body weight (scaling coefficient $b = -0.25 \pm 0.03$). (B) Dependence of NCX1 (*SLC8A1*) mRNA expression levels on body weight (slope of fitted line was not significantly different to zero). (C) Dependence of SCN5A mRNA expression levels on body weight (scaling coefficient $b = -0.11 \pm 0.02$).

Constraints on Cardiac Ion Channel Sequence

Comparisons of the deduced amino acid sequence of the mouse and human voltage gated sodium, calcium and potassium channels, the calcium-activated and inward rectifier potassium channels and the HCN channels are shown in Figure 8. The majority of them have a sequence identity above 90%, suggesting the amino acid sequences of these proteins are highly constrained. The average percentage change in amino acid sequence identity for all channels in the figure is 7.1%. There is no evidence that the channels involved in the scaling ventricular myocyte electrophysiology have an unusually high rate of sequence change (Fig. 8). The specific values of their sequence identity are listed in table 1.

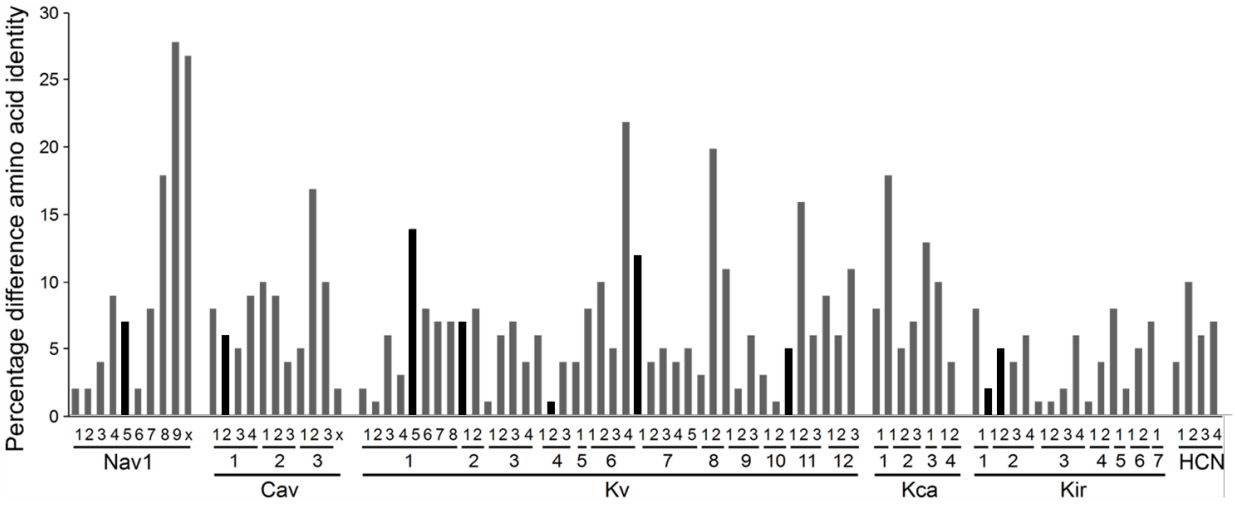

Figure 8. Sequence comparison between mouse and human of the major ion channel genes expressed in the cardiac electrophysiological system

Percentage differences in amino acid identity in the following groups of proteins (labeled under the x-axis): voltage gated sodium, calcium and potassium channels, the calcium-activated and inward rectifier potassium channels and the HCN channels. Channels mentioned in this chapter are marked by black bars.

DISCUSSION

Despite the large number of studies on the physiology and molecular biology of cardiac myocyte electrophysiology, this is the first study on the mechanisms by which cardiac electrophysiology evolves within the mammalian lineage. There are two basic ways in which the electrophysiological properties of any electrically excitable cell can evolve, either by changes in channel and transporter expression levels or by changes in protein sequence and function. Although these are not mutually exclusive alternatives, the results described in this chapter suggest that regulation of expression levels is the primary means by which ventricular electrophysiological function has been modified during the course of mammalian evolution.

Evolution of Action Potential Morphology

Mammalian ventricular myocytes can display one of two different action potential morphologies: either a spike and dome morphology or a triangular morphology. The spike and dome action potential morphology, which is observed in most mammals, is evolutionarily ancient. The I_{Ks} and I_{Kr} channels, which produce action potential repolarization in these species, are also the major repolarizing currents in the hearts of non-mammalian vertebrates, which have similar spike and dome action potential morphologies (Hume et al. 1986; Vornanen et al. 2002). Expression of either I_{to} or I_{Kur} has not been described in the ventricular myocytes of non-mammalian vertebrates. The triangular waveform appears to be an innovation that is restricted to small rodents with very rapid heart rates and reflects the acquisition of a novel trait in these species. The shift to the triangular waveform morphology is produced by the increased expression of two rapidly activating potassium currents, I_{to} and I_{Kur}. The experimental evidence

presented in this chapter suggests that the switch in this particular physiological trait is due primarily to regulatory evolution modifying the expression of the Kv4.2 and Kv2.1 genes, with little or no role for structural evolution in determining this trait. It has been shown previously that artificially increasing Kv4 α-subunit mRNA expression is, by itself, sufficient to produce the expected change in action potential morphology (Hoppe et al. 2000; Zobel et al. 2002).

The analysis of Kv4.2 and Kv2.1 proximal promoter function described in this chapter suggests that the evolution of *cis*-regulatory function is likely to be the predominant factor contributing to the changes in Kv4.2 and Kv2.1 gene expression seen in small mammals. However, a role for changes in transcription factor network function cannot be excluded without a complete analysis of the expression levels of the transcription factors that are important for regulating expression of these genes, which currently remain, in large part, unknown.

Evolution of Action Potential Duration

The evolution of action potential duration is a complex phenomenon, involving a relatively large number of different genes (shown in part in Table 1). In addition, the trait grades smoothly across the entire mammalian phylogeny and requires a complex set of changes including graded changes in the expression of multiple genes, in addition to the "on" or "off" changes in Kv2.1 and Kv4.2 gene expression. The complex nature of this evolution is illustrated by the paradoxical changes in calcium channel expression, with expression levels of this current being primarily constrained by the role of this current in excitation-contraction coupling rather than in regulating action potential duration.

Scaling of action potential duration does not appear to require significant changes in the function of any of the main proteins controlling cellular electrophysiology. The coding regions of ion channel and transporter genes are highly conserved in mammals and the number of voltage-gated ion channel genes is unchanged within the mammalian lineage, with no known loss or gain of ion channel α-subunit genes (Moulton et al. 2003; Yu et al. 2005; Demuth et al. 2006) (Fig. 8). Comparisons of the deduced amino acid sequences of the channels and transporters that contribute to the electrophysiological phenotype of ventricular myocytes are shown in Figure 8 and Table 1. For those genes that are functionally important in all mammals, there is no evidence for significant changes in the functional properties of their protein products. The function of the cardiac sodium channel (I_{Na}) is generally assumed to be invariant across mammalian phylogeny (Pandit et al. 2001) and the function of the inward rectifier (I_{K1}) is unchanged from similar currents found in simple invertebrates (Hagiwara et al. 1976). For the calcium current, as described in this chapter, there are minor changes in the biophysical function of the channel, but these changes do not contribute in any obvious way to the changes in action potential duration. The sequence of the calcium channel α-subunit is highly conserved for such a large protein containing several loosely structured regions (Table 1) and the minor changes in the biophysical function of this channel may reflect changes in the stoichiometry of the accessory subunits associated with the main subunit. For the Ca^{2+}-ATPase, its key functional property, the specific activity of the pump, is unchanged across mammalian phylogeny (Hamilton and Ianuzzo 1991; Hove-Madsen and Bers 1993; Su et al. 2003; Vangheluwe et al. 2005) whereas its expression levels change significantly.

As described in the results, there was no significant change in the function of the I_{Ks} and I_{Kr} channels, which control action potential repolarization in larger mammals. The increase in

KCNQ1 and KCNH2 mRNA expression is consistent with the increased current expression in guinea pig myocytes (Lu et al. 2001), although it is likely that other channel subunits also regulate the expression of these currents. Of the channels that are important for action potential repolarization in small mammals, only the Kv1.5 gene is less than 94% identical in mouse-human sequence comparisons. The relevant comparison for these channels, however, is within the subset of small mammals where these channels are expressed, and in this case sequence identity is much higher (Table 1).

Taken together, the evidence suggests that regulatory evolution is predominant in the evolution of action potential duration in the ventricular myocytes of mammals. A similar conclusion has been made for the evolution of a non-mammalian electrophysiological system, the giant axon of squid (Rosenthal and Bezanilla 2002). This conclusion does not exclude the possibility that one or more channels shows some gene encoded change in functional properties but clearly the major thrust of evolutionary mediated modifications is at the level of channel expression.

Whether the graded changes in expression seen for multiple genes, including KCNQ1, KCNH2, SCN5A and SERCA2, primarily reflect *cis*-regulatory evolution, as seems most likely for the Kv2.1 and Kv4.2 genes, remains an open question. There are quantitative changes in transcription factor gene expression in the ventricular myocytes from different mammalian species (Rosati et al. 2006), possibly reflecting evolution of the cardiac regulatory network within the mammalian lineage. Determining whether changes in the transcription factor network contribute to the graded changes in ion channel and transporter gene expression will require a more detailed understanding of the regulation of the relevant genes.

Table 1. Comparison of Cardiac Channel and Transporter Deduced Amino Acid Sequences

Universally important for mammalian ventricular myocyte function

Current or Transporter	Primary Subunit	Sequence Identity Human-Mouse
I_{Na}	SCN5A	94
$I_{Ca,L}$	$Ca_V1.2$ (CACNA1C)	94
I_{K1}	Kir2.1 (KCNJ2)	98
I_{K1}	Kir2.2 (KCNJ12)	96
Ca^{2+}-ATPase	SERCA2 (ATP2A2)	99
Na-Ca exchanger	NCX1 (SLC8A1)	95

Functionally important only in larger mammals

		Human-Mouse	Human-Guinea Pig
I_{Ks}	KCNQ1	90	91
I_{Kr}	KCNH2	96	96

Functionally important only in small mammals

		Human-Mouse	Rat-Mouse
$I_{to,f}$	Kv4.2 (KCND2)	99	100
I_{Kur}	Kv2.1 (KCNB1)	94	97
I_{Kur}	Kv1.5 (KCNA5)	86	96

CONCLUSIONS

The evolution of ventricular myocyte electrophysiology appears to conform, in broad outline, to the principles derived from the study of developmental system evolution (Carroll 2005; Carroll et al. 2005; Wray 2007). In particular, differences in the functional properties of ion channels and transporters appear to be relatively small compared to the multiple, relatively large changes in channel and transporter expression levels. As demonstrated in this chapter, action potential repolarization and calcium handling evolve in mammals primarily by changes in the level of expression of the relevant ion channels and transporters, in general agreement with the concept that regulatory evolution is the predominant mechanism underlying the evolution of complex multicellular organisms. Although this issue is confused in the physiological and modeling literature, because multiple and shifting combinations of gene products can contribute to single physiologically identified currents, future efforts in this area should benefit from a recognition of the relative unity of the molecular underpinnings of mammalian cardiac electrophysiology.

Chapter 3

Evolution of CpG Island Promoter Function Underlies Changes in KChIP2 Potassium Channel Subunit Gene Expression in Mammalian Heart

INTRODUCTION

The large differences in body mass amongst mammals require significant changes in heart rate and ventricular action potential duration in order to scale cardiac physiological function to body mass (Schmidt-Nielsen 1984; Rosati et al. 2008). These changes in cardiac function are produced by systematic changes in myocyte electrophysiological function and in the pattern and level of expression of multiple voltage-gated ion channels and transporters (Rosati et al. 2008). Some of the most prominent changes are seen in the changing role of the transient outward potassium current (I_{to}). The I_{to} current is a rapidly activating and inactivating current that is expressed in the ventricular myocytes of most, but not all, mammalian hearts (Niwa and Nerbonne 2010). Expression of this current in heart appears to be an innovation of mammals. This current has not been described in the hearts of non-mammalian vertebrates. An essentially identical current (known as I_A) is, however, expressed in the brains of most vertebrate and many invertebrate species (Covarrubias et al. 2008). A subset of the genes that encode the neuronal I_A current in mammals have been co-opted for I_{to} expression in heart (Rosati et al. 2008; Niwa and Nerbonne 2010).

The ventricular action potential in most non-rodent mammals has a 'spike and dome' morphology, with a long plateau phase before action potential repolarization. In these species, I_{to} modifies the early phase of action potential morphology, altering the initial rate of calcium ion entry and the strength of myocyte contraction (Dong et al. 2010). The I_{to} channel is comprised of an α-subunit encoded by the Kv4.3 gene (KCND3) and an auxiliary subunit encoded by the KChIP2 gene (KCNIP2) in these species (Niwa and Nerbonne 2010). Differences in I_{to} and KChIP2 expression within the ventricles (Antzelevitch et al. 1999; Rosati et al. 2003) contribute

to regional differences in ventricular contractility and coordination of ventricular contraction (Dong et al. 2010). The broad phylogenetic distribution of this particular pattern of I_{to} gene expression (Niwa and Nerbonne 2010) suggests that it was established early in mammalian evolution.

I_{to} and KChIP2 expression varies significantly from the common mammalian pattern in some rodents. In guinea pig, I_{to} expression (Findlay 2003) and KChIP2 expression has been lost, although the action potential is similar in most other respects to other non-rodent mammals. In contrast, mouse and closely related species express I_{to} at very high levels. In these species the ventricular action potential is very short with a triangular waveform (Pandit et al. 2001; Rosati et al. 2008; Niwa and Nerbonne 2010), due to the large size and rapid activation of the I_{to} current. The short action potential duration and altered morphology contribute to the scaling of ventricular action potential duration (Rosati et al. 2008). In mouse and related species, I_{to} is encoded by both Kv4.3 and a second alpha subunit gene Kv4.2, which is only expressed in the hearts of this subset of rodents (Rosati et al. 2008). Cardiac Kv4.2 gene expression is produced by evolutionarily mediated changes in the *cis*-regulatory function of the Kv4.2 gene in these species (Rosati et al. 2008). There is a complementary increase in KChIP2 gene expression in these species that also contributes to increased I_{to} expression.

Despite complex biosynthetic pathways, voltage gated ion channel expression in heart is primarily determined by the level of channel gene transcription (Rosati and McKinnon 2004; Chandler et al. 2009). The size of the I_{to} current is directly dependent upon the level of KChIP2 gene expression (Kuo et al. 2001; Rosati et al. 2003). The large changes in KChIP2 gene expression in mammalian heart and compact gene structure make it a favorable model in which to study the contribution of *cis*-regulatory evolution to the evolution of physiological function in

mammals. The results presented in this chapter demonstrate that the KChIP2 gene contains a CpG island promoter that is not simply permissive for gene transcription but also contributes significantly to the tissue specificity of gene expression and is a primary locus for the evolution of KChIP2 gene expression patterns in mammalian heart.

MATERIALS AND METHODS

Analysis of KChIP2 and Luciferase mRNA Expression

Analysis of mRNA expression in left ventricle wall was performed using real-time PCR as described in *Chapter 2*. Animals were euthanized and the hearts were quickly removed before further dissection. Human RNA samples were obtained from two independent commercial suppliers (Ambion and BioChain). For luciferase mRNA quantitation, rat neonatal myocytes were isolated, transfected and cultured for 48 hours, as described below. After culture, cells were lysed by adding RLT buffer and passing the lysate over a Qiashredder column (Qiagen, Novato, CA). Total RNA was prepared from tissues and cells using Qiagen RNeasy columns with DNase treatment. RNA samples were quantitated, re-diluted to give nominally equal concentrations and quantitated a second time using spectrophotometric analysis.

cDNAs were prepared from a starting RNA amount of 5 μg per sample. *In vitro* reverse-transcription was performed using Superscript III reverse transcriptase (Invitrogen), as described previously (Rosati et al. 2004). Real-time PCR was performed using the SYBR Green QuantiTect PCR Kit (Qiagen) with a 7300 Real-time PCR System (Applied Biosystems). Experimental samples were analyzed in triplicate. Threshold crossing points were converted to expression values automatically (Larionov et al. 2005). Real-time PCR products were analyzed by gel electrophoresis and sequenced to confirm specificity of the amplification. Gene expression across RNA samples was normalized using 18S and 28S rRNAs as internal controls.

Multiple (typically three) primer pairs were used to analyze expression in order to detect primer dependent artifacts. The results from each primer pair were averaged. Primer sequences used for real-time PCR are listed in Table 1.

Table 1. Real-time PCR Primers

Gene	Pair#	Sequence (5’ to 3’)
18S	1	CCTGCGGCTTAATTTGACTC (fwd)
		CGGACATCTAAGGGCATCAC (rev)
	2	GTTCCGACCATAAACGATGC (fwd)
		AACTAAGAACGGCCATGCAC (rev)
	3	CCCGAAGCTTTACTTTGAA (fwd)
		GCATCGTTTATGGTCGGAAC (rev)
28S	1	TGGGTTTTAAGCAGGAGGTG (fwd)
		TCCTCAGCCAAGCACATACA (rev)
	2	AAAGGGAGTCGGGTTCAGAT (fwd)
		AGAGGCTGTTCACCTTGGAG (rev)
	3	TCCGAAGTTTCCCTCAGGAT (fwd)
		CCTTTTCTGGGGTCTGATGA (rev)
KChIP2	1	GAATGTCCCAGCGGAATTGT (fwd)
		AGCCATCCTTGTTGAGGTCATA (rev)
	2	TCTCTTCAATGCCTTTGACACC (fwd)
		CTTGTTCCTGTCCATCTTCTGGA (rev)
	3	CAGTTTTGAGGACTTTGTGGCT (fwd)
		TGCATGGACCTCATGATGTTC (rev)
	4	TATGACCTCAACAAGGATGGCT (fwd)
		TAGATGACATTGTCAAAGAGCTGC (rev)
Luciferase	1	TGGCAGAAGCTATGAAACGA (fwd)
		CATCGACTGAAATCCCTGGT (rev)
	2	ACGCCTTGATTGACAAGGAT (fwd)
		TCGCGGTTGTTACTTGACTG (rev)
	3	TTCCATTCCATCACGGTTTT (fwd)
		CGTATCCCTGGAAGATGGAA (rev)

BAC Library Screening

BAC clones encompassing the KChIP2 proximal promoter regions of guinea pig and hamster were identified in BAC libraries (BACPAC Resources Center, CHORI, Oakland, CA) using a non-radioactive probe labeled with Digoxigenin-11-dUTP (DIG-11-dUTP alkali-labile, Roche). Probe sequences were based on cDNA sequences or conserved regions from multiple species. A 40-base pair double-stranded DNA probe was synthesized using two 24-mer oligonucleotides with overlapping 3'ends (5'GGAGCCGTCGAGATCTCGAGAGTC 3' and 5'TAAGGAGAGTTTGTCCGACTCTCG 3'), using Klenow fragment DNA Polymerase and a mixture of dNTPs and DIG-dUTP. Hybridization was carried out using buffers optimized for DIG labeled probe (DIG Easy Hyb, Roche). Signals were developed using immunological detection method with anti-DIG-AP, Fab fragments (Roche) and CDP-Star (Roche). Positive BAC clones identified from the screening were then obtained from the BACPAC Resources Center. The BAC clones were analyzed by fingerprinting, end sequencing and finally sequencing of the specific region of interest.

Isolation, Subcloning and Sequencing of Genomic DNA Regions

For human, mouse, rat and guinea pig, initial selection of genomic fragments was based on sequences from genome databases (Homo sapiens Build 36 for the human, Mus musculus Build 36 for the mouse, Rattus norvegicus RGSC v3.4 for rat, Cavia porcellus Broad/cavPor3 Assembly for the guinea pig). Human and mouse BAC clones containing the KChIP2 proximal promoter region were obtained from the BACPAC Resources Center (CHORI). For the rat, genomic DNA was used as a template to amplify the region of interest.

The genome sequences of the remainder mammalian species were not available. For hamster, the specific KChIP2 DNA fragment was isolated from the BAC clone by a combination of restriction mapping and southern blotting and then subcloned into pBluescript SK. For Petromyscus (rock mouse), Anomalurus beecrofti (Beecroft's flying squirrel), Dipodomys heermanni (Heermann's kangaroo rat) and Tamias striatus (eastern chipmunk), the specific KChIP2 DNA fragments were isolated from genomic DNA by PCR amplification using a pair of primers designed at highly conserved regions around the KChIP2 proximal promoter region and then subcloned into pBluescript SK. The KChIP2 sequences of these species were obtained from sequencing these intermediate subclones and were confirmed by sequencing multiple independent isolates.

Comparisons of the KChIP2 proximal promoter sequences were performed using the Vista (Frazer et al. 2004) and ClustalW (Larkin et al. 2007; Goujon et al. 2010) alignment programs. Conserved regions were used as landmarks to select orthologous sequences, although these were not exactly identical in length. All sequences terminated immediately before the initiator methionine in the first exon of the KChIP2 gene. The lengths of DNA fragments for the KChIP2 proximal promoter region were: 2,256 bp (mouse), 2,596 bp (guinea pig) and 2,760 bp (human). The lengths of DNA fragments for the KChIP2 CpG island region were: 453 bp (mouse), 457 bp (rat), 454 bp (hamster), 443bp (Petromyscus), 463 bp (Anomalurus), 436 bp (Dipodomys), 395 bp (guinea pig), 462 bp (Tamias) and 457 bp (human).

Genomic regions were obtained using high fidelity PCR amplification with either Expand Long Template PCR system (Roche) or Platinum Pfx DNA polymerase (Invitrogen), subcloned into the pGL2 luciferase reporter vector (Promega) and confirmed by sequencing.

Transcription Start Site (TSS) Mapping by RNA Ligase-Mediated RACE PCR

The transcription start site of the KChIP2 gene was mapped in mouse, guinea pig and human with the RNA Ligase Mediated RACE PCR technique (Maruyama and Sugano 1994) using the Ambion First Choice RLM-RACE Kit (Applied Biosystems, Carlsbad, CA). Guinea pig brain and mouse brain and heart RNA were prepared as described previously (Rosati et al. 2008). Human brain and heart RNA were obtained from commercial suppliers (BioChain and Ambion, respectively).

Briefly, 10 μg of total RNA were ethanol-precipitated and treated with Calf Intestine Alkaline Phosphatase (CIP) to remove the terminal 5' phosphate group from degraded and uncapped RNAs. The samples were purified by phenol/chloroform and chloroform extraction, precipitated with isopropanol and finally treated with Tobacco Acid Pyrophosphatase (TAP) to remove the mRNA cap structure. An aliquot of the RNA sample was not treated with TAP and kept as a negative ('TAP-minus') control. An adapter was then ligated to the 5'-end of the RNA molecules using T4 single strand RNA ligase. The previous CIP treatment step prevents adapter ligation to degraded/uncapped RNA molecules and ligation to capped RNAs cannot occur without removal of the cap structure. The ligated RNA was reverse transcribed at 50 ℃ using M-MLV Reverse Transcriptase and gene-specific primers (Table 2), The cDNAs obtained were then subjected to a first round of nested PCR (primers listed in Table 3). A second round of PCR (inner PCR) was performed by using 2 μl of the first PCR reaction as template, and 3' primers (Table 4). The inner PCR reactions were purified using the Qiaquick PCR Purification kit (Qiagen), subcloned into pBluescript SK and sequenced.

Table 2. Reverse transcription gene-specific primers

Mouse: 5’CGCTGGGACATTCGTTCTTGAA 3’, 5’GCGTAGTTGCTGGAGTCTCCTTG 3’

Guinea Pig: 5’ GCATAGGTGCTAGAGTCTCCTTGAGG 3’

Human: 5’ TGCGCGTGAATTTGGTTTGC 3’, 5’AGGTGCTGGAGTCTCCTTGA 3’

Table 3. First round nested PCR primers

Mouse: 5’ AGGATAGGGCGCTCACACA 3’,
5’TCAGGGCTTTTTTACTGGGC 3’

Guinea Pig: 5’ GGACAAGGCGCTTGCTCAAAC 3’,
5’TCAGCGCTTTTTTAGTGGGC 3’

Human: 5’GCGCTCGAGTACTGTGCTGTCGGGGCT 3’,
5’GCGCTCGAGAAACTCTCCTTGCGGCCCTG 3’

Table 4. Second round nested PCR primers

Mouse: 5’GCGGAATTCAGCGACCTGCTGGGGCT 3’,
5’GCGGAATTCATAGGAGCCGTCCAAATCTC 3’

Guinea Pig: 5’GCGGAATTCTGAAGAGCCGAGGGGTCGT 3’,
5’ GCGGAATTCCGTAGGAGCCGTCGAGATCTC 3’

Human: 5’GCGCTCGAGTACTGTGCTGTCGGGGCT 3’,
5’GCGCTCGAGAAACTCTCCTTGCGGCCCTG 3’

Neonatal Myocyte Transfection, Culture and Luciferase Assay

Rat cardiac myocytes were isolated from P2-P3 animals and cultured as described previously (Yin et al. 2004). Ferret cardiac ventricular myocytes were isolated from E34 animals using the same procedure and then handled similarly to the rat myocytes. Cell transfection was performed using the Rat Cardiomyocyte Nucleofector Kit (Amaxa, Lonza, Walkersville, MD) in a Nucleofector I device (Amaxa). Each sample included an internal control Renilla luciferase plasmid (phRL-SV40). Experiments always included a negative control sample (pGL2-basic), and a positive control (pGL2-control) when appropriate. After electroporation the myocytes were plated onto fibronectin-gelatin coated 12-well plates and cultured at 37 ℃ in 5% CO_2 for 48 hours. Firefly and Renilla luciferase activities were measured using the Dual Luciferase Reporter Assay Kit (Promega) in a Lumat luminometer (Berthold).

RESULTS

Expression of the KChIP2 Gene in Cardiac Ventricle

KChIP2 mRNA expression in the left ventricular wall of hearts from six different species was determined (Fig. 1A). KChIP2 mRNA was expressed at moderate levels in non-rodent mammals. Expression was high in mouse and rat, consistent with the high level of I_{to} expression in these species (Rosati et al. 2008; Niwa and Nerbonne 2010). There was an almost complete absence of KChIP2 expression in the guinea pig ventricle, concordant with the lack of I_{to} expression in this species (Findlay 2003).

KChIP2 gene regulatory function was initially analyzed in three species: mouse, representative of small rodents that have a large I_{to}; guinea pig, a rodent that lacks significant KChIP2 and I_{to} expression; and human, representative of the majority of mammals that have a relatively small but functionally important I_{to}.

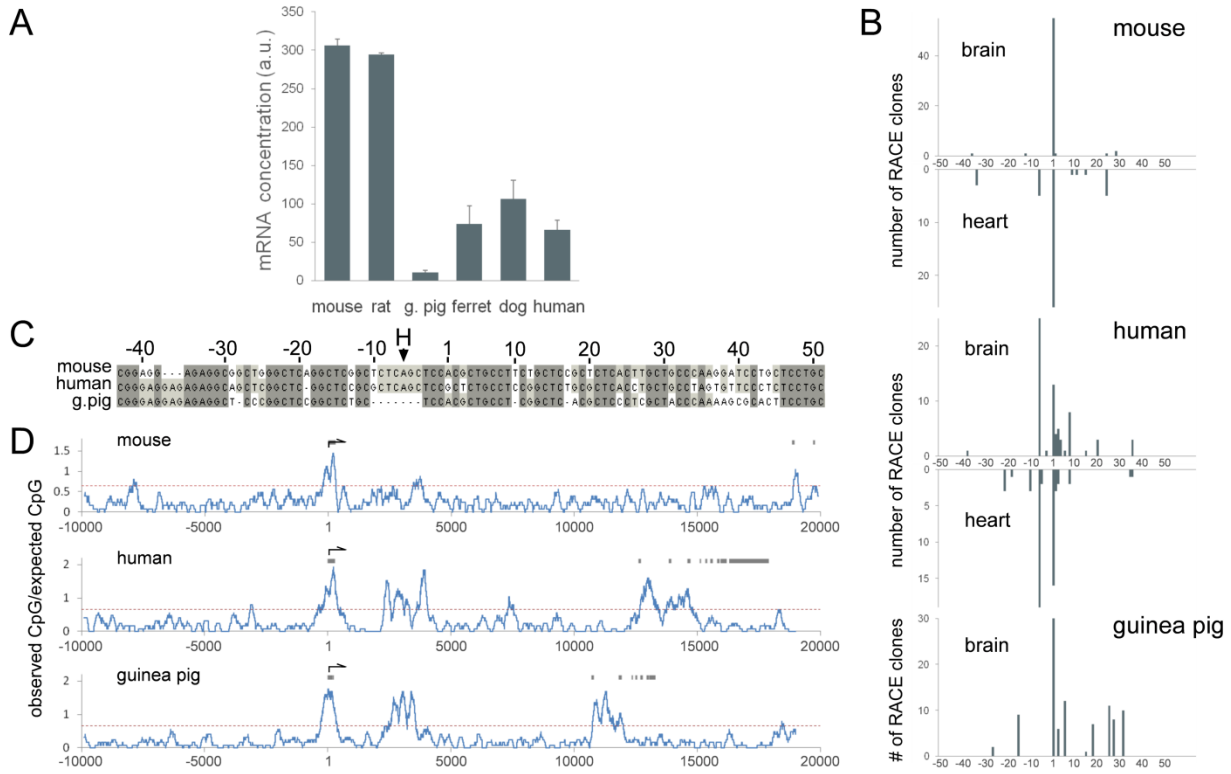

Figure 1. KChIP2 mRNA expression and transcription start site mapping.

(A) Comparison of KChIP2 (KCNIP2) mRNA expression in the left ventricular wall of six mammalian species. Histogram shows means ± S.D. (N = 3). (B) Mapping of the KChIP2 transcription start sites using mouse and human heart and brain mRNA and guinea pig brain mRNA. The y-axis indicates the number of RACE PCR clones that were sequenced and mapped to the respective nucleotide position indicated on the x-axis. (C) Alignment of mouse, human and guinea pig sequences encompassing the transcription start sites shown in (B). Numbering of the x-axis is relative to the primary transcription start site (+1) in mouse and guinea pig and the second most common start site in human. The primary TSS in human is marked with an 'H'. (D) Analysis of CpG frequency around the KChIP2 transcription start site of the mouse, human and guinea pig genes. The standard threshold for CpG island prediction ($observed_{CpG}$ /$expected_{CpG}$ >0.65) (33) is marked with a dashed red line. The lower CpG frequency in the mouse KChIP2 gene and the loss of apparently non-functional CpG islands is reflective of genome-wide trends in this species (34). The transcription start site was aligned for all three species and is marked by an arrow. The exons are marked by grey bars. At the most commonly used TSS in each species, the [-1,+1] dinucleotide was C:A, a pyrimidine:purine pair, which conforms to the consensus at this location (13). In the human the second most commonly used site, equivalent to the primary site in mouse and guinea pig, was also a pyrimidine:purine pair, although in this case a C:G pair. The plots use a 200-bp window to calculate obs_{CpG}/exp_{CpG}.

KChIP2 Transcription Start Site Mapping

The transcription start site (TSS) for the KChIP2 gene was mapped in mouse and human heart and brain and guinea pig brain (Fig. 1B). Mapping of the TSS in guinea pig heart was not attempted due to the very low level of transcripts in this tissue. In the mouse, transcription was initiated primarily at a single primary transcription start site. The human and guinea pig transcription start sites were more dispersed. Multiple transcription start sites were found in these species, although they were restricted to a relatively small region. Notably, for both mouse and human, the same transcription start sites are used in heart and brain, indicating that the same promoter is used in both tissues.

The sequence around the transcription start site of the three species is generally well conserved, although it contains some small deletions (Fig. 1C). The transcription start sites for all three species are located within a CpG island (Fig. 1D) and the promoter region in all three species has the typical properties of a CpG island promoter (Sandelin et al. 2007). In particular, this region lacks a consensus TATA box or BRE, Inr and DPE elements with the expected relationship to the transcription start site (Smale and Kadonaga 2003). The highly focused nature of the mouse TSS is relatively unusual for this class of promoters, with the human and guinea pig TSS patterns being more typical (Sandelin et al. 2007).

Comparison of KChIP2 Proximal Promoter Function and mRNA Expression

The KChIP2 gene is located within a gene-rich region of chromosomes 19 and 10 in mouse and human, respectively. The gene is closely bounded in the 5' direction by another transcription unit (C10orf76), resulting in a relatively compact upstream regulatory region.

Equivalent, approximately 2.5 kb, 5' intergenic regions containing the core promoter were selected from mouse, guinea pig and human genomic sequences and then tested using an *in vitro* transcription assay in cultured rat myocytes. There was a good correspondence between the function of this region and the relative level of mRNA expression in cardiac ventricles from the corresponding species (Fig. 2A and B), suggesting that this region was likely to make a primary contribution to the species differences in KChIP2 transcriptional function in heart.

The presence of 5'UTR sequence in the constructs raised the possibility that some of the differences in reporter gene expression between the different species could be due to differences in the translational efficiency of the transcribed mRNAs. To test this possibility, transcription from the reporter genes was measured directly using real-time PCR (Fig. 2C). The species differences in transcriptional activity were maintained when assessed directly from mRNA levels.

The transcription activity assays were performed using cultured rat myocytes. The use of this culture system assumes that the evolution of KChIP2 *cis*-regulatory function is fast relative to any potential evolutionarily mediated changes in transcription factor network function. This assumption is consistent with the fact that, with the exception of cellular electrophysiology, myocyte morphology and function are generally very well conserved in mammals (Rosati et al. 2008). The observation that the mouse, guinea pig and human KChIP2 promoter activity matches relative mRNA abundance rather than the degree of phylogenetic relatedness to the cell culture system also supports this assumption (Fig. 2A and B).

The effect of cell species is directly tested using cultured ferret embryonic ventricular myocytes. Ferret is an out-group relative to Euarchontoglires (the superclade containing mouse, guinea pig and human) and both KChIP2 mRNA (Fig. 1A) and I_{to} (Patel and Campbell 2005) are

expressed in ferret heart at similar levels to that seen in human. The differences in mouse, guinea pig and human KChIP2 transcriptional activity are retained in the ferret cultures (Fig. 2D) and are independent of both the species (ferret versus rat) and developmental stage (embryonic versus neonatal) of the culture system. This observation supports the general hypothesis that *cis*-regulatory function is the primary mechanism responsible for changes in ion channel expression in heart and that transcription factor function and expression remain relatively invariant in mammalian heart (Rosati et al. 2008).

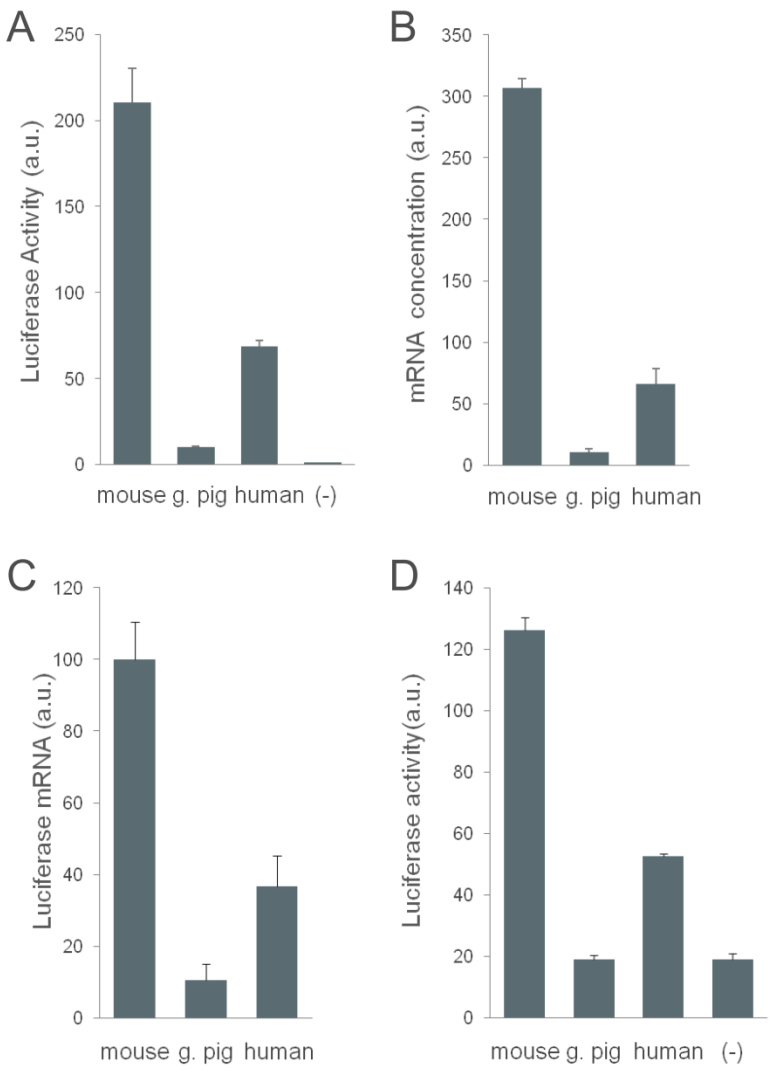

Figure 2. KChIP2 proximal promoter function matches with mRNA expression.

(A) Comparison of mouse, guinea pig and human KChIP2 proximal promoter region activity using an *in vitro* transcription assay in neonatal rat cardiomyocytes. (B) Expression of KChIP2 mRNA in the left ventricle of mouse, guinea pig and human heart. The data are replotted from Figure 1A to aid comparison. (C) Comparison of firefly luciferase mRNA abundance when driven from mouse, guinea pig and human KChIP2 proximal promoter region constructs. (D) Comparison of mouse, guinea pig and human KChIP2 proximal promoter activity in cultured embryonic ferret cardiomyocytes. Values for the negative control construct were relatively high compared to the rat cultures primarily because of the difficulty in obtaining large number of ferret myocytes for transfection. Error bars are SEM (N = 3-6).

KChIP2 Proximal Promoter Function

An alignment of the proximal promoter region from mouse, human and guinea pig shows that regions upstream of the CpG island are relatively poorly conserved (Fig. 3A). The conserved regions at the 5' end of this sequence are associated with the upstream genes transcription unit.

To isolate the regions responsible for the species differences in promoter function, a series of 5' deletions were performed (Fig. 3B). Increasingly large deletions had relatively little effect on both the absolute level of activity (Fig. 3C) and the relative level of activity (Fig. 3D) of promoter function for the three species.

Notably, even the shortest sequence, which encompasses the CpG island containing only the core promoter and 5’ UTR, retained most of the difference in expression between the mouse, human and guinea pig genes (Fig. 3C and D), suggesting that the primary differences between the species are located within the CpG island.

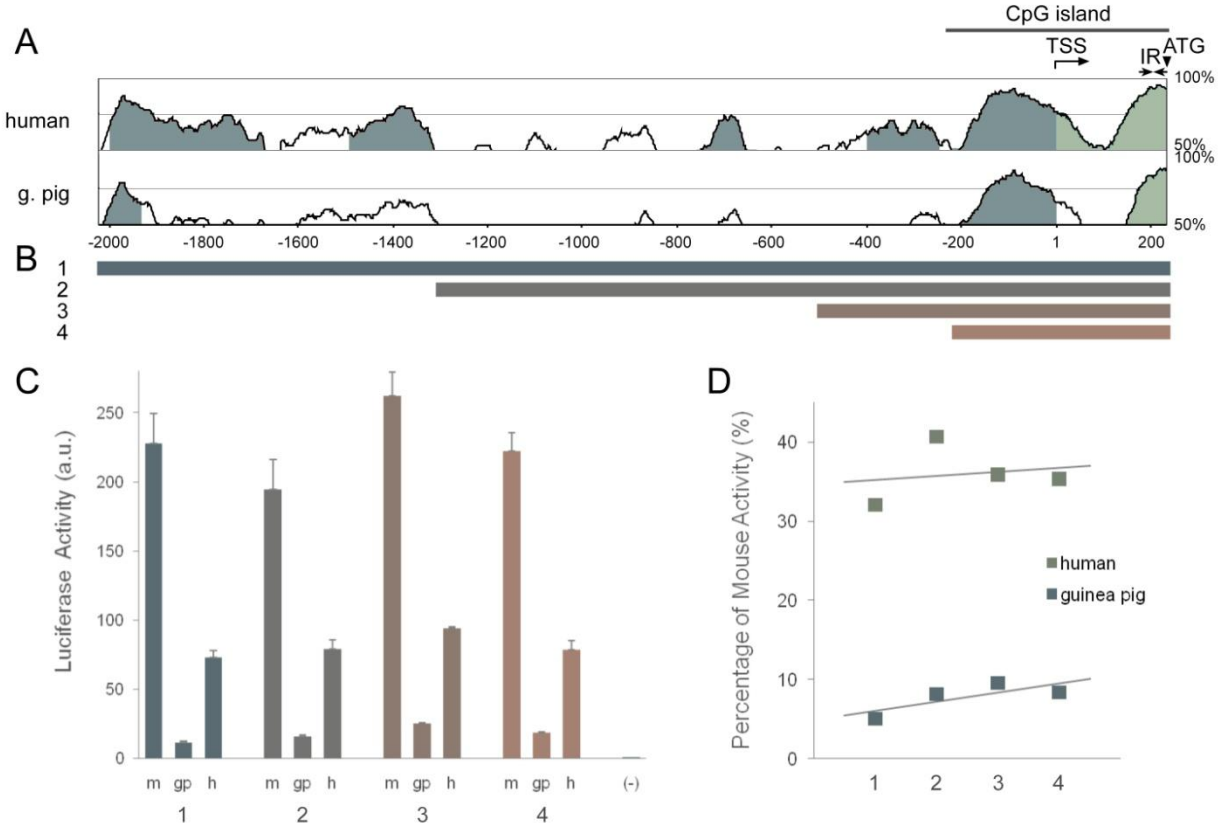

Figure 3. Dissection of KChIP2 proximal promoter function.

(A) VISTA alignment of the KChIP2 proximal promoter regions. Human and guinea pig were compared to mouse as the base sequence. Three features are marked, the C_PG island region, the transcription start site (TSS) and an inverted repeat in the 5' UTR (IR). The sequences end immediately upstream of the initiator methionine codon in exon 1 of the gene (ATG). Conserved sequences in VISTA (70%/100 bp cutoff) are colored according to the annotation (UTRs - light green and non-coding - dark green). (B) Clones used for 5' deletion analysis of the KChIP2 proximal promoter function. The colors of the bars representing the different length clones match the corresponding histogram bars in panel (C). (C) Comparison of transcriptional activity of mouse, guinea pig and human 5' deletion constructs. Error bars are SEM (N = 6). (D) Human and guinea pig promoter activity as a percentage of mouse promoter activity for the four clones.

Substitution of the CpG Island between Mouse and Guinea Pig

To further confirm that the CpG island region plays the predominant role in determining the species differences in promoter function, this region was swapped between the mouse and guinea pig proximal regulatory regions (Fig. 4A). Substituting the guinea pig sequence into the mouse background produced a more than 4-fold reduction in expression relative to the mouse sequence (Fig. 4B). The converse experiment produced a more than 8-fold increase in expression relative to the guinea pig sequence.

The upstream 5' regulatory region clearly modifies the activity of the CpG island to some extent, as seen by comparison of mouse to the guinea pig-mouse hybrid and guinea pig to the mouse-guinea pig hybrid (Fig. 4A and B). Nonetheless, it is clear that the CpG island is the major determinant of the species differences in KChIP2 promoter function.

Localization of Sequence Changes within the CpG Island Responsible for Changes in Functional Activity

A series of swaps between the mouse and guinea pig CpG island were performed in order to localize the sequences responsible for the differences in transcriptional activity. This region was divided into 4 domains (Fig. 4C): regions 'a' and 'b' correspond to roughly equal halves of the core promoter, with 'b' containing the transcription start site. Region 'c' corresponds to a poorly conserved region of the 5'UTR that is largely deleted in guinea pig and 'd' corresponds to a well conserved region of the 5'UTR that contains a conserved inverted repeat. Transcription assays showed that region 'd' did not contribute to the functional differences (Fig. 4C and D). The other three regions contributed approximately equally. Considerable effort was expended to

localize specific nucleotide changes responsible for these differences. Individual sequence changes had very modest effects on function, suggesting that the concerted effect of multiple changes are required to produce these differences in regulatory activity, as has been found in other systems (Frankel et al. 2011).

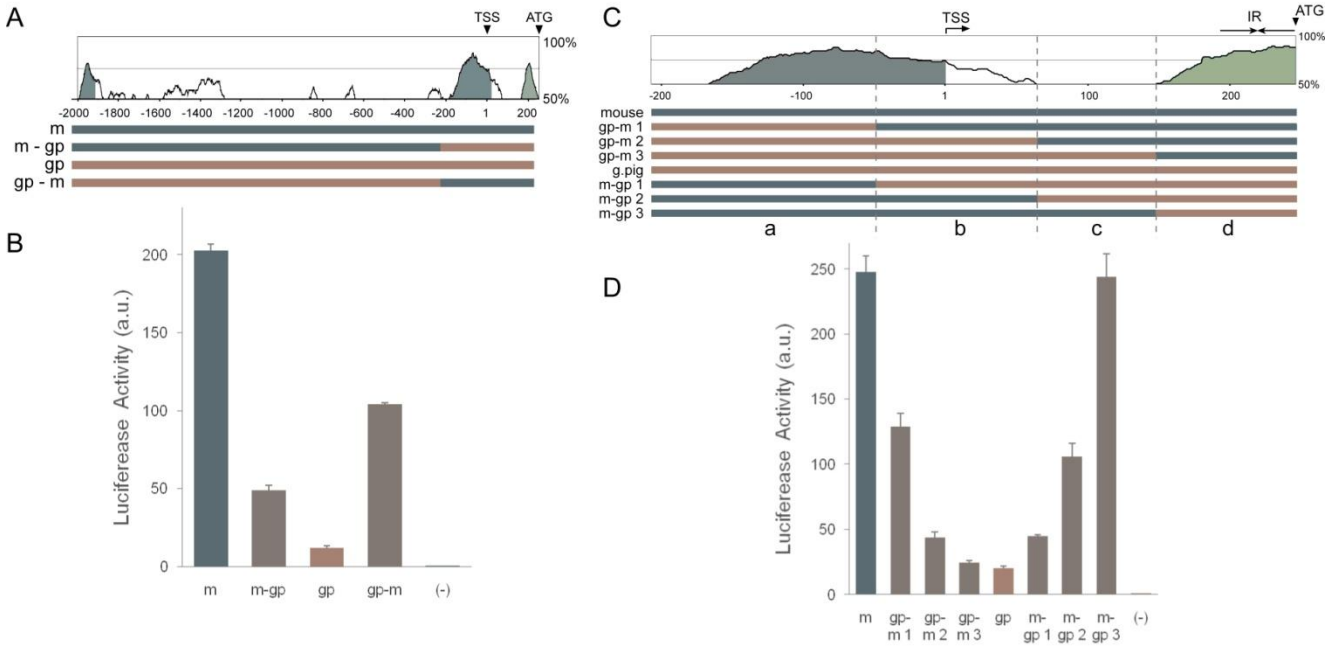

Figure 4. The CpG island core promoter is the major locus of evolution mediated changes.

(A) VISTA alignment of mouse and guinea pig KChIP2 proximal promoter regions (equivalent to clone 1 in Figure 3), with mouse as the base sequence. The colored bars underneath show the swap of CpG domains between mouse (teal) and guinea pig (tan). (B) Comparison of swapped regions in an *in vitro* transcription assay. Error bars are SEM (N = 3). (C) VISTA alignment of mouse and guinea pig KChIP2 CpG island (equivalent to clone 4 in Figure 3), with mouse as the base sequence. Four regions are marked 'a' and 'b' roughly split the core promoter in half, 'c' corresponds to a poorly conserved region of the 5'UTR that is largely lost in guinea pig and 'd' corresponds to a well conserved region of the 5' UTR that contains a conserved inverted repeat. The colored bars underneath show the swap of core promoter and 5'UTR domains between mouse (teal) and guinea pig (tan). (D) Comparison of swapped regions in an *in vitro* transcription assay. Error bars are SEM (N = 3).

Phylogenetic Comparison of KChIP2 CpG Island Promoter Function

Expression of KChIP2 varies most markedly in rodents. The function of the CpG island promoter from eight rodents and three non-rodents was compared (Fig. 5A). High KChIP2 promoter function appears to be phylogenetically restricted to mouse and closely related species. Most rodents have intermediate function, similar to the level seen in non-rodents. Very low KChIP2 promoter function was restricted to guinea pig and chipmunk (*Tamias striatus*).

KChIP2 Proximal Promoter Function in Neurons

Mouse, guinea pig and human KChIP2 proximal promoter function was tested in cultured rat cortical neurons. Mouse and human promoter function was indistinguishable in neurons (Fig. 5B). Guinea pig promoter activity in neurons was reduced to approximately 37% of the mouse and human level. This level was significantly higher than that seen in myocytes (Fig. 2A) but remains lower than mouse and human. There are no established species differences in I_A function in mammalian neurons and it is unlikely that KChIP2 expression in equivalent neurons varies significantly between these species.

The reduction in guinea pig KChIP2 promoter activity in neurons suggests that changes in a neuron-specific enhancer element may be required to compensate for the weaker promoter function in neurons. Such an element was not identified in functional tests using the large first intron.

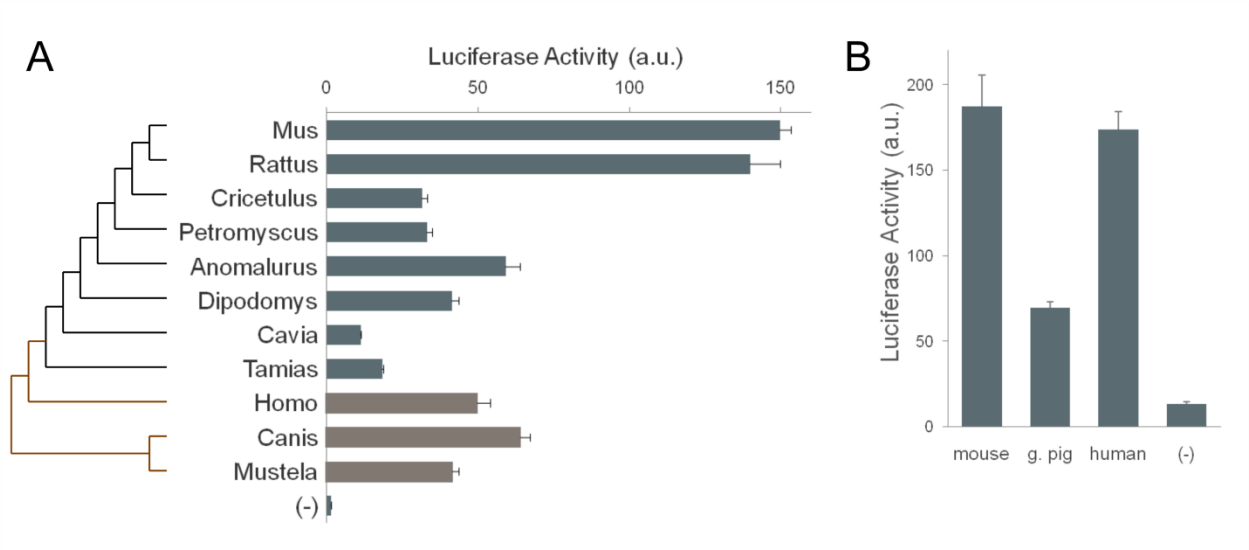

Figure 5. KChIP2 core promoter function in eight rodent species and proximal promoter function in neurons.

(A) Analysis of KChIP2 core promoter function in eight rodents (green bars) and three out-group species (brown bars): *Mus musculus*, *Rattus norvegicus*, *Cricetus cricetus* (hamster), *Petromyscus* (rock mouse), *Anomalurus beecrofti* (Beecroft's flying squirrel), *Dipodomys heermanni* (Heermann's kangaroo rat), *Cavia porcellus* (domestic guinea pig), *Tamias striatus* (eastern chipmunk), *Homo sapiens sapiens*, *Canis lupus familiaris* (dog), *Mustela putorius furo* (ferret). (B) Comparison of mouse, guinea pig and human KChIP2 proximal promoter activity in cultured rat cortical neurons. Error bars are SEM (N = 6-8).

DISCUSSION

The results reported here support the hypothesis that the large differences in the level of KChIP2 expression in mammalian heart are primarily due to evolutionarily mediated changes in the *cis*-regulatory function of the gene. This is demonstrated by the close match between KChIP2 mRNA expression and promoter function for different species and by the independence of the relative promoter function from the phylogenetic origin of the cultured cells in which functional promoter tests were performed.

Expression of the KChIP2 gene is primarily restricted to electrically excitable cells and this gene is expressed in both cardiac myocytes and a subset of neurons (Rosati et al. 2001; Xiong et al. 2004). Transcription in both brain and heart tissues is initiated from the same CpG island promoter. Surprisingly, a major locus of evolutionary change for KChIP2 gene expression in heart lies within this CpG island core promoter. The species differences in KChIP2 mRNA expression in heart were matched by similar differences in the functional activity of this relatively small CpG island promoter from the same species.

Prior studies on the evolution of *cis*-regulatory function have generally found that evolutionarily mediated changes in gene regulatory function were localized to tissue specific enhancer/repressor elements separate from the core promoter (Rebeiz et al. 2009; Chan et al. 2010). Evolution of these tissue-restrictive elements is considered an effective way to modify regulatory function in a tissue specific way, thereby limiting the pleiotropic effects of changes in gene regulatory function (Stern 2000). Evolution of KChIP2 regulatory function deviates from this pattern in that a major locus of change is the CpG island promoter itself.

The changes in regulatory function of the KChIP2 core promoter in cardiac tissue are, to some degree, tissue specific. For example, there are relatively large differences in mouse and human KChIP2 core promoter function in heart with essentially no difference in neuronal function. There are, however, limits to the tissue-specificity of these changes. In the more extreme case of guinea pig, where KChIP2 expression in cardiac myocytes is largely eliminated, there was a significant reduction in neuronal function, although this was not as extreme as the reduction seen in myocytes. It is possible that compensatory changes may occur in other regulatory regions of the guinea pig gene, although these were not identified. The results suggest that tissue selective changes in CpG island core promoter function are possible, although there are limitations in isolating the effect of these changes.

Approximately half of the tissue-restricted genes in mammals have CpG island promoters (Mohn and Schubeler 2009) and the KChIP2 gene is an apparently typical example of this class of genes. Results for the KChIP2 gene suggest that, at least for some of these tissue-specific genes, the CpG island promoter is not merely permissive for gene expression but can be a significant contributor to tissue selective expression. As such, for this class of promoters, the core promoter may itself be an important locus for evolutionarily mediated changes in tissue-selective regulatory function.

There is significant variation in the physiological function of the I_{to} current in different rodent hearts. In mouse and closely related species, the I_{to} current acquires a new function, becoming the major current underlying action potential repolarization (Rosati et al. 2008). The large I_{to} current produces a ventricular action potential of very short duration that matches the very fast heart rates in these species. Enhanced KChIP2 gene regulatory function makes an essential contribution to the required changes in cardiac electrophysiological function in these

species. For guinea pig (Cavia), and possibly *Tamias*, the ventricular action potential retains the classic spike and dome morphology seen in most mammals, albeit without the initial rapid phase 1 repolarization contributed by the I_{to} current. The degenerative loss of I_{to} current expression in guinea pig heart may reflect reduced importance of I_{to} for coordinating contractile function in these relatively small hearts, or the reduced requirement for the spare repolarization capacity provided by the I_{to} in hearts that already have relatively large repolarizing I_{Ks} and I_{Kr} currents.

Expression of most voltage-gated ion channels in heart is transcriptionally regulated (Rosati and McKinnon 2004; Chandler et al. 2009). A general property of excitable cells is that they are computational systems, in the sense that the output of the system is determined by the sum of the various currents that are expressed in the cell (Rosati and McKinnon 2009). As a consequence, relatively modest quantitative changes in voltage-gated ion channel expression and channel gene *cis*-regulatory function can have large effects on cellular electrophysiological function. The evolution of KChIP2 *cis*-regulatory function within the rodent clade is an example of how ion channel gene *cis*-regulatory function can evolve over relatively short phylogenetic distances in a quantitative fashion to significantly alter electrophysiological function. Evolution of *cis*-regulatory function is a flexible and efficient way to modify cellular electrophysiological function and would seem to be the most reliable way to match channel expression levels to optimal electrophysiological function. It has been suggested that relatively complex cellular homeostatic mechanisms could be used to match voltage-gated ion channel expression levels to the required cellular electrophysiological function (Liu et al. 1998). A simpler alternative is that the *cis*-regulatory function of ion channel genes can evolve over time to achieve this matching, in much the same way that the evolution of *cis*-regulatory function establishes a wide range of phenotypic properties in most other cell types (Carroll et al. 2004; Peter and Davidson 2011).

This is not to say that there is not some environment specific tuning of voltage-gated ion channel gene expression levels within individual cells, but it seems most likely that *cis*-regulatory evolution is the primary mechanism used to achieve appropriate channel expression levels in electrically excitable cells (Rosati and McKinnon 2009).

Chapter 4

Cis-Regulatory Function and Evolution of the KChIP2 Gene: Other Aspects

INTRODUCTION

In *Chapter 3*, we showed that evolution of the KChIP2 gene expression in the mammalian heart is mediated by changes in *cis*-regulatory function. In particular, the CpG island core promoter is the major locus of change during evolution. As the major determinant of species-specific differences in the heart, the CpG island has a function *in vitro* that closely matches with the KChIP2 expression *in vivo* (Fig. 1). This is an exceptionally interesting case that a core promoter region contains so much of a gene's regulatory function and controls expression in such a precise way without the assistance of additional enhancer elements.

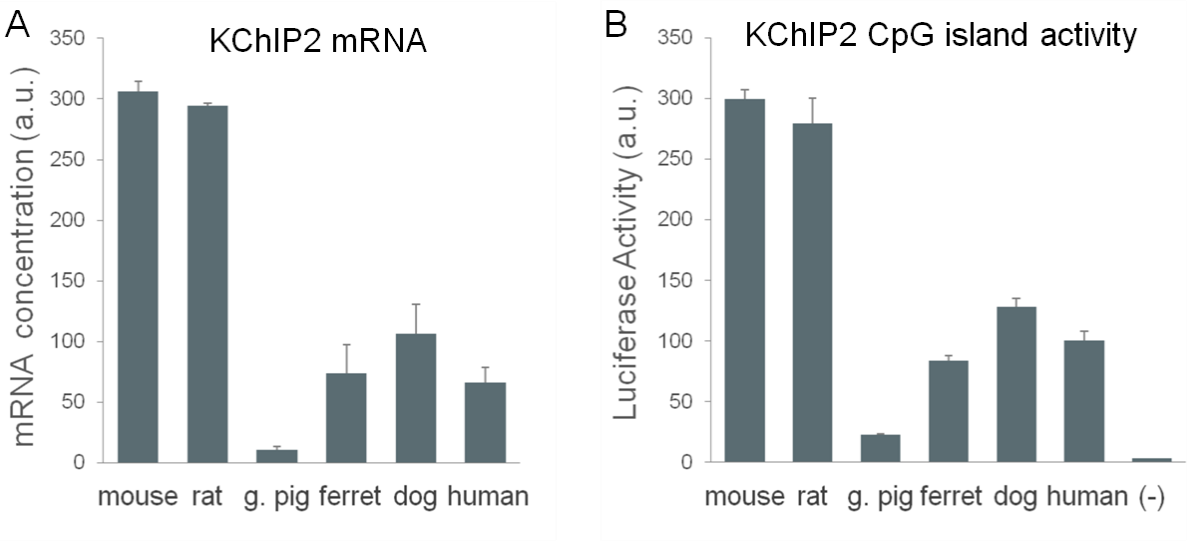

Figure 1. KChIP2 CpG island function recapitulates mRNA expression level in mammals

(A) KChIP2 mRNA expression in the left ventricular wall of six mammalian species (see *Chapter 3*). The histogram shows means ± S.D. (n = 3). (B) Analysis of the KChIP2 core promoter function in the same species shown in A. Error bars are SEM (n = 6-8).

Although the general mechanism of KChIP2 evolution in the heart has been pinpointed (*Chapter 3*), there are still several unresolved issues about the *cis*-regulation of this gene.

The first question is whether the evolution-mediated changes can be localized at the nucleotide level. Some evo-devo studies have clearly shown that single nucleotide variation during evolution can affect gene expression. For example, in one study on the morphological evolution of trichomes in some closely related *Drosophila* species, a few single-nucleotide mutations in an enhancer of the transcription factor Shavenbaby (Svb) were found responsible for the changes in the expression of this gene (Frankel et al. 2011). In another study on the adaptation of pigmentation in different populations of *Drosophila Melanganster,* five single-nucleotide mutations in the 2.4kb of the *ebony* abdominal enhancer were shown to determine the degree of fly abdominal pigmentation (Rebeiz et al. 2009). However, such findings seem possible only for relatively closely-related species, as the swap experiments inside the CpG island regions of two relatively distantly-related mammalian species, mouse and guinea pig, showed evenly distributed changes across the whole CpG island region except for the conserved 5'-UTR (*Chapter 3*, Fig. 4C&D). In order to identify such subtle changes, we decided to examine mammalian species which are phylogenetically very close, yet whose KChIP2 promoters show significantly different degrees of activity. We were able to find such species in the muroid clade (Fig. 8 and *Chapter 3*, Fig. 5A), such as hamster and gerbil (Jansa and Weksler 2004). We performed swap experiments between the two species and mouse/rat and the closer phylogenic differences allow us to identify single-nucleotide changes.

Another unresolved issue is the evolution of tissue specificity of the KChIP2 gene expression. The expression pattern of KChIP2 in the mammalian brains is strikingly different from that of the heart, with expression levels remaining relatively constant across all the species

examined, including guinea pig, where cardiac expression of KChIP2 is little or none (*Chapter 3*, Fig. 1A). The tissue-specific differences may partially reside in the CpG island promoter, as suggested by the evidence that the mouse-human differences are completely eliminated and the mouse-guinea pig differences reduced in a luciferase assay in neurons (*Chapter 3*, Fig. 5B). Nonetheless, neither the CpG island nor the whole 5' upstream region can fully recapitulate the pattern of KChIP2 mRNA expression in brain. Hence, additional tissue-specific *cis*-regulatory regions outside the 5' upstream region are to be identified in order to explain the expression levels of KChIP2 in this tissue. The intron region is a strong candidate for this search, as a major component of the non-coding DNA sequences (Jareborg et al. 1999) and was frequently found to contain regulatory elements (Bornstein et al. 1987; Aronow et al. 1989; Smith et al. 1996; Blackwood and Kadonaga 1998; Fedorova and Fedorov 2003; Schauer et al. 2009).

As important *cis*-regulatory regions of the KChIP2 gene are being identified, it is interesting to test whether and how these regions respond to transcription factors known to modulate the cardiac electrophysiological function or KChIP2 expression. The Iroquois homeobox genes Irx3 and Irx5 are expressed in a transmural gradient across the cardiac ventricles in both small and large mammals, with the highest level of expression in the endocardium (Rosati et al. 2006). This gradient is opposite to the transmural gradient in I_{to} current (with the exception of guinea pig). Such regional variations in transcription factor expression may explain the transcriptional variation of the molecular determinants of I_{to} gradient (KChIP2 in large mammals and Kv4.2 in small mammals). In mouse and rat, Irx5 was shown to directly regulate Kv4.2 transcription (Costantini et al. 2005; He et al. 2009). In larger mammals, whether Irx5 directly regulates KChIP2 expression is not known (Costantini et al. 2005; Gaborit et al. 2010).

In contrast to Irx3 and Irx5, the transcription factor FoxP2 was shown to have a transmural gradient concordant with that of Kv4.2 and KChIP2 (Rosati et al. 2006). In addition, a member of Sp1 and Kruppel-like transcription factor family, Klf15, was shown to control the circadian rhythmicity of cardiac function in the mouse, via regulation of KChIP2 gene expression (Jeyaraj et al. 2012).

Finally, while mapping the KChIP2 TSS (*Chapter 3*, Fig. 1), I found an interesting structure located in the KChIP2 CpG island - an inverted repeat - that can potentially form a highly thermodynamically stable stem-loop structure in the conserved 5'-UTR. It is well known that secondary structure in the 5'-UTR can regulate gene expression through various mechanisms affecting transcriptional efficiency, mRNA stability and translational efficiency (Pelletier and Sonenberg 1985; Baim and Sherman 1988; Emory et al. 1992; Bevilacqua and Blose 2008; Scott et al. 2009). Although the mouse-guinea pig swap experiments showed that the 5'-UTR does not carry species-specific functions (*Chapter 3*, Fig. 4C&D), the inverted repeat structure, which is also conserved, might carry some important regulatory function common in all species.

In this chapter, I report the results of studies on the various aspects of the KChIP2 *cis*-regulatory function described above. These results are organized and presented according to the gene structure, thereby starting from the CpG island and the inverted repeat contained in it, moving to regions outside the proximal promoter and, finally, testing the effects of transcription factors on these regions.

MATERIALS AND METHODS

The methods used in this chapter are the same as those in *Chapter 3*. Additional methods are listed below.

Site-Directed Mutagenesis

For fine resolution mapping of gene function, site-directed mutagenesis was used to create small deletions or modify individual base pairs. We used a modification of the procedure described by Sang et al (Sang et al. 1996), in which two primers are used to perform inverse PCR of the insert and vector. For site-directed mutagenesis, one of the primers contained a mutated base at the 5' end of the oligonucleotide. For deletion analysis, the primers were designed to leave a small gap, which became the desired deletion following re-ligation of the amplified product. In this procedure, a small amount (50 ng) of template plasmid DNA was amplified using a low number of cycles (typically 10-15) and a high fidelity DNA Polymerase (Pfx from Invitrogen or Pfu from Stratagene). The original template DNA was removed after the PCR reaction by digestion with Dpn I endonuclease, which targets the sequence Gm6ATC, where the A residue is methylated. Digestion with Dpn I selects against the parental DNA in the reaction mix because this DNA is Dam-methylated, whereas the PCR products are not.

RESULTS

1. KChIP2 Gene Structure

KChIP2 is a relatively compact gene located in a gene-rich region (Fig. 2B). The whole transcription unit is only 18kb in human, which is strikingly smaller in size than all the other members of the KChIP gene family (KChIP1: 390kb; KChIP3: 90kb; KChIP4: 1,240kb). The smaller size of the gene does not mean that the *cis*-regulation of this gene is less complicated but it suggests that it would be easier to identify specific *cis*-regulatory elements, compared to DNA regions of larger size, which are more challenging to study.

We can identify three major regions in the KChIP2 gene that are most likely to harbor regulatory elements: the 5' upstream intergenic region, the large first intron (Intron 1), and the 3' downstream intergenic region (Fig. 1B).

The 5' upstream region was extensively characterized, as reported in *Chapter 3*. An interspecies Vista alignment between human, mouse and guinea pig reveals that there are two relatively well-conserved regions inside this major region: the upstream portion which overlaps with the 3'-UTR of another transcript (C10orf76) and the downstream portion which is the CpG island (Fig. 2A). While the CpG island turned out to be the primary locus for evolution mediated changes in KChIP2 gene expression, we showed that the upstream portion of this 5' region does not contain any important *cis*-regulatory element for the KChIP2 gene (*Chapter 3*, Fig. 3),.

The large first intron is a candidate region that may contribute to the evolution of tissue-specificity in KChIP2 expression, as the 5' upstream region (including the CpG island) did not fully recapitulate the KChIP2 gene expression in the brain. Relative to the compact size of the

rest of this gene, the first KChIP2 intron is extremely large, thereby representing a major portion of the gene body (Fig. 2B). Again using an interspecies alignment between human, mouse and guinea pig, we identified two conserved regions in the first intron, which we named “intron 1A” and “1B” regions (“in1A” and “in1B”, Fig. 2C). While in1A is relatively well conserved in the three species, the in1B region is very poorly conserved in the guinea pig (Fig. 2C).

The 3’ intergenic region, which also coincides with the 5’ upstream region of an adjacent gene (MGEA5), was not considered for further studies, as it is very likely to contain regulatory elements for MGEA5 rather than for KChIP2. Both of the other two major regions, the 5’ upstream proximal promoter region and the first intron, were tested in *in vitro* transcription assays in order to identify important regulatory elements.

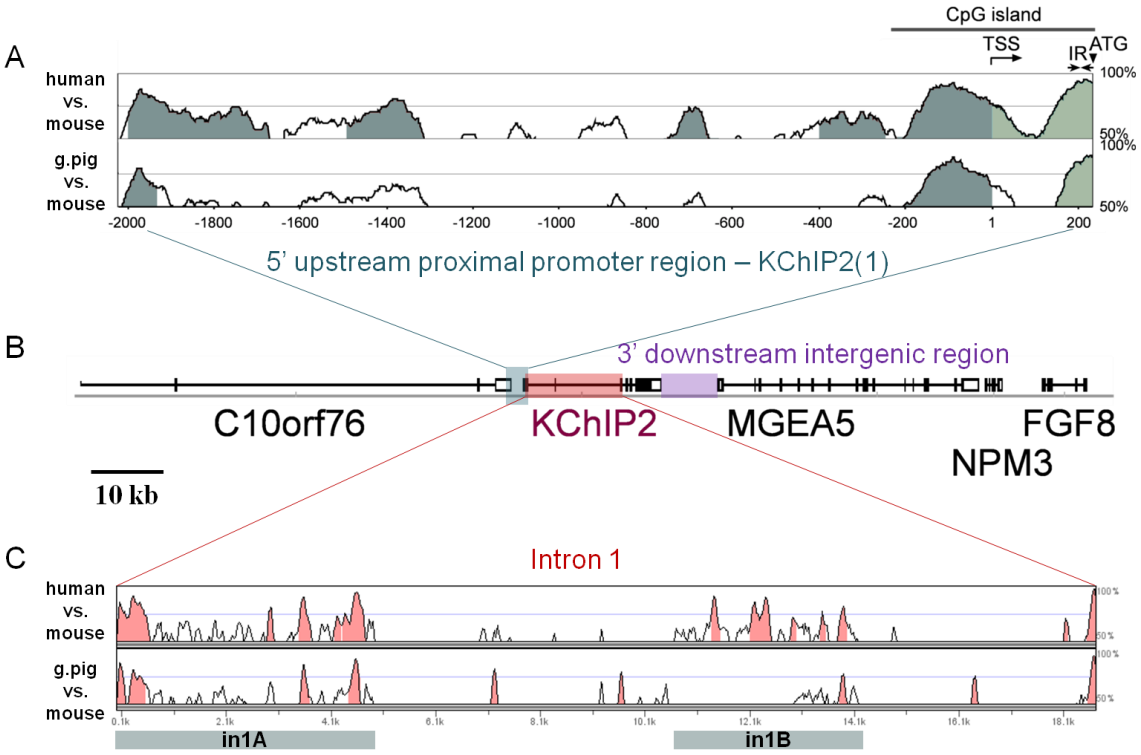

Figure 2. The KChIP2 gene structure

(A) Vista alignment of KChIP2 5' upstream regulatory region of human (top) and guinea pig (guinea pig, bottom), using mouse as the reference sequence. Three features are marked, the CpG island region, the transcription start site (TSS) and an inverted repeat (IR) in the 5' UTR. The sequences end immediately upstream of the initiator methionine codon in exon 1 of the gene (ATG). Conserved sequences in VISTA (70%/100 bp cutoff) are colored according to the annotation (UTRs - light green and non-coding - teal). (B) Structure of KChIP2 and surrounding genes on human chromosome 10. The 5' upstream proximal promoter region is shaded blue and the first intron is shaded rose. There is an exon labeled inside the rose area, but it only exists in a minor fraction of KChIP2 transcripts. (C) Vista alignment of KChIP2 first intron (Intron1) of human (top) and guinea pig (guinea pig, bottom), using mouse as the reference sequence. Two most interesting regions are labeled as in1A and in1B underneath the alignment map.

2. KChIP2 CpG Island

The capability of the KChIP2 CpG island to recapitulate the cardiac expression pattern of this gene across mammalian species makes it a most interesting *cis*-regulatory region to study. A lot of efforts were spent to study the function and evolution of the CpG island. Swap experiments were carried out to finalize the important evolution-mediated changes. Mutation experiments were designed to examine some interesting features of this region, which were annotated in Figure 3 together with other known features like the TSS and the inverted repeat.

Given its functional importance, the CpG island region is surprisingly short (about 450bp). It has two well conserved regions separated by a poorly-conserved one in the middle (Fig. 3A). The TSS locates in the first conserved peak, while the inverted repeat locates in the second conserved peak.

In the mouse-guinea pig swap experiments, the CpG island was divided into four regions (*a*, *b*, *c* and *d*, Fig. 3A&B). Region *a* contains a predicted Sp1 binding site (GGGGCGGGG) present in both mouse and human but not guinea pig, due to a two-nucleotide mutation at the 5' end of the recognition site ("GG" versus "CA"). As Sp1 is one of the most potent transcription activators identified in eukaryotes (Kaczynski et al. 2003), loss of Sp1 binding at this site may have contributed to the low level of CpG island promoter activity in guinea pig. The contribution of the mutation of this site is investigated in paragraph 2.5. Region *b* has the TSSs located in the center. Region *c* is the most poorly conserved region in the CpG island. According to the mouse-guinea pig swap experiments (*Chapter 3*, Fig. 4C&D), these three regions contain species-specific changes that seem to be evenly distributed throughout *a*-*b*-*c*. Finally, consistent with the lack of species-specific effects in the swap experiments, region *d* is well conserved across the species. A special feature of this region is the inverted repeat (IR, ~50bp long), located at the 3'

end. In order to further analyze the contribution of these sub-regions on the evolution of the KChIP2 CpG island function, swap experiments between mouse and a few other species were carried out. The results are described in paragraph 2.1 to 2.4.

In the ClustalW alignment of sequences from seven mammalian species (Fig. 3B), the guinea pig sequence is shown to be the least related to the mouse by being listed at the bottom. Clearly, other constraints for the evolution of the KChIP2 gene override the phylogenetic relationship among species, as guinea pig is more distantly related to the other rodents (mouse, rat and hamster) in terms of KChIP2 sequence than non-rodent mammals (human, dog and rabbit).

Finally, four human single nucleotide polymorphisms (SNPs) are located in the KChIP2 CpG island region: rs35519717 (SNP1), rs113576926 (SNP2), rs35051533 (SNP3) and rs60274016 (SNP4) (Fig. 3B & Fig. 11A). SNP1 is in a conserved region, at the boundary between region *a* and *b*. SNP2 is in region *b*. SNP3 and SNP4 are in the poorly conserved region *c*. SNPs in human populations are the genetic basis for individual differences and susceptibility to disease. Because of the importance of the CpG island in the evolution and function of this gene, it is interesting to test whether these nucleotide variations can result in a change in transcriptional activity of the KChIP2 promoter. The results are described in paragraph 2.6.

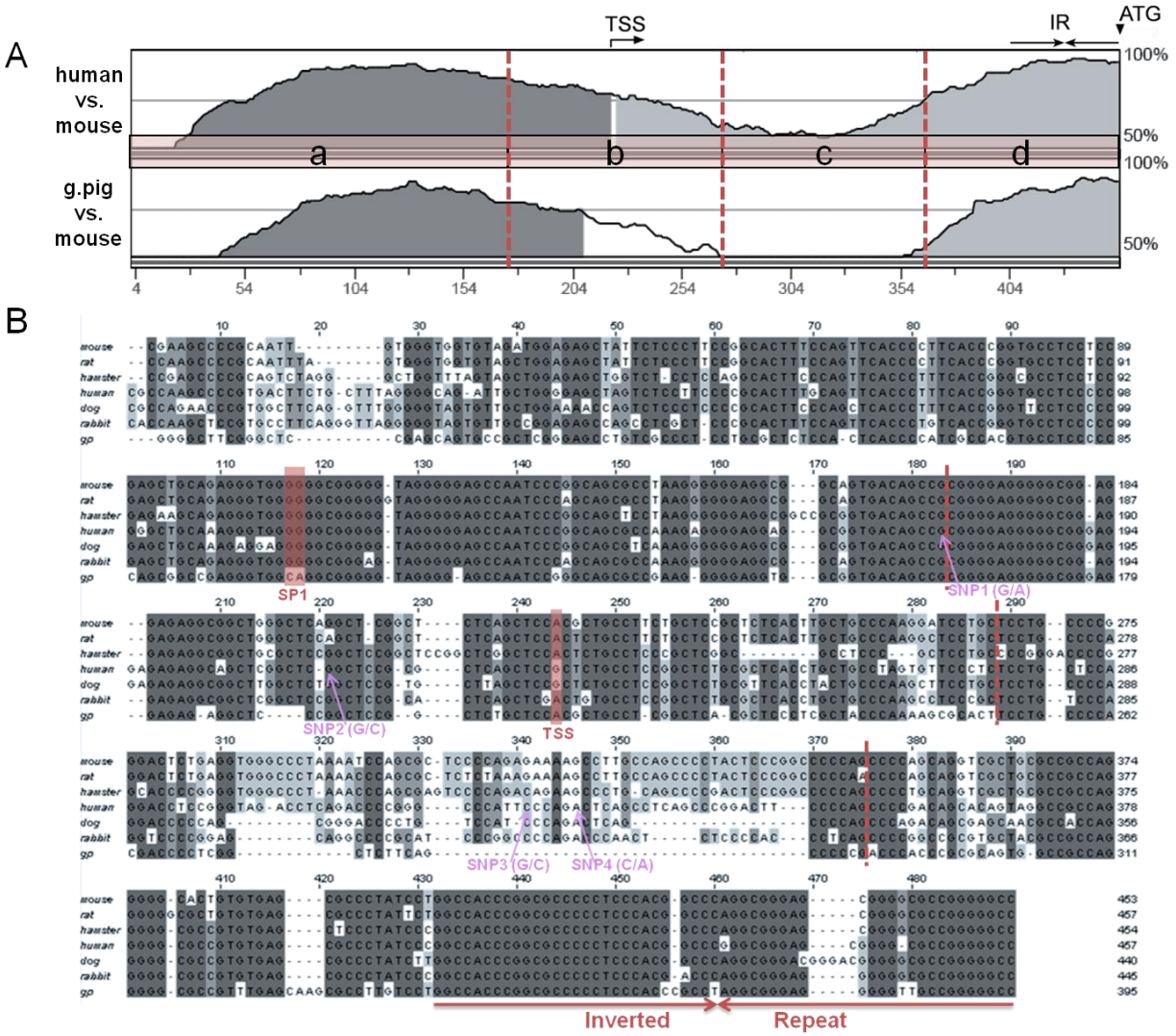

Figure 3. KChIP2 CpG island sequence alignment and annotation

(A) Vista alignment of the KChIP2 CpG island region of human (top) and guinea pig (bottom), using mouse as the reference sequence. Based on the conservation map, this region can be divided into 4 portions (red dashed lines), named *a*, *b*, *c* and *d*, respectively. (B) ClustalW sequence alignment of the KChIP2 CpG island in seven mammalian species: mouse, rat, hamster, human, dog, rabbit and guinea pig (gp). The degree of sequence identity is shown in shaded color (gray). The red dashed lines correspond to the ones in (A). The four SNPs identified in the human population are labeled in purple (arrows and text below). Other features are labeled (red) in these sequences, namely two nucleotides at a potential Sp1 binding sites that are divergent only in the guinea pig ("Sp1"); the primary "TSS" in mouse; the "Inverted Repeat".

2.1 Mouse-human swaps within the CpG island

To identify smaller regions responsible for the differences in KChIP2 expression between mouse and human, a similar strategy to the mouse-guinea pig swaps was used. Using the same four divisions inside the CpG island region (*a* to *d*), a similar set of DNA constructs were made by swapping mouse and human fragments (Fig. 4A&B). These new constructs were then tested in a luciferase assay to assess their *cis*-regulatory function. The results obtained were quite different from those obtained from the mouse-guinea pig swap experiments reported in *Chapter 3*. Instead of a progressive increase/decrease in regulatory function observed in the former swaps, the mouse-human swaps resulted in a variable pattern of changes, without an identifiable trend (Fig. 4C).

A first observation is that swapping the human *a* region with the mouse one (h-m1 swap) caused an increase in transcriptional activity (Fig. 4C). However, further addition of the human *b* region (h-m2 swap) had a dramatic effect by decreasing the promoter activity down to a level much lower than the original mouse construct and comparable with the overall lower level of activity of the human construct (Fig. 4C). Consistently, such effects are confirmed in reciprocal swap experiments, where the correspondent human regions were replaced with mouse regions (human→m-h1→m-h2). These effects of swapping are not caused by formation of new element at the junction of regions *a* and *b*, as the junctional sequences are identical between the two species (Fig. 3B). Therefore, it seems that the human *a* region contains some stronger activating elements than the correspondent mouse region, while the mouse seems to contain some stronger elements in region *b*. This might also partly explain the lack of difference between mouse and human promoter activities, when later only the *a+b* regions are tested (Fig. 9), since each species

would, in this case, have a strong activating element, only located in a different region (*a* for the human, *b* for the mouse).

Swapping the *c* region between mouse and human yielded inconsistent results. While replacement of the mouse *c* region with the human (h-m2→h-m3) suggested that this region does not carry any species-specific differences, swap of the human *c* region with mouse (m-h2→m-h3) resulted in a significant increase in transcriptional activity. This suggests the possibility of species-specific synergistic interactions between different *cis*-regulatory elements. Probably because of the long period of independent evolution since the last common ancestor of mouse and human, the mouse and human sequences themselves have co-evolved within the CpG island region that in our case the lack of such a synergy would cause the inconsistent results from swapping region *c*.

In keeping with what was observed in the mouse-guinea pig swap experiments, even in this series of substitutions (mouse-human/human-mouse), it appears that the conserved *d* region does not carry any species-specific differences. This is indicated in Figure 4C by comparison of either h-m3 with human, or of m-h3 with mouse.

Altogether, out of the four regions inside the KChIP2 CpG island, region *b* appears to be the most important for the mouse-human differences in KChIP2 gene expression, while region *c* may be responsible for some of the differences between these two species. Although containing species-specific changes, region *a* has an effect that is opposite to the species-specific differences and can be counteracted by region *b*.

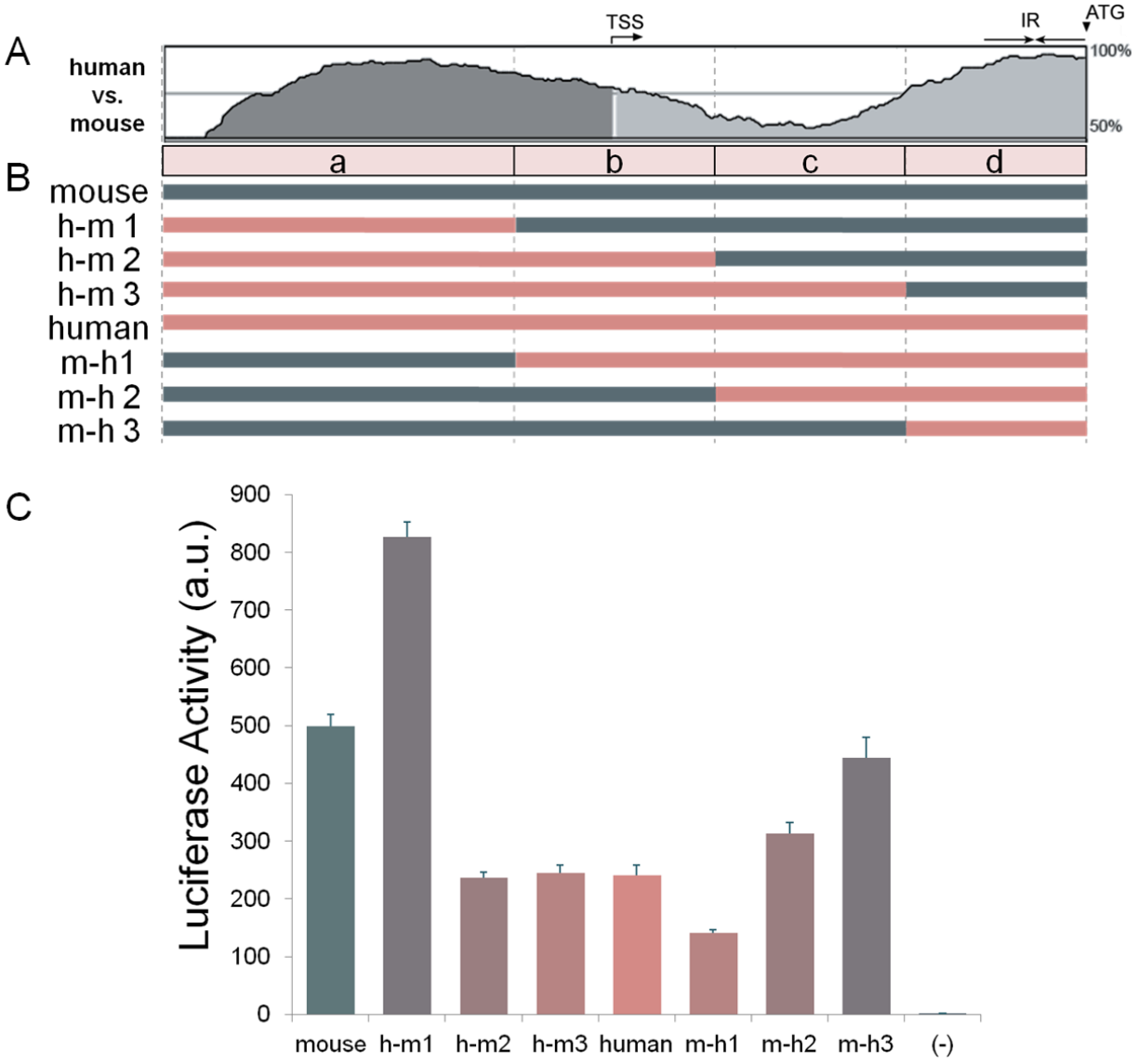

Figure 4. Effects of mouse-human swaps on the KChIP2 CpG island promoter activity

(A) Vista alignment of human and mouse KChIP2 CpG island region, using mouse as the reference sequence. The CpG island sequence is divided into 4 parts (*a*, *b*, *c* and *d*) similarly to what shown for the mouse-guinea pig swap experiments (*Chapter 3*, Fig. 4C). (B) Scheme of the swap clones represented by the colored horizontal bars, with mouse colored teal and human colored orange. (B) Comparison of the *cis*-regulatory activity of the clones in an *in vitro* transcription assay. Error bars are SEM (n=3). The columns are colored according to the composition of the respective clones by mixing specific amount of teal (mouse) and orange (human).

2.2 Mouse-hamster and rat-hamster swaps within the CpG island

Due to the relatively large sequence differences, neither the mouse-guinea pig nor mouse-human swap experiments allow us to identify nucleotide level changes that underlie species-specific differences in the cardiac KChIP2 gene expression. As a result, another species in the muroid clade of rodents, hamster, was chosen for comparison with the mouse. It is closely related to mouse and rat but its level of KChIP2 promoter activity is significantly lower (*Chapter 3*, Fig. 5).

Based on sequence similarity and the convenience of the experimental design, the whole CpG island region was divided into three instead of four by means of two conserved restriction sites (Fig. 5). The first region (region *a*) was kept the same as the previous mouse-human swap experiment, while the rest of the sequence (regions *b*, *c* and *d*) was divided into two instead of three, named *b'* and *c'*. Each of the three regions (*a*, *b'*, *c'*) was swapped independently between hamster and mouse and the results are summarized in Figures 6 and 7. In addition to the mouse-hamster swaps, rat-hamster swaps were also made to independently confirm the results. Here the rat was considered to behave the same way as mouse, as the KChIP2 CpG islands from the two species have very similar sequence (Fig. 3B) and identical function (Fig. 1B).

It is clearly advantageous to do the swap experiment between more closely species, as revealed by these experiments that the results were more straightforward for interpretation. Moreover, the overall pattern of changes observed following the hamster swap experiments was reproducible between mouse and rat (Fig. 6E vs. 6F, and Fig. 7E vs. 7F). In general, the results showed that regions *a* and *c'*, located on either end of the CpG island drove minor changes in *cis*-regulatory activity when swapped between mouse/rat and hamster. Noticeably, the least

conserved region *b'*, which encompasses the TSS, turned out to be the most important determinant of the species-specific differences.

At difference with the complex results observed in the mouse-human swaps, the changes in *cis*-regulatory function observed following the swap in one direction (hamster to mouse/rat) were almost perfectly matched by the changes produced by swapping in the opposite direction (mouse/rat to hamster). For example, replacing the region *b'* of the mouse with the hamster one caused a dramatic decline in promoter activity (Fig. 6E), while replacing the same region in hamster with the mouse *b'* caused a dramatic increase in *cis*-regulatory activity (Fig. 7E).

In conclusion, the region immediately surrounding the TSS (region *b'*) contributes to the majority of the species-specific differences in KChIP2 cardiac gene expression between mouse/rat and a closely related species, hamster.

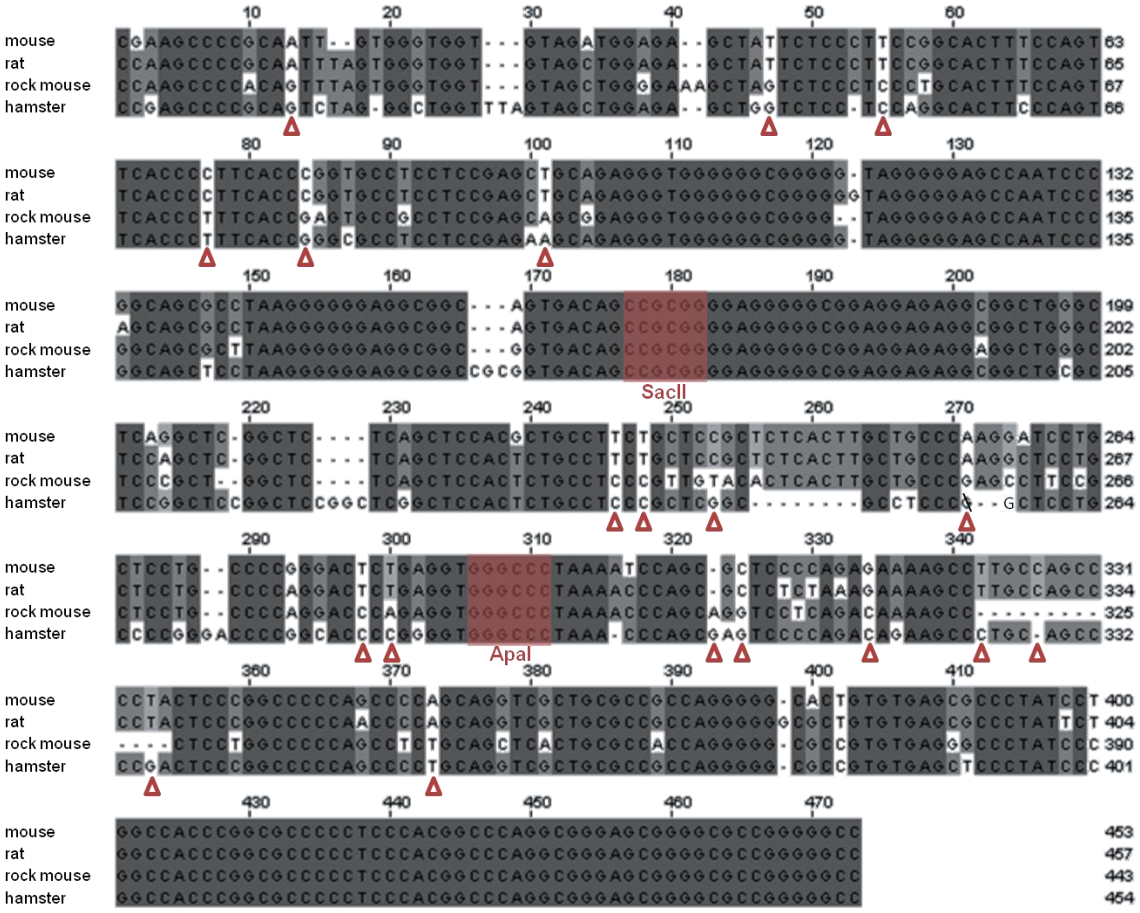

Figure 5. Design of point mutation and swap clones in mouse and hamster CpG islands

ClustalW alignment of mouse, rat, rock mouse and hamster CpG islands. The degree of sequence identity is shown in shaded color (gray). The red triangles mark the nucleotides that were selected for point mutations. The two red shaded boxes mark the boundaries of the swap regions, which are restrictive sites for SacII and ApaI, respectively. The CpG islands are divided into three parts by the two restrictive sites. Accordingly, the point mutations are also separated into three blocks.

2.3 Point mutations in mouse and hamster KChIP2 CpG island

In parallel with the swap clones, we tried to identify single nucleotides responsible for differences in the KChIP2 *cis*-regulatory function between rodents by analyzing the effects of single nucleotide substitutions.

Based on sequence conservation (Fig. 5), we selected a total of 19 single-nucleotide mutations. In an attempt to reduce the number of candidate mutations, I included rock mouse in the sequence comparison (Fig. 5). In this rodent species, the KChIP2 CpG island has a similar activity as the hamster. Therefore, only the single nucleotide variations that are the same in mouse and rat but different in both hamster and rock mouse were chosen.

Based on the same divisions used for the mouse/rat-hamster swap clones that split the CpG island into three regions (*a*, *b'* and *c'*), these 19 mutation sites were divided into three groups (mut1, mut2, mut3) according to which regions they are located in, with about six mutations in each group (Fig. 5). For each group, either the mouse nucleotides were mutated into the corresponding hamster ones (m_mut1, m_mut2, m_mut3) (Fig. 6B) or the hamster nucleotides were mutated into the corresponding mouse ones (ha_mut1, ha_mut2, ha_mut3) (Fig. 7B). The results of these experiments were compared to those obtained when swapping the whole regions described in paragraph 2.2 (Fig. 6D vs. 6E & Fig. 7D vs. 7E).

When the single nucleotide mutations were introduced in the mouse sequence, there were only minor changes in promoter activity for the first group (m_mut1). On the other hand, the second (m_mut2) and third (m_mut3) group of substitutions had significant effects (Fig. 6D). Substitutions in region *b'* (m_mut2) resulted in a marked decrease of promoter activity, which confirmed the importance of this region already observed in the swap experiments described in

paragraph 2.2. Although the amplitude of the effect was smaller than the corresponding swap experiment (m-ha-m, Fig. 6E), it is striking that the six point mutations in this region could capture so much of the functional changes, especially given the relatively poor level of conservation of region *b'*.

However, none of the mouse-hamster substitution groups caused a large increase in the hamster CpG island promoter activity (Fig. 7D), in striking contrast with the swap results (Fig. 7E&F), but also with the results of the corresponding point mutations in mouse (Fig. 6D). This happened because the DNA sequences are poorly conserved and there are large deletions and insertions in the hamster sequence (Fig. 5) that were missed by the point mutations. This suggests that this point mutation approach is not working well for sequences that are poorly conserved, especially the ones that carry large insertion and deletions.

In conclusion, the point mutation experiments partly confirmed the importance of the poorly conserved *b'* region for the evolution of the KChIP2 gene expression in rodents.

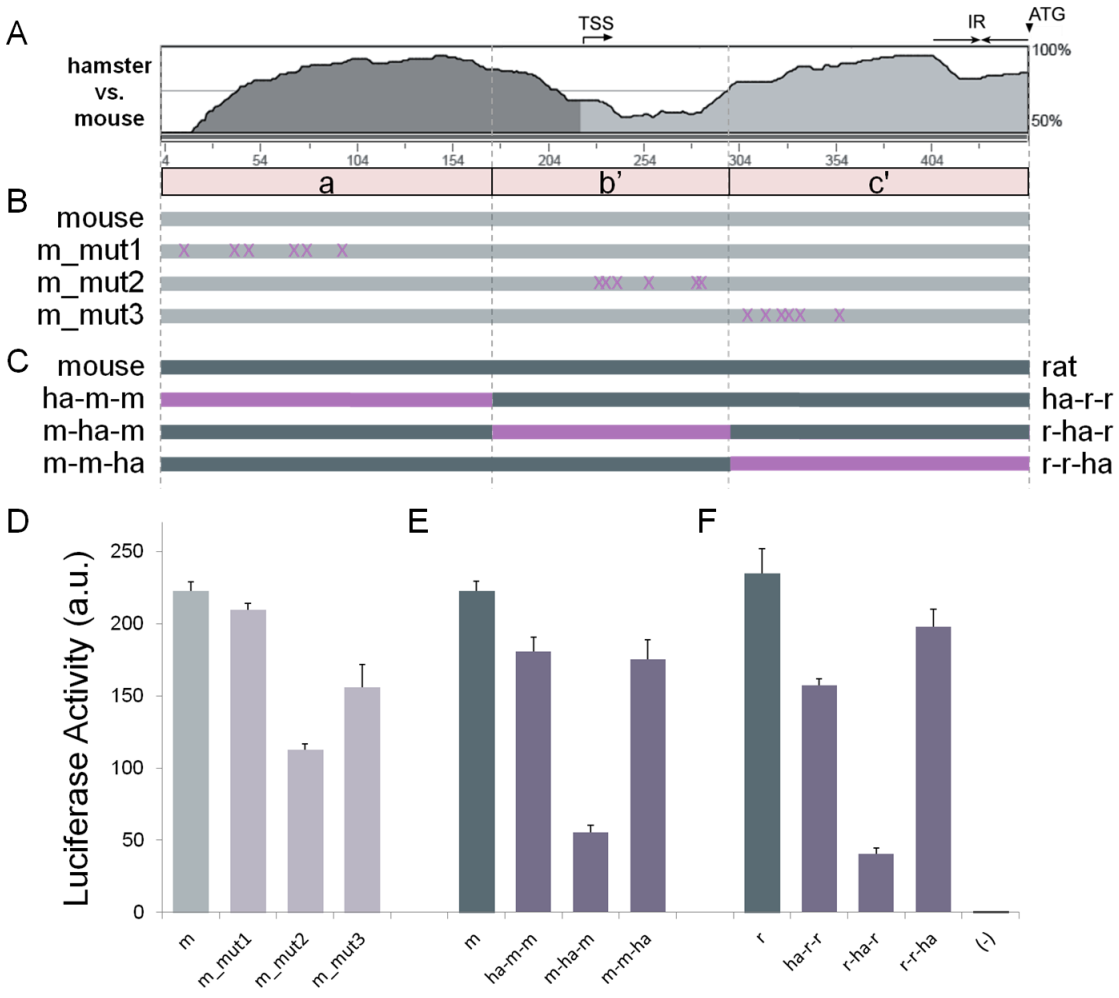

Figure 6. Effects of hamster point mutation substitutions and hamster region swap on the mouse and rat KChIP2 CpG island

(A) Vista alignment of hamster and mouse KChIP2 CpG island region, using mouse as the reference sequence. The whole region is divided into 3 parts, named *a*, *b'* and *c'*. (B) Location of the point mutations in the mouse sequence. The teal horizontal bars represent the original mouse clone and the X symbols on the bars represent the position of the specific mouse nucleotides that were changed into hamster ones. Each mutation clone carries six mutations on one of the three regions. (C) Scheme of the swap constructs. The colored horizontal bars represent the composition of the swap clones with mouse and rat colored teal and hamster colored purple. (D-F) *Cis*-regulatory activity of the respective clones in an *in vitro* luciferase assay. Error bars are SEM (n=3). The columns are colored according to the composition of the respective clones by mixing specific amount of teal (mouse or rat) and purple (hamster). The results of the mouse to hamster mutation substitutions are shown in (D). Results for the mouse-hamster swaps are shown in E and for the rat-hamster swaps in (F).

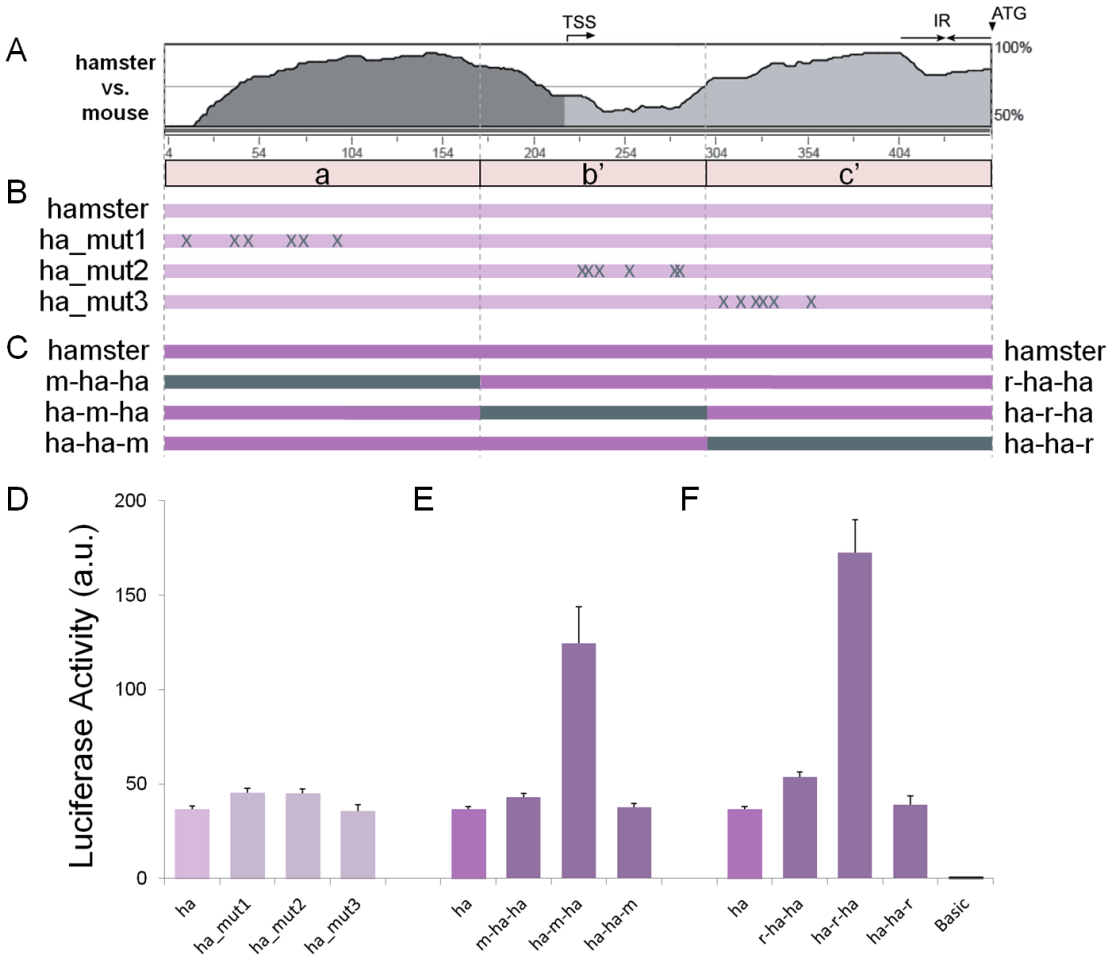

Figure 7. Effects of mouse point mutation substitutions and mouse region swap on the hamster KChIP2 CpG island

(A) Vista alignment of hamster and mouse KChIP2 CpG island region, using mouse as the reference sequence. The whole region is divided into 3 parts, named *a*, *b'* and *c'*. (B) Location of the point mutations in the hamster sequence. The purple horizontal bars represent the original hamster clone and the X symbols on the bars represent the position of the specific hamster nucleotides that were changed into mouse ones. Each mutation clone carries six mutations on one of the three regions. (C) Scheme of the swap constructs. The colored horizontal bars represent the composition of the swap clones with mouse and rat colored teal and hamster colored purple. (D-F) *Cis*-regulatory activity of the respective clones in an *in vitro* luciferase assay. Error bars are SEM (n=3). The columns are colored according to the composition of the respective clones by mixing specific amount of teal (mouse or rat) and purple (hamster). The results of the hamster to mouse mutation substitutions are shown in (D). Results for the hamster-mouse swaps are shown in E and for the hamster-rat swaps in (F).

2.4 Mouse-gerbil and rat-gerbil swaps within the KChIP2CpG island

The results from the mouse single nucleotide substitution in the hamster (Fig. 7A) raise the possibility that hamster may not be phylogenetically close enough for identifying functional changes of the KChIP2 CpG island at the nucleotide level. In order to rule out this possibility, we searched for species that are even more closely related to mouse and rat, and gerbil seemed a good candidate (Fig. 8). As DNA sequences and BAC libraries for gerbil were not available, the genomic DNA of gerbil was obtained commercially (Zyagen) and the KChIP2 proximal region was PCR amplified, subcloned and then sequenced. As shown in Figure 9A, compared to hamster, the gerbil KChIP2 CpG island has a much smaller number of changes relative to mouse and rat, consistent with its phylogenetic proximity to these species (Fig. 8), and no large deletions or insertions were observed. Particularly, the middle *b'* region is no longer the least conserved region. Only eight single-nucleotide changes were observed in this region (Fig. 9A). Instead, the third (*c'*) region appears to contain the largest number of nucleotide changes.

Similarly to hamster, the gerbil KChIP2 CpG island showed a relatively low level of *cis*-regulatory activity (Fig 9B&C), despite the high-level of sequence identity compared to mouse. As a result, the comparison between gerbil and mouse seemed an ideal system for studying the rapid evolution of the KChIP2 CpG island function.

A set of swap clones between mouse and gerbil were made, dividing the CpG island into three parts using the same divisions used for the mouse-hamster swap experiment (*a*, *b'* and *c'*). Similarly to the approach used for the hamster-mouse swaps, replacements of each region were made and parallel experiments using the rat KChIP2 CpG island were performed to validate the results.

Somewhat surprisingly, the largest change in promoter activity occurred when the conserved *b'* region was swapped (Fig. 9B). Swapping of either region *a* or *c'* did not result in any significant change in activity (Fig. 9B). Most importantly, these results were reproducible in the swaps in both directions, with the mouse to gerbil swap producing a large decrease and the gerbil to mouse a large increase in promoter activity. Furthermore, these findings were also confirmed in the rat-gerbil swaps (Fig. 9C). Interestingly, although the *b'* region is no longer the least conserved region in the mouse-gerbil comparison, it still carries most of the evolutionary-mediated changes, similar to what was found in the mouse-hamster comparison study.

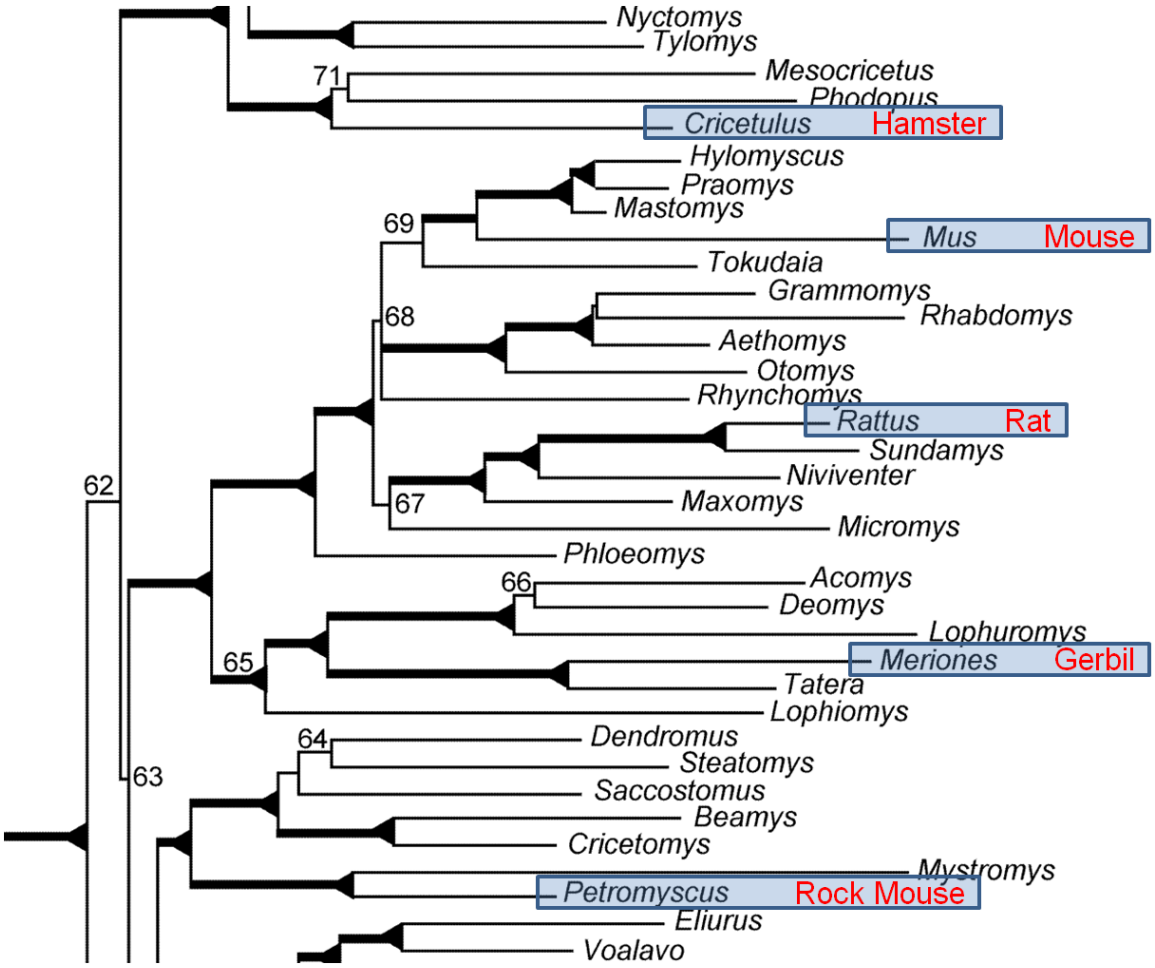

Figure 8. Phylogenetic map of species closely related to mouse and rat

Figure adapted from Jansa and Weksler 2004, which gave a detailed phylogenetic analysis of muroid rodents. Only a part of the muriod phylogenetic map is shown. The species mentioned in this chapter are highlighted by the blue box. The common names of the species are provided (red text).

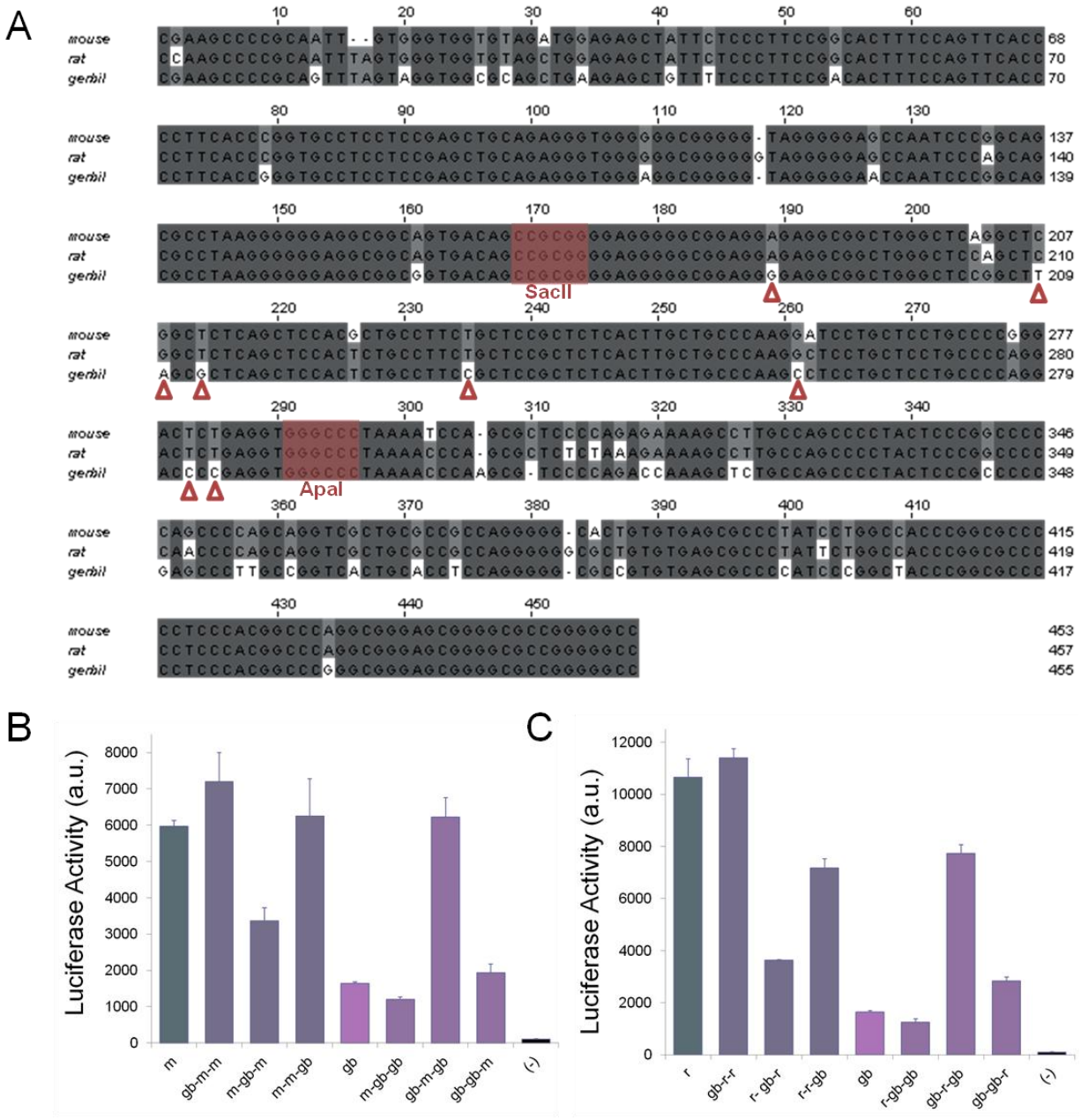

Figure 9. Effects of mouse-gerbil and rat-gerbil swaps within the KChIP2 CpG island

(A) ClustalW alignment of mouse, rat and gerbil CpG islands. The degree of sequence identity is shown in shaded color (gray). The red triangles mark the nucleotides that are different in gerbil in the *b'* region. The two red shaded boxes mark the boundaries of the swapped regions, which were the same as the ones used in the swap experiments with hamster. They are restrictive sites for SacII and ApaI, respectively. Similarly, the CpG islands are divided into three parts by the two restrictive sites. (B) Comparison of the *cis*-regulatory activity of the swap clones in an *in vitro* transcription assay. Error bars are SEM (n=3). The columns are colored according to the composition of the respective clones by mixing specific amount of teal (mouse or rat) and purple (gerbil).

2.5 Lack of predicted Sp1-binding site in guinea pig

As described above, a potential Sp1 binding site is present in the KChIP2 CpG island of all the other mammals but guinea pig (Fig. 3B). To test whether the lack of this site contributes to the overall low KChIP2 expression in this species, a functional Sp1 binding site was created in the guinea pig KChIP2 GpG island by replacing the two nucleotides "CA" with "GG" as annotated in Figure 3B. Conversely, the mouse and human Sp1 binding sites were mutated by changing the "GG" into "CA". These modifications were inserted in construct containing only regions *a* and *b*, i.e. lacking most of the 5'UTR (Fig. 10B).

Interestingly, elimination of the 5'-UTR resulted in a dramatic increase (more than ten folds in guinea pig and human) of *cis*-regulatory activity in all three species (Fig. 10C).

Consistent with the idea that losing the Sp1 site is important for the loss of KChIP2 promoter activity in the guinea pig heart, the creation of an Sp1 binding site in guinea pig produced an increase in promoter activity (Fig. 10C). However, no significant change was observed following elimination of the Sp1 binding site in the mouse, while there was an increase of activity in the human, which is opposite to what expected.

In summary, these results suggest that loss of the predicated Sp1 binding site may have contributed to the guinea-pig specific loss of cardiac KChIP2 expression. As the transcription factor binding site prediction program cannot predict function, the lack of effects in mouse and human suggests that this site might not be functional in the two species despite its presence.

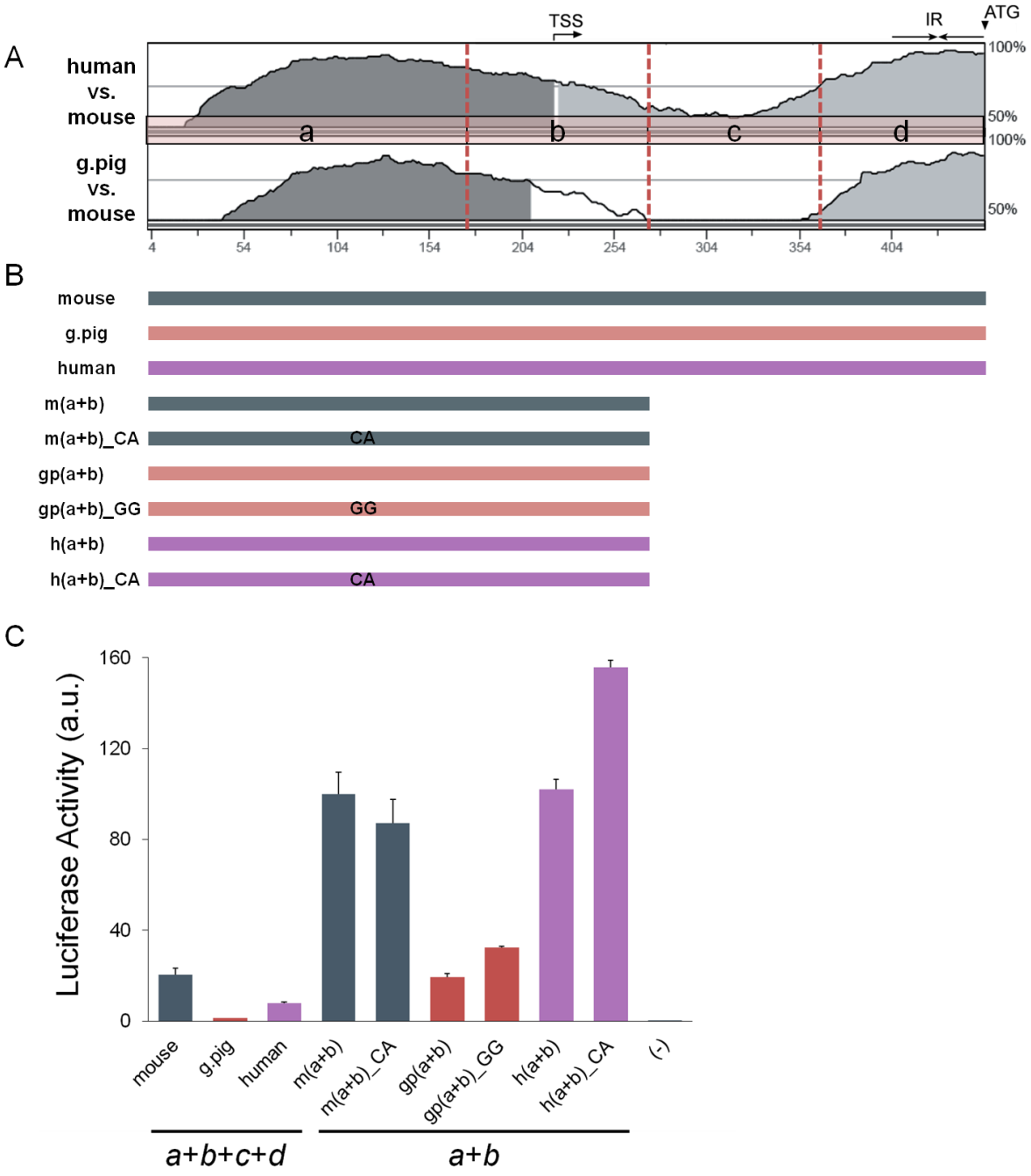

Figure 10. Effects of losing and gaining a predicted Sp1 binding site in the mouse, guinea pig and human KChIP2 CpG island

(A) Vista alignment of KChIP2 CpG island region of human (top) and guinea pig (bottom), using mouse as the reference sequence. (B) Scheme of the clones with each species represented by a differently-colored horizontal bars. For the mutation clones, the two nucleotide mutations at the Sp1 site were labeled on the horizontal bars. (C) Comparison of the *cis*-regulatory activity of the clones in an *in vitro* transcription assay. Error bars are SEM (n=3). The species are colored with their respective colors (mouse - teal, guinea pig - red, human - purple).

2.6 Analysis of single nucleotide polymorphisms (SNPs) in the human KChIP2 CpG island

In order to examine the potential contribution of each SNP to the KChIP2 promoter activity in humans, we made constructs carrying every variant of the single nucleotide, for each of the four identified SNPs. SNP1 is located in a region that appears to be very important for the CpG island function based on its highly conserved nature. There is no variation in this 24bp region across the mammalian species. One variant at SNP1 seemed to have increased the CpG island activity but this change was not significant (Fig. 11B). The SNP2 variant did not produce any change in *cis*-regulatory activity. However, single nucleotide change at SNP3 produced a modest level of change and variation at SNP4 produced a large difference in *cis*-regulatory function, although both were located in a poorly-conserved region of the CpG island.

In conclusion, at least two of the four SNPs in the KChIP2 CpG island can significantly affect the human KChIP2 gene expression level in the heart.

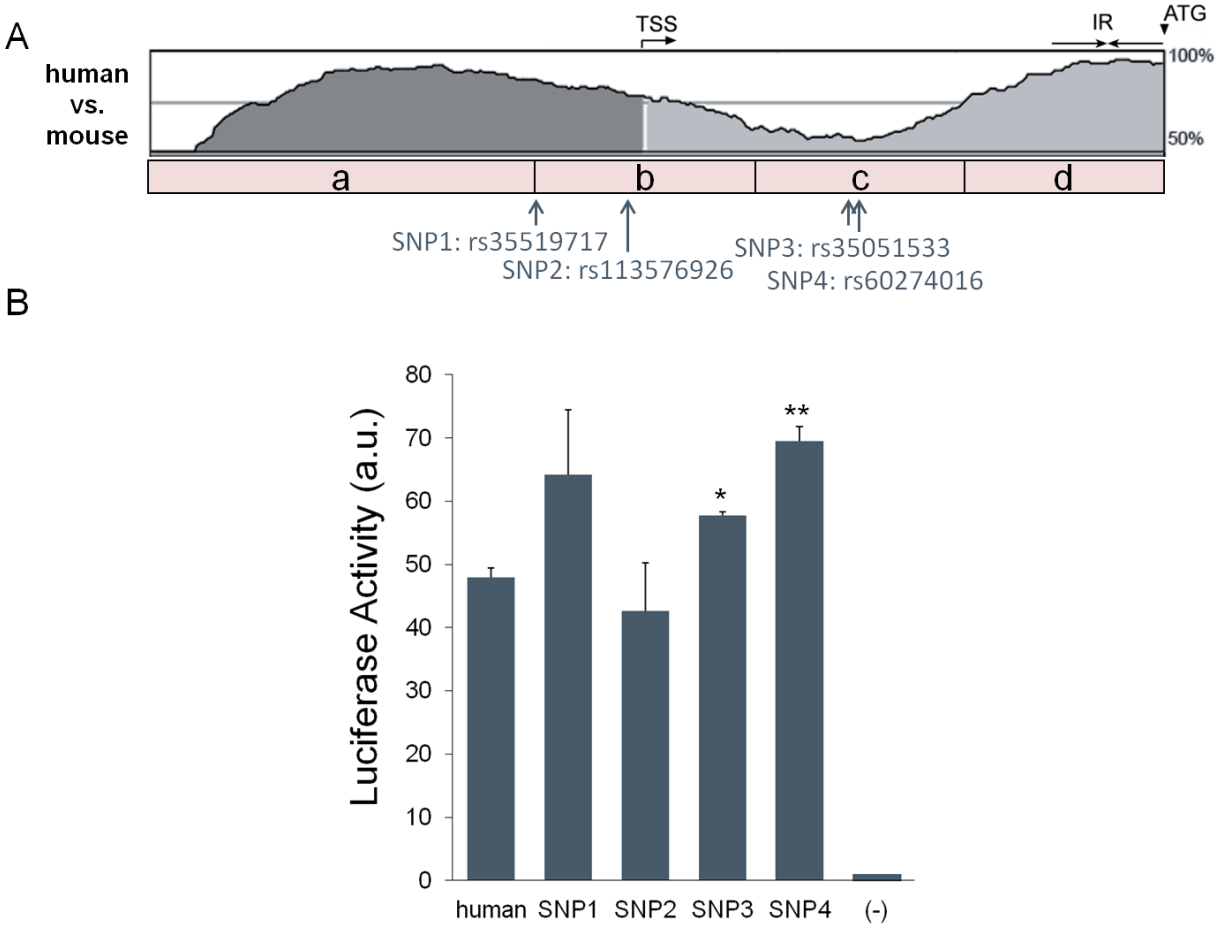

Figure 11. Effects of SNP variations on the promoter activity of the human KChIP2 CpG island

(A) Positions of the four SNPs annotated on the vista alignment map. (B) Comparison of the *cis*-regulatory activity of every SNP variant in an *in vitro* transcription assay. The detailed nucleotide information for each SNP is shown in Figure 3. Error bars are SEM (n=3). *P<0.05, **P<0.005, student's t-test.

3. The Conserved 5'-UTR and the Inverted Repeat

The conserved 5'- untranslated region (UTR) does not contribute to species-dependent changes in KChIP2 *cis*-regulatory function, as shown by both the mouse-guinea pig swap (*Chapter 3*, Fig. 4C&D) and the mouse-human swap (Fig. 4) experiments. However, deletion of this region (and part of the poorly-conserved UTR) resulted in a dramatic increase of activity in all species (Fig. 10). This indicates the presence of elements with strong inhibitory function in the UTR, although this is not contributing to the species-specific variation in KChIP2 gene expression.

There are two noticeable features in the conserved UTR: (1) this region is highly GC-rich at the 3'end (close to the start codon), with GC percentages of 90.6% in mouse, 92.5% in human and 85.2% in guinea pig; (2) this 53-54 base-pair long 3' GC-rich sequence is self-complementary containing an inverted repeat (IR, Fig. 12A&B). Due to the high GC content, this IR can potentially form a secondary stem-loop structure that is thermodynamically highly stable (Fig. 13A).

To analyze the function of the IR, we first deleted it from a construct containing the full-length proximal KChIP2 promoter. Deletion of the IR resulted an increase in *cis*-regulatory activity in all three species tested (Fig. 12C). The relative level of *cis*-regulatory activity characteristic of the three species (high in mouse, low in guinea pig and medium in human) was maintained. Consistent with its conserved sequence and structure (Fig. 12A), the IR appears to have an inhibitory function that is also conserved among species.

3.1 Disruption of the potential secondary structure in the inverted repeat

One possible mechanism of the inhibition by the IR is the potential formation of a stem-loop secondary structure that could either inhibit transcription or negatively affect post-transcriptional processes (Pelletier and Sonenberg 1985; Baim and Sherman 1988; Emory et al. 1992; Bevilacqua and Blose 2008; Scott et al. 2009). To test whether the secondary structure of the IR (Fig. 13A) plays a role in the inhibitory function, half of the self-complementary region was inverted without changing the nucleotide sequence (Fig. 13B). A secondary structure would be completely disrupted by this sequence inversion.

Disruption of the potential stem-loop structure by inverting half of the IR region did result in an increase in *cis*-regulatory activity in all species (Fig. 13C). However, the size of change is much smaller than the deletion. This suggests that the secondary structure is not a major cause of the inhibition. Instead, the sequence itself may contain binding sites for repressive transcription factors. Although the sequence inversion did its best in preserving a potential transcription factor binding site, it could still disrupt transcription factor interaction and therefore cause a change in *cis*-regulatory activity.

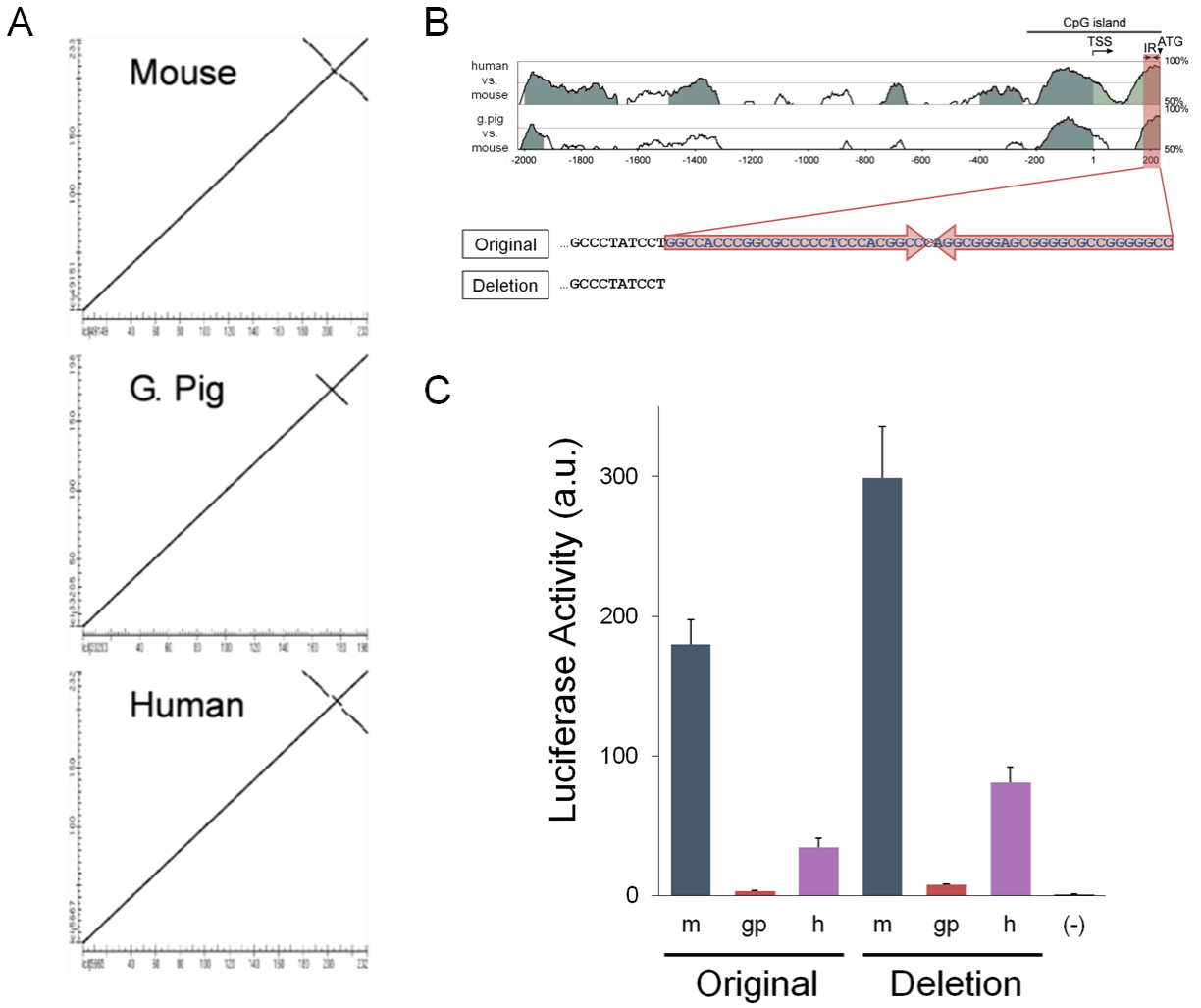

Figure 12. Deletion of the inverted repeat in the conserved 5'-UTR

(A) Dot matrix view of the self-alignment of mouse, guinea pig and human 5'-UTR sequences in NCBI nucleotide BLAST. There is an inverted repeat (IR) present in all three species. (B) Location and sequence of the IR. The red shadow on the vista alignment map highlights the location of the IR. Underneath the map is the mouse IR sequence with the two internal complementary regions labeled by the arrows. The deletion clone lacks this IR sequence. (C) *Cis*-regulatory activity of the original and deletion clones of the three species in an *in vitro* transcription assay. Mouse, guinea pig and human are represented by different colors. Error bars are SEM (n=3).

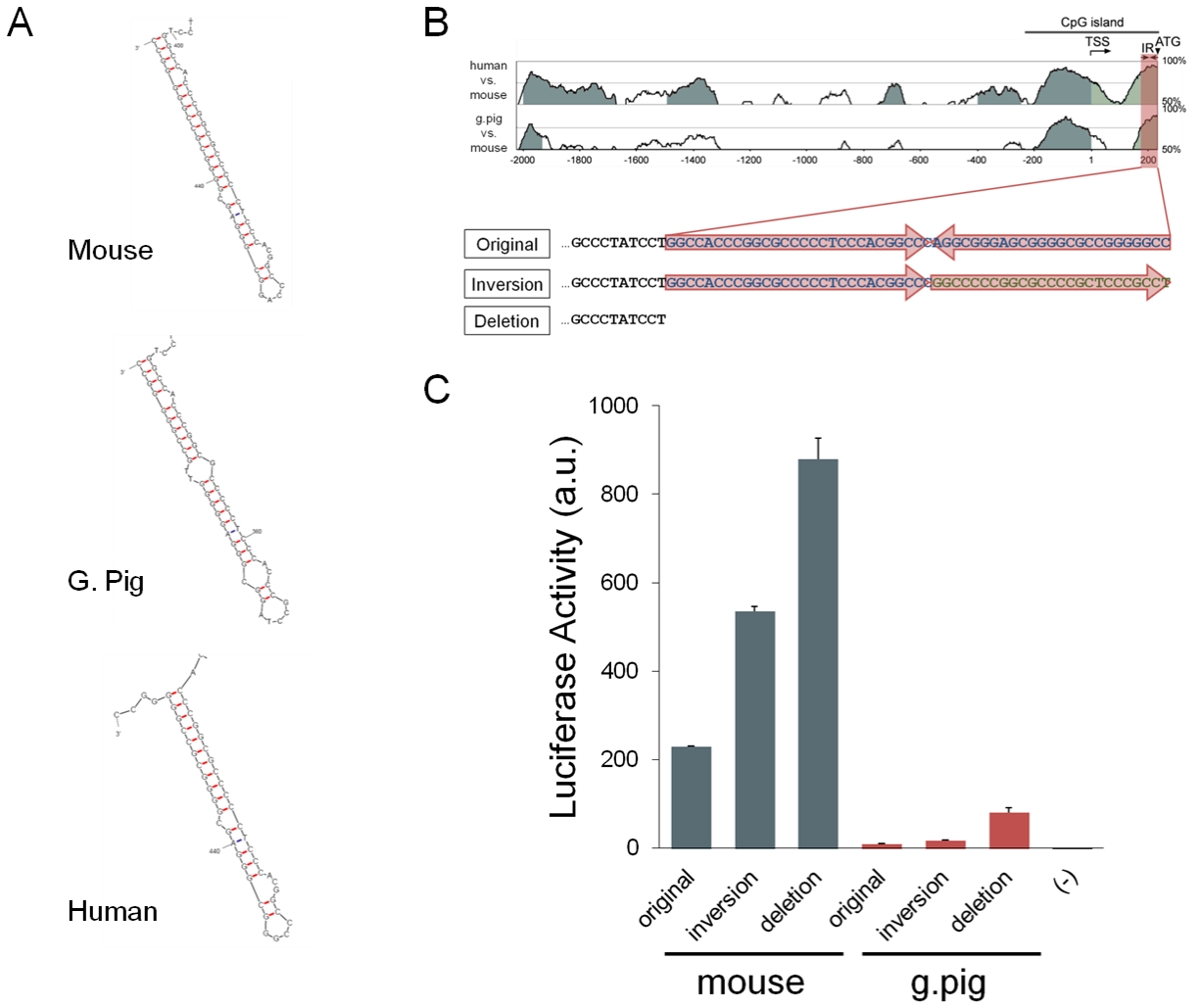

Figure 13. Disruption of the inverted repeat structure in the conserved 5'-UTR

(A) Stem-loop structure formed by the IR in mouse, guinea pig and human. (B) Scheme of inversion and deletion clones. The red shadow on the vista alignment map highlights the location of the IR. Underneath the map is the mouse IR sequence with the two internal complementary regions labeled by the arrows. The inversion clone has the last half of IR inverted. The deletion clone lacks the IR sequence. (C) *Cis*-regulatory activity of the original, inversion and deletion clones of mouse and guinea pig in an *in vitro* transcription assay. Mouse and guinea pig are represented by different colors. Error bars are SEM (n=3).

3.2 Deletion in KChIP2 IR mRNA

In sequencing the 5'-end of KChIP2 mRNA clones for TSS mapping, I observed an unexpected phenomenon: a significant fraction of the KChIP2 mRNAs contained the same sequence deletion of about 50bp, right upstream of the start codon (Fig. 14A). This is where the IR is located and the deleted sequence approximately covers the whole length of the IR.

A more careful examination of all the TSS mapping clones revealed that there were two types of deletion: a short and long one (Fig. 14B). Both types of deletions ended at the same nucleotide position in the 3' end. The short deletion was the most common type and had the same length (53bp) in mouse and human. The longer deletion was 77bp in mouse and 93bp in human. The short deletion exactly covered the length of the IR in both species. However, it did not completely overlap with the IR, as there were 7bp left on the 3' end (Fig. 14B). Nonetheless, the majority of the IR is deleted in both types of deletion.

Interestingly, the frequency of deletions varied between species and tissue types (Fig. 14C). No deletion was observed in the human brain, while most of the mouse heart mRNAs have the deletions. In general, less deletions were observed in the brain: none in human mRNA clones and only in 20% of the mouse clones. The heart had a higher frequency of deletions: about 50% of the human clones and 80% of the mouse clones contained such deletions.

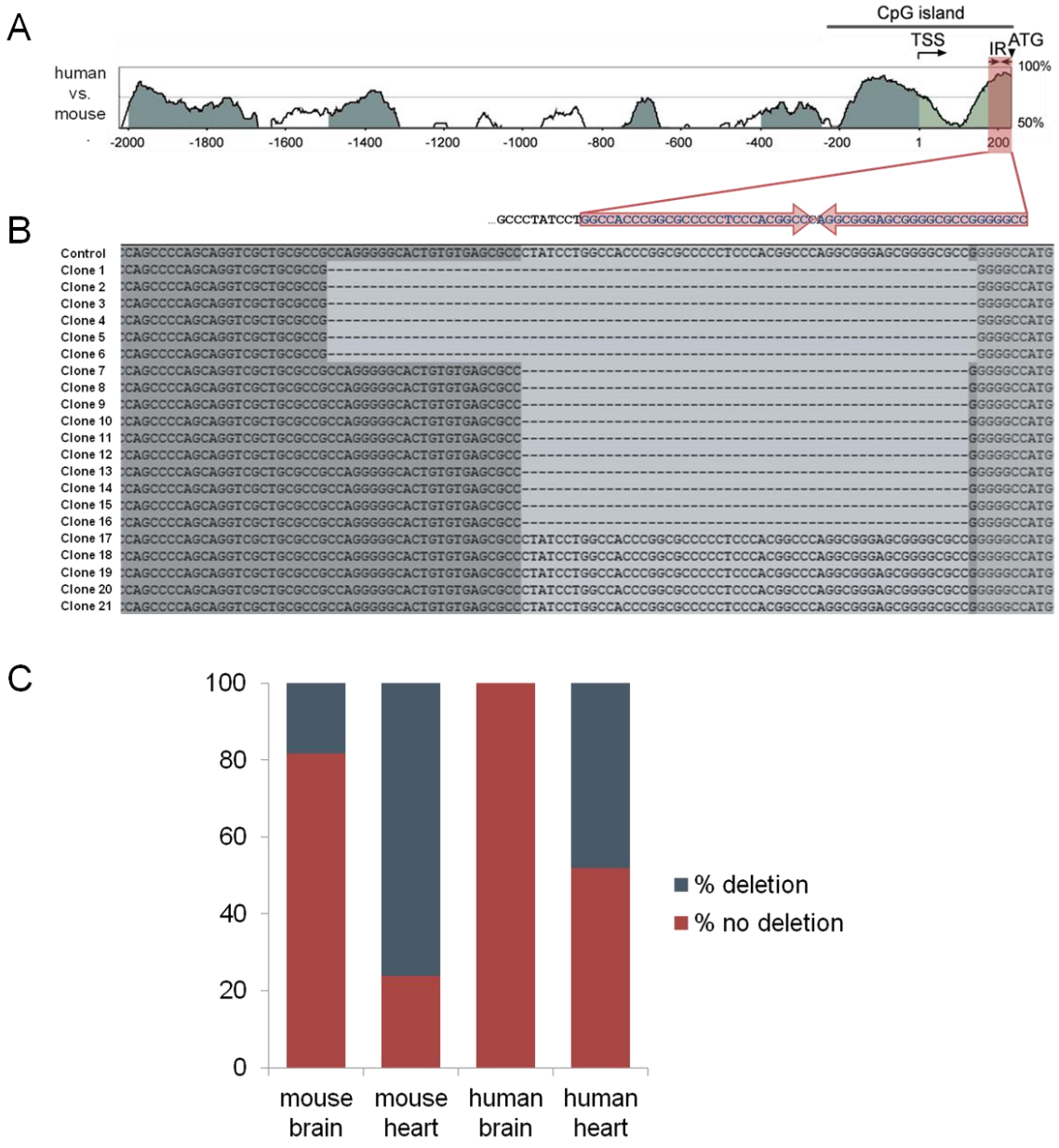

Figure 14. IR-deletions in KChIP2 mRNA clones

(A) Vista alignment of human and mouse KChIP2 5' upstream regulatory region, using mouse as the reference sequence. The red shadow on the vista alignment map highlights the location of the IR. (B) Alignment of KChIP2 cDNA sequences in mouse heart. A total of 21 clones are sequenced and a majority of them contain deletion of sequence around the IR. Placed on top of the alignment is the mouse IR sequence with the two internal complementary regions labeled by the arrows. (C) Percentage of cDNA clones that carry (% deletion, in teal) and do not carry (% no deletion, in red) the sequence deletion in mouse and human heart and brain.

4. Analysis of the *Cis*-Regulatory Function of the First Intron of the KChIP2 Gene

In contrast to the generally compact gene structure of KChIP2, the first intron (called "Intron1" henceforward) is large and represents more than half of the whole gene transcription unit (Fig. 2C). To identify the presence of *cis*-regulatory elements, regions of Intron1 were isolated and inserted upstream of the full length proximal KChIP2 promoter region, which, in turn, is upstream to the luciferase reporter gene in the construct. As shown in previous paragraphs, the *cis*-regulatory activity of each construct was then measured as luciferase activity in rat neonatal cardiomyocytes or cortical neurons.

Based on sequence conservation, we identified two conserved regions (in1A and in1B) in Intron1 (Fig. 2C). The relatively conserved nature of these two regions indicates that they are likely to be the most important *cis*-regulatory regions in Intron1. We made plasmid DNA constructs containing either of these regions and the proximal KChIP2 promoter upstream from the luciferase reporter gene for mouse and human (Fig. 15A&B). For the guinea pig, only the in1A region was studied due to failure in amplifying the 1B region.

Surprisingly, Intron1 seemed to have a general inhibitory effect on KChIP2 promoter activity in the heart (Fig. 15C). The inhibitory effect of in1A was particularly strong in all three species. In1B caused a dramatic decrease in mouse KChIP2 promoter activity and a more modest but significant decrease in human. Interestingly, insertion of either region of Intron1 eliminated the mouse-human differences in promoter activity.

A speculation about the function of Intron1 is that it may contribute to evolution of tissue specificity of the KChIP2 gene expression. To test this hypothesis, the *cis*-regulatory function of the Intron1 clones was assayed in neurons. Intron1 function in the brain was dramatically

different from the one in the heart (Fig. 15D). In all three species, none of the intronic regions tested caused any change in *cis*-regulatory activity.

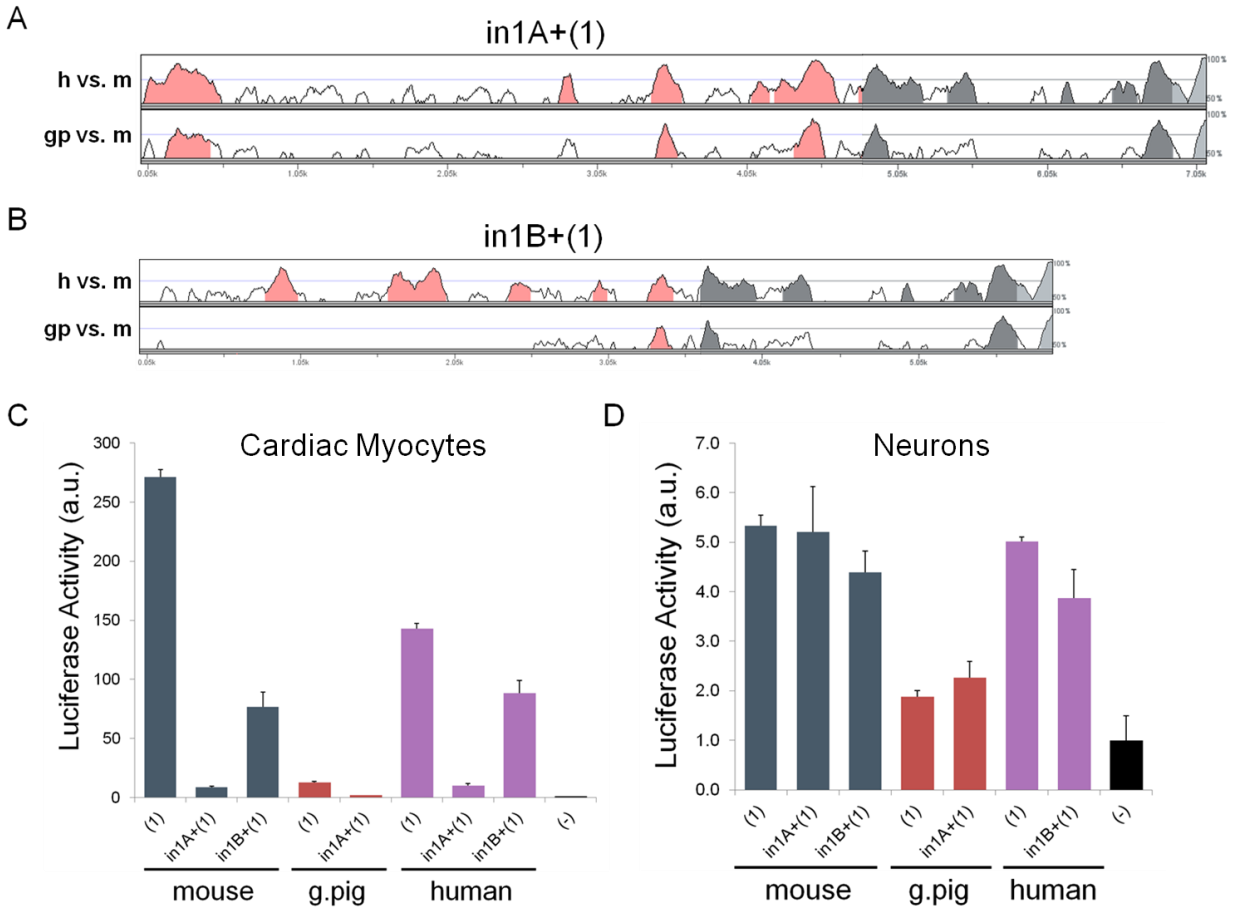

Figure 15. Analysis of the KChIP2 Intron1 *cis*-regulatory function in the heart and brain

(A, B) Vista alignment of human (top) and guinea pig (guinea pig, bottom) Intron1 clones, using mouse as the reference sequence. The intron portion is colored pink and the 5'-proximal promoter region is colored teal. (A) Clones containing the in1A region upstream of the 5'-proximal promoter region. (B) Clones containing the in1B region upstream of the 5'-proximal promoter region. (C, D) Comparison of the *cis*-regulatory activity of the Intron1 clones for mouse, guinea pig and human in an *in vitro* luciferase assay in cardiac myocytes (C) and neurons (D). Results for the different species are labeled in different colors (mouse - teal, guinea pig - red, human - purple). Error bars are SEM (n=3).

5. Transcription Factor Modulation of KChIP2 *Cis*-Regulatory Function

The transcription factor Irx5 has been shown to be responsible for determining the transmural gradient in expression of the Kv4.2 gene in mouse by inhibiting expression of this gene in the endocardium (Costantini et al. 2005). Moreover, He et al. (2009) showed that Irx5 inhibits the rat Kv4.2 promoter function *in vitro* at a low concentration of the transcription factor but not at higher concentrations. We have confirmed these results on our mouse Kv4.2 proximal promoter clone (Fig. 16A).

Since the transmural gradient in Irx5 expression is conserved in different mammalian species (Rosati et al. 2006), we hypothesized that Irx5 could determine the transmural gradient in KChIP2 expression in larger mammals, where this gene is responsible for the transmural gradient in I_{to}, rather than Kv4.2, which is not expressed in the hearts of these species (Dixon et al. 1996; Rosati et al. 2001). In particular, we tested whether Irx5 could inhibit the KChIP2 promoter activity, similarly to its effect on the expression of the Kv4.2 gene. At difference with what we expected, Irx5 increased human KChIP2 *cis*-regulatory activity in a dose-dependent manner (Fig. 16B).

Irx3 is another member of the Iroquois family of transcription factors and, similarly to Irx5, is expressed in a transmural gradient, which is opposite to that of KChIP2 (Rosati et al., 2006). We tested whether this transcription factor contributed to the gradient in KChIP2 gene expression and found that, although in a dose-independent manner, Irx3 expression also causes an increase in the human KChIP2 *cis*-regulatory activity (Fig. 16 C).

Interactions inside the Iroquiois family of transcription factors had been reported (He et al. 2009) and the loss of Irx3 was shown to antagonize the effect of Irx5 deletion (Gaborit et al.

2012). It is of interest to test the effect of the two factors in combination. Consistent with the enhancing effect observed individually, Irx3 and Irx5 in combination also caused an increase in *cis*-regulatory activity (Fig. 16D). In this case, addition of Irx3 seems to null the dose-dependent effect of Irx5, as increasing the concentration of both factors at the same time does not result in additional increases in promoter activity.

The transcription factor FoxP2 is expressed in a transmural gradient in rodent hearts which has the same direction as the KChIP2 gradient and is therefore a candidate as a positive regulator of the KChIP2 gene expression. As expected, we observed a modest, dose-independent increase in KChIP2 promoter activity when FoxP2 was coexpressed with the KChIP2 promoter in neonatal cardiac myocytes (Fig. 16E).

As FoxP2 displays an opposing transmural gradient expression to that of Irx3 and Irx5, it is of interest to test whether it interacts with the other two factors or not. Consistent with the independent assay results, combination of the three transcription factors resulted in an increase in KChIP2 promoter activity (Fig. 16F).

Clearly all three transcription factors are interacting with the proximal promoter region of the KChIP2 gene by affecting its transcriptional activity (Fig. 16B-F). However, both the Irx3 and Irx5 have an effect opposite to what is expected from the *in-vivo* expression pattern (Rosati et al. 2006). It is therefore suspected that these transcription factors may have additional interacting *cis*-regulatory regions. The Intron1 regions were shown to be important for other aspects of KChIP2 function (Fig. 15) and may as well be a candidate region for the additional interactions. As a result, the effect of all three factors on the transcriptional activity of clones containing both the Intron1 and the proximal promoter regions are tested. Interestingly, the enhancing effect remained when the Intron1 regions are included (Fig. 16F). This result confirms

the enhancing effect of these transcription factors on KChIP2 *cis*-regulatory activity and also suggests that the Intron1 is probably not affecting the interaction of the transcription factors with the KChIP2 proximal promoter region.

The transcription factor Klf15 was found to control rhythmic cardiac KChIP2 expression by positively affecting the transcriptional activity of rat KChIP2 proximal promoter in the heart (Jeyaraj et al. 2012). In order to confirm this finding and to test whether the effect of Klf15 on KChIP2 expression are species-specific or can, conversely, be extended to other species, particularly human, we analyzed the effect of Klf15 on both mouse and human KChIP2 proximal promoter region (Fig. 16G). In keeping with the Jeyaraj et al. findings, Klf15 increased KChIP2 *cis*-regulatory activity in a dose-dependent manner in both mouse and human. This suggests that Klf15 does not contribute to the species-specific variation in KChIP2 expression, but rather has a conserved physiological role that is likely to be important in all species.

The Klf15 results confirmed that the KChIP2 cis-regulatory region can respond to know modification factors similar to physiological conditions. But none of the transcription factors tested above contributed to the species-specific differences. Although transcription factor prediction programs tend to give too many false positives, the small number (eight) of nucleotide changes between mouse and gerbil allows the bioinformatics tools to be useful. I searched the 123 base pair region *b'* in TRANSFAC database and it gave 133 and 147 predicted binding sites for mouse and gerbil, respectively. A total of 18 sites were identified to be different between the two species. They were mapped to the *b'* region, as shown in Figure 17.

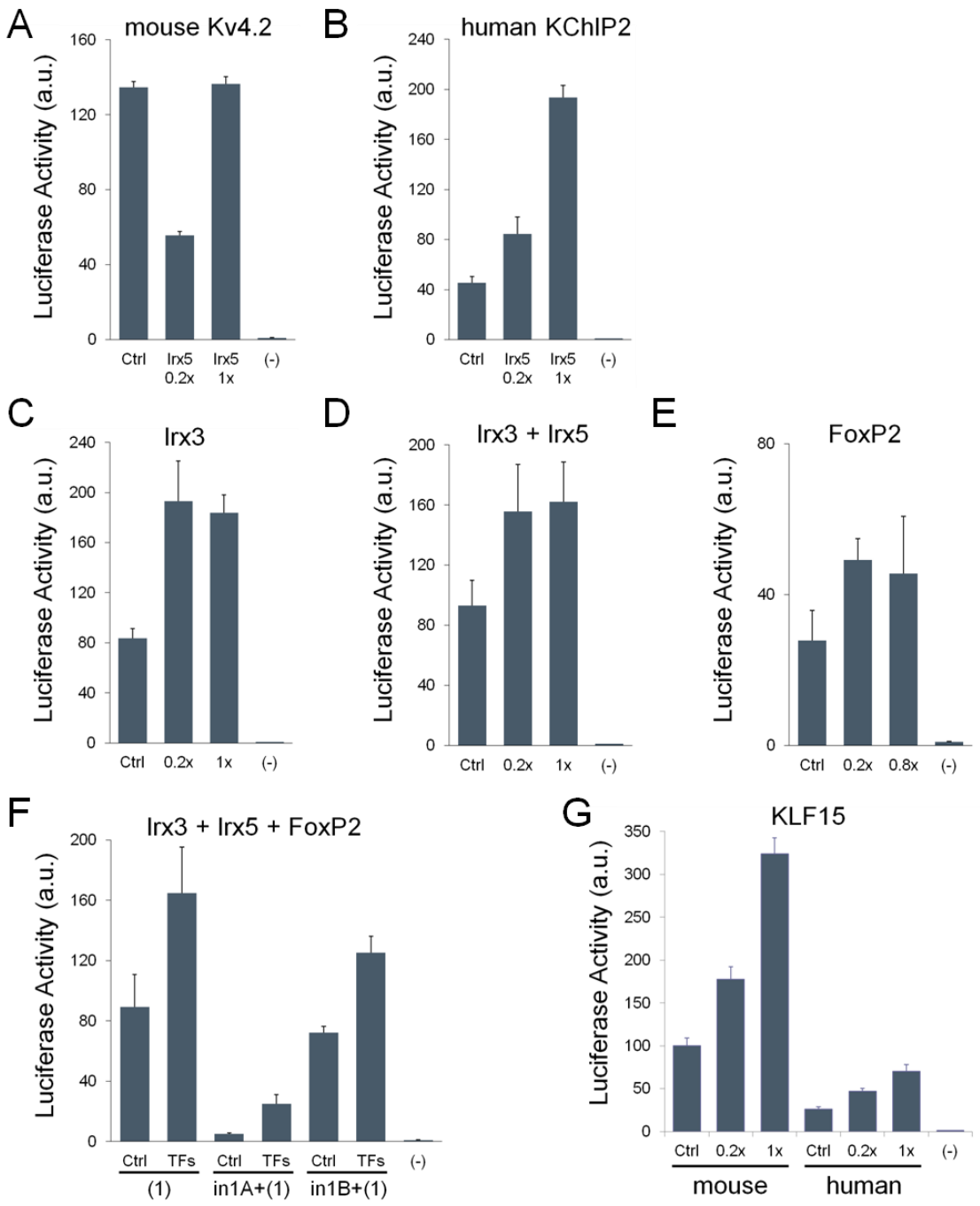

Figure 16. Modulation of the promoter activity by transcription factors

(A-B) Effect of Irx5 on mouse Kv4.2 (A) and human KChIP2 (B) proximal promoter *cis*-regulatory function. (C-G) Effect of various transcription factors or transcription factor mixtures on human KChIP2 *cis*-regulatory function: (C) Irx3; (D) mixture of Irx3 and 5; (E) FoxP2; (F) mixture of Irx3, Irx5 and FoxP2; and (G) KLF15. All the tests used the 5' upstream proximal promoter region. In (F), the intron clones are also included. In (G), effects on the mouse proximal promoter are also tested. Error bars are SEM (n=3).

A

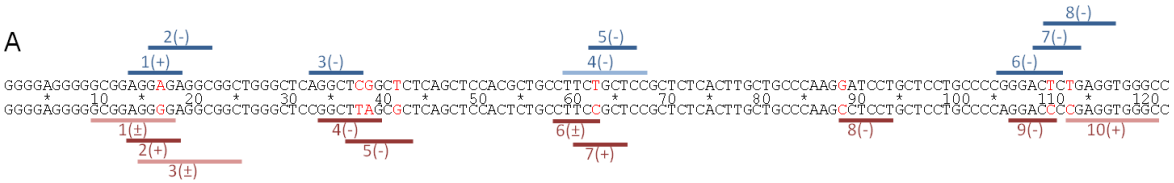

B

Index	TRANSFAC Identifier	Position	Strand	Mismatches	Score	Binding Factors	Sequence
1	MOUSE$PCP2_01	14	(+)	0	100	RXR-beta, T3R-alpha1, T3R-beta1	AGGAGA
2	MOUSE$AACR_02	16	(-)	0	100		GCCTCTC
3	HS$APOB_11	33	(-)	0	100	LF-A1	GAGCCT
4	RAT$GSTP_07	60	(-)	1	87.5	NF-1A, SF-A	GGAGCAGGA
5	RAT$VEGF_02	63	(-)	0	100	ER-alpha, ER-beta	GAGCA
6	HS$EGFR_12	106	(-)	0	100	RPF1, Sp1	GAGTCCC
7	RAT$POMC_03	110	(-)	0	100	GR	CAGAG
8	HS$M2DRA_01	111	(-)	0	100		ACCTCAGA

C

Index	TRANSFAC Identifier	Position	Strand	Mismatches	Score	Binding Factors	Sequence
1	HS$AAC_10	9	(+)	1	88.89	Sp1	GGGGGAGGGG
	HS$MIP_03	10	(+)	1	87.5	Sp1	GGGGAGGGG
	HS$ZG_06	10	(-)	1	87.5	Sp1	CCCCTCCCC
	HS$NPY_04	12	(-)	0	100	Sp1	CCCCTCC
	HS$GPC_06	13	(-)	1	90	Sp1	CCCCTCCCCTC
2	MOUSE$AQP7_01	14	(+)	0	100	PPAR-alpha, PPAR-gamma, RXR-alpha	AGGGGA
3	HS$TPI_01	15	(+)	1	90	Sp1	GGGGCGGCGGC
	HS$PFKM_03	15	(+)	1	88.89		GGGGAGGAGG
	HS$MIP_03	15	(+)	1	87.5	Sp1	GGGGAGGGG
	HS$ZG_06	15	(-)	1	87.5	Sp1	CCCCTCCCC
	HS$AAC_13	15	(-)	1	90	Sp1	GCCCCCTCCCC
4	RAT$POMC_15	34	(-)	0	100	Otx1, Otx2, Pitx1, Pitx3	CTAAGCC
5	HS$E2F2_05	37	(-)	0	100	E2F	GCGCTAA
6	XENLA$RPL14_01	59	(+)	0	100	HrpF, XrpFI	CTTCC
	MOUSE$RPL32_01	59	(-)	0	100	f(alpha)-f(epsilon), HrpF, XrpFI	GGAAG
	HS$TNFA_02	59	(-)	0	100		GGAAG
	HS$TNFA_03	59	(-)	0	100		GGAAG
7	HS$EGFR_16	61	(+)	0	100		TCCGCT
8	HS$AACS_02	89	(-)	0	100	ARP-1	AGGAGG
9	HS$HH4_02	107	(-)	0	100	H4TF-2	GGTCC
10	HS$GFAP_04	113	(+)	1	88.89	AP-1, AP-2alphaA, AP-2alphaB, NF-1	CGGGGTGGGC

Figure 17. Predicted transcription factor binding sites in mouse and gerbil *b'* region

(A) Location of predicted transcription factor binding sites in mouse (top) and gerbil (bottom) sequence of region *b'*. The eight nucleotides that are different between gerbil and mouse/rat were colored red. Predicted transcription factor binding sites (data from TRANSFAC database) are marked by blue (mouse) or red (gerbil) bars. Each binding site is labeled on top (for mouse) or underneath (for gerbil) with the index number and the strand. (+): the sense strand; (-): the negative strand). The detailed annotations of each binding site are listed in (B) and (C). (B) Transcription factor binding sites that are present in mouse but not gerbil. (C) Transcription factor binding sites that are present in gerbil but not mouse.

DISCUSSION

The highly variable pattern of the KChIP2 gene expression in mammalian hearts provides an ideal system for the study of the evolution of gene regulatory function. In the previous chapter, we identified the general mechanism for the evolution of cardiac KChIP2 expression. In this chapter, further aspects of the KChIP2 regulatory function were studied and new insights were gained about the mechanism of the evolution and regulation of this gene.

First, more species were included in the comparison of the KChIP2 CpG island function and nucleotide level changes were identified to contribute to evolution of KChIP2 gene expression. The initial comparison between mouse and guinea pig KChIP2 CpG island suggested that the species specific effects are evenly distributed across a ~350 bp region (*a*+*b*+*c*, *Chapter 3*, Fig. 4C&D), which is still too broad for the search of specific transcription factor binding sites. According to Rebeiz et al. and Frankel et al., identification of specific nucleotide changes are possible if closely-related species can be used (Rebeiz et al. 2009; Frankel et al. 2011). Fortunately, the rapid evolution of KChIP2 *cis*-regulatory function (*Chapter 3*, Fig. 5A) in rodents provides the opportunity to achieve such a goal. By comparing the CpG island function in more closely related species such as hamster and gerbil using swap experiments, I showed that a ~120bp region (region *b'*) was most important for the variation of KChIP2 expression in the muroid clade (Fig. 6, 7 & 9). And strikingly, only eight nucleotides in the mouse-gerbil comparison are responsible for the majority of the changes in *cis*-regulatory function (Fig. 9). This finding is promising as it will allow us to identify the potential transcription factors whose binding sites changed during mammalian evolution (Fig. 17).

Besides the swap experiments which identified nucleotide-level changes for KChIP2 evolution, single-nucleotide mutation experiments were carried out to investigate the *cis*-regulatory function of the CpG island promoter. A few findings were made and they were summarized as follows.

(1) Mutation of six nucleotides in the mouse CpG island to the hamster version caused a significant decrease of the mouse *cis*-regulatory activity, bringing it closer to the KChIP2 promoter activity in hamster (Fig. 6). These six nucleotides either overlap with or locate close to the eight-nucleotides identified in the mouse-gerbil swap experiments (Fig. 5 & 9A). As a transcription factor recognition motif is typically 6-20 bp long (Bilu and Barkai 2005; Zambelli et al. 2012), there are various ways of affecting a transcription factor event (which determines the transcriptional output) by changing one or multiple the nucleotides in the recognition sequence (Spivakov et al. 2012; Whitfield et al. 2012). However, this does not mean that transcription factor binding is generally sensitive to any variation in its recognition sequence. Instead, there is a position weight matrix used to describe the binding preference at a specific nucleotide position inside the recognition motif (Stormo 2000; Whitfield et al. 2012). Some positions are strongly selective while the others can be highly tolerant to variations (Spivakov et al. 2012; Vernot et al. 2012). Changes at nucleotide positions that are non-selective will not result in a change in function. This also partly explains the failure of the correlating six mutations in hamster in showing a corresponding change in transcriptional activity (Fig. 7D).

(2) Despite the lack of effects in mouse and human, a two-nucleotide mutation in a potential Sp1 recognition site can partially recover the KChIP2 promoter function in the guinea pig heart (Fig. 9). Correlated with the distinct low level of promoter function, the guinea pig KChIP2 CpG island sequence is most distant to mouse and rat among all the other mammalian

species. In comparison to other species, there are large changes inside the guinea pig sequence including large deletions and insertion (Fig. 3). It is therefore striking that a two-nucleotide change could be identified to have a noticeable effect on the CpG island function. Although the result in guinea pig confirms the enhancing effect of the Sp1 binding element (Kaczynski et al. 2003), it does not necessarily mean that this predicted binding site is functional in mouse and human, given the fact that a prediction program usually gives too many false positives by simply matching the DNA motifs in the genome (Won et al. 2010). The loss of the predicted Sp1 binding site in mouse did not result in any change in *cis*-regulatory activity and there is a contradicatory increase of activity in human after the mutation possibly by influencing nearby transcription factor interations.

(3) Single nucleotide variation at two human SNP sites was shown to cause significant differences in promoter activity (Fig. 10) and may contribute to individual variability in cardiac electrophysiology phenotype in the human population. SNPs inside the coding regions, particularly the ones that cause nonsynonymous mutations, has been extensively characterized and implicated in human disease (Walsh and Engle 2010). Although 88% of the variations identified by genome wide association studies are located in regulatory regions (Hindorff et al. 2009), these SNPS are poorly studied due to the difficulty in identifying the functional output and resulting phenotype (Boyle et al. 2012). However, recent advances of high-throughput sequencing-based whole genome studies have associated a large number of such SNPs to functional changes revealed by ChIP-seq, DNaseI hypersensitivity, chromatin state and expression information (Boyle et al. 2012; Schaub et al. 2012). Consistent with these general findings about the importance of SNPs inside the regulatory region in human disease and individual variation, the two SNPs inside the KChIP2 CpG island was found to cause a

functional change by affecting the expression of the gene. Given the importance of KChIP2 in cardiac electrophysiological function (Sah et al. 2003; Jeyaraj et al. 2012), these SNPs may also be a substrate for the individual variations in human cardiac disease susceptibility.

Another interesting aspect about the CpG island is the conserved 5'-UTR (cUTR). Although it does not contribute to species-specific differences in cardiac KChIP2 expression (Fig. 4, 6, 7 &8, and *Chapter 3*, Fig. 4C&D), we found that it has a dramatic impact on the overall promoter activity of KChIP2. Deletion of the majority of the 5'-UTR caused a dramatic increase in *cis*-regulatory activity (up to 14-fold) in all species tested (Fig. 9C), which indicated an unusually strong inhibitory effect from this region. This effect could be caused by either transcriptional or post-transcriptional mechanisms, as on one hand, the 5'-UTR is frequently found to contain *cis*-regulatory elements for transcription factor binding (Amrolia et al. 1995; Tang et al. 1997; Bianchi et al. 2009; Minervini et al. 2010), and on the other hand, the 5'-UTR is crucial in post-transcriptional regulation of gene expression "through the modulation of nucleo-cytoplasmic mRNA transport, translation efficiency, subcellular localization and message stability" (Mignone et al. 2002; Pesole et al. 2002). In addition, a special sequence feature was identified in this region – a GC-rich inverted repeat (IR) – that can potentially form a highly stable stem-loop structure. The stem-loop structures are known to be capable of affecting protein expression through various transcriptional and post transcriptional mechanisms (Pelletier and Sonenberg 1985; Baim and Sherman 1988; Emory et al. 1992; Bevilacqua and Blose 2008; Scott et al. 2009). This naturally leads us to hypothesize that formation of the secondary structure is the mechanism of inhibition from the 5'-UTR. Consistent with the inhibitory role of the UTR, deletion of the IR caused a non-species specific increase in KChIP2 *cis*-regulatory activity (Fig. 11). Disruption of its potential secondary structure also caused a non-species specific increase in

KChIP2 *cis*-regulatory activity (Fig. 12), however, with a much smaller size of change. To summarize the experiments (Fig. 9, 11&12), the size of change displayed a pattern like this: deletion of cUTR > deletion of IR > inversion of IR. The limited effect by the disruption of the potential secondary structure suggests that formation of stem-loop structure is not the mechanism for inhibition from the 5'-UTR. It is not yet clear how the cUTR exerts an inhibitory function on the regulation of KChIP2 gene expression, although the increasing size of effect with increasing size of sequence deletion (from the shorter IR to the longer cUTR) could suggest a transcriptional mechanism that quantitatively more of the repressive transcription factor binding sites were deleted in larger sequence deletions. Further experiments need to be done to show whether the changes were caused by transcriptional or post-transcriptional mechanisms.

Interestingly, the IR seems to be deleted in some of the KChIP2 mRNA transcripts in a species- and tissue-specific fashion (Fig. 13). It is not clear how this cleavage of RNA inside the 5'-UTR is produced. It looks like tissue-specific splicing but it is highly unlikely to be so, as no splice sites were observed at either end of the sequence and it lacks additional features to serve as an alternatively spliced intron (Tarn and Steitz 1997; Wu and Krainer 1999; Matlin et al. 2005). There are other reported RNA cleavage mechanisms such as riboswitches that usually reside in the 5'-UTR and some of which have self-cleavage activity (Mandal and Breaker 2004; Roth and Breaker 2009) and miRNA and siRNA-mediated RNA cleavage (Meister et al. 2004). Further experiments need to be done in order to clarify the underlying mechanisms.

Further, we extended the study of the KChIP2 *cis*-regulatory activity to regions outside the proximal promoter. In particular, we found Intron1 responsible for the tissue-selective expression of the KChIP2 gene. This region has a very strong inhibitory effect on KChIP2 promoter function in the heart (Fig. 15C) but no inhibition of the promoter activity was observed

in the brain (Fig. 15D). Up to this point, all the potentially important KChIP2 *cis*-regulatory regions were explored (see *Results*, paragraph 1) and the overall mechanisms for *cis*-regulation of KChIP2 gene expression were elucidated. For the two tissue types where KChIP2 is expressed, the cardiac expression is mainly controlled by the CpG island inside proximal promoter region (Fig. 1) and the neuronal expression is more complicated, requiring additional regulation from the Intron1 (Fig. 15).

Finally, we tested the function of several transcription factors on the mouse and human KChIP2 *cis*-regulatory sequences. These factors (Irx5, Irx3, FoxP2, Klf15) were known to modulate the cardiac electrophysiological function, possibly through interactions with KChIP2 (Costantini et al. 2005; Rosati et al. 2006; He et al. 2009; Gaborit et al. 2012; Jeyaraj et al. 2012). The assay results confirmed that these factors do interact with KChIP2 (Fig. 16) and indicated the importance of KChIP2 in mediating the modulation of cardiac function by transcription factors. Particularly, the KChIP2 proximal promoter region responded to the modulation of Klf15 (Fig. 16G), in accord with the physiological responses *in-vivo* (Jeyaraj et al. 2012). This confirms the functionality of our KChIP2 proximal promoter constructs. Together with their ability to reflect the *in-vivo* expression level of this gene (Fig. 1), the KChIP2 proximal promoter construct can be a valid *in-vitro* model for studying the cardiac regulation of KChIP2 gene. On the other hand, the unexpected responses towards Irx3 and Irx5 (Fig. 16B, C, D&F), the transcription factors that are important for the establishment of transmural expression gradient of ion channels and currents (Costantini et al. 2005; Gaborit et al. 2012), opened more questions regarding the mechanism for the establishment of KChIP2 and I_{to} regional variation in human hearts.

In conclusion, this chapter provides a more complete picture about the transcriptional regulation of the KChIP2 gene but also set up the foundational work for future studies. This gene has the following three features that made it valuable to study: the highly variable species-specific expression pattern, the dramatic tissue-specific variation between heart and brain, and the regional variation within the mammalian myocardium. For each of the features, this chapter opened a new scope to study. First, the rapid evolution of KChIP2 in the muroid clade provides an unprecedented opportunity to identify individual nucleotides and specific transcription factor binding sites that changed in closely related species. Secondly, identification of the Intron1 as the additional contributor of tissue-selection expression require further work to dissect out more specific *cis*-regulatory elements inside this region. Finally, the validity of the KChIP2 proximal promoter region as a model for studying KChIP2 gene regulation allows future pursuit of the mechanism of KChIP2 and I_{to} gradient expression in large mammals like the human.

Chapter 5

Regulatory Evolution of Other Ion Channel Genes: HCN4, Kv4.3 and SERCA

INTRODUCTION

As described in *Chapters 1 and 2*, the heart rate and ventricular action potential duration are scaled in mammals, in order to maintain an adequate level of blood pressure for effective tissue perfusion. In the present Chapter, I am reporting some preliminary results on the investigation of possible molecular mechanisms by which the scaling of these cardiac electrophysiological traits is achieved. These experiments are to be seen as a continuation of the work described in *Chapter 2* and are part of an ongoing work.

The heart rate is dictated by a small cardiac region known as the sinoatrial node (SAN). The classical pacemaker current is known as the hyperpolarization-activated cation current ("funny" current, I_f), which plays an important role in the generation of rhythmic electrical activity in the heart (DiFrancesco 2010). It depolarizes the cell in response to hyperpolarization at the end of the action potential phase and causes diastolic depolarization of the SAN cells (DiFrancesco et al. 1986; Baruscotti et al. 2010). There has been some controversy over what constitutes the primary pacemaker current in the SAN (Bers 2006; Barbuti and DiFrancesco 2008; Lakatta et al. 2008). It appears most likely that the coordinated action of multiple different membrane currents as well as intracellular calcium metabolism contribute to normal pacemaking (Tellez et al. 2006; Mangoni and Nargeot 2008). The distributed nature of pacemaker function in the SAN is illustrated by the fact that knockout of the HCN4 gene, which eliminates approximately 75% of the I_f current, the textbook pacemaker current, does not result in complete loss of pacemaking function in mice, although there is significant disruption of this function (Herrmann et al. 2007). Despite this controversy, it is clear that the I_f current is critical in the

pacemaking function. We decided to first focus on studying the role of this current in the scaling of heart rate.

The duration of the diastolic depolarization determines the heart rate and therefore changing the pacemaker current would be an efficient mechanism to achieve scaling of heart rate. In particular, a smaller I_f would be expected to result in a more slowly depolarizing membrane potential during the diastolic interval, producing a reduced firing frequency in SAN cells and hence a slower pacing rate, typical of larger mammals. Therefore, we hypothesized that larger mammals have a smaller I_f than smaller mammals and that the smaller size of this current is determined by a lower levels of gene expression. The hyperpolarization-activated cyclic nucleotide-gated (HCN) channels are the molecular basis for I_f (Ludwig et al. 1998; Shi et al, 1999; Baruscotti and Difrancesco 2004). In this chapter, I will present an analysis of the evolution of the *cis*-regulatory function of HCN4, which contributes to the majority of the I_f current in the SAN (Shi et al. 1999).

A different set of currents are changed for the scaling of ventricular action potential, some of which have been discussed and studied in *Chapter 2*. One notable feature is that the repolarization phase of the ventricular action potential varies dramatically in duration across mammals (*Chapter 2*, Fig. 2). One efficient mechanism to scale the ventricular action potential duration is changing the repolarization currents. As shown in *Chapter 2*, changes in the expression of Kv4.2-dependent I_{to} current and the Kv2.1-dependent I_{Kur} current are responsible for the generation of two distinct action potential morphologies – spike-and-dome and triangular. Moreover, for larger mammals with a spike-and-dome morphology, changes in the expression of KCNQ1 (underlying the I_{Ks} current) and KCNH2 (I_{Kr} current) genes contribute to the scaling of the action potential duration.

Among the repolarization currents, whose expression levels have changed among species during evolution, the I_{to} current is the one with the most heterogeneous molecular basis (see *Chapter 1*). Its underlying principal subunit (pore-forming subunit) varies between large mammals (Kv4.3 only) and small rodents (Kv4.2 and Kv4.3), and transmural expression of this current is determined by the principal (rodents) or the auxiliary subunit KChIP2 (larger mammals), depending on the species (except for the ferret, which has gradient expression of both the principal and auxiliary subunits) (Dixon and McKinnon 1994; Brahmajothi et al. 1999; Rosati et al. 2001; Patel et al. 2002). In *Chapters 2 and 3*, we have reported studies on two of the major components of I_{to}: Kv4.2 displays a stepwise expression pattern across mammalian species (*Chapter 2*) and KChIP2 displays a highly-variable pattern of expression (*Chapter 3*). We showed that *cis*-regulatory evolution is the mechanism for the species-dependent variation in the expression of both genes. In this chapter, I will report the analysis of the *cis*-regulatory function of the third component of I_{to} - the Kv4.3 gene.

Another way to achieve scaling of the action potential duration is by changing the duration of the plateau phase, which is controlled by the duration and size of Ca^{2+} influx in the myocyte (Hamilton and Ianuzzo 1991; Bers 2002; Su et al. 2003). When an excitation arrives, depolarization of the cell membrane opens the L-type calcium channels, which further triggers Ca^{2+} release through ryanodine receptors located on the membranes of the sarcoplasmic reticulum (SR). This release causes a dramatic increase of the cytosolic Ca^{2+} concentration, which switches on the contractile machinery in cardiac myocytes (Bers 2002). This whole process mediated by Ca^{2+} is known as “excitation-contraction coupling”. At the end of the action potential, the membrane potential is repolarized to resting level and the cytosolic Ca^{2+} is cleared by the Ca^{2+} uptake systems.

A larger Ca^{2+} influx and a slower or less efficient Ca^{2+} uptake would result in elongation of the action potential. As shown in *Chapter 1*, the main constraint determining the size of Ca^{2+} influx through the L-type calcium channels is not scaling of the action potential duration, but maintenance of the excitation-contraction coupling. In smaller mammals, the requirement for a shorter plateau phase in the presence of a larger L-type Ca^{2+} current, creates a demand for an increased Ca^{2+} uptake. This is accomplished by scaling expression of the sarcoplasmic reticulum (SR) Ca^{2+}-ATPase (SERCA) pump (Hamilton and Ianuzzo 1991; Hove-Madsen and Bers 1993; Su et al. 2003; Vangheluwe et al. 2005) via *cis*-regulatory evolution (*Chapter 1*, Fig. 6).

The SERCA2 (or ATPA2) gene encodes the SR Ca^{2+} ATPase, which pumps two Ca^{2+} ions into the SR at the cost of one ATP molecule. The SR Ca^{2+} ATPase, together with the Na^{+}/Ca^{2+} exchanger on the membrane (which exchanges one Ca^{2+} ion for three Na^{+} ions), actively maintain a low internal Ca^{2+} concentration which is critical for the normal function of the cell (Bers 2002; Clapham 2007). The SR Ca^{2+} ATPase is the dominant Ca^{2+} uptake system in the myocytes of all mammals (Bassani et al. 1994; Bers 2002). In smaller mammals, there is an increase of Ca^{2+} ATPase expression and thus an even greater role in Ca^{2+} uptake due to the requirement of more efficient uptake. Ca^{2+} ATPase is responsible for as high as 92% of total Ca^{2+} uptake in mouse in contrast to 70% in rabbit (Bassani et al. 1994). In this chapter, I will report a further analysis of the *cis*-regulatory function of the SERCA2 gene.

ANALYSIS OF THE CARDIAC EXPRESSION AND *CIS*-REGULATORY FUNCTION OF THE HCN4 GENE

The HCN4 gene encodes the pore-forming subunit for I_f in heart, with the highest expression in the SAN (Shi et al. 1999; Baruscotti and Difrancesco 2004; DiFrancesco 2010). It is a relatively simple gene, with no alternatively spliced transcripts detected. The whole transcription unit is 50kb. Analysis of the genomic sequence of this gene identified a CpG island in the promoter region (Fig. 1A), which appears to be more conserved than the rest of the non-coding region.

Electrophysiological recordings obtained in SAN cells from different mammalian species seem to confirm a decreasing trend in I_f expression with increasing body size (Fig. 1B), as we previously hypothesized. To test whether such species-dependent variation is caused by changes in the *cis*-regulatory function of the HCN4 gene, the *cis*-regulatory activity of the HCN4 upstream proximal promoter region was compared in mouse and human (Fig. 1A).

No change in the *cis*-regulatory function of this region was found between mouse and human (Fig. 1C). This suggests that the proximal promoter (including the CpG island promoter) by itself is not responsible for the species-dependent differences of this gene. It is likely that *cis*-regulatory elements located outside of this region contribute to the species differences in the expression of this current, which is quite probable, given the large size of the remaining upstream intergenic region (74kb total).

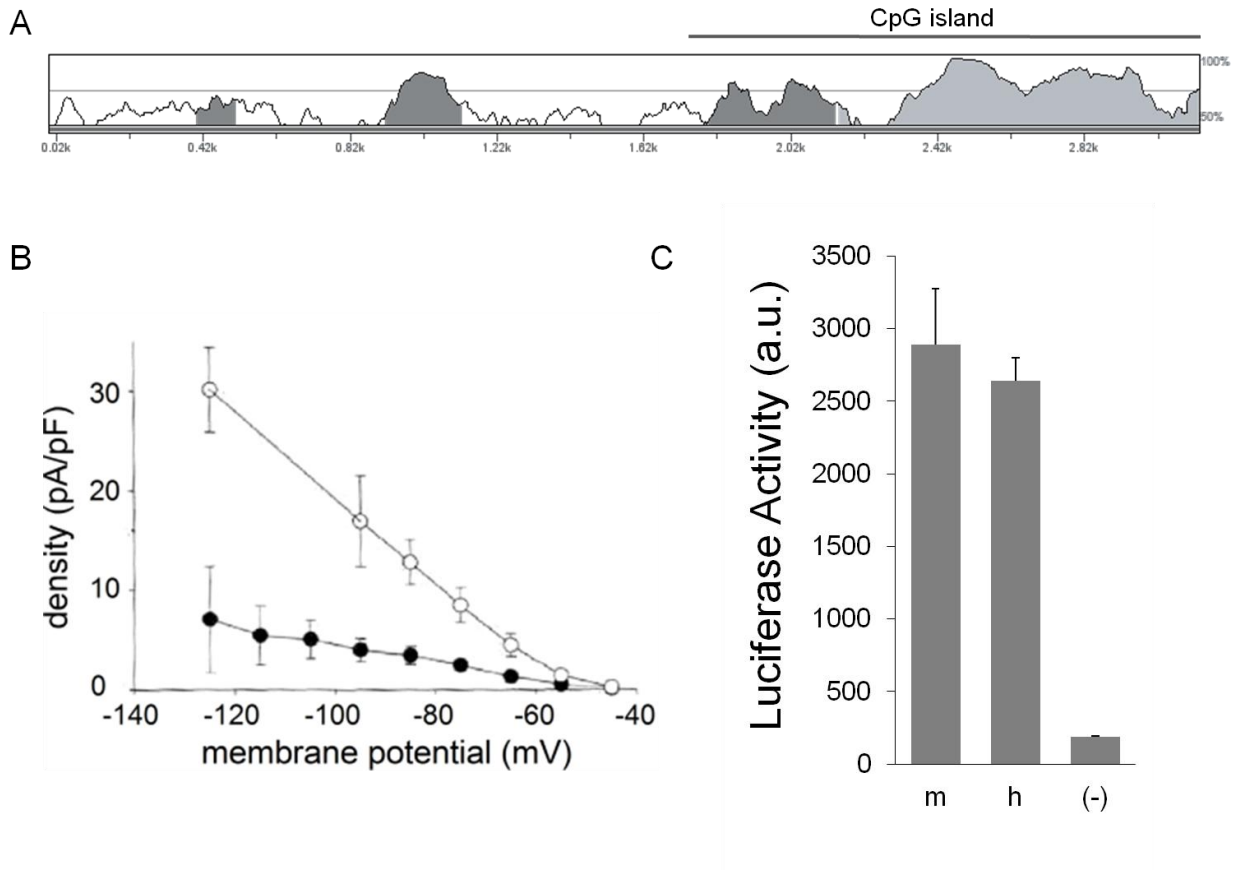

Figure 1. Sequence analysis, expression (current) and *cis*-regulatory function of the HCN4 gene

(A) Vista alignment of HCN4 5' upstream regulatory region of human and mouse. The CpG island region is marked. The sequences end immediately upstream of the initiator methionine codon in exon 1 of the gene (ATG). Conserved sequences in VISTA (70%/100 bp cutoff) are colored according to the annotation (UTRs - light gray and non-coding - dark gray). (B) Fully activated I-V relation for I_f in canine (filled symbols) and rabbit (open symbols) SAN cells. Error bars are SEM. Data are from 9 canine and 4 rabbit SAN cells (D. McKinnon, unpublished results). (C) Comparison of *cis*-regulatory activity of the mouse and human clones in an *in vitro* transcription assay. Error bars are SEM (n=3).

ANALYSIS OF THE CARDIAC EXPRESSION AND *CIS*-REGULATORY FUNCTION OF THE K_V4.3 GENE

Kv4.3 is the principal subunit underlying I_{to} in most mammals, except for small rodents that require a short triangular action potential and additionally express Kv4.2 in order to produce a large I_{to} current (Dixon et al. 1996; Patel and Campbell 2005; Niwa and Nerbonne 2010). Kv4.3 displays a highly variable pattern of expression across mammalian species (Fig. 2). Notably, in keeping with the lack of I_{to} current in guinea pig, expression of Kv4.3 in this species is extremely low. We sought to determine whether *cis*-regulatory changes were involved in the evolution of Kv4.3 expression.

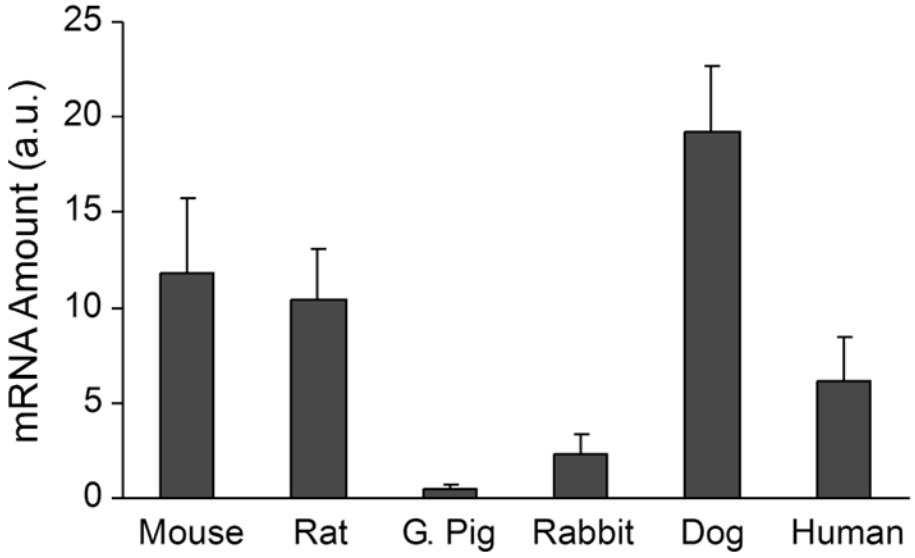

Figure 2. Kv4.3 mRNA expression in mammalian ventricles

Real-time PCR analysis of Kv4.3 mRNA expression in the left ventricular wall of six mammalian species. Histogram shows means ± SD (n = 3).

In order to perform this analysis, we studied the 5' upstream regulatory region of this gene. The Kv4.3 gene also has a CpG island promoter, in which three relatively conserved regions could be identified (Fig. 3A). For each species chosen for this analysis (mouse and guinea pig), three constructs containing three, two, or one of these regions were generated (Fig. 3B).

Consistently with the lower level of Kv4.3 mRNA expression in this species, the guinea pig promoter has much weaker *cis*-regulatory activity than the mouse one (Fig. 3C). Interestingly, progressive deletion of sequence in the 5' end of the first construct ("1" in Fig. 3B) did not result in any change in *cis*-regulatory activity, even when part of the CpG island was missing. As shown, the shortest conserved CpG island region ("3", Fig. 3B) determines most of the species-specific differences in Kv4.3 gene expression.

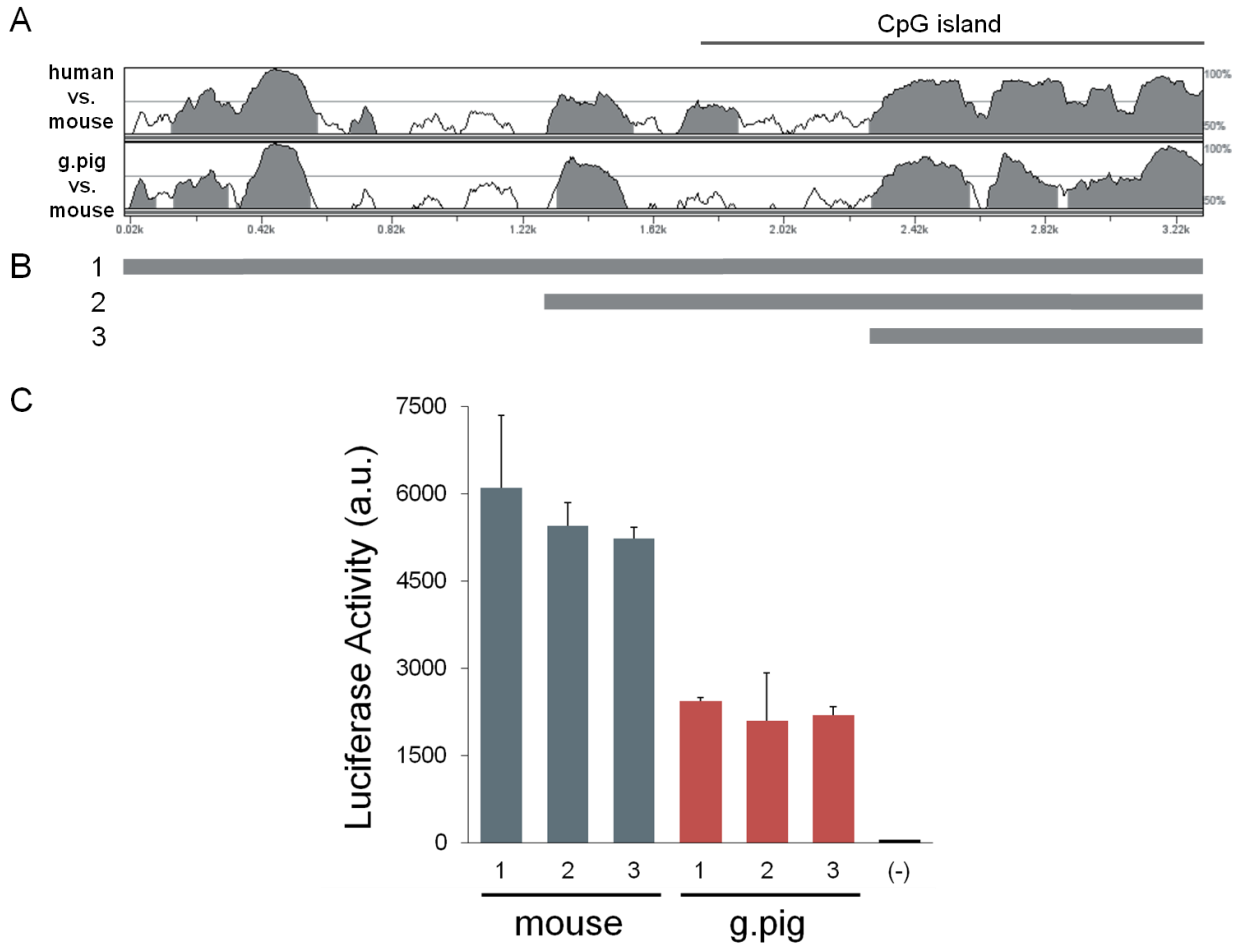

Figure 3. Analysis of Kv4.3 *cis*-regulatory function in mouse and guinea pig

(A) Vista alignment of Kv4.3 5' upstream regulatory region of human (top) and guinea pig (bottom), using mouse as the reference sequence. The CpG island region is marked. The sequences end at the first 5'-UTR of the gene in mouse (the human does not have this UTR). Conserved sequences in VISTA (70%/100 bp cutoff) are colored according to the annotation. (B) Clones used for 5' deletion analysis of the Kv4.3 proximal promoter function. (C) Comparison of *cis*-regulatory activity of the mouse (colored teal) and guinea pig (colored red) clones in an *in vitro* transcription assay. Error bars are SEM (n=3).

ANALYSIS OF THE C*IS*-REGULATORY FUNCTION OF SERCA2

The systematic variation of the SERCA2 mRNA expression with mammalian body size makes this gene a good candidate for studying the evolution of its *cis*-regulatory function (*Chapter 1*, Fig. 6A). The whole transcription unit of SERCA2 is 70kb, with 62kb upstream and 22kb downstream intergenic region. Interestingly, this gene also has a CpG island promoter (Fig. 4A).

Similarly to what was shown above for the HCN4 gene, we analyzed the *cis*-regulatory function of the upstream regulatory region, this time in mouse and human. In contrast to the marked differences in SERCA2 mRNA expression between the mouse and human ventricles, no significant difference in the promoter activity was observed for the tested regions (Fig. 4B). This was not entirely surprising, given that this is a relatively large gene with long intergenic and intronic regions. It seems clear that further and farther regions of the SERCA2A gene will need to be tested in order to identify *cis*-regulatory regions responsible of the species-specific changes in gene expression that occurred during evolution.

In addition, deletion of the 5' sequences ("2" versus "1" in Fig. 4A) did not result in a change in the level of *cis*-regulatory activity in both species, indicating the deleted region is not important for the species-specific changes. Notably, all clones have an activity level that is higher than the positive control (+), which is rare for most other genes tested (Fig. 4C). Although the promoter activity did not vary between species, its relatively high level of activity matches with the generally strong SERCA2 expression in mammalian hearts (Bers 2002).

The relatively high level of promoter activity in SERCA2 is an advantage for the dissection of its *cis*-regulatory function. The SERCA2 promoter is one of the strongest ion channel promoters that we have tested. Most ion channel gene promoters, for example, HCN4 and KChIP2, have a relatively lower level of promoter activity in comparing to the positive control (Fig. 4C). For some genes such as Kv4.2 and Kv2.1, their promoter activity is too low to be further studied, as the experimental noises can easily override the actual changes in signal. In contrast, SERCA2 is a promising gene to study given its advantage in the assay system, in addition to its importance in the scaling of action potential duration.

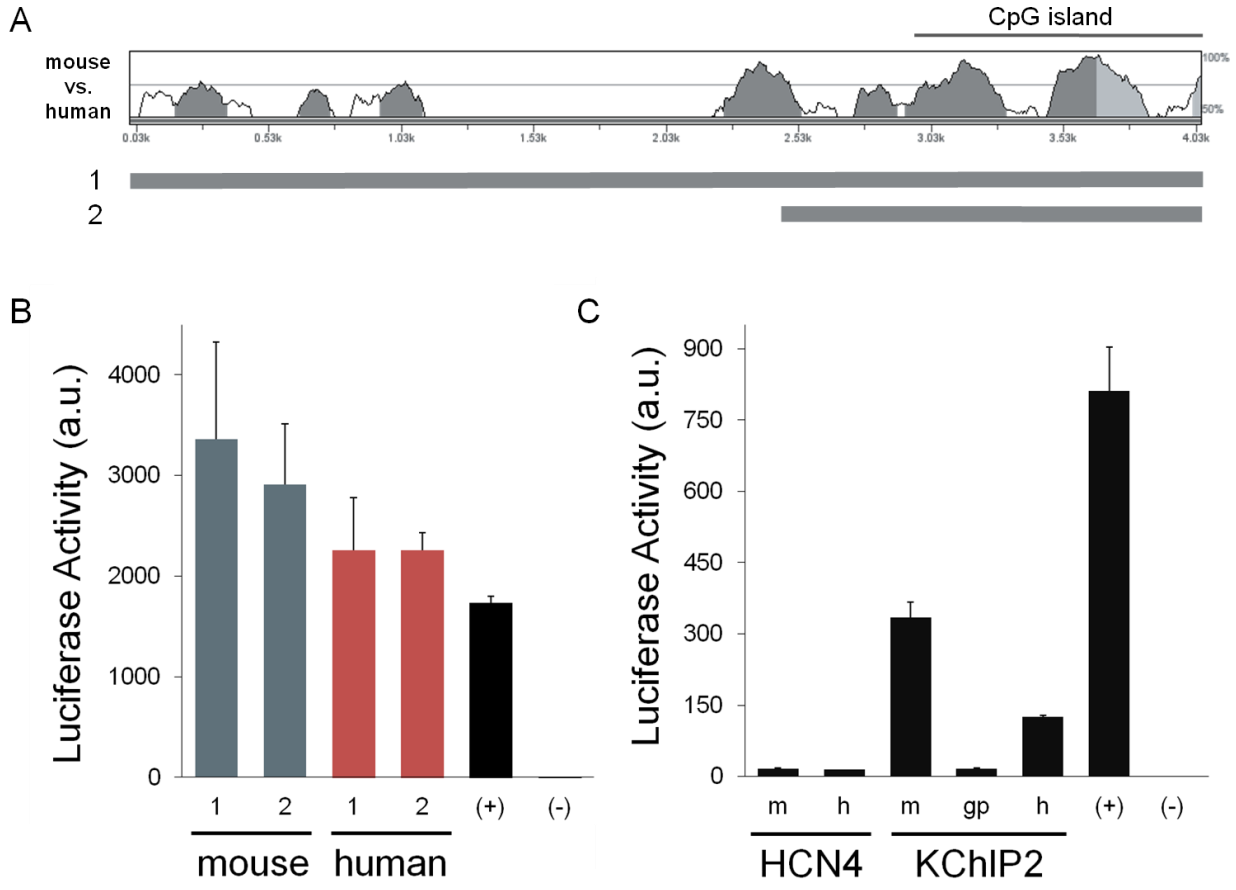

Figure 4. Analysis of SERCA2 *cis*-regulatory function in mouse and human

(A) Vista alignment of SERCA2 5' upstream regulatory region of mouse and human. The CpG island region is marked. The sequences end at a conserved location inside the 5'-UTR. Conserved sequences in VISTA (70%/100 bp cutoff) are colored according to the annotation (UTRs - light gray and non-coding - dark gray). The horizontal bars underneath the alignment pane show the location of clones used in the *in vitro* assay. (B) *Cis*-regulatory activity of the mouse (colored teal) and human (colored red) SERCA2 clones in an *in vitro* transcription assay. Error bars are SEM (n=3). (C) Comparison of *cis*-regulatory activity of the HCN4 and KChIP2 promoter clones with the positive control.

DISCUSSION

In mammalian evolution, scaling of cellular electrophysiology requires systematic changes in heart rate and action potential duration (Schmidt-Nielsen 1984; Rosati et al. 2008). To achieve such scaling, we showed in this chapter and *Chapter 2* that variations in the ventricular repolarization currents, pacemaker current, and calcium uptake system are three important physiological mechanisms used. Such physiological variations are in turn produced or contributed by regulatory changes of three ion channel and transporter genes respectively – Kv4.3, HCN4 and SERCA2. Analysis of the *cis*-regulatory function of these three genes is the topic of this chapter. All three genes are typical examples of regulatory evolution and we hypothesize that *cis*-regulatory evolution is also the predominant mechanism of evolution of the expression of these genes.

We showed here that the Kv4.3 gene is a clear example of *cis*-regulatory evolution. The changes in Kv4.3 *cis*-regulatory function between mouse and guinea pig matched with the cardiac mRNA expression of the gene in these species (Fig. 2&3). For HCN4 and SERCA2, the proximal promoter region by itself did not match with the mRNA expression variation among the species (Fig. 1&4). Given that we only analyzed an overall small portion of the intergenic and intragenic non-coding regions for the HCN4 and SERCA2 genes, larger and more distant regions need to be tested in order to identify the responsible *cis*-regulatory changes.

The larger size of the non-coding regions, including the CpG island, makes it more challenging to study the *cis*-regulatory function in these genes, compared to more compact genes such as KChIP2, and implies that regulation of their expression is more complex. Lenhard et al. classify the CpG island promoters into two categories: a ubiquitous type with short CpG islands,

usually associated with ubiquitously expressed genes and dispersed TSS distribution, and a developmentally regulated type with long CpG islands that associate with developmental genes and complex chromatin marks, including polycomb group proteins and H3K27me3 and H3K4me3 (Lenhard et al. 2012). The length of the CpG islands is a major difference in these two categories of promoters. It is suggested that the regulation of the latter gene type with long CpG islands is more complicated, usually involving a large number of enhancers and have diverse promoter states depending on the epigenetic modifications (Ernst et al. 2011).

As perhaps expected for such general categorizations, this classification does not fit perfectly with the genes we have analyzed. In fact the KChIP2 gene, which has a relatively short CpG island (586bp), is not ubiquitously expressed and, most strikingly in the mouse, does not have a dispersed TSS distribution (*Chapter 3*, Fig.1B). However, the inability of the upstream proximal promoter regions to recapitulate the expression levels of the HCN4 and SERCA2 genes, both belonging to the second type of CpG island promoter (CpG island sizes are 2108bp and 1735bp, respectively), does reflect the higher regulatory complexity of this category of promoters.

This seems an important result, as it contrasts with the new regulatory mechanism we have described for KChIP2. Studies on the mechanism of evolution of gene regulation had frequently identified distal enhancers as the mediator of regulatory changes (Carroll 2005; McGregor et al. 2007; Rebeiz et al. 2009; Chan et al. 2010). However, our studies on the KChIP2 gene had revealed a new mechanism for the evolution of gene regulation, which is primarily determined by the CpG island core promoter (*Chapter 3* & *Chapter 4*). It seems the evolutionary mechanism of HCN4 and SERCA2 has fallen into the classical category of

enhancer-mediated evolution and the core-promoter based mechanism is not valid for these genes.

The comparative genomics strategy, exclusively used in my dissertation research, facilitates identification and exclusion of unimportant *cis*-regulatory regions, based on sequence conservation. For example, both the 5'-deletion clones of Kv4.3 and SERCA2 successfully eliminated unnecessary regions based on this strategy (Fig. 3&4). However, for identification of distal elements, other techniques may be more effective and efficient. Recent advances on high-throughput sequencing-based whole genome DNase I hypersensitivity site analysis and transcription factor binding region analysis (ChIP-seq, which combines chromatin immunoprecipitation with high-throughput sequencing), provided a wealth of new information on the *cis*-regulation of the genome (Bernstein et al. 2012). A better understanding of the HCN4 and SERCA2 gene regulatory function and the identification of distant *cis*-regulatory elements for these genes can be achieved by a combination of the available whole-genome *cis*-regulatory databases and techniques with comparative genomics tools.

Chapter 6

Regulation of L-Type Calcium Channel

INTRODUCTION

The robustness of biological systems reflects the ability of the system to maintain normal function following a significant perturbation (Wagner, 2007). For the cardiac electrophysiological system, robustness corresponds to the ability to maintain stable electrical function and excitation-contraction coupling following pathological, pharmacological or genetic insults to the system. Two broad classes of mechanisms can potentially contribute to the robustness of biological systems.

One possibility is that feedback loops could monitor and maintain system states and actively respond to perturbation, as envisioned by classical control theory (Sauro, 2009). In principle, homeostatic feedback loops could act to maintain a specific state in electrophysiological systems, such as a particular action potential morphology or firing pattern, by regulating basal ion channel expression levels in a coordinated fashion. Such a mechanism requires very accurate monitoring of the state of the system in order to provide useful regulatory feedback (Liu et al, 1998). For the regulation of electrophysiological function and the expression of voltage-gated ion channels, only a limited amount of feedback information about the system state is available, primarily in the form of calcium fluxes, and this information may be inadequate to regulate the relatively large number of different components in the system (Rosati and McKinnon, 2004).

Alternatively, the networks that underlie a particular biological function could have evolved to be relatively stable in response to at least some perturbations and thereby maintain function without the requirement to accurately monitor the overall system state. In principle, the biosynthetic networks that underlie the expression of functional channels in the cell membrane

could function in this way (Rosati and McKinnon, 2004). Robust biosynthetic networks could act to maintain electrical stability by buffering channel expression levels during a variety of disturbances affecting mRNA or protein expression levels, without directly monitoring electrophysiological function.

Surprisingly, this second form of robustness appears to be relatively rare. Heterozygous null mutations of the SCN5A, KCNQ1, KCNH2 and KCNJ2 genes in humans all produce haploinsufficiencies due to destabilization of cardiac electrical function (Sanguinetti et al, 1996; Chen et al, 1998; Wang et al, 1999; Fodstad et al, 2004). Similarly, heterozygous knockouts of the SCN5A and KChIP2 genes in mice produce an approximately 50% reduction in the expression of the I_{Na} and I_{to} currents respectively, in cardiac myocytes (Kuo et al, 2001; Papadatos et al, 2002). Null mutations in one allele of multiple different ion channel genes expressed in mouse brain also result in significant reductions in basal channel expression or related impairments of electrophysiological function (Planells-Cases et al, 2000; Ahern et al, 2001; Osanai et al, 2006; Yu et al, 2006; Brew et al, 2007; Tzingounis and Nicoll, 2008). Although most ion channels have relatively complex biosynthesis pathways (Deutsch, 2003; Delisle et al, 2004), it appears that for many physiologically important channels there is no mechanism that acts to maintain stable basal channel expression levels following the loss of one allele.

It was argued previously that heterozygous knockouts of ion channel genes are a good system in which to study the robustness of basal ion channel expression *in vivo* (Rosati and McKinnon, 2004). A valid criticism of conventional knockout technology is that mutations that are present throughout the course of development can modify normal development and ion

channel expression, thereby confusing interpretation of the results seen in the adult. For this reason, we have used an inducible knockout system in the current study.

The Cav1.2 gene, which encodes the vast majority of the L-type calcium current in the adult heart (Bodi et al, 2005; Rosati et al, 2007), was chosen to study because prior studies suggest that expression of this channel is relatively robust in many pathophysiological conditions affecting ventricular function, at least in comparison to most other ion channels (Beuckelmann et al., 1991; Schroder et al, 1998; He et al, 2001; Chen et al, 2002; Piacentino et al, 2003; Tomaselli and Marban, 1999; Pitt et al, 2006).

MATERIALS & METHODS

Homozygote and Heterozygote Inducible Knockout Mice

Mice bearing two *loxP* sites flanking exon 2 of the Cav1.2 (CACNA1C) gene ("floxed" allele) have been described previously (White et al, 2008). These mice were bred with transgenic mice carrying a transgene comprised of an α-MHC promoter driving a tamoxifen-inducible Cre recombinase (Mer-Cre-Mer), which targets expression of this recombinase to the heart (Sohal et al, 2001). To simplify the production of mice for experimental analysis, mice homozygote for both the floxed Cav1.2 gene and the transgene ($Cav1.2^{f/f}$ and $Cre^{+/+}$) were bred. Homozygosity was confirmed by breeding the homozygous mice with wild-type animals and then verifying heterozygosity of the pups. Through selective breeding of these animals, mice that carried the Cre transgene and were either homozygous or heterozygous for the floxed $Ca_v1.2$ allele were obtained for the experiments.

There was no leakage of Cre activity and Cav1.2 gene recombination was undetectable in heart tissue prior to tamoxifen treatment. Recombination following tamoxifen treatment was cardiac tissue specific, and was not observed in non-cardiac tissues.

In the standard experimental protocol, Cav1.2 gene knockout was induced in 6-7 week-old mice of either sex by i.p. injection of approximately 100 μl of 10 mg/ml tamoxifen free base (Sigma T5648) in peanut oil (Sigma P2144) per day for 5 consecutive days. After the end of the injection period the mice were left for 2-3 weeks to allow for decay of mRNA and protein products from the targeted gene before subsequent analysis. This time interval was judged to be adequate based on the survival time of the homozygous mice (6.9 ± 3 days). This waiting period also allowed for wash-out of any acute effects of the tamoxifen treatment, if present.

For the study of Cav1.2 mRNA and protein decay times, the standard tamoxifen treatment protocol was modified in two ways in order to better synchronize gene knockout. The mice were placed on a soy-free diet for 1 week before receiving a single injection of tamoxifen (50 mg kg^{-1} day^{-1}). These two changes were taken in order to minimize the overlap between the tamoxifen treatment period and the decay of Cav1.2 protein. The soy-free diet may improve the effectiveness of the tamoxifen treatment, since it does not contain phyto-oestrogens, which means that the Cav1.2 protein decay time may not be directly comparable to the survival times observed using the standard protocol.

It has been suggested that induction of Cre recombinase expression (Koitabashi et al, 2009) can induce transient cardiomyopathy. Our lab obtained more efficient gene ablation than described in this report using a lower tamoxifen dose. Under our experimental conditions, no changes in calcium channel or auxiliary subunit gene expression were observed in tamoxifen treated Cre mice ($Cre^{+/-}$), nor were there significant changes in the expression of the calcium handling genes SERCA2A, phospholamban or NCX1 in the experimental mice (not shown). Notably, even in the tamoxifen treated heterozygous knockout mice there was no change in cardiac contractile function.

Genotyping

To assess the outcome of breedings, mouse genomic DNA was extracted from 2-3 mm long toe or tail biopsies using phenol extraction. To confirm genotypes in animals sacrificed for biochemical or electrophysiological experiments, genomic DNA was prepared from liver tissue using the DNeasy Tissue Kit (Qiagen).

Genotyping was performed using real-time PCR. This allowed to reliably rule out false positive results due to contamination of the PCR assay. The complete genotyping procedure consisted of separate assays to identify the knock-in ("floxed") allele, the wild-type allele and knock-out allele following recombination. The following primer pairs were used:

Cre recombinase:

3'CATTTGGGCCAGCTAAACAT 5' and 3'TAAGCAATCCCCAGAAATGC 5';

Cav1.2 knock-in allele:

3' GGGGGAACTTCCTGACTAGG 5' and 3' ATCTTTGGTTCAGGGATGCTT 5';

Cav1.2 wild-type and knock-out alleles:

3' GTTCCTGCAATAGCTTGAGGG 5' and 3' CATGGAGTCTGGGGGGAGGTC 5'.

Primers directed against the Kv1.2 gene were used as an internal control for normalization between samples (3' TGGCTTCTCTTTGAATACCCAGA 5' and 3' TTGCTGGGACAGGCAAAGAA 5'). A positive and a negative control sample were included in each experiment.

Echocardiography

Transthoracic echocardiography was performed in anesthetized animals (1-2% isoflurane) using a Vevo 770 ultrasound device (VisualSonics, Canada) with a 30-MHz transducer. The Vevo Measurement and Calculations software package was used to generate left ventricular measurements and calculations derived from the tracings of the collected echocardiographic data. The following parameters were obtained using M-mode transthoracic views: left ventricular end-systolic diameter (LVESD), left ventricular end-diastolic diameter

(LVEDD), ejection fraction (EF). Contractile function was calculated as fractional shortening = (LVEDD – LVESD)/LVEDD x 100%.

Analysis of Calcium Channel Subunit mRNA Expression

Analysis of mRNA expression was performed using real-time PCR as described in *Chapter 2* . For RNA isolation, mice were euthanized with halothane and the hearts were quickly removed. The left ventricular free wall and septum were dissected and frozen in liquid N_2. Total RNA was prepared using Qiagen RNeasy columns with DNase treatment. RNA samples were quantitated, re-diluted to give nominally equal concentrations and quantitated a second time using spectrophotometric analysis. Human RNA samples were obtained from two independent commercial suppliers (Ambion, Inc., Austin, TX, USA and BioChain Institute Inc., Hayward, CA, USA).

cDNAs were prepared from a starting RNA amount of 5 μg per sample. *In vitro* reverse-transcription was performed as described previously (Rosati et al, 2004). Real-time PCR was performed using the SYBR Green QuantiTect PCR Kit (Qiagen) with a 7300 Real-time PCR System (ABI). Experimental samples were analyzed in triplicate. Threshold crossing points were converted to expression values automatically (Larionov et al, 2005). Real-time PCR products were analyzed by gel electrophoresis and sequenced to confirm specificity of the amplification. Gene expression across RNA samples was normalized using 18S and 28S rRNAs as internal controls.

Multiple primer pairs were used to analyze expression of every gene tested in order to detect primer dependent artifacts. The results from each primer pair were averaged. For

quantitation of the Cav1.2 gene, the following primer pairs were used:

(1) 3'ATGCCAACATGAATGCCAAT 5' and 3'CCATTCAACAATGCTTATGCAC 5';

(2) 3' CAGCTCATGCCAACATGAAT 5' and 3' TGCTTCTTGGGTTTCCCATA 5';

(3) 3' CTACTCCAGGGGCAGCACT 5' and 3' TTTCCATTCAACAATGCTTATG 5'.

Detection and Quantitation of Cav1.2 Protein by Western Blot

Protein samples were prepared from tissue samples that were frozen in liquid N_2 and then homogenized in ice-cold lysis buffer (50 mM Tris-HCl, pH 7.4), containing several protease inhibitors (Complete Mini Protease Inhibitor Cocktail tablets, Roche). The homogenates were cleared by centrifugation at 1,000g at 4 ℃ for 10 minutes. The supernatant was then centrifuged at 48,000g at 4 ℃ for 45 minutes. The pellet containing membrane proteins was resuspended in lysis buffer and rehomogenized and sonicated to get complete resuspension. Protein samples were quantitated, re-diluted to give nominally equal concentrations and quantitated a second time colorimetrically (BCA, Pierce).

Samples, 2.5 μg of membrane proteins in LDS Sample Buffer (Novex, Invitrogen) with 10% DTT, were heated at 70 ℃ for 10 min, prior to loading on a pre-cast 4-12% Bis-Tris gel (NuPage, Invitrogen). Electrophoretic separation of the proteins was carried out in SDS-MOPS Running Buffer. Proteins were then blotted onto PVDF membranes. After a blocking step, the membranes were incubated overnight at 4 ℃ in blocking solution with the primary antibodies (anti-Cav1.2, 1:200, Alomone Labs, Cat#ACC-003 and anti-actin (internal control), 1:1,000, Chemicon, Cat# MAB1501). Incubation in alkaline phosphatase-conjugated secondary antibodies (Tropix, Applied Biosystems, 1:10,000, anti-rabbit for the Cav1.2 or anti-mouse for Actin) was performed at RT for 1 hour. The membranes were exposed to chemiluminescent

substrate (CSPD, Tropix, Applied Biosystems) and luminescence was quantified using a Kodak Image Station 440CF.

Mouse Ventricular Myocyte Isolation

Cardiac myocytes were isolated from the ventricles of 9-11 week-old mice using a method described previously (Rosati et al, 2008). Mice were euthanized by intraperitoneal injection of 100 mg/kg of sodium pentobarbital. The heart was quickly removed and rinsed in three changes of cold Basic Solution (BS) (112 mM NaCl, 5.4 mM KCl, 1.7 mM NaH_2PO_4, 1.6 mM $MgCl_2$, 4.2 mM $NaHCO_3$, 20 mM HEPES, 5.4 mM glucose, 4.1 mM L-glutamine, 10 mM taurine, Minimal Essential Medium vitamins and amino acids, pH 7.4) containing 20 units/ml of heparin. The aorta was cannulated using a 22-gauge blunt needle and the heart was rinsed with oxygenated BS containing 1 mg/ml 2,3-butanedione monoxime at 37 ℃ on a Langendorff apparatus for 10 minutes. Digestion of the myocardium was performed using 36 μg/ml Liberase Blendzyme 4 (Roche) in oxygenated BS for 5-7 minutes. After digestion, the heart was rinsed in KB solution (74.56 mM KCl, 30 mM K_2HPO_4, 5 mM $MgSO_4$, 5 mM pyruvic acid, 5 mM β-hydroxybutyric acid, 5 mM creatine, 20 mM taurine, 10 mM glucose, 0.5 mM EGTA, 5 mM HEPES and 5 mM Na_2-ATP, pH 7.2). The atria were subsequently trimmed off and the ventricles were minced in KB. The tissue was collected in a 15 ml conical tube and further dissociated by gentle trituration. The cell suspension was filtered through a 210 μm nylon mesh and allowed to sediment. The pellet was washed once in KB before the cells were used.

Recording of Calcium Currents

Only rod-shaped calcium-tolerant myocytes were used for electrophysiological recordings, which were performed at room temperature (23 ℃). Gigaseals were obtained using 1.5-3 MΩ borosilicate glass pipettes and whole-cell L-type Ca^{2+} currents ($I_{Ca,L}$) were measured in voltage-clamp mode using an Axopatch 200A amplifier with a Digidata 1322A digitizer and the pClamp 8 software package (all from Axon Instruments). The experimental recording conditions for $I_{Ca,L}$ have been previously described (Rosati et al, 2008). Briefly, the internal solution contained (mM): Cs-aspartate 115, CsCl 20, EGTA 11, HEPES 10, $MgCl_2$ 2.5 and Mg-ATP 2 (pH 7.2). The Na^+- and K^+-free bath solution contained (mM): TEA-Cl 137, CsCl 5.4, $CaCl_2$ 2, $MgCl_2$ 1, HEPES 5, glucose 10 and 4-aminopyridine 3 (pH 7.4). For $I_{Ca,L}$ peak determination, the current was activated from a holding potential of -50 mV by 10 mV steps, ranging from -50 to +60 mV. The maximum absolute value of the current obtained (in pA) was divided by the cell capacitance (in pF).

di-8-ANEPPS Staining and Confocal Imaging

Glass bottom dishes (MatTek Corporation) were coated with poly-D-Lysine (1mg/ml, Sigma) and laminin (0.1mg/ml, BD Biosciences) for 30 minutes at 37 ℃. A suspension of isolated myocytes was added to the coated glass bottom well, incubated for 1h at room temperature (RT) and then rinsed once with KB. The cells were then stained in 75 μM di-8-ANEPPS (Invitrogen). Confocal imaging was performed after a 10-minute incubation and a subsequent wash with KB.

Imaging was performed on an Olympus Fluoview FV1000 microscope, with a 488 nm excitation wavelength for di-8-ANEPPS. X-Y scan images (10.0 μs/pixel) were Kalman-averaged twice. Data analysis was performed using custom routines written in Matlab.

Kinetic Model and Data Fitting

The kinetic model was coded using Python and the data values were fitted using a Simplex search algorithm from a standard Python library.

Five free parameters were used for data fitting: *k1*, *k4*, *d1*, K (the saturation constant) and a constant, which scaled the number of active channels to the peak current density. The other rate constants in the model were constrained as follows: $k2 = k1/4$, $k3 = k1 \cdot 2$, $k5 = k4 \cdot 10$, $d2 = d1/40$. These constraints were chosen to produce a predominance of inactive channels in the cell membrane, as suggested by charge movement measurements (Bean and Rios, 1989; Hadley and Lederer, 1991), and to produce a higher rate of degradation of the Cav1.2 protein in its unassembled form relative to the assembled forms, which has been demonstrated in some channel biosynthesis systems (Merlie and Smith, 1986). It was assumed that the channel assembly step (*k2*) was saturable, with Michaelis-Menten kinetics. Without this assumption Cav1.2 protein and current levels would scale linearly and infinitely with the amount of Cav1.2 mRNA, which is biologically unrealistic. The transport to the cell membrane step is also likely to be saturable, but adding this feature to the model had little relatively little effect and was omitted for simplicity.

RESULTS

Validation of the Inducible Knockout System Using Homozygous Floxed Cav1.2 Mice

Homozygous floxed Cav1.2 mice (also transgenic for a cardiac-specific tamoxifen-inducible Cre recombinase) were used to confirm that both the genetic modification and the tamoxifen treatment worked as expected. Homozygous mice were treated for five days by i.p. injection of 100 μl of tamoxifen in peanut oil (33 mg/kg/day). As expected for a complete deletion of the Cav1.2 gene, the tamoxifen-treated mice died rapidly following treatment. Homozygous animals had an average survival time of 6.9 ± 3 days (mean ± S.D., n = 14) following the five day injection period (Fig. 1A). This time interval presumably reflects in part the decay times of the Cav1.2 mRNA and proteins following gene knock-out. No mice injected with peanut oil alone (the drug vehicle) died during the same time period, and these mice had long-term viability (tested up to two months).

Mice examined within 2 days of death using echocardiography displayed a profound decrease in myocardial contractility, as assessed by fractional shortening, consistent with a large reduction in calcium current expression (Fig. 1B and C). There was also a significant increase in ventricular end diastolic volume (Fig. 1D).

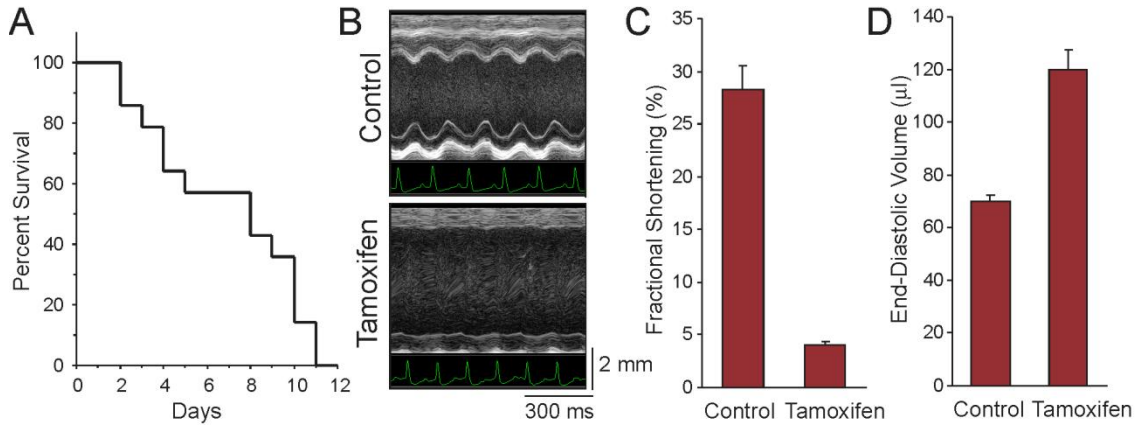

Figure 1. Effect of homozygous Cav1.2 knockout on survival and cardiac function

(A) Kaplan–Meier cumulative survival plot of homozygous floxed Cav1.2 mice also expressing a tamoxifen-inducible, cardiac-specific Cre recombinase. Mice were treated for five days by i.p. injection of 100 µl of tamoxifen in peanut oil (10 mg/ml). Average survival time was 6.9 ± 3 days (mean ± S.D., n = 14) after the end of the injection period. No control mice died during the same time period. B. Echocardiographic analysis of control and homozygous floxed $Ca_v1.2$ mice following tamoxifen injection. Histograms show average data for fractional shortening (C) and end-diastolic volume (D) for control and tamoxifen treated homozygous floxed Cav1.2 mice. Data are from tamoxifen treated mice within 2 days of death and control mice following peanut oil (drug vehicle) injection tested during the same time period. Error bars are SEM and n = 8 and 6 respectively. In both cases values for treated animals were significantly ($P<0.001$) different to control values.

To analyze mRNA and protein expression in the homozygous mice, the physiological status of tamoxifen-treated mice was followed longitudinally using echocardiography and mice were sacrificed and tested for mRNA and protein expression when fractional shortening fell below 5%.

In the tamoxifen-treated homozygous mice, Cav1.2 mRNA expression was reduced to 11±1% relative to controls (Fig. 2A). Assuming that Cav1.2 mRNA expression is restricted solely to myocytes expressing the α-MHC gene, then, based on the mRNA results, the efficiency of gene deletion is approximately 89% under our experimental conditions. If non-trivial amounts of Cav1.2 mRNA are expressed in non-myocytes in the ventricle wall, then the efficiency would be somewhat higher.

There was a very limited compensatory increase in Cav1.3 mRNA expression in the adult homozygous Cav1.2 knockouts (Fig. 2B), much smaller than has been described in embryonic hearts using conventional Cav1.2 knockouts (Xu et al, 2003). Notably, Cav1.3 mRNA expression remained more than an order of magnitude smaller that that required to compensate for the loss of Cav1.2 mRNA expression (Fig. 2C). Expression of other members of the Cav1 gene family, as well as Cav3 family genes, also remained at similarly low, or lower, levels relative to Cav1.2 gene expression in control hearts (not shown).

Cav1.2 protein expression in homozygous mice was analyzed by western blotting. Because linearity can be a problem with these assays, a range of conditions were tested in order to optimize the assay. The assay for Cav1.2 protein detection was found to be linear over the range 0-3 μg of membrane protein per sample (Fig. 2D). For all subsequent experiments, 2.5 μg of membrane protein were used in each independent sample.

There was a dramatic reduction in Cav1.2 protein expression in the homozygous animals (Fig. 2E and F). Cav1.2 protein was expressed at low but detectable levels in the hearts of homozygous knockout animals with severely compromised cardiac function. The average level of expression was 19 ± 9% of control values (mean ± s.e.m, n = 10 and 6 for control and treated animals respectively). This result confirms the specificity of the Cav1.2 antibody used in the western blot assay. A complete loss of Cav1.2 protein would not be expected under these conditions because the mice were sacrificed before the protein had declined to baseline levels, which are clearly not consistent with survival.

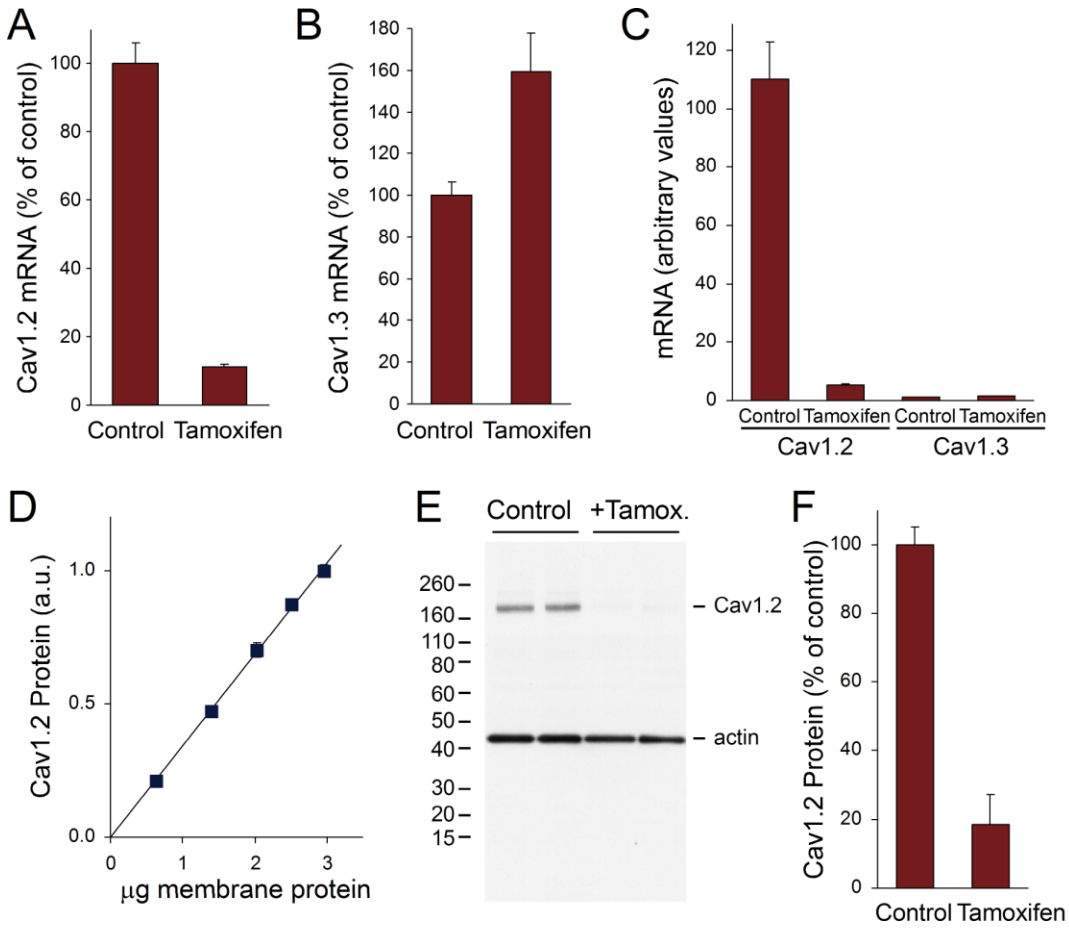

Figure 2. Effect of homozygous Cav1.2 knockout on calcium channel mRNA and protein expression

(A) Analysis of Cav1.2 mRNA expression in the left ventricles of homozygous Cav1.2 KO mice. Cav1.2 mRNA abundance was reduced to 11 ±1% of control values in homozygous tamoxifen treated mice ($P<0.0001$, $n = 7$). (B) Cav1.3 mRNA expression in the left ventricles of homozygous Cav1.2 KO mice was increased 59% compared to controls ($P<0.01$). (C) Comparison of the relative levels of Cav1.2 and Cav1.3 mRNA expression in control and homozygous KO mice. (D) Standard curve for Cav1.2 detection by western blot analysis, 0-3 µg of membrane protein was used in assay. Data points are means ±s.e.m ($n = 6$). Error bars are hidden by the symbols. (E) Western blot analysis of Cav1.2 protein expression in the left ventricles of control and tamoxifen-treated homozygous Cav1.2 KO mice. The upper band corresponds to Cav1.2 protein and the lower band to actin, which served as an internal control for equal lane loading. (F) Histogram showing average data for homozygous KO mice. Cav1.2 protein abundance was reduced to 19 ±9% of control values in homozygous mice ($n = 10$ and 6 for control and treated animals respectively).

Analysis of Heterozygous Floxed Mice Following Induction of Cav1.2 Gene Deletion

The effect of tamoxifen treatment appears to reach completion within 2 weeks following the end of tamoxifen injections (Fig. 1A). As a consequence, all physiological and biochemical experiments on heterozygous mice were performed 2 to 4 weeks after the completion of the tamoxifen injections. In contrast to the results for the homozygous mice, no heterozygous mice died during this 2-4 week period following tamoxifen injection. No fatalities were observed in a subset of treated heterozygous mice that were examined over a longer 2 month period.

Again, in contrast to the results for the homozygous mice, echocardiographic analysis of cardiac function in the heterozygous floxed Cav1.2 mice revealed no differences in the functional properties of the hearts between control and treated animals. Fractional shortening was unchanged (25.3 ±1% versus 25.1 ±1% for control and treated animals respectively, mean ± s.e.m, n = 11 and 12) nor was end-diastolic volume significantly changed (65±2.5 μl versus 65±2.8 μl, mean ± s.e.m, n = 11 and 12 respectively).

Calcium Current Expression in Heterozygous Cav1.2 KO Mice

There was no change in peak current density in myocytes obtained from control and tamoxifen-treated heterozygous floxed mice (Fig. 3A). There was no significant difference in cell capacitance between the two groups (146 ± 51 vs. 127 ± 38 pF for control and tamoxifen treated respectively, mean ± SD, n =27 and 21).

The biophysical properties of the currents in the tamoxifen treated animals were also unchanged (Fig. 3B). The I-V relationships for currents obtained from the two sets of mice are

virtually identical (Fig. 3C). The rate of inactivation and steady-state inactivation curves are similarly unchanged (Fig. 3D and E).

In summary, there was no significant change in $I_{Ca,L}$ density or any of the tested biophysical properties in myocytes from the heterozygous knockout mice compared to controls.

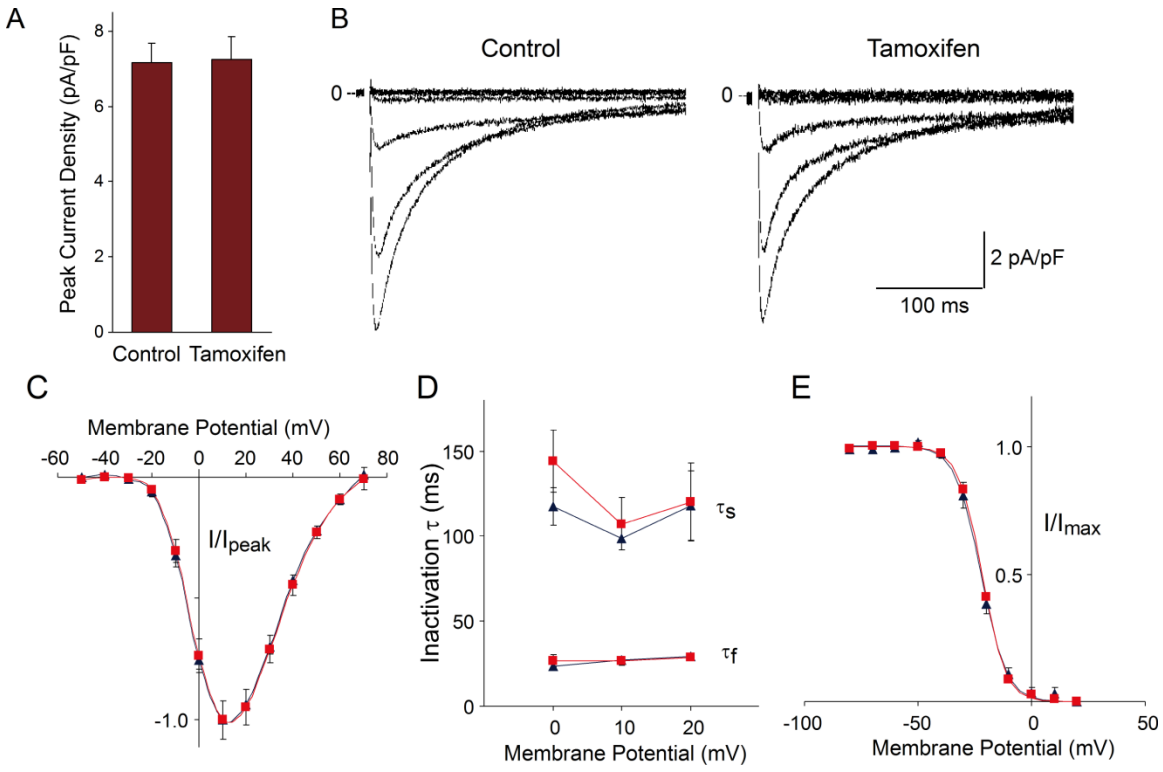

Figure 3. Effect of heterozygous Cav1.2 knockout on L-type calcium current expression and function

(A) Bar graph comparing peak calcium current expression in ventricular myocytes obtained from heterozygous floxed Cav1.2 mice treated with peanut oil alone (control) or with tamoxifen (7.2 ± 1 and 7.3 ± 1 pA pF^{-1}, n = 27 and 21 respectively, mean ± SEM). Error bars are SEM. (B) Recordings of calcium currents from myocytes obtained from control and tamoxifen-treated mice. Holding potential was −50 mV, and currents were elicited by voltage steps over the range −30 to +10 mV. (C) Normalized *I–V* curves for $I_{Ca,L}$ in ventricular myocytes from control and tamoxifen-treated mice. (D) Inactivation time constants for $I_{Ca,L}$. The data were fitted with a biexponential curve with two time constants (τ_f and τ_s). (E) Steady-state inactivation for $I_{Ca,L}$. Data were fitted with Boltzmann curves ($V_{1/2}$ = −21.6 ± 1.3 and −21.4 ± 0.4; k = 6.2 ± 0.5 and 5.6 ± 0.2; n = 11). Data points are means ± SEM, and symbols are control (blue triangles) and tamoxifen-treated (red squares). Recordings were made on myocytes obtained from mice 3–5 weeks after the initiation of tamoxifen injections.

Reduced Cav1.2 mRNA and Protein Expression in Heterozygous Cav1.2 KO Mice

Cav1.2 mRNA expression in the left ventricle of heterozygous floxed mice treated with tamoxifen or with peanut oil alone was compared using real-time PCR. In tamoxifen-treated heterozygous mice Cav1.2 mRNA expression was reduced to 58% relative to controls (Fig. 4A). This value was not significantly different to the value of 55.5% interpolated from the homozygote mouse data, assuming a similar efficiency for recombination and negligible non-myocyte Cav1.2 mRNA expression. This suggests that there is no significant compensation of mRNA expression from the remaining intact Cav1.2 allele in the heterozygous knockout mice.

There was a modest but significant ($P < 0.001$) reduction in Cav1.2 protein expression in tamoxifen-treated heterozygous mice relative to control animals. Cav1.2 expression in tamoxifen-treated animals was 79 ± 2% of controls (mean ± s.e.m, n = 19 and 18 for control and treated animals). There was no change in actin expression in these same tissue samples. Expression of actin, which acted as the internal control, was 101 ± 2% of control values (mean ± s.e.m, n = 19 and 18 for control and treated animals).

No Change in Cav1.2 Related Gene Expression in Heterozygous Knockout Mice

The expression of genes whose upregulation could potentially explain the unchanged levels of $I_{Ca,L}$ found in heterozygous Cav1.2 knockout mice was examined. In particular, no change in Cav1.3 mRNA expression was found following heterozygous Cav1.2 gene knockout. Cav1.1 and Cav1.4 mRNAs were expressed at very low or undetectable levels. Similarly, no change in Cavβ2, Cavα2δ-1 and Cavα2δ-2 mRNA was observed. These mRNAs encode

auxiliary subunits that have been shown to cause an increase in Cav1.2 current or to be associated with the alpha subunit in cardiac myocytes (Bodi et al, 2005).

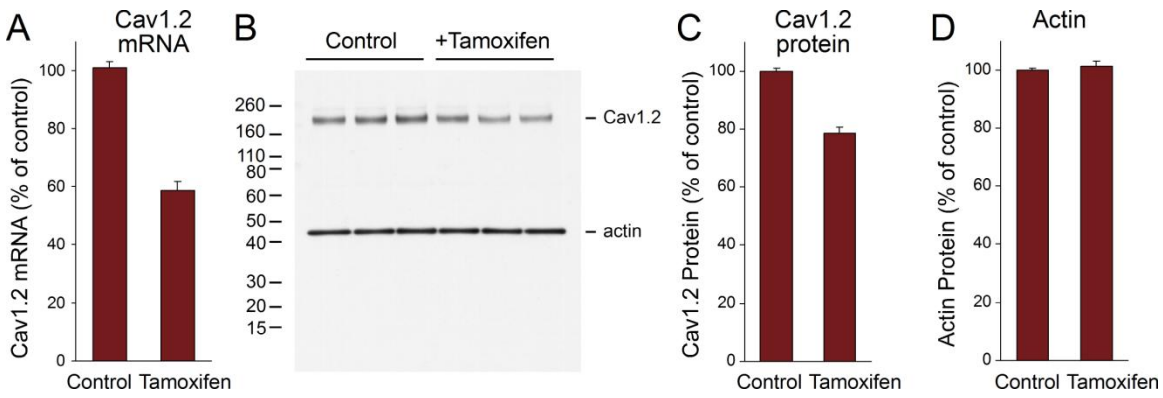

Figure 4. Effect of heterozygous Cav1.2 knockout on calcium channel mRNA and protein expression

(A). Analysis of Cav1.2 mRNA expression in the left ventricles of heterozygous Cav1.2 KO mice was determined using real-time PCR. Cav1.2 mRNA abundance was reduced to 58 ± 3% of control values in heterozygous mice ($P < 0.0001$, $n = 13$ and 10 respectively). Error bars are SEM B. Western blot analysis of Cav1.2 protein expression in cell membranes from the left ventricles of control and tamoxifen-treated heterozygous Cav1.2 KO mice. Upper band corresponds to Cav1.2 protein and lower band to actin, which served as an internal control. Histograms show average data for Cav1.2 (C) and actin (D) expression. Cav1.2 protein abundance was reduced to 79 ± 2% of control values in heterozygous mice ($P < 0.0001$) whereas actin expression was unchanged ($n = 19$ and 18 for control and treated animals, respectively).

Disruption of T-tubule Network Structure in Homozygous but not Heterozygous Knockout Mice

A majority of calcium channels are located in the T-tubule membrane (Scriven et al, 2000) and changes in channel expression could potentially be reflected in changes in this structure.

There was significant disruption of the T-tubule network in the Cav1.2 homozygous knockout mice (Fig. 5A). In contrast, no change was observed in the heterozygous mice. A spatial fast Fourier transform, which is a sensitive measure of the regularity of T-tubule structure, was used to analyze the data. T-tubules form at the Z-line in a regular pattern on an approximately 2 μm grid and this organization is reflected in the peak seen in the spatial power spectrum at 1/2 μm^{-1}, and at multiples of this value (Fig. 5B). The power in this peak is greatly reduced in cells from the homozygous knockout mice (Fig. 5C) but is unchanged in the heterozygous knockout mice (Fig. 5D).

The disruption of the T-tubule network structure observed in the homozygous mice is very striking. It may either reflect a direct dependency of the T-tubule structure on Cav1.2 channel expression or be secondary to the heart failure induced by Cav1.2 loss. For the heterozygous knockout mice, there is no change in the T-tubule network structure and compensation of calcium current expression is clearly unrelated to changes in T-tubule structure.

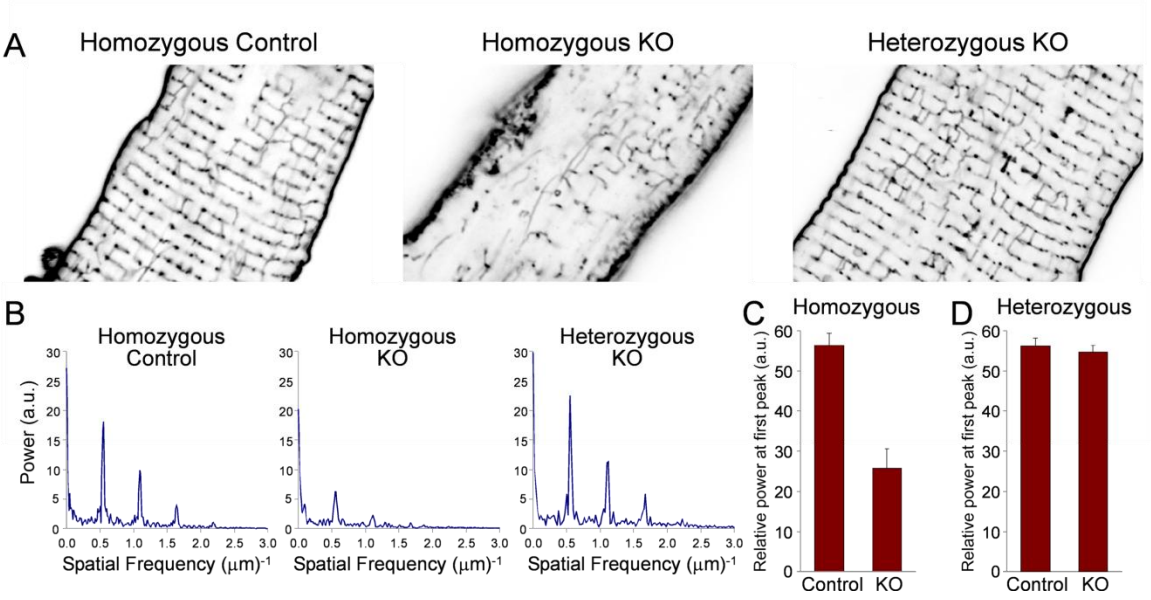

Figure 5. Analysis of T-tubule networks in control, homozygous and heterozygous Cav1.2 KO mice

(A) Images of the T-tubule network in isolated myocytes were obtained using confocal microscopy and di-8-ANEPPS staining. The images were inverted to improve the clarity with which the T-tubule network can be seen. There is reduced regularity of the T-tubule network in the cells from the homozygous KO mice and an increased number and length of longitudinal elements, relative to the control. (B) Spatial power spectrum for cells from untreated homozygous floxed mice, homozygous and heterozygous Cav1.2 KO mice. The plots show power (y-axis) as a function of spatial frequency (x-axis) with a strong peak at approximately$1/2\mu m^{-1}$ and multiples thereof. (C) Average power at the first peak ($\approx 1/2\mu m^{-1}$) in the spatial power spectrum of myocytes from untreated homozygous floxed mice and homozygous knockout mice ($P<0.0001$, n = 12 and 10 respectively). (D) Average power at the first peak in the spatial power spectrum for untreated heterozygous floxed mice and heterozygous knockout mice. There was no significant difference in the means (n = 28). Data points are means ± SEM

Effects of Blockade of the Calcium Current on Cav1.2 mRNA and Protein Expression

It has been proposed that calcium fluxes can actively regulate calcium channel expression, based on results using Verapmil treatment *in vivo* (Schroder et al, 2007). To test this possibility the effects of Verapamil treatment on Cav1.2 protein expression, were examined. In preliminary experiments, even relatively high doses of Verapamil (up to 25 mg/kg/day for 4 days) had no effect on Cav1.2 protein expression. The highest dosage of Verapamil that could be tolerated without significant lethality was 75 mg/kg/day split into two daily doses. For mice injected subcutaneously with Verapamil (75 mg/kg/day for 3.5 days) there was no change in Cav1.2 protein expression relative to control animals (Fig. 6A). No change in Cav1.2 mRNA expression was observed in the same animals.

Because of the voltage dependence of Verapamil blockade, there was some question as to whether even sublethal doses of the drug could effectively block the ventricular calcium channel *in vivo*. When examined using echocardiography, no significant change in cardiac contractility was observed in the drug treated animals (data not shown).

Variation in Cav1.2 mRNA Expression

The effective buffering of experimentally induced changes in Cav1.2 mRNA expression raised the possibility that relaxation of *cis*-regulatory control of Cav1.2 gene expression could potentially occur. One study of Cav1.2 mRNA expression in tissue samples from human ventricle has reported an unusually high degree of variablity, with a normalized mean and standard deviation of 100 ± 51 (Wang et al, 2006). A second study, also using human ventricle, found a much tighter distribution, 100 ± 30 (mean $\pm$ SD) (Gaborit et al, 2007).

In mouse ventricle no unusual variation in Cav1.2 expression 100 ± 17 (mean ± SD) (Fig. 6C) is observed. The tighter distribution in mouse probably reflects the use of inbred animals and the more consistent age and condition of the tissue samples. Three human heart RNA samples (see Methods) were also examined and a relatively tight grouping of normalized expression values (119, 86, 95) were found. Although a small sample size, this result is not consistent with the very broad distribution of Cav1.2 mRNA expression levels described by Wang et al (2006).

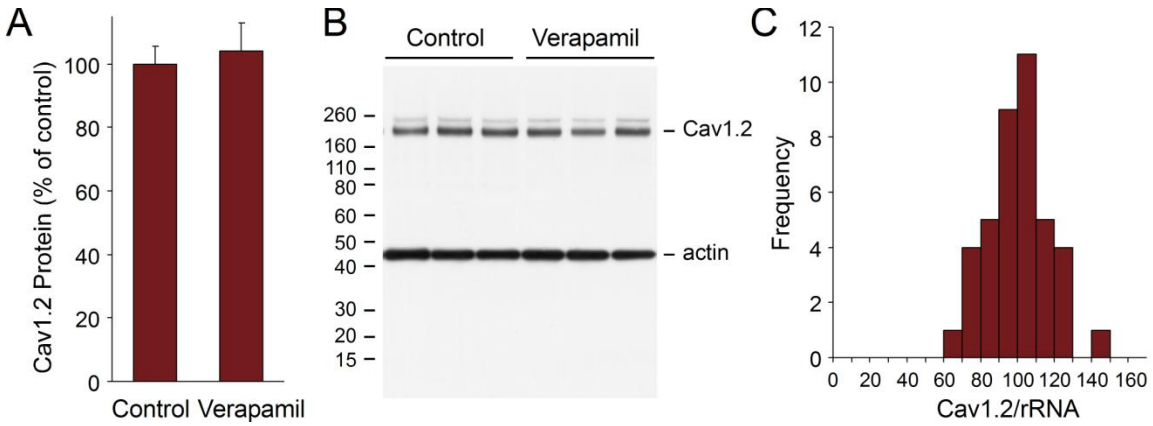

Figure 6. Effect of verapamil on Cav1.2 protein expression and variation of Cav1.2 mRNA in mice

(A) Analysis of Cav1.2 protein following Verapamil treatment (75 mg/kg/day for 3.5 days). Histogram shows average data for Cav1.2 expression (100 ± 5 and 104 ± 9, n = 6 and 10 respectively, mean ± SEM). Cav1.2 protein abundance was unchanged in Verapamil treated mice compared to control mice injected with the same volume of the vehicle (water). (B) Western blot analysis of Cav1.2 protein expression in cell membranes from left ventricles of control and Verapamil-treated mice. Upper band corresponds to Cav1.2 protein and lower band to actin, which served as an internal control. The higher molecular weight band above the Cav1.2 band is a non-specific signal detected intermittently by the anti-Cav1.2 antibody. (C) Histogram shows expression of Cav1.2 mRNA in 40 control mouse ventricles from 8-10 week old mice of either sex. The difference between the lowest and highest expressing animal was 2.4-fold with a normalized mean and standard deviation of 100 ± 17. Data are normalized to ribosomal RNA and expressed as a percentage of the mean.

Model of Cav1.2 Biosynthesis

To begin to understand the biosynthesis of the Cav1.2 channel, the decay of the Cav1.2 mRNA and protein was examined following gene knockout in homozygous mice (Fig. 6A and B). Induction of knockout in these experiments used a single tamoxifen injection at time zero (see Methods). The decay of Cav1.2 mRNA was quite rapid, with a time constant of 14.7 hours. The steady-state baseline value was 12%, similar to that observed using our standard knockout protocol (Fig. 2A). The decay of Cav1.2 protein was more complex, beginning after a noticeable delay. This delay suggests that only the later steps in the biosynthesis of the Cav1.2 subunit are effectively seen by the western blot assay. The early intermediates are either relatively rare, have short half lives or are not efficiently captured by the membrane protein preparation procedure.

The results from the heterozygous knockout mice show that, relative to the reduction in Cav1.2 mRNA, calcium current density is buffered more effectively than total Cav1.2 protein (Fig. 3A and Fig. 4C). A simple model of channel biosynthesis (Fig. 6C) can account for these results, assuming that there is at least one saturating step in the biosynthetic pathway (see Methods). This model, when fitted to the current and protein data simultaneously, produces a good fit of the experimental data (Fig. 6B, D and E). The model predicts that there should be a small reduction in calcium current in the heterozygous knockouts that is within experimental error.

The key feature of this model is that at least one step in the biosynthetic pathway is saturated under wild-type conditions (Fig. 6C). Without the assumption of at least one saturable step, Cav1.2 protein and current levels would scale linearly and infinitely with the amount of Cav1.2 mRNA. The complex dependency of calcium channel expression on multiple subunits (Bodi et al, 2005; Kobayashi et al, 2007) suggests that the assembly step is likely to be limiting,

as assumed in the model. It is notable that calcium current expression is also buffered following reduction of Cavβ2 subunit expression in adult mice (Meissner et al, 2009), which is consistent with the assembly step also being saturated for Cavβ2. The large mismatch between calcium channel gating charge and the number of functional channels in the cell membrane (Bean and Rios, 1989; Hadley and Lederer, 1991) and the resultant relatively high level of channel expression in the cell membrane suggests that transport to the cell membrane may also be saturated.

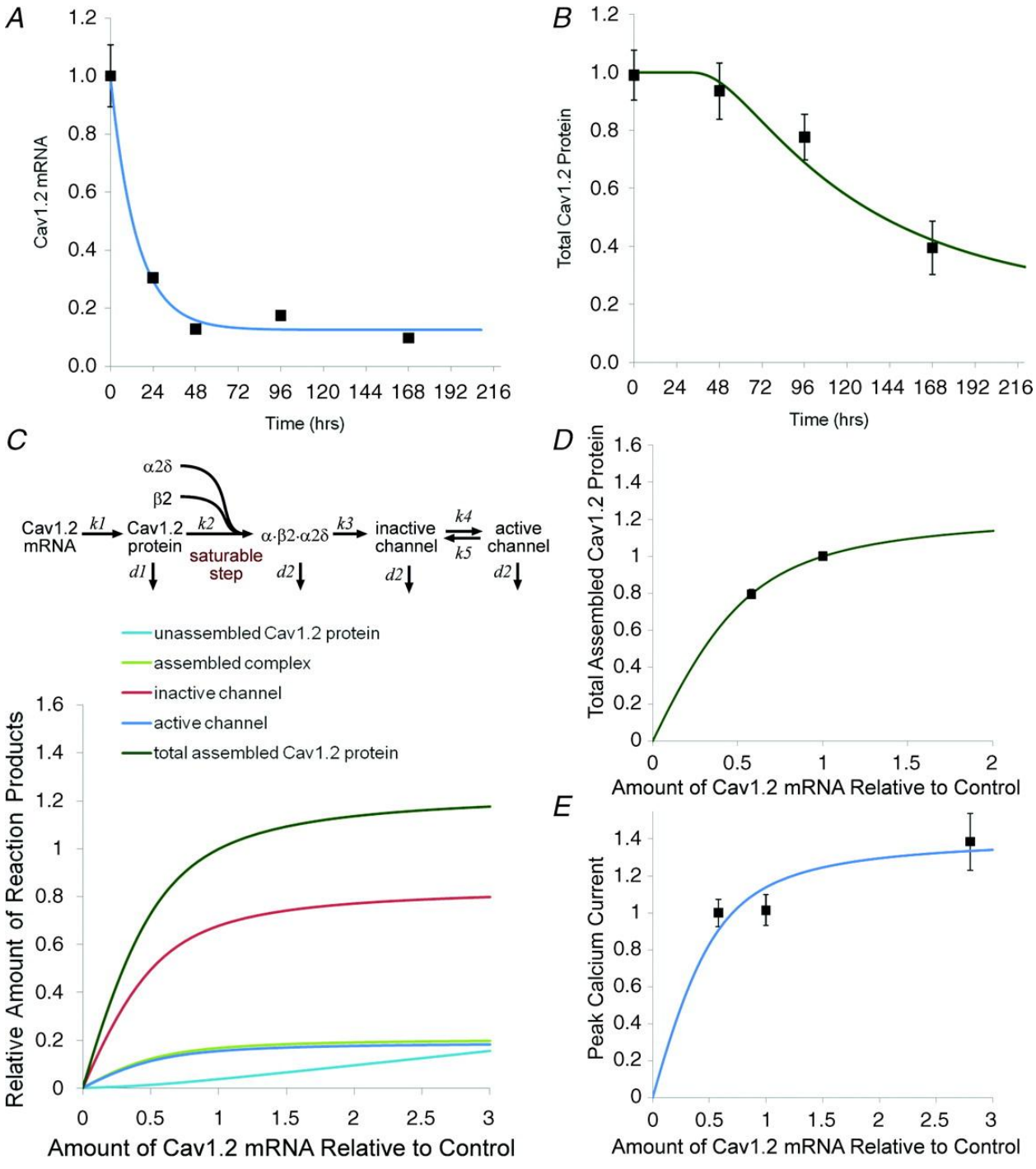
A
Cav1.2 mRNA
Time (hrs)
B
Total Cav1.2 Protein
Time (hrs)
C
α2δ
β2
Cav1.2 mRNA
k1
Cav1.2 protein
k2
saturable step
α·β2·α2δ
k3
inactive channel
k4
k5
active channel
d1
d2
d2
d2
unassembled Cav1.2 protein
assembled complex
inactive channel
active channel
total assembled Cav1.2 protein
Relative Amount of Reaction Products
Amount of Cav1.2 mRNA Relative to Control
D
Total Assembled Cav1.2 Protein
Amount of Cav1.2 mRNA Relative to Control
E
Peak Calcium Current
Amount of Cav1.2 mRNA Relative to Control

Figure 7. Decay of Cav1.2 mRNA and protein following homozygous Cav1.2 knockout and a model of Cav1.2 channel biosynthesis

(A) Decay of Cav1.2 mRNA in homozygous knockout mice following a single tamoxifen injection (see Methods). Data points show mean ± SEM (n = 3–7). Data were fitted with a single exponential: τ = 14.7 h, baseline = 0.12. (B) Decay of Cav1.2 protein in the same mice shown in (A). Curve was fitted using the kinetic model shown in panel (C). (C) Kinetic model of Cav1.2 channel biosynthesis. The amount of the four forms of the Cav1.2 protein plus total assembled Cav1.2 protein is plotted as a function of the amount of Cav1.2 mRNA. Total assembled Cav1.2 protein corresponds to the Western blot measurements shown in Fig. 4C and the corresponding fit is shown in panel (D). Active protein corresponds to the number of functional channels corresponding to peak calcium current shown in Fig. 3A and the corresponding fit is shown in panel (E). Data for peak current following overexpression of Cav1.2 mRNA also shown in panel *E* are taken from Muth et al. (1999). Note that total protein and peak current have different dependencies on the amount of Cav1.2 mRNA. The small decline in peak calcium current predicted by the model for the heterozygous knockout mice would not be readily detected experimentally. Values are expressed relative to control levels and in some cases the symbols obscure the error bars. Fit parameters were: $k_1 = 0.029\ h^{-1}$, $k_4 = 0.032\ h^{-1}$, K (the saturation constant) = 0.0092. The decay rate for the assembled protein was taken from the fit to the protein decay data shown in panel *B*, $d_2 = 0.012\ h^{-1}$. The other parameters were constrained by these values (see Methods).

DISCUSSION

The effects of conditional knockout of the Cav1.2 gene in mouse heart were studied. The homozygous Cav1.2 knockout is lethal, without evidence for any effective compensatory responses in the adult heart. In contrast, following heterozygous knockout of the Cav1.2 gene in the adult heart, expression of the L-type calcium current is maintained at close to control levels. In marked contrast to previous studies on the heterozygous knockout of cardiac channel genes (Kuo et al. 2001; Papadatos et al. 2002), L-type calcium current expression is effectively buffered following deletion of one allele of the Cav1.2 gene. There are two alternative mechanisms that could account for this result.

One possibility is that the maintenance of stable calcium current expression following genetic perturbation is an intrinsic property of the channel biosynthetic network. Such a mechanism does not necessarily require either monitoring of electrophysiological function nor any form of feedback loop in order to effectively buffer channel expression. Even a very simple model of the calcium channel biosynthetic pathway (Fig. 7) can account for the data. Although this model undoubtedly lacks some features of the actual pathway, it is reasonable to consider this kind of mechanism to be the null hypothesis before evaluating other, more complicated alternatives.

The alternative hypothesis is that L-type calcium current expression levels are maintained by a feedback loop. Three potential feedback mechanisms could regulate calcium channel expression.

First, changes in cardiac function could result in feedback via the sympathetic nervous system modifying the function of existing channels, as has been proposed to occur during heart

failure (Schroder et al. 1998; Chen et al, 2002). Significant changes in the biophysical properties of $I_{Ca,L}$ have been reported under these conditions (Chen et al, 2002). No change in the biophysical properties of the calcium current was observed in the present study (Fig. 3), suggesting that sympathetic feedback is unlikely to be a major compensatory mechanism.

A second possibility is that the calcium channel C-terminal tail, which can act as a transcription factor, might form part of a feedback loop to regulate expression of the channel at the level of transcription (Gomez-Ospina et al, 2006; Schroder et al, 2009). In the current study, buffering of calcium current expression following loss of one Cav1.2 allele is predominantly post-transcriptional. There is no significant increase in transcription from the remaining Cav1.2 allele or from auxiliary subunit genes, suggesting that changes in gene regulation are of limited importance.

A third possibility is that calcium flux through the channel might provide a feedback signal that can be monitored to regulate Cav1.2 channel expression. Based on evidence obtained using the calcium channel blocker verapamil, it has been suggested that reduced calcium influx can trigger an increase in Cav1.2 channel expression (Schroder et al, 2007). No effect of Verapamil on Cav1.2 mRNA or protein expression is observed. These results are in agreement with multiple prior studies showing that there is no change in calcium channel protein expression following Verapamil treatment, as assessed by dihydropyridine binding analysis (McCaughran and Juno, 1988; Lonsberry et al, 1992; 1994; Chapados et al, 1992).

Moreover, the use of calcium fluxes to regulate basal calcium channel expression in a negative feedback loop may be inherently problematic (Rosati and McKinnon, 2004). In such a system, a sustained fall in calcium influx would result in a compensatory increase in current expression and a return to normal levels of calcium influx. Because calcium fluxes are the only

established linkage between electrical activity and cell signaling/transcription, this mechanism would eliminate most of the useful information available to the cell about its own electrical activity, effectively short-circuiting this signaling pathway. It would seem more valuable to have the calcium channel and the fluxes that it mediates function as an independent indicator of electrical function, thereby preserving the information from calcium fluxes for other regulatory functions. The central role of the calcium channel in cell signaling is what makes this channel such a strong candidate for the evolution of a robust network to maintain basal channel expression levels relatively stable.

There may be particular selective pressure to maintain stable expression of the calcium channel in cardiac myocytes. This channel has an unusually complex role in the physiology of the myocyte and this creates multiple constraints on the optimal size of the calcium current. At a minimum two criteria constrain the upper and lower bounds of normal calcium current expression. The current must be large enough to trigger excitation-contraction coupling (Rosati et al, 2008) but not so large as to result in calcium overload (Muth et al, 2001; Rosati et al, 2008). These relatively tight constraints on calcium current expression may create selective pressure for the evolution of mechanisms that produce more effective buffering of channel expression than is seen for many other channels (Kuo et al, 2001; Papadatos et al, 2002; Planells-Cases et al, 2000; Ahern et al, 2001; Osanai et al, 2006; Yu et al, 2006; Brew et al, 2007; Tzingounis and Nicoll, 2008).

There are clearly limitations associated with the reliance on a passive buffering mechanism. A 280% increase in Cav1.2 mRNA expression in transgenic mice is buffered to a more modest 30-50% increase in calcium current (Muth et al, 1999; 2001). This increase is large enough, however, to induce hypertrophy, presumably secondary to calcium overload, which

ultimately leads to heart failure, indicating an effective failure of the buffering system (Muth et al, 1999; 2001; Wang et al 2009). A true homeostatic feedback system would be able to maintain close to constant levels of current expression over this relatively modest range of mRNA values. It is possible that the Cav1.2 heterozygous knockout mice will also be more prone to pathologies than wild-type mice, due to reduced calcium channel protein expression, when examined for longer time periods or under more stressful conditions.

The lack of effective response to the homozygous knock-out of the Cav1.2 gene is also revealing. This is a life-threatening situation, where reasonable compensatory solutions exist, either up-regulation of expression of Cav1.3, which is expressed at relatively high levels in normal embryonic heart, or up-regulation of other Cav1 or Cav2 genes. In addition, there are several potential feedback signals, including dramatically reduced calcium flux, contractility and cardiac output. Despite these apparently favorable circumstances, there is no effective compensatory response. Clearly, there is no generalized homoeostatic regulatory system that can respond to changes in channel expression and/or physiological function in order to mediate a useful compensatory response.

Genetic mutations affecting the cardiac electrophysiological system are relatively rare in natural populations and are unlikely to have been a significant factor affecting the evolution of robustness in this system. This rarity almost certainly accounts in large part for the general fragility of the cardiac electrophysiological system to these kinds of genetic perturbations (Sanguinetti et al, 1996; Chen et al, 1998; Wang et al, 1999; Fodstad et al, 2004). Genetic mutations, either natural or experimentally induced, can however reveal the robustness or fragility of a system to non-genetic perturbations (Wagner, 2004). The stability of calcium current expression following heterozygous Cav1.2 gene deletion suggests that there has been

strong selective pressure to develop mechanisms to maintain stable levels of basal calcium current expression, either during the course of normal physiology or in common pathological conditions affecting the heart.

Chapter 7

Summary and Discussion

The results presented in this dissertation demonstrate that the cardiac electrophysiological system is an ideal system for the study of the evolution of gene regulatory function. The relatively simple physiology of the heart allowed us to study the evolution of expression of several cardiac ion channel genes, in a systematic way. It is concluded that the evolution mechanisms described for the developmental systems can also be applied to the physiological system, using the cardiac cellular electrophysiological system as an example (*Chapter 2*). We showed that regulatory evolution is the predominant mechanism for the evolution of mammalian cardiac electrophysiological system and we suggested that *cis*-regulatory evolution plays a key role in this process, supporting the conclusions drawn from the "evo-devo" studies, as described in *Chapter 1*.

On the other hand, at difference with the "evo-devo" principles, our studies on the KChIP2 gene revealed novel molecular mechanisms of evolution (*Chapter 3*). In particular, we demonstrated that CpG island promoters can be the main elements responsible for evolution of species-specific expression of genes (in our case, ion channel genes), independently from other distant regulatory elements. This finding brings important insights on the functions of this prevalent but understudied class of gene promoters. More details about this aspect will be discussed below.

Focusing on the KChIP2 CpG island promoter, we successfully identified nucleotide-level changes that are responsible for the species-specific changes, using species that are very closely related in the muroid clade (*Chapter 4*). In particular, the ~120bp region surrounding the transcription start site was shown to be the primary region for the evolution of KChIP2 *cis*-regulatory function in the hearts of these species and only eight (or less) nucleotide changes in this region were identified to determine the species-specific variation.

Except for the species-specific variation, the evolution of tissue-specific variation in gene expression was also addressed. Surprisingly, the CpG island promoter also showed a tissue-selective function (*Chapter 3*). However, expression of KChIP2 in the brain is apparently more complicated than the cardiac expression, additionally requiring the Intron1 regions for its regulation (*Chapter 4*). The KChIP2 gene was concluded to be a valuable system for the study of mammalian gene regulation for its complex expression phenotypes (species-dependent, tissue-dependent and region-dependent variations) that are approachable for study. Further studies on a few other ion channel genes that are also implicated in the scaling of cardiac electrophysiological system - Kv4.3, HCN4 and SERCA2 - showed the difficulty of studying *cis*-regulatory evolution in most mammalian genes and the advantage of the KChIP2 for having a relatively compact gene structure (*Chapter 5*).

Chapters 2-5 largely focus on transcriptional regulation. In *Chapter 6*, we studied the post-transcriptional regulation of the L-type calcium channel, which was shown to have robust regulation under pathological conditions and appears to be different to most other ion channels genes whose expression levels are hardwired in the genome (*Chapter 1*). By examining the response to changes in Cav1.2 gene dosage in adult mice, it was found that L-type calcium channel biosynthesis involves one or more saturated steps, which act to buffer changes in both Cav1.2 channel protein and L-type calcium current expression (*Chapter 6*).

In the following paragraphs, I would like to first discuss similarities between the cardiac electrophysiological system and developmental system and analyze the reasons why the same conclusions are reached for the mechanisms of their evolution. Then I will emphasize on the novel mechanism of core-promoter-mediated evolution found in KChIP2 and the importance of the CpG island promoter. And finally, possible future directions are discussed.

PARALLELING WITH EVO-DEVO: REGULATORY EVOLUTION IN THE CARDIAC ELECTROPHYSIOLOGICAL SYSTEM

Based on hypotheses about mechanisms of evolution proposed by evolutionary developmental biology ("evo-devo") studies, we analyzed the relative importance of regulatory evolution (the evolution of gene regulation) versus structural evolution (the evolution of protein structure and function) in determining the evolution of a physiological system - the cardiac electrophysiological system.

Similarly to developmental systems, regulatory evolution was shown as the primary mechanism for the evolution of the cardiac electrophysiological system. This result was expected, based on two key similarities between the two systems: (1) both systems have a large and essentially computational component and (2) due to pleiotropy, structural evolution has the potential to create significant problems in both systems. In addition, like the developmental systems, *cis*-regulatory evolution is the specific primary mechanism for regulatory evolution in the electrophysiological system.

Computational Nature of the Cardiac Electrophysiological System

Previous studies on proteins acting in physiological systems, such as light-sensitive rhodopsins (Yokoyama 2002), melanocortin receptors in skin patterning (Logan et al. 2003) and olfactory/taste/pheromone receptors (Fischer et al. 2005; Grus et al. 2005; Niimura and Nei 2007) have proposed structural evolution as the main mechanism for evolution of physiological

systems. A limitation of these studies is that they are focusing on individual molecules that are expressed in highly-specialized tissue-type. In order to really understand the evolution of a physiological system, it is important to study the system as a whole rather than focusing on individual molecules.

The cellular electrophysiological system of ventricular myocytes, for example, produces various complex processes such as generation of an action potential, triggering of a cell contractile response, maintenance of specific ion concentrations by ionic pumps and transporters, among the most notable ones. Such processes are controlled by several proteins that function in a coordinated and interdependent fashion. In order to study the mechanism of the evolution of such a complex system as a whole, it is important to first define the nature of the tasks that this system is performing, that is, whether computational or physical (Rosati and McKinnon 2009).

A biological system can evolve either through structural evolution or regulatory evolution, or both. The relative contribution of either mechanism will be determined by the relative balance of physical and computational tasks that a biological system has to perform. Physiological systems that directly interface with the environment will almost always perform some kind of physical task, like the examples given in the beginning. In the majority of these cases, structural evolution will be required for the tasks themselves to evolve.

In contrast, the cardiac electrophysiological system is clearly a computational one. The scaling of cellular electrophysiological properties of the heart with body size essentially relies on changes in the output of its computational function (square pulse generator, *Chapter 1*, Fig. 3). We studied evolution of this system as a whole by focusing on the changes in two related traits across the mammalian phylogeny (action potential morphology and action potential duration)

and revealed that regulatory evolution is the predominant evolution mechanisms, as expected for a computational system.

Constrained Protein Sequence and Function in the Cardiac Electrophysiological System

The advantage of regulatory over structural evolution is that it is able to avoid pleiotropic effects. The importance of pleiotropy as a constraint favoring regulatory evolution in developmental systems has been discussed at length (Stern, 2000; Carroll, 2005) and essentially identical arguments can be applied to electrophysiological systems. In brief, both systems depend on a large, but relatively fixed, set of proteins that are broadly expressed in a large number of highly differentiated cell types. As a consequence, structural evolution, by changing the function of a protein that is important for the function of a range of differentiated cells, has a high probability of producing pleiotropic effects. In contrast, regulatory evolution, particularly the evolution of *cis*-regulatory modules, can produce cell type specific effects, thereby avoiding, or limiting, pleiotropic effects.

Ion channels form a large gene family in most animals (Moulton et al, 2003; Yu and Catterall, 2004), nonetheless there is a relatively small number of channels compared to the very large number of distinct types of excitable cells in a typical animal. In particular, there is an enormous number of phenotypically distinct neurons (Stevens, 1998; Bota et al, 2003). Most electrically excitable cells express a large fraction of the total number of ion channel genes (Dixon and McKinnon, 1996; Gaborit et al, 2007). As a consequence, there are relatively few voltage-gated ion channels that are restricted to a single cell type and the constraints on channel function are relatively tight for the majority of voltage-gated channels.

A comparisons of amino acid sequences of the major ion channels between mouse and human (*Chapter 2*, Fig. 8) revealed the highly constrained nature of protein sequence in the cardiac electrophysiological system. Most of the proteins are highly conserved with a sequence similarity above 90% between mouse and human (*Chapter 2*, Fig. 8).

Although sequence identity is only a rough measure of the conservation of channel function, the high level of sequence similarity supports the hypothesis of a highly constrained function for these genes. As shown in *Chapter 2*, although expressed at a different level, the biophysical properties of the KCNQ1 and KCNH2 channels in guinea pig do not change compared to a larger species (human). Similarly, the L-type calcium current function remains unchanged in all species, although its expression levels vary with the animal body size. The KCNH2 (Kv11.1 in Figure 8 of *Chapter 2*) and the Cav1.2 channels have a sequence similarity between mouse and human of 96% and 94% respectively and they are not among the most conserved channels. KCNQ1 (Kv7.1 in Figure 8 of *Chapter 2*) has a sequence identity of 90%, which is lower than the average. Yet, for all these channels, no functional differences are caused by the differences in amino acid sequence between species. To further support these observations, we have compared the function of an even less conserved channel, Kv1.5 (86% sequence similarity) from either mouse or human, using a heterologous expression system. Again, despite the relatively large sequence differences, no significant change in function was observed between these orthologous channels (*Chapter 2*, Fig. 3).

In conclusion, under pleiotropic constraints, the coding sequences and functional properties of ion channels in the mammalian electrophysiological system have remained relatively unchanged during evolution. Given the conserved nature of mammalian ion channel coding sequences and gene number, regulatory evolution has to be the primary mechanism used

for the generation of different electrophysiological phenotypes during the course of evolution in most mammalian electrophysiological systems.

Cis-Regulatory Evolution in the Cardiac Electrophysiological System

As mentioned above, our studies on the evolution of the cardiac electrophysiological system revealed a similarity with the evo-devo theories, in that *cis*-regulatory evolution, rather than reorganization of transcription factor networks, emerges as the primary mechanism in regulatory evolution. These results were obtained by analysis of the molecular basis of two simple traits - the evolution of ventricular action potential morphology and the species dependent variation in the expression of the KChIP2 and Kv4.3 gene.

In the case of ventricular action potential morphology, the step-wise change in transcriptional activity of the Kv2.1 and Kv4.2 proximal promoter regions that occurs between small rodents and large mammals closely matches the expression pattern of mRNA and the corresponding repolarization currents and it is therefore responsible for the triangular action potential morphology found in the hearts of smaller mammals. In the case of the KChIP2 gene, the highly variable pattern in cardiac KChIP2 mRNA expression among mammalian species is recapitulated by the variation in *cis*-regulatory function of the KChIP2 proximal promoter region. And for the Kv4.3 gene, the changes in the *cis*-regulatory function between mouse and guinea pig matched with the cardiac mRNA expression in these species.

EVOLUTIONARY ROLE OF CpG ISLAND PROMOTERS

Despite the many similarities between the evolution of cardiac electrophysiology and developmental systems, one of our results on the *cis*-regulatory mechanisms of evolution is completely novel. In particular, the evolutionary changes in the cardiac KChIP2 expression almost completely reside in the core promoter of this gene, rather than being driven by *cis*-regulatory changes in distal elements, as described in the evo-devo models of gene regulation (Carroll 2005).

Enhancer-Mediated *Cis*-Regulatory Evolution

The *cis*-regulatory regions for any given gene include the following elements: promoters, enhancers, insulators, silencers and locus control regions (Maston et al. 2006). Among these, the promoters and enhancers are the best-recognized elements, key to the regulation of gene expression. A transcript is correlated with a single promoter but its expression is usually regulated by multiple enhancers (Arnone and Davidson 1997; Panne 2008). The distinction between promoter and enhancer elements has been vague in the roles they play during evolution and the *cis*-regulatory evolution has also been called "promoter evolution" (Wray et al. 2003; Hoekstra and Coyne 2007). Here, we would like to make a distinction between the promoter-mediated and enhancer-mediated *cis*-regulatory mechanisms. The central role of core promoters as the binding site of RNA polymerase and integration center of regulatory signals can impose a certain level of constraint on the evolution of these regions (Donald and Cashmore 1990; Munoz-Antonia et al. 1996; Jarrard et al. 1998; Butler and Kadonaga 2002). In contrast, there is more

flexibility in changing the function of enhancers (Ludwig et al. 2000; Crocker et al. 2008; Visel et al. 2009; Crocker et al. 2010; Spivakov et al. 2012).

Enhancers are best known for their control of tissue-specificity and timing of gene expression (Struhl 2001). The highly specific nature of their function in transcriptional regulation lends enhancers to the fine-tuning of gene expression (Crocker et al. 2008; Crocker et al. 2010), while avoiding the problem of pleiotropy during evolution. This is also the advantage of *cis*-regulatory evolution over rewiring of the transcription factor network (Wray et al. 2003; Oliveri et al. 2008). Evo-devo studies have revealed plenty of systems, in which gain and loss of distal enhancers fine-tune the transcription process during evolution (Carroll 2005; McGregor et al. 2007; Rebeiz et al. 2009; Chan et al. 2010).

CpG Island Core Promoter as the Main Contributor to *Cis*-Regulatory Evolution

The finding that the KChIP2 core promoter alone can recapitulate the regulatory evolution of this gene in mammalian hearts, without the presence of distal enhancer elements, was surprising and remarkable. Even more surprisingly, we showed that this region also contributes to tissue-specific expression of the KChIP2 gene.

What is special about the KChIP2 core promoter is the CpG-dinucleotide richness in its sequence – characteristic of CpG island promoters. CpG islands are a unique feature of the vertebrate genome (Tweedie et al. 1997; Glass et al. 2007; Sharif et al. 2010). These 200bp to a few kb long sequences seem to serve as landing marks for RNA polymerase II by distinguishing themselves from the vast sea of CpG-low and hyper-methylated genomic sequences (Duncan and Miller 1980; Bird 1987; Larsen et al. 1992; Ioshikhes and Zhang 2000). Different to all the other

known promoter elements that require a specific consensus sequence, for example, "TATAAA" for the TATA box promoter, CpG island promoters do not share a specific consensus sequence except for the CpG richness (Smale and Kadonaga 2003). The mechanism of transcription at this class of promoters is not known, but it is thought that the CpG island core promoter generally provides a platform for the binding of transcription factors and transcription initiation (Blackledge and Klose 2011). The relatively long length of CpG island promoters and the lack of sharing any consensus sequences (Butler and Kadonaga 2002) suggest that there is adequate freedom of change inside the sequence to fine-tune gene expression, hence its role in evolution as demonstrated in the KChIP2 gene.

In addition to KChIP2, all the other genes whose *cis*-regulatory function we assayed in this research – Kv2.1, Kv4.2, Kv4.3, HCN4 and SERCA2 –also use CpG islands as their promoters. All the *cis*-regulatory regions tested in the luciferase reporter assays contain most or part of the CpG island promoters. Four (KChIP2, Kv2.1, Kv4.2, Kv4.3) out of the six genes had their CpG island promoter-containing regions showing patterns of *cis*-regulatory activity that match with their mRNA expression in the heart. In particular, the CpG island core promoter of the KChIP2 gene was isolated for study and was shown as the main contributor of *cis*-regulatory evolution of the gene. We hypothesize that the CpG island promoters can, more in general, contribute to the evolution of *cis*-regulatory function.

Significance of the Role of the Core CpG Island Promoter in *Cis*-Regulatory Evolution

After examining all the important ion channel and transporter genes expressed in the heart in the UCSC genome browser, surprisingly, we found that more than 90% of them are

associated with a CpG island promoter (*Chapter 1*, Table 1). This means that the function of the cardiac electrophysiological system is primarily controlled by this class of promoters. Given the significant contribution of CpG island promoters to the evolution of the genes that were tested so far, this class of promoters seems also to be a key player in the evolution of the cardiac electrophysiological system.

The importance of CpG island promoters in evolution was not recognized in evo-devo studies, probably due to the fact that some of the most widely used model organisms, such as Drosophila (Prud'homme et al. 2006; McGregor et al. 2007; Rebeiz et al. 2009; Frankel et al. 2011) and fish (Colosimo et al. 2005; Chan et al. 2010), do not have or rarely use CpG island as promoters, in contrast to the ubiquitous use of CpG island promoters in mammals (Glass et al. 2007; Sharif et al. 2010). In mammalian genome, more than half of the genes are found to be associated with CpG island promoters (Saxonov et al. 2006).

Finally, I would like to comment on the significance of studying the CpG island promoter at the nucleotide level. As the largest class of promoters in mammals and the primary transcription sites of 72% of human protein-coding genes, it is surprising how little is known about the functional properties of CpG island promoters, in contrast to conventional promoters that contain a TATA box or other well defined localization elements for RNA polymerase II binding (Butler and Kadonaga 2002; Saxonov et al. 2006; Sandelin et al. 2007). As CpG islands usually lack methylation, they are frequently mentioned in epigenetic studies and have been associated with a few histone modifications (Fazzari and Greally 2004; Blackledge and Klose 2011; Orlando et al. 2012). Nonetheless, the transcription mechanisms from this type of promoter are unknown. Our research has started to shed light on this topic, by dissecting the CpG island promoter function at the nucleotide level. We found that, as little as eight-nucleotide

changes in the KChIP2 CpG island promoter underlie the majority of species-specific differences in the cardiac expression of this gene between mouse and gerbil (*Chapter 4*, Fig. 8). The analysis the function of CpG island promoter at such high resolution can be highly informative about the mechanism of transcription at this class of promoters, by allowing identification of specific transcription factors that are obviously important for the transcription at this class of promoter.

FUTURE DIRECTIONS

Comparative genomics is a widely used approach in the study of molecular evolution (Wray et al. 2003; Meireles-Filho and Stark 2009). Making use of comparative genomics, we have analyzed the role of *cis*-regulatory evolution in the cardiac electrophysiological system. As there is no documented data on transcription factor binding in the regulatory regions we have studied and the bioinformatics transcription factor binding site prediction programs give too many false-positive results, the strategy of combining comparative genomics with deletion and swap assays appears to be the best way to identify potential functional *cis*-regulatory elements.

Although comparative genomics can help refine the number and length of candidate *cis*-regulatory regions, it is labor intensive, and can be inefficient in some cases (Ludwig 2002). In this approach, a candidate region that is most likely to contain important *cis*-regulatory elements is first chosen for analysis. In our case, we analyzed at first the 5' upstream proximal promoter region of our genes of interest. For the Kv2.1, Kv4.2, KChIP2 and Kv4.3 genes, these *cis*-regulatory regions contained at least some of the functional changes that occurred during mammalian evolution. When a relatively small number of functional *cis*-changes are identified, for example, the eight-nucleotide differences between mouse and gerbil, the bioinformatics tools then become extremely helpful in identifying the potential factors that are functioning in *trans* (*Chapter 4*, Fig. 17).

With the advancement and application of high-throughput sequencing to whole genome studies (e.g. the ENCODE project, Bernstein et al. 2012), the availability of data from mRNA-seq (which measures the transcription level for all genes in the genome), DNaseI-seq (which shows the genomic sequences that are protected from DNaseI digestion by transcription factor

binding), transcription factor ChIP-seq (which gives a genome-wide binding map for specific transcription factors) and others (e.g. FAIRE-seq for isolation of *cis*-regulatory elements, MRE-seq and MeDIP-seq for methylated and non-methylated CpGs, etc.) can aid tremendously the search of *cis*-regulatory elements.

However, caution must be used in relying on the data provided by these techniques, as the regulatory map of a given gene will be different in different cell types, developmental stages and biological/experimental conditions and, ultimately, the function of the candidate elements identified using these techniques has to be verified with functional experiments. Analysis of the *cis*-regulatory function of the candidate genomic region remains the most labor intensive step. Although researchers have tried to assay a large number of candidate regulatory regions at a time using high-throughput methods (Nam et al. 2010), the step of isolating and cloning each specific region cannot be avoided. Nonetheless, the availability of these high throughput data will help minimize the amount of work needed by allowing researchers to focus on the strongest candidate regions.

In conclusion, new high throughput technologies and whole genome studies have provided a better vision of the genome regulatory map. It will be easier to select candidate regions to study the *cis*-regulatory function of mammalian genes. The availability of high-throughput sequencing methods has also made it possible to more easily identify and study groups of genes involved in a specific function or disease. As the regulatory genomic maps for more organisms, other than mouse and human, are studied in the future, comparative genomic techniques will be no longer limited to the comparison of DNA sequence, but can be extended to the comparison of the regulatory maps therefore providing new and more global data on how these networks evolve and function.

References

Ahern CA, Powers PA, Biddlecome GH, Roethe L, Vallejo P, Mortenson L, Strube C, Campbell KP, Coronado R & Gregg RG (2001). Modulation of L-type Ca^{2+} current but not activation of Ca^{2+} release by the gamma1 subunit of the dihydropyridine receptor of skeletal muscle. *BMC Physiol* **1**, 8.

Amrolia, P. J., J. M. Cunningham, P. Ney, A. W. Nienhuis and S. M. Jane (1995). "Identification of two novel regulatory elements within the 5'-untranslated region of the human A gamma-globin gene." J Biol Chem **270**(21): 12892-12898.

Antequera, F. and A. Bird (1999). "CpG islands as genomic footprints of promoters that are associated with replication origins." Curr Biol **9**(17): R661-667.

Antequera, F., M. Tamame, J. R. Villanueva and T. Santos (1984). "DNA methylation in the fungi." J Biol Chem **259**(13): 8033-8036.

Antzelevitch, C., W. Shimizu, G. X. Yan, S. Sicouri, J. Weissenburger, V. V. Nesterenko, A. Burashnikov, J. Di Diego, J. Saffitz and G. P. Thomas (1999). "The M cell: its contribution to the ECG and to normal and abnormal electrical function of the heart." J Cardiovasc Electrophysiol **10**(8): 1124-1152.

Arikkath, J. and K. P. Campbell (2003). "Auxiliary subunits: essential components of the voltage-gated calcium channel complex." Curr Opin Neurobiol **13**(3): 298-307.

Arnone, M. I. and E. H. Davidson (1997). "The hardwiring of development: organization and function of genomic regulatory systems." Development **124**(10): 1851-1864.

Aronow, B., D. Lattier, R. Silbiger, M. Dusing, J. Hutton, G. Jones, J. Stock, J. McNeish, S. Potter, D. Witte and et al. (1989). "Evidence for a complex regulatory array in the first intron of the human adenosine deaminase gene." Genes Dev **3**(9): 1384-1400.

Attwell, D. and S. B. Laughlin (2001). "An energy budget for signaling in the grey matter of the brain." J Cereb Blood Flow Metab **21**(10): 1133-1145.

Baim, S. B. and F. Sherman (1988). "mRNA structures influencing translation in the yeast Saccharomyces cerevisiae." Mol Cell Biol **8**(4): 1591-1601.

Baruscotti, M., A. Barbuti and A. Bucchi (2010). "The cardiac pacemaker current." J Mol Cell Cardiol **48**(1): 55-64.

Baruscotti, M. and D. Difrancesco (2004). "Pacemaker channels." Ann N Y Acad Sci **1015**: 111-121.

Bassani, J. W., R. A. Bassani and D. M. Bers (1994). "Relaxation in rabbit and rat cardiac cells: species-dependent differences in cellular mechanisms." J Physiol **476**(2): 279-293.

Berk, A. J. (2000). "TBP-like factors come into focus." Cell **103**(1): 5-8.

Bernstein, B. E., E. Birney, I. Dunham, E. D. Green, C. Gunter and M. Snyder (2012). "An integrated encyclopedia of DNA elements in the human genome." Nature **489**(7414): 57-74.

Bean BP, Rios E (1989). Nonlinear charge movement in mammalian cardiac ventricular cells. Components from Na and Ca channel gating. *J Gen Physiol* **94**, 65-93.

Bers, D. M. (2002). "Cardiac excitation-contraction coupling." Nature **415**(6868): 198-205.

Bevilacqua, P. C. and J. M. Blose (2008). "Structures, kinetics, thermodynamics, and biological functions of RNA hairpins." Annu Rev Phys Chem **59**: 79-103.

Bezzina, C. R., W. Shimizu, P. Yang, T. T. Koopmann, M. W. Tanck, Y. Miyamoto, S. Kamakura, D. M. Roden and A. A. Wilde (2006). "Common sodium channel promoter haplotype in asian subjects underlies variability in cardiac conduction." Circulation **113**(3): 338-344.

Bianchi, M., R. Crinelli, E. Giacomini, E. Carloni and M. Magnani (2009). "A potent enhancer element in the 5'-UTR intron is crucial for transcriptional regulation of the human ubiquitin C gene." Gene **448**(1): 88-101.

Bilu, Y. and N. Barkai (2005). "The design of transcription-factor binding sites is affected by combinatorial regulation." Genome Biol **6**(12): R103.

Bird, A. P.Beuckelmann DJ, Nabauer M & Erdmann E (1991). Characteristics of calcium-current in isolated human ventricular myocytes from patients with terminal heart failure. *J Mol Cell Cardiol* **23**, 929-37.

Bird, A. P. (1986). "CpG-rich islands and the function of DNA methylation." Nature **321**(6067): 209-213.

Bird, A. P. (1987). "CpG islands as gene markers in the vertebrate nucleus." Trends in Genetics **3**(0): 342-347.

Bird, A. P. and M. H. Taggart (1980). "Variable patterns of total DNA and rDNA methylation in animals." Nucleic Acids Res **8**(7): 1485-1497.

Bird, A. P., M. H. Taggart and B. A. Smith (1979). "Methylated and unmethylated DNA compartments in the sea urchin genome." Cell **17**(4): 889-901.

Blackledge, N. P. and R. J. Klose (2011). "CpG island chromatin: A platform for gene regulation." Epigenetics **6**(2).

Blackwood, E. M. and J. T. Kadonaga (1998). "Going the distance: a current view of enhancer action." Science **281**(5373): 60-63

Birney, E., J. A. Stamatoyannopoulos, A. Dutta, R. Guigo, T. R. Gingeras, E. H. Margulies, Z. Weng, M. Snyder, E. T. Dermitzakis, R. E. Thurman, M. S. Kuehn, C. M. Taylor, S. Neph, C. M. Koch, S. Asthana, A. Malhotra, I. Adzhubei, J. A. Greenbaum, R. M. Andrews, P. Flicek, P. J. Boyle, H. Cao, N. P. Carter, G. K. Clelland, S. Davis, N. Day, P. Dhami, S. C. Dillon, M. O. Dorschner, H. Fiegler, P. G. Giresi, J. Goldy, M. Hawrylycz, A. Haydock, R. Humbert, K. D. James, B. E. Johnson, E. M. Johnson, T. T. Frum, E. R. Rosenzweig, N. Karnani, K. Lee, G. C. Lefebvre, P. A. Navas, F. Neri, S. C. Parker, P. J. Sabo, R. Sandstrom, A. Shafer, D. Vetrie, M. Weaver, S. Wilcox, M. Yu, F. S. Collins, J. Dekker, J. D. Lieb, T. D. Tullius, G. E. Crawford, S. Sunyaev, W. S. Noble, I. Dunham, F. Denoeud, A. Reymond, P. Kapranov, J. Rozowsky, D. Zheng, R. Castelo, A. Frankish, J. Harrow, S. Ghosh, A. Sandelin, I. L. Hofacker, R. Baertsch, D. Keefe, S. Dike, J. Cheng, H. A. Hirsch, E. A. Sekinger, J. Lagarde, J. F. Abril, A. Shahab, C. Flamm, C. Fried, J. Hackermuller, J. Hertel, M. Lindemeyer, K. Missal, A. Tanzer, S. Washietl, J. Korbel, O. Emanuelsson, J. S. Pedersen, N. Holroyd, R. Taylor, D. Swarbreck, N. Matthews, M. C. Dickson, D. J. Thomas, M. T. Weirauch, J. Gilbert, J. Drenkow, I. Bell, X. Zhao, K. G. Srinivasan, W. K. Sung, H. S. Ooi, K. P. Chiu, S. Foissac, T. Alioto, M. Brent, L. Pachter, M. L. Tress, A. Valencia, S. W. Choo, C. Y. Choo, C. Ucla, C. Manzano, C. Wyss, E. Cheung, T. G. Clark, J. B. Brown, M. Ganesh, S. Patel, H. Tammana, J. Chrast, C. N. Henrichsen, C. Kai, J. Kawai, U. Nagalakshmi, J. Wu, Z. Lian, J. Lian, P. Newburger, X. Zhang, P. Bickel, J. S. Mattick, P. Carninci, Y. Hayashizaki, S. Weissman, T. Hubbard, R. M. Myers, J. Rogers, P. F. Stadler, T. M. Lowe, C. L. Wei, Y. Ruan, K. Struhl, M. Gerstein, S. E. Antonarakis, Y. Fu, E. D. Green, U. Karaoz, A. Siepel, J. Taylor, L. A. Liefer, K. A. Wetterstrand, P. J. Good, E. A. Feingold, M. S. Guyer, G. M. Cooper, G. Asimenos, C. N. Dewey, M. Hou, S. Nikolaev, J. I. Montoya-Burgos, A. Loytynoja, S. Whelan, F. Pardi, T. Massingham, H. Huang, N. R. Zhang, I. Holmes, J. C. Mullikin, A. Ureta-Vidal, B. Paten, M. Seringhaus, D. Church, K. Rosenbloom, W. J. Kent, E. A. Stone, S. Batzoglou, N. Goldman, R. C. Hardison, D. Haussler, W. Miller, A. Sidow, N. D. Trinklein, Z. D. Zhang, L. Barrera, R. Stuart, D. C. King, A. Ameur, S. Enroth, M. C. Bieda, J. Kim, A. A. Bhinge, N. Jiang, J. Liu, F. Yao, V. B. Vega, C. W. Lee, P. Ng, A. Yang, Z. Moqtaderi, Z. Zhu, X. Xu, S. Squazzo, M. J. Oberley, D. Inman, M. A. Singer, T. A. Richmond, K. J. Munn, A. Rada-Iglesias, O. Wallerman, J. Komorowski, J. C. Fowler, P. Couttet, A. W. Bruce, O. M. Dovey, P. D. Ellis, C. F. Langford, D. A. Nix, G. Euskirchen, S. Hartman, A. E. Urban, P. Kraus, S. Van Calcar, N. Heintzman, T. H. Kim, K. Wang, C. Qu, G. Hon, R. Luna, C. K. Glass, M. G. Rosenfeld, S. F. Aldred, S. J. Cooper, A. Halees, J. M. Lin, H. P. Shulha, M. Xu, J. N. Haidar, Y. Yu, V. R. Iyer, R. D. Green, C. Wadelius, P. J. Farnham, B. Ren, R. A. Harte, A. S. Hinrichs, H. Trumbower, H. Clawson, J. Hillman-Jackson, A. S. Zweig, K. Smith, A. Thakkapallayil, G. Barber, R. M. Kuhn, D. Karolchik, L. Armengol, C. P. Bird, P. I. de Bakker, A. D. Kern, N. Lopez-Bigas, J. D. Martin, B. E. Stranger, A. Woodroffe, E. Davydov, A. Dimas, E. Eyras, I. B. Hallgrimsdottir, J. Huppert, M. C. Zody, G. R. Abecasis, X. Estivill, G. G. Bouffard, X. Guan, N. F. Hansen, J. R. Idol, V. V. Maduro, B. Maskeri, J. C. McDowell, M. Park, P. J. Thomas, A. C. Young, R. W. Blakesley, D. M. Muzny, E. Sodergren,

D. A. Wheeler, K. C. Worley, H. Jiang, G. M. Weinstock, R. A. Gibbs, T. Graves, R. Fulton, E. R. Mardis, R. K. Wilson, M. Clamp, J. Cuff, S. Gnerre, D. B. Jaffe, J. L. Chang, K. Lindblad-Toh, E. S. Lander, M. Koriabine, M. Nefedov, K. Osoegawa, Y. Yoshinaga, B. Zhu and P. J. de Jong (2007). "Identification and analysis of functional elements in 1% of the human genome by the ENCODE pilot project." Nature **447**(7146): 799-816.

Bishopric, N. H. (2005). "Evolution of the heart from bacteria to man." Ann N Y Acad Sci **1047**: 13-29.

Bodi, I., G. Mikala, S. E. Koch, S. A. Akhter and A. Schwartz (2005). "The L-type calcium channel in the heart: the beat goes on." J Clin Invest **115**(12): 3306-3317.

Bornstein, P., J. McKay, J. K. Morishima, S. Devarayalu and R. E. Gelinas (1987). "Regulatory elements in the first intron contribute to transcriptional control of the human alpha 1(I) collagen gene." Proc Natl Acad Sci U S A **84**(24): 8869-8873.

Boyle, A. P., E. L. Hong, M. Hariharan, Y. Cheng, M. A. Schaub, M. Kasowski, K. J. Karczewski, J. Park, B. C. Hitz, S. Weng, J. M. Cherry and M. Snyder (2012). "Annotation of functional variation in personal genomes using RegulomeDB." Genome Res **22**(9): 1790-1797.

Brahmajothi, M. V., D. L. Campbell, R. L. Rasmusson, M. J. Morales, J. S. Trimmer, J. M. Nerbonne and H. C. Strauss (1999). "Distinct transient outward potassium current (Ito) phenotypes and distribution of fast-inactivating potassium channel alpha subunits in ferret left ventricular myocytes." J Gen Physiol **113**(4): 581-600.

Brandeis, M., D. Frank, I. Keshet, Z. Siegfried, M. Mendelsohn, A. Nemes, V. Temper, A. Razin and H. Cedar (1994). "Sp1 elements protect a CpG island from de novo methylation." Nature **371**(6496): 435-438.

Brew HM, Gittelman JX, Silverstein RS, Hanks TD, Demas VP, Robinson LC, Robbins CA, McKee-Johnson J, Chiu SY, Messing A & Tempel BL (2007). Seizures and reduced life span in mice lacking the potassium channel subunit Kv1.2, but hypoexcitability and enlarged Kv1 currents in auditory neurons. *J Neurophysiol* **98**, 1501-25.

Bru-Mercier, G., E. Deroubaix, V. Capuano, Y. Ruchon, C. Rucker-Martin, A. Coulombe and J. F. Renaud (2003). "Expression of heart K+ channels in adrenalectomized and catecholamine-depleted reserpine-treated rats." J Mol Cell Cardiol **35**(2): 153-163.

Butler, J. E. and J. T. Kadonaga (2002). "The RNA polymerase II core promoter: a key component in the regulation of gene expression." Genes Dev **16**(20): 2583-2592.

Carninci, P., A. Sandelin, B. Lenhard, S. Katayama, K. Shimokawa, J. Ponjavic, C. A. Semple, M. S. Taylor, P. G. Engstrom, M. C. Frith, A. R. Forrest, W. B. Alkema, S. L. Tan, C. Plessy, R.

Kodzius, T. Ravasi, T. Kasukawa, S. Fukuda, M. Kanamori-Katayama, Y. Kitazume, H. Kawaji, C. Kai, M. Nakamura, H. Konno, K. Nakano, S. Mottagui-Tabar, P. Arner, A. Chesi, S. Gustincich, F. Persichetti, H. Suzuki, S. M. Grimmond, C. A. Wells, V. Orlando, C. Wahlestedt, E. T. Liu, M. Harbers, J. Kawai, V. B. Bajic, D. A. Hume and Y. Hayashizaki (2006). "Genome-wide analysis of mammalian promoter architecture and evolution." Nat Genet **38**(6): 626-635.

Carroll, S. B., J. K. Grenier and S. D. Weatherbee (2001). From DNA to diversity : molecular genetics and the evolution of animal design. Oxford, Blackwell Science.

Carroll, S. B. (2005). "Evolution at two levels: on genes and form." PLoS Biol **3**(7): e245.

Carroll, S. B., J. K. Grenier and S. D. Weatherbee (2004). From DNA to Diversity: Molecular Genetics and the Evolution of Animal Design Blackwell Science, Malden, USA.

Carroll, S. B., J. K. Grenier and S. D. Weatherbee (2005). From DNA to diversity : molecular genetics and the evolution of animal design. Malden, Mass. ; Oxford, Blackwell Pub.

Catterall, W. A. (2000). "Structure and regulation of voltage-gated Ca2+ channels." Annu Rev Cell Dev Biol **16**: 521-555.

Chan, Y. F., M. E. Marks, F. C. Jones, G. Villarreal, Jr., M. D. Shapiro, S. D. Brady, A. M. Southwick, D. M. Absher, J. Grimwood, J. Schmutz, R. M. Myers, D. Petrov, B. Jonsson, D. Schluter, M. A. Bell and D. M. Kingsley (2010). "Adaptive evolution of pelvic reduction in sticklebacks by recurrent deletion of a Pitx1 enhancer." Science **327**(5963): 302-305.

Chandler, N. J., I. D. Greener, J. O. Tellez, S. Inada, H. Musa, P. Molenaar, D. Difrancesco, M. Baruscotti, R. Longhi, R. H. Anderson, R. Billeter, V. Sharma, D. C. Sigg, M. R. Boyett and H. Dobrzynski (2009). "Molecular architecture of the human sinus node: insights into the function of the cardiac pacemaker." Circulation **119**(12): 1562-1575.

Clapham, D. E. (2007). "Calcium signaling." Cell **131**(6): 1047-1058.

Colosimo, P. F., K. E. Hosemann, S. Balabhadra, G. Villarreal, Jr., M. Dickson, J. Grimwood, J. Schmutz, R. M. Myers, D. Schluter and D. M. Kingsley (2005). "Widespread parallel evolution in sticklebacks by repeated fixation of Ectodysplasin alleles." Science **307**(5717): 1928-1933.

Chapados RA, Gruver EJ, Ingwall JS, Marsh JD & Gwathmey JK (1992). Chronic administration of cardiovascular drugs: altered energetics and transmembrane signaling. *Am J Physiol* **263**, H1576-H1586.

Chen, Q., G. E. Kirsch, D. Zhang, R. Brugada, J. Brugada, P. Brugada, D. Potenza, A. Moya, M. Borggrefe, G. Breithardt, R. Ortiz-Lopez, Z. Wang, C. Antzelevitch, R. E. O'Brien, E. Schulze-

Bahr, M. T. Keating, J. A. Towbin and Q. Wang (1998). "Genetic basis and molecular mechanism for idiopathic ventricular fibrillation." Nature **392**(6673): 293-296.

Chen X, Piacentino V, Furukawa S, Goldman B, Margulies KB & Houser SR (2002). L-type Ca^{2+} channel density and regulation are altered in failing human ventricular myocytes and recover after support with mechanical assist devices. *Circ Res* **91**, 517-24.

Choi, J. K. (2010). "Contrasting chromatin organization of CpG islands and exons in the human genome." Genome Biol **11**(7): R70.

Core, L. J., J. J. Waterfall and J. T. Lis (2008). "Nascent RNA sequencing reveals widespread pausing and divergent initiation at human promoters." Science **322**(5909): 1845-1848.

Costantini, D. L., E. P. Arruda, P. Agarwal, K. H. Kim, Y. Zhu, W. Zhu, M. Lebel, C. W. Cheng, C. Y. Park, S. A. Pierce, A. Guerchicoff, G. D. Pollevick, T. Y. Chan, M. G. Kabir, S. H. Cheng, M. Husain, C. Antzelevitch, D. Srivastava, G. J. Gross, C. C. Hui, P. H. Backx and B. G. Bruneau (2005). "The homeodomain transcription factor Irx5 establishes the mouse cardiac ventricular repolarization gradient." Cell **123**(2): 347-358.

Coulondre, C., J. H. Miller, P. J. Farabaugh and W. Gilbert (1978). "Molecular basis of base substitution hotspots in Escherichia coli." Nature **274**(5673): 775-780.

Covarrubias, M., A. Bhattacharji, J. A. De Santiago-Castillo, K. Dougherty, Y. A. Kaulin, T. R. Na-Phuket and G. Wang (2008). "The neuronal Kv4 channel complex." Neurochem Res **33**(8): 1558-1567.

Cowan, W. M., K. L. Kopnisky and S. E. Hyman (2002). "The human genome project and its impact on psychiatry." Annu Rev Neurosci **25**: 1-50.

Crocker, J., N. Potter and A. Erives (2010). "Dynamic evolution of precise regulatory encodings creates the clustered site signature of enhancers." Nat Commun **1**: 99.

Crocker, J., Y. Tamori and A. Erives (2008). "Evolution acts on enhancer organization to fine-tune gradient threshold readouts." PLoS Biol **6**(11): e263.

Davison (2001). Genomic Regulatory Systems: Development and Evolution, San Diego: Academic Press.

Deaton, A. M. and A. Bird (2011). "CpG islands and the regulation of transcription." Genes Dev **25**(10): 1010-1022.

Dekker, J., K. Rippe, M. Dekker and N. Kleckner (2002). "Capturing chromosome conformation." Science **295**(5558): 1306-1311.

Delgado, S., M. Gomez, A. Bird and F. Antequera (1998). "Initiation of DNA replication at CpG islands in mammalian chromosomes." EMBO J **17**(8): 2426-2435.

Delisle BP, Anson BD, Rajamani S & January CT (2004). Biology of cardiac arrhythmias: ion channel protein trafficking. *Circ Res* **94**, 1418-28.

Demuth, J. P., T. De Bie, J. E. Stajich, N. Cristianini and M. W. Hahn (2006). "The evolution of mammalian gene families." PLoS One **1**: e85.

Deutschbauer, A. M., D. F. Jaramillo, M. Proctor, J. Kumm, M. E. Hillenmeyer, R. W. Davis, C. Nislow and G. Giaever (2005). "Mechanisms of haploinsufficiency revealed by genome-wide profiling in yeast." Genetics **169**(4): 1915-1925.

DiFrancesco, D. (2010). "The role of the funny current in pacemaker activity." Circ Res **106**(3): 434-446.

DiFrancesco, D., A. Ferroni, M. Mazzanti and C. Tromba (1986). "Properties of the hyperpolarizing-activated current (if) in cells isolated from the rabbit sino-atrial node." J Physiol **377**: 61-88.

Dixon, J. E. and D. McKinnon (1994). "Quantitative analysis of potassium channel mRNA expression in atrial and ventricular muscle of rats." Circ Res **75**(2): 252-260.

Dixon, J. E., W.Deutsch C (2003). The birth of a channel. *Neuron* **40**, 265-76.

Fodstad H, Swan H, Auberson M, Gautschi I, Loffing J, Schild L & Kontula K (2004). Loss-of-function mutations of the K(+) channel gene KCNJ2 constitute a rare cause of long QT syndrome. *J Mol Cell Cardiol* **37**, 593-602.

Dixon, J. E., W. Shi, H. S. Wang, C. McDonald, H. Yu, R. S. Wymore, I. S. Cohen and D. McKinnon (1996). "Role of the Kv4.3 K+ channel in ventricular muscle. A molecular correlate for the transient outward current." Circ Res **79**(4): 659-668.

Donald, R. G. and A. R. Cashmore (1990). "Mutation of either G box or I box sequences profoundly affects expression from the Arabidopsis rbcS-1A promoter." EMBO J **9**(6): 1717-1726.

Dong, M., X. Sun, A. A. Prinz and H. S. Wang (2006). "Effect of simulated I(to) on guinea pig and canine ventricular action potential morphology." Am J Physiol Heart Circ Physiol **291**(2): H631-637.

Dong, M., S. Yan, Y. Chen, P. J. Niklewski, X. Sun, K. Chenault and H. S. Wang (2010). "Role of the transient outward current in regulating mechanical properties of canine ventricular myocytes." J Cardiovasc Electrophysiol **21**(6): 697-703.

Dostie, J., T. A. Richmond, R. A. Arnaout, R. R. Selzer, W. L. Lee, T. A. Honan, E. D. Rubio, A. Krumm, J. Lamb, C. Nusbaum, R. D. Green and J. Dekker (2006). "Chromosome Conformation Capture Carbon Copy (5C): a massively parallel solution for mapping interactions between genomic elements." Genome Res **16**(10): 1299-1309.

Duncan, B. K. and J. H. Miller (1980). "Mutagenic deamination of cytosine residues in DNA." Nature **287**(5782): 560-561.

Elzinga, G. and N. Westerhof (1991). "Matching between ventricle and arterial load. An evolutionary process." Circ Res **68**(6): 1495-1500.

Emory, S. A., P. Bouvet and J. G. Belasco (1992). "A 5'-terminal stem-loop structure can stabilize mRNA in Escherichia coli." Genes Dev **6**(1): 135-148.

Ernst, J., P. Kheradpour, T. S. Mikkelsen, N. Shoresh, L. D. Ward, C. B. Epstein, X. Zhang, L. Wang, R. Issner, M. Coyne, M. Ku, T. Durham, M. Kellis and B. E. Bernstein (2011). "Mapping and analysis of chromatin state dynamics in nine human cell types." Nature **473**(7345): 43-49.

Fazzari, M. J. and J. M. Greally (2004). "Epigenomics: beyond CpG islands." Nat Rev Genet **5**(6): 446-455.

Fedorova, L. and A. Fedorov (2003). "Introns in gene evolution." Genetica **118**(2-3): 123-131.

Ficz, G., M. R. Branco, S. Seisenberger, F. Santos, F. Krueger, T. A. Hore, C. J. Marques, S. Andrews and W. Reik (2011). "Dynamic regulation of 5-hydroxymethylcytosine in mouse ES cells and during differentiation." Nature **473**(7347): 398-402.

Findlay, I. (2003). "Is there an A-type K+ current in guinea pig ventricular myocytes?" American Journal of Physiology-Heart and Circulatory Physiology **284**(2): H598-H604.

Fischer, A., Y. Gilad, O. Man and S. Paabo (2005). "Evolution of bitter taste receptors in humans and apes." Mol Biol Evol **22**(3): 432-436.

Fodstad, H., H. Swan, M. Auberson, I. Gautschi, J. Loffing, L. Schild and K. Kontula (2004). "Loss-of-function mutations of the K(+) channel gene KCNJ2 constitute a rare cause of long QT syndrome." J Mol Cell Cardiol **37**(2): 593-602.

Frankel, N., D. F. Erezyilmaz, A. P. McGregor, S. Wang, F. Payre and D. L. Stern (2011). "Morphological evolution caused by many subtle-effect substitutions in regulatory DNA." Nature **474**(7353): 598-603.

Frazer, K. A., L. Pachter, A. Poliakov, E. M. Rubin and I. Dubchak (2004). "VISTA: computational tools for comparative genomics." Nucleic Acids Res **32**(Web Server issue): W273-279.

Gaborit, N., R. Sakuma, J. N. Wylie, K. H. Kim, S. S. Zhang, C. C. Hui and B. G. Bruneau (2012). "Cooperative and antagonistic roles for Irx3 and Irx5 in cardiac morphogenesis and postnatal physiology." Development **139**(21): 4007-4019.

Gaborit, N., A. Varro, S. Le Bouter, V. Szuts, D. Escande, S. Nattel and S. Demolombe (2010). "Gender-related differences in ion-channel and transporter subunit expression in non-diseased human hearts." J Mol Cell Cardiol **49**(4): 639-646.

Gardiner-Garden, M. and M. Frommer (1987). "CpG islands in vertebrate genomes." J Mol Biol **196**(2): 261-282.

Gilchrist, D. A., G. Fromm, G. dos Santos, L. N. Pham, I. E. McDaniel, A. Burkholder, D. C. Fargo and K. Adelman (2012). "Regulating the regulators: the pervasive effects of Pol II pausing on stimulus-responsive gene networks." Genes Dev **26**(9): 933-944.

Glass, J. L., R. F. Thompson, B. Khulan, M. E. Figueroa, E. N. Olivier, E. J. Oakley, G. Van Zant, E. E. Bouhassira, A. Melnick, A. Golden, M. J. Fazzari and J. M. Greally (2007). "CG dinucleotide clustering is a species-specific property of the genome." Nucleic Acids Res **35**(20): 6798-6807.

Gompel, N., B. Prud'homme, P. J. Wittkopp, V. A. Kassner and S. B. Carroll (2005). "Chance caught on the wing: *cis*-regulatory evolution and the origin of pigment patterns in Drosophila." Nature **433**(7025): 481-487.

Gomez-Ospina N, Tsuruta F, Barreto-Chang O , Hu L & Dolmetsch R (2006). The C terminus of the L-type voltage-gated calcium channel Ca(V)1.2 encodes a transcription factor. *Cell* **127**, 591-606.

Goujon, M., H. McWilliam, W. Li, F. Valentin, S. Squizzato, J. Paern and R. Lopez (2010). "A new bioinformatics analysis tools framework at EMBL-EBI." Nucleic Acids Res **38**(Web Server issue): W695-699.

Grus, W. E., P. Shi, Y. P. Zhang and J. Zhang (2005). "Dramatic variation of the vomeronasal pheromone receptor gene repertoire among five orders of placental and marsupial mammals." Proc Natl Acad Sci U S A **102**(16): 5767-5772.

Guenther, M. G., S. S. Levine, L. A. Boyer, R. Jaenisch and R. A. Young (2007). "A chromatin landmark and transcription initiation at most promoters in human cells." Cell **130**(1): 77-88.

Guo, W., W. E. Jung, C. Marionneau, F. Aimond, H. Xu, K. A. Yamada, T. L. Schwarz, S. Demolombe and J. M. Nerbonne (2005). "Targeted deletion of Kv4.2 eliminates I(to,f) and results in electrical and molecular remodeling, with no evidence of ventricular hypertrophy or myocardial dysfunction." Circ Res **97**(12): 1342-1350.

Hackenberg, M., G. Barturen, P. Carpena, P. L. Luque-Escamilla, C. Previti and J. L. Oliver (2010). "Prediction of CpG-island function: CpG clustering vs. sliding-window methods." BMC Genomics **11**: 327.

Hackenberg, M., C. Previti, P. L. Luque-Escamilla, P. Carpena, J. Martinez-Aroza and J. L. Oliver (2006). "CpGcluster: a distance-based algorithm for CpG-island detection." BMC Bioinformatics **7**: 446.

Hadley RW, Lederer WJ (1991). Properties of L-type calcium channel gating current in isolated guinea pig ventricular myocytes. *J Gen Physiol* **98**, 265-85.

Hagiwara, S., S. Miyazaki and N. P. Rosenthal (1976). "Potassium current and the effect of cesium on this current during anomalous rectification of the egg cell membrane of a starfish." J Gen Physiol **67**(6): 621-638.

Hamilton, N. and C. D. Ianuzzo (1991). "Contractile and calcium regulating capacities of myocardia of different sized mammals scale with resting heart rate." Mol Cell Biochem **106**(2): 133-141.

Han, L. and Z. Zhao (2009). "CpG islands or CpG clusters: how to identify functional GC-rich regions in a genome?" BMC Bioinformatics **10**: 65.

Hargreaves, D. C., T. Horng and R. Medzhitov (2009). "Control of inducible gene expression by signal-dependent transcriptional elongation." Cell **138**(1): 129-145.

He J, Conklin MW, Foell JD, Wolff MR, Haworth RA, Coronado R & Kamp TJ (2001). Reduction in density of transverse tubules and L-type Ca(2+) channels in canine tachycardia-induced heart failure. *Cardiovasc Res* **49**, 298-307.

He, W., Y. Jia and K. Takimoto (2009). "Interaction between transcription factors Iroquois proteins 4 and 5 controls cardiac potassium channel Kv4.2 gene transcription." Cardiovasc Res **81**(1): 64-71.

Herrmann, S., J. Stieber, G. Stockl, F. Hofmann and A. Ludwig (2007). "HCN4 provides a 'depolarization reserve' and is not required for heart rate acceleration in mice." EMBO J **26**(21): 4423-4432.

Hindorff, L. A., P. Sethupathy, H. A. Junkins, E. M. Ramos, J. P. Mehta, F. S. Collins and T. A. Manolio (2009). "Potential etiologic and functional implications of genome-wide association loci for human diseases and traits." Proc Natl Acad Sci U S A **106**(23): 9362-9367.

Hoekstra, H. E. and J. A. Coyne (2007). "The locus of evolution: evo devo and the genetics of adaptation." Evolution **61**(5): 995-1016.

Hofmann, F., M. Biel and V. Flockerzi (1994). "Molecular basis for Ca2+ channel diversity." Annu Rev Neurosci **17**: 399-418.

Holt, J. P., E. A. Rhode and H. Kines (1968). "Ventricular volumes and body weight in mammals." Am J Physiol **215**(3): 704-715.

Hong, T. T., J. W. Smyth, D. Gao, K. Y. Chu, J. M. Vogan, T. S. Fong, B. C. Jensen, H. M. Colecraft and R. M. Shaw (2010). "BIN1 localizes the L-type calcium channel to cardiac T-tubules." PLoS Biol **8**(2): e1000312.

Hoppe, U. C., E. Marban and D. C. Johns (2000). "Molecular dissection of cardiac repolarization by *in vivo* Kv4.3 gene transfer." J Clin Invest **105**(8): 1077-1084.

Hove-Madsen, L. and D. M. Bers (1993). "Sarcoplasmic reticulum Ca2+ uptake and thapsigargin sensitivity in permeabilized rabbit and rat ventricular myocytes." Circ Res **73**(5): 820-828.

Hume, J. R., W. Giles, K. Robinson, E. F. Shibata, R. D. Nathan, K. Kanai and R. Rasmusson (1986). "A time- and voltage-dependent K+ current in single cardiac cells from bullfrog atrium." J Gen Physiol **88**(6): 777-798.

Illingworth, R. S., U. Gruenewald-Schneider, S. Webb, A. R. Kerr, K. D. James, D. J. Turner, C. Smith, D. J. Harrison, R. Andrews and A. P. Bird (2010). "Orphan CpG islands identify numerous conserved promoters in the mammalian genome." PLoS Genet **6**(9).

Ioshikhes, I. P. and M. Q. Zhang (2000). "Large-scale human promoter mapping using CpG islands." Nat Genet **26**(1): 61-63.

Irizarry, R. A., H. Wu and A. P. Feinberg (2009). "A species-generalized probabilistic model-based definition of CpG islands." Mamm Genome **20**(9-10): 674-680.

Jansa, S. A. and M. Weksler (2004). "Phylogeny of muroid rodents: relationships within and among major lineages as determined by IRBP gene sequences." Mol Phylogenet Evol **31**(1): 256-276.

Jareborg, N., E. Birney and R. Durbin (1999). "Comparative analysis of noncoding regions of 77 orthologous mouse and human gene pairs." Genome Res **9**(9): 815-824.

Jarrard, D. F., H. Kinoshita, Y. Shi, C. Sandefur, D. Hoff, L. F. Meisner, C. Chang, J. G. Herman, W. B. Isaacs and N. Nassif (1998). "Methylation of the androgen receptor promoter CpG island is associated with loss of androgen receptor expression in prostate cancer cells." Cancer Res **58**(23): 5310-5314.

Jacob, F. (1977). "Evolution and tinkering." Science **196**(4295): 1161-1166.

Jenuwein, T. and C. D. Allis (2001). "Translating the histone code." Science **293**(5532): 1074-1080.

Jeyaraj, D., S. M. Haldar, X. Wan, M. D. McCauley, J. A. Ripperger, K. Hu, Y. Lu, B. L. Eapen, N. Sharma, E. Ficker, M. J. Cutler, J. Gulick, A. Sanbe, J. Robbins, S. Demolombe, R. V. Kondratov, S. A. Shea, U. Albrecht, X. H. Wehrens, D. S. Rosenbaum and M. K. Jain (2012). "Circadian rhythms govern cardiac repolarization and arrhythmogenesis." Nature **483**(7387): 96-99.

Kaczynski, J., T. Cook and R. Urrutia (2003). "Sp1- and Kruppel-like transcription factors." Genome Biol **4**(2): 206.

Karlic, R., H. R. Chung, J. Lasserre, K. Vlahovicek and M. Vingron (2010). "Histone modification levels are predictive for gene expression." Proc Natl Acad Sci U S A **107**(7): 2926-2931.

King, M. C. and A. C. Wilson (1975). "Evolution at two levels in humans and chimpanzees." Science **188**(4184): 107-116.

Kobayashi, T., Y. Yamada, M. Nagashima, S. Seki, M. Tsutsuura, Y. Ito, I. Sakuma, H. Hamada, T. Abe and N. Tohse (2003). "Contribution of KChIP2 to the developmental increase in transient outward current of rat cardiomyocytes." J Mol Cell Cardiol **35**(9): 1073-1082.

Kobayashi T, Yamada Y, Fukao M, Tsutsuura M & Tohse N (2007). Regulation of Cav1.2 current: interaction with intracellular molecules. *J Pharmacol Sci* **103**, 347-53.

Koitabashi N, Bedja D, Zaiman AL, Pinto YM, Zhang M, Gabrielson KL, Takimoto E & Kass DA (2009). Avoidance of transient cardiomyopathy in cardiomyocyte-targeted tamoxifen-induced MerCreMer gene deletion models. *Circ Res* **105**, 12-5.

Koch, C. (1999). Biophysics of computation : information processing in single neurons. Oxford, Oxford University Press.

Kuo, H. C., C. F. Cheng, R. B. Clark, J. J. Lin, J. L. Lin, M. Hoshijima, V. T. Nguyen-Tran, Y. Gu, Y. Ikeda, P. H. Chu, J. Ross, W. R. Giles and K. R. Chien (2001). "A defect in the Kv channel-interacting protein 2 (KChIP2) gene leads to a complete loss of I(to) and confers susceptibility to ventricular tachycardia." Cell **107**(6): 801-813.

Lakatta, E. G., T. M. Vinogradova and V. A. Maltsev (2008). "The missing link in the mystery of normal automaticity of cardiac pacemaker cells." Ann N Y Acad Sci **1123**: 41-57.

Larionov, A., A. Krause and W. Miller (2005). "A standard curve based method for relative real time PCR data processing." BMC Bioinformatics **6**: 62.

Larkin, M. A., G. Blackshields, N. P. Brown, R. Chenna, P. A. McGettigan, H. McWilliam, F. Valentin, I. M. Wallace, A. Wilm, R. Lopez, J. D. Thompson, T. J. Gibson and D. G. Higgins (2007). "Clustal W and Clustal X version 2.0." Bioinformatics **23**(21): 2947-2948.

Larsen, F., G. Gundersen, R. Lopez and H. Prydz (1992). "CpG islands as gene markers in the human genome." Genomics **13**(4): 1095-1107.

Lenhard, B., A. Sandelin and P. Carninci (2012). "Metazoan promoters: emerging characteristics and insights into transcriptional regulation." Nat Rev Genet **13**(4): 233-245.

Lieberman-Aiden, E., N. L. van Berkum, L. Williams, M. Imakaev, T. Ragoczy, A. Telling, I. Amit, B. R. Lajoie, P. J. Sabo, M. O. Dorschner, R. Sandstrom, B. Bernstein, M. A. Bender, M. Groudine, A. Gnirke, J. Stamatoyannopoulos, L. A. Mirny, E. S. Lander and J. Dekker (2009). "Comprehensive mapping of long-range interactions reveals folding principles of the human genome." Science **326**(5950): 289-293.

Liu, Z., J.Lee, J. H., C. M. Tate, J. S. You and D. G. Skalnik (2007). "Identification and characterization of the human Set1B histone H3-Lys4 methyltransferase complex." J Biol Chem **282**(18): 13419-13428.

Liu, Z., J. Golowasch, E. Marder and L. F. Abbott (1998). "A model neuron with activity-dependent conductances regulated by multiple calcium sensors." J Neurosci **18**(7): 2309-2320.

Logan, D. W., R. J. Bryson-Richardson, K. E. Pagan, M. S. Taylor, P. D. Currie and I. J. Jackson (2003). "The structure and evolution of the melanocortin and MCH receptors in fish and mammals." Genomics **81**(2): 184-191.

Lonsberry BB, Czubryt MP, Dubo DF, Gilchrist JS, Docherty JC, Maddaford TG & Pierce GN

(1992). Effect of chronic administration of verapamil on Ca++ channel density in rat tissue. *J Pharmacol Exp Ther* **263**, 540-5.

Lonsberry BB, Dubo DF, Thomas SM, Docherty JC, Maddaford TG & Pierce GN (1994). Effect of high-dose verapamil administration on the Ca2+ channel density in rat cardiac tissue. *Pharmacology* **49**, 23-32.

Loughrey, C. M., G. L. Smith and K. E. MacEachern (2004). "Comparison of Ca2+ release and uptake characteristics of the sarcoplasmic reticulum in isolated horse and rabbit cardiomyocytes." Am J Physiol Heart Circ Physiol **287**(3): H1149-1159.

Lu, Z., K. Kamiya, T. Opthof, K. Yasui and I. Kodama (2001). "Density and kinetics of I(Kr) and I(Ks) in guinea pig and rabbit ventricular myocytes explain different efficacy of I(Ks) blockade at high heart rate in guinea pig and rabbit: implications for arrhythmogenesis in humans." Circulation **104**(8): 951-956.

Ludwig, A., X. Zong, M. Jeglitsch, F. Hofmann and M. Biel (1998). "A family of hyperpolarization-activated mammalian cation channels." Nature **393**(6685): 587-591.

Ludwig, M. Z. (2002). "Functional evolution of noncoding DNA." Curr Opin Genet Dev **12**(6): 634-639.

Ludwig, M. Z., C. Bergman, N. H. Patel and M. Kreitman (2000). "Evidence for stabilizing selection in a eukaryotic enhancer element." Nature **403**(6769): 564-567.

Mandal, M. and R. R. Breaker (2004). "Gene regulation by riboswitches." Nat Rev Mol Cell Biol **5**(6): 451-463.

Mangoni, M. E. and J. Nargeot (2008). "Genesis and regulation of the heart automaticity." Physiol Rev **88**(3): 919-982.

Macleod, D., J. Charlton, J. Mullins and A. P. Bird (1994). "Sp1 sites in the mouse aprt gene promoter are required to prevent methylation of the CpG island." Genes Dev **8**(19): 2282-2292.

Maruyama, K. and S. Sugano (1994). "Oligo-capping: a simple method to replace the cap structure of eukaryotic mRNAs with oligoribonucleotides." Gene **138**(1-2): 171-174.

Maston, G. A., S. K. Evans and M. R. Green (2006). "Transcriptional regulatory elements in the human genome." Annu Rev Genomics Hum Genet **7**: 29-59.

Matlin, A. J., F. Clark and C. W. Smith (2005). "Understanding alternative splicing: towards a cellular code." Nat Rev Mol Cell Biol **6**(5): 386-398.

Maunakea, A. K., R. P. Nagarajan, M. Bilenky, T. J. Ballinger, C. D'Souza, S. D. Fouse, B. E. Johnson, C. Hong, C. Nielsen, Y. Zhao, G. Turecki, A. Delaney, R. Varhol, N. Thiessen, K. Shchors, V. M. Heine, D. H. Rowitch, X. Xing, C. Fiore, M. Schillebeeckx, S. J. Jones, D. Haussler, M. A. Marra, M. Hirst, T. Wang and J. F. Costello (2010). "Conserved role of intragenic DNA methylation in regulating alternative promoters." Nature **466**(7303): 253-257.

McGregor, A. P., V. Orgogozo, I. Delon, J. Zanet, D. G. Srinivasan, F. Payre and D. L. Stern (2007). "Morphological evolution through multiple *cis*-regulatory mutations at a single gene." Nature **448**(7153): 587-590.

Meireles-Filho, A. C. and A. Stark (2009). "Comparative genomics of gene regulation-conservation and divergence of *cis*-regulatory information." Curr Opin Genet Dev **19**(6): 565-570.

Meister, G., M. Landthaler, A. Patkaniowska, Y. Dorsett, G. Teng and T. Tuschl (2004). "Human Argonaute2 mediates RNA cleavage targeted by miRNAs and siRNAs." Mol Cell **15**(2): 185-197.

Mignone, F., C. Gissi, S. Liuni and G. Pesole (2002). "Untranslated regions of mRNAs." Genome Biol **3**(3): REVIEWS0004.

Minervini, C. F., S. Ruggieri, M. Traversa, L. D'Aiuto, R. M. Marsano, D. Leronni, I. Centomani, C. De Giovanni and L. Viggiano (2010). "Evidences for insulator activity of the 5'UTR of the Drosophila melanogaster LTR-retrotransposon ZAM." Mol Genet Genomics **283**(5): 503-509.

McCaughran JA, Juno CJ (1988). Calcium channel blockade with verapamil. Effects on blood pressure, renal, and myocardial adrenergic, cholinergic, and calcium channel receptors in inbred Dahl hypertension-sensitive (S/JR) and hypertension-resistant (R/JR) rats. *Am J Hypertens* **1**, 255S-62S.

Meissner M, Weissgerber P, Londono JEC, Molkentin JD, Nilius B, Flockerzi V & Freichel M (2009). Temporally regulated inactivation of the loxP-targeted CaVß2 gene in the adult mouse heart. *Naunyn Schmiedebergs Arch. Pharmacol.* **379 Suppl. 1**, 30-1.

Merlie JP, Smith MM (1986). Synthesis and assembly of acetylcholine receptor, a multisubunit membrane glycoprotein. *J. Mem. Biol.* **91**, 1-10.

Muth JN, Bodi I, Lewis W, Varadi G & Schwartz A (2001). A Ca^{2+}-dependent transgenic model of cardiac hypertrophy: A role for protein kinase Calpha. *Circulation* **103**, 140-7.

Muth JN, Yamaguchi H, Mikala G, Grupp IL, Lewis W, Cheng H, Song LS, Lakatta EG, Varadi G & Schwartz A (1999). Cardiac-specific overexpression of the alpha(1) subunit of the L-type

voltage-dependent Ca(2+) channel in transgenic mice. Loss of isoproterenol-induced contraction. *J Biol Chem* **274**, 21503-6.

Mohn, F. and D. Schubeler (2009). "Genetics and epigenetics: stability and plasticity during cellular differentiation." Trends Genet **25**(3): 129-136.

Moulton, G., T. K. Attwood, D. J. Parry-Smith and J. C. Packer (2003). "Phylogenomic analysis and evolution of the potassium channel gene family." Receptors Channels **9**(6): 363-377.

Mountcastle, V. B. (1980). Medical physiology. St. Louis ; London, Mosby.

Mouse Genome Sequencing, C., R. H. Waterston, K. Lindblad-Toh, E. Birney, J. Rogers, J. F. Abril, P. Agarwal, R. Agarwala, R. Ainscough, M. Alexandersson, P. An, S. E. Antonarakis, J. Attwood, R. Baertsch, J. Bailey, K. Barlow, S. Beck, E. Berry, B. Birren, T. Bloom, P. Bork, M. Botcherby, N. Bray, M. R. Brent, D. G. Brown, S. D. Brown, C. Bult, J. Burton, J. Butler, R. D. Campbell, P. Carninci, S. Cawley, F. Chiaromonte, A. T. Chinwalla, D. M. Church, M. Clamp, C. Clee, F. S. Collins, L. L. Cook, R. R. Copley, A. Coulson, O. Couronne, J. Cuff, V. Curwen, T. Cutts, M. Daly, R. David, J. Davies, K. D. Delehaunty, J. Deri, E. T. Dermitzakis, C. Dewey, N. J. Dickens, M. Diekhans, S. Dodge, I. Dubchak, D. M. Dunn, S. R. Eddy, L. Elnitski, R. D. Emes, P. Eswara, E. Eyras, A. Felsenfeld, G. A. Fewell, P. Flicek, K. Foley, W. N. Frankel, L. A. Fulton, R. S. Fulton, T. S. Furey, D. Gage, R. A. Gibbs, G. Glusman, S. Gnerre, N. Goldman, L. Goodstadt, D. Grafham, T. A. Graves, E. D. Green, S. Gregory, R. Guigo, M. Guyer, R. C. Hardison, D. Haussler, Y. Hayashizaki, L. W. Hillier, A. Hinrichs, W. Hlavina, T. Holzer, F. Hsu, A. Hua, T. Hubbard, A. Hunt, I. Jackson, D. B. Jaffe, L. S. Johnson, M. Jones, T. A. Jones, A. Joy, M. Kamal, E. K. Karlsson, D. Karolchik, A. Kasprzyk, J. Kawai, E. Keibler, C. Kells, W. J. Kent, A. Kirby, D. L. Kolbe, I. Korf, R. S. Kucherlapati, E. J. Kulbokas, D. Kulp, T. Landers, J. P. Leger, S. Leonard, I. Letunic, R. Levine, J. Li, M. Li, C. Lloyd, S. Lucas, B. Ma, D. R. Maglott, E. R. Mardis, L. Matthews, E. Mauceli, J. H. Mayer, M. McCarthy, W. R. McCombie, S. McLaren, K. McLay, J. D. McPherson, J. Meldrim, B. Meredith, J. P. Mesirov, W. Miller, T. L. Miner, E. Mongin, K. T. Montgomery, M. Morgan, R. Mott, J. C. Mullikin, D. M. Muzny, W. E. Nash, J. O. Nelson, M. N. Nhan, R. Nicol, Z. Ning, C. Nusbaum, M. J. O'Connor, Y. Okazaki, K. Oliver, E. Overton-Larty, L. Pachter, G. Parra, K. H. Pepin, J. Peterson, P. Pevzner, R. Plumb, C. S. Pohl, A. Poliakov, T. C. Ponce, C. P. Ponting, S. Potter, M. Quail, A. Reymond, B. A. Roe, K. M. Roskin, E. M. Rubin, A. G. Rust, R. Santos, V. Sapojnikov, B. Schultz, J. Schultz, M. S. Schwartz, S. Schwartz, C. Scott, S. Seaman, S. Searle, T. Sharpe, A. Sheridan, R. Shownkeen, S. Sims, J. B. Singer, G. Slater, A. Smit, D. R. Smith, B. Spencer, A. Stabenau, N. Stange-Thomann, C. Sugnet, M. Suyama, G. Tesler, J. Thompson, D. Torrents, E. Trevaskis, J. Tromp, C. Ucla, A. Ureta-Vidal, J. P. Vinson, A. C. Von Niederhausern, C. M. Wade, M. Wall, R. J. Weber, R. B. Weiss, M. C. Wendl, A. P. West, K. Wetterstrand, R. Wheeler, S. Whelan, J. Wierzbowski, D. Willey, S. Williams, R. K. Wilson, E. Winter, K. C. Worley, D. Wyman, S. Yang, S. P. Yang, E. M. Zdobnov, M. C. Zody and E. S. Lander (2002). "Initial sequencing and comparative analysis of the mouse genome." Nature **420**(6915): 520-562.

Munoz-Antonia, T., X. Li, M. Reiss, R. Jackson and S. Antonia (1996). "A mutation in the transforming growth factor beta type II receptor gene promoter associated with loss of gene expression." Cancer Res **56**(21): 4831-4835.

Nam, J., P. Dong, R. Tarpine, S. Istrail and E. H. Davidson (2010). "Functional *cis*-regulatory genomics for systems biology." Proc Natl Acad Sci U S A **107**(8): 3930-3935.

Nerbonne, J. M. and R. S. Kass (2005). "Molecular physiology of cardiac repolarization." Physiol Rev **85**(4): 1205-1253.

Ni, T., D. L. Corcoran, E. A. Rach, S. Song, E. P. Spana, Y. Gao, U. Ohler and J. Zhu (2010). "A paired-end sequencing strategy to map the complex landscape of transcription initiation." Nat Methods **7**(7): 521-527.

Niimura, Y. and M. Nei (2007). "Extensive gains and losses of olfactory receptor genes in mammalian evolution." PLoS One **2**(8): e708.

Nicolas, M., D. Dememes, A. Martin, S. Kupershmidt and J. Barhanin (2001). "KCNQ1/KCNE1 potassium channels in mammalian vestibular dark cells." Hear Res **153**(1-2): 132-145.

Niwa, N. and J. M. Nerbonne (2010). "Molecular determinants of cardiac transient outward potassium current (I(to)) expression and regulation." J Mol Cell Cardiol **48**(1): 12-25.

Niwa, N., W. Wang, Q. Sha, C. Marionneau and J. M. Nerbonne (2008). "Kv4.3 is not required for the generation of functional Ito,f channels in adult mouse ventricles." J Mol Cell Cardiol **44**(1): 95-104.

Nozaki, T., N. Yachie, R. Ogawa, A. Kratz, R. Saito and M. Tomita (2011). "Tight associations between transcription promoter type and epigenetic variation in histone positioning and modification." BMC Genomics **12**: 416.

Ohler, U. (2006). "Identification of core promoter modules in Drosophila and their application in accurate transcription start site prediction." Nucleic Acids Res **34**(20): 5943-5950.

Oliveri, P., Q. Tu and E. H. Davidson (2008). "Global regulatory logic for specification of an embryonic cell lineage." Proc Natl Acad Sci U S A **105**(16): 5955-5962.

Orchard, C. H., M. Pasek and F. Brette (2009). "The role of mammalian cardiac t-tubules in excitation-contraction coupling: experimental and computational approaches." Exp Physiol **94**(5): 509-519.

Orlando, D. A., M. G. Guenther, G. M. Frampton and R. A. Young (2012). "CpG island structure and trithorax/polycomb chromatin domains in human cells." Genomics.

Ooi, S. K., C. Qiu, E. Bernstein, K. Li, D. Jia, Z. Yang, H. Erdjument-Bromage, P. Tempst, S. P. Lin, C. D. Allis, X. Cheng and T. H. Bestor (2007). "DNMT3L connects unmethylated lysine 4 of histone H3 to de novo methylation of DNA." Nature **448**(7154): 714-717.

Osanai M, Saegusa H, Kazuno AA, Nagayama S, Hu Q, Zong S, Murakoshi T & Tanabe T (2006). Altered cerebellar function in mice lacking $Ca_V2.3$ Ca^{2+} channel. *Biochem Biophys Res Commun* **344**, 920-5.

Pandit, S. V., R. B. Clark, W. R. Giles and S. S. Demir (2001). "A mathematical model of action potential heterogeneity in adult rat left ventricular myocytes." Biophys J **81**(6): 3029-3051.

Panne, D. (2008). "The enhanceosome." Curr Opin Struct Biol **18**(2): 236-242.

Papadatos, G. A., P. M. Wallerstein, C. E. Head, R. Ratcliff, P. A. Brady, K. Benndorf, R. C. Saumarez, A. E. Trezise, C. L. Huang, J. I. Vandenberg, W. H. Colledge and A. A. Grace (2002). "Slowed conduction and ventricular tachycardia after targeted disruption of the cardiac sodium channel gene Scn5a." Proc Natl Acad Sci U S A **99**(9): 6210-6215.

Patel, S. P. and D. L. Campbell (2005). "Transient outward potassium current, 'Ito', phenotypes in the mammalian left ventricle: underlying molecular, cellular and biophysical mechanisms." J Physiol **569**(Pt 1): 7-39.

Patel, S. P., D. L. Campbell, M. J. Morales and H. C. Strauss (2002). "Heterogeneous expression of KChIP2 isoforms in the ferret heart." J Physiol **539**(Pt 3): 649-656.

Pelletier, J. and N. Sonenberg (1985). "Insertion mutagenesis to increase secondary structure within the 5' noncoding region of a eukaryotic mRNA reduces translational efficiency." Cell **40**(3): 515-526.

Pesole, G., S. Liuni, G. Grillo, F. Licciulli, F. Mignone, C. Gissi and C. Saccone (2002). "UTRdb and UTRsite: specialized databases of sequences and functional elements of 5' and 3' untranslated regions of eukaryotic mRNAs. Update 2002." Nucleic Acids Res **30**(1): 335-340.

Peter, I. S. and E. H. Davidson (2011). "Evolution of gene regulatory networks controlling body plan development." Cell **144**(6): 970-985.

Piacentino III V, Weber CR, Chen X, Weisser-Thomas J, Margulies KB, Bers DM & Houser SR (2003). Cellular basis of abnormal calcium transients of failing human ventricular myocytes. *Circ Res* **92**, 651-8.

Pinto, R. D., R. C. Elson, A. Szucs, M. I. Rabinovich, A. I. Selverston and H. D. Abarbanel (2001). "Extended dynamic clamp: controlling up to four neurons using a single desktop computer and interface." J Neurosci Methods **108**(1): 39-48.

Pitt GS, Dun W & Boyden PA (2006). Remodeled cardiac calcium channels. *J Mol Cell Cardiol* **41**, 373-88.

Planells-Cases R, Caprini M, Zhang J, Rockenstein EM, Rivera RR, Murre C, Masliah E & Montal M (2000). Neuronal death and perinatal lethality in voltage-gated sodium channel alpha(II)-deficient mice. *Biophys J* **78**, 2878-91.

Pond, A. L. and J. M. Nerbonne (2001). "ERG proteins and functional cardiac I(Kr) channels in rat, mouse, and human heart." Trends Cardiovasc Med **11**(7): 286-294.

Ponger, L., L. Duret and D. Mouchiroud (2001). "Determinants of CpG islands: expression in early embryo and isochore structure." Genome Res **11**(11): 1854-1860.

Popovic, Z. B., K. E. Richards, N. L. Greenberg, A. Rovner, J. Drinko, Y. Cheng, M. S. Penn, K. Fukamachi, N. Mal, B. D. Levine, M. J. Garcia and J. D. Thomas (2006). "Scaling of diastolic intraventricular pressure gradients is related to filling time duration." Am J Physiol Heart Circ Physiol **291**(2): H762-769.

Prothero, J. (1979). "Heart weight as a function of body weight in mammals." Growth **43**(3): 139-150.

Prud'homme, B., N. Gompel, A. Rokas, V. A. Kassner, T. M. Williams, S. D. Yeh, J. R. True and S. B. Carroll (2006). "Repeated morphological evolution through *cis*-regulatory changes in a pleiotropic gene." Nature **440**(7087): 1050-1053.

Rach, E. A., D. R. Winter, A. M. Benjamin, D. L. Corcoran, T. Ni, J. Zhu and U. Ohler (2011). "Transcription initiation patterns indicate divergent strategies for gene regulation at the chromatin level." PLoS Genet **7**(1): e1001274.

Ramirez-Carrozzi, V. R., D. Braas, D. M. Bhatt, C. S. Cheng, C. Hong, K. R. Doty, J. C. Black, A. Hoffmann, M. Carey and S. T. Smale (2009). "A unifying model for the selective regulation of inducible transcription by CpG islands and nucleosome remodeling." Cell **138**(1): 114-128.

Rebeiz, M., J. E. Pool, V. A. Kassner, C. F. Aquadro and S. B. Carroll (2009). "Stepwise modification of a modular enhancer underlies adaptation in a Drosophila population." Science **326**(5960): 1663-1667.

Rhodes, K. J., K. I. Carroll, M. A. Sung, L. C. Doliveira, M. M. Monaghan, S. L. Burke, B. W. Strassle, L. Buchwalder, M. Menegola, J. Cao, W. F. An and J. S. Trimmer (2004). "KChIPs and

Kv4 alpha subunits as integral components of A-type potassium channels in mammalian brain." J Neurosci **24**(36): 7903-7915.

Rivas, A. and H. W. Francis (2005). "Inner ear abnormalities in a Kcnq1 (Kvlqt1) knockout mouse: a model of Jervell and Lange-Nielsen syndrome." Otol Neurotol **26**(3): 415-424.

Rosati, B., M. Dong, L. Cheng, S. R. Liou, Q. Yan, J. Y. Park, E. Shiang, M. Sanguinetti, H. S. Wang and D. McKinnon (2008). "Evolution of ventricular myocyte electrophysiology." Physiol Genomics **35**(3): 262-272.

Rosati, B., W. Dun, M. Hirose, P. A. Boyden and D. McKinnon (2007). "Molecular basis of the T- and L-type Ca2+ currents in canine Purkinje fibres." J Physiol **579**(Pt 2): 465-471.

Rosati, B., F. Grau, A. Kuehler, S. Rodriguez and D. McKinnon (2004). "Comparison of different probe-level analysis techniques for oligonucleotide microarrays." Biotechniques **36**(2): 316-322.

Rosati, B., F. Grau and D. McKinnon (2006). "Regional variation in mRNA transcript abundance within the ventricular wall." J Mol Cell Cardiol **40**(2): 295-302.

Rosati, B., F. Grau, S. Rodriguez, H. Li, J. M. Nerbonne and D. McKinnon (2003). "Concordant expression of KChIP2 mRNA, protein and transient outward current throughout the canine ventricle." J Physiol **548**(Pt 3): 815-822.

Rosati, B. and D. McKinnon (2004). "Regulation of ion channel expression." Circ Res **94**(7): 874-883.

Rosati, B. and D. McKinnon (2009). "Structural and regulatory evolution of cellular electrophysiological systems." Evol Dev **11**(5): 610-618.

Rosati, B., Z. Pan, S. Lypen, H. S. Wang, I. Cohen, J. E. Dixon and D. McKinnon (2001). "Regulation of KChIP2 potassium channel beta subunit gene expression underlies the gradient of transient outward current in canine and human ventricle." J Physiol **533**(Pt 1): 119-125.

Rosenthal, J. J. and F. Bezanilla (2002). "A comparison of propagated action potentials from tropical and temperate squid axons: different durations and conduction velocities correlate with ionic conductance levels." J Exp Biol **205**(Pt 12): 1819-1830.

Roth, A. and R. R. Breaker (2009). "The structural and functional diversity of metabolite-binding riboswitches." Annu Rev Biochem **78**: 305-334.

Rudy, Y. and J. R. Silva (2006). "Computational biology in the study of cardiac ion channels and cell electrophysiology." Q Rev Biophys **39**(1): 57-116.

Sadoshima, J. and S. Izumo (1997). "The cellular and molecular response of cardiac myocytes to mechanical stress." Annu Rev Physiol **59**: 551-571.

Sah, R., R. J. Ramirez, G. Y. Oudit, D. Gidrewicz, M. G. Trivieri, C. Zobel and P. H. Backx (2003). "Regulation of cardiac excitation-contraction coupling by action potential repolarization: role of the transient outward potassium current (I(to))." J Physiol **546**(Pt 1): 5-18.

Sandelin, A., P. Carninci, B. Lenhard, J. Ponjavic, Y. Hayashizaki and D. A. Hume (2007). "Mammalian RNA polymerase II core promoters: insights from genome-wide studies." Nat Rev Genet **8**(6): 424-436.

Sang, N., G. Condorelli, A. De Luca, T. K. MacLachlan and A. Giordano (1996). "Generation of site-directed mutagenesis by extralong, high-fidelity polymerase chain reaction." Anal Biochem **233**(1): 142-144.

Sanguinetti, M. C., M. E. Curran, P. S. Spector and M. T. Keating (1996). "Spectrum of HERG K+-channel dysfunction in an inherited cardiac arrhythmia." Proc Natl Acad Sci U S A **93**(5): 2208-2212.

Sanguinetti, M. C., M. E. Curran, A. Zou, J. Shen, P. S. Spector, D. L. Atkinson and M. T. Keating (1996). "Coassembly of K(V)LQT1 and minK (IsK) proteins to form cardiac I(Ks) potassium channel." Nature **384**(6604): 80-83.

Sanguinetti, M. C., C. Jiang, M. E. Curran and M. T. Keating (1995). "A mechanistic link between an inherited and an acquired cardiac arrhythmia: HERG encodes the IKr potassium channel." Cell **81**(2): 299-307.

Sanyal, A., B. R. Lajoie, G. Jain and J. Dekker (2012). "The long-range interaction landscape of gene promoters." Nature **489**(7414): 109-113.

Sauro HM (2009). Network dynamics. *Methods Mol Biol* **541**, 269. Schroder E, Byse M & Satin J (2009). L-type calcium channel C terminus autoregulates transcription. *Circ Res* **104**, 1373-81.

Saxonov, S., P. Berg and D. L. Brutlag (2006). "A genome-wide analysis of CpG dinucleotides in the human genome distinguishes two distinct classes of promoters." Proc Natl Acad Sci U S A **103**(5): 1412-1417.

Schaub, M. A., A. P. Boyle, A. Kundaje, S. Batzoglou and M. Snyder (2012). "Linking disease associations with regulatory information in the human genome." Genome Res **22**(9): 1748-1759.

Schauer, S. E., P. M. Schluter, R. Baskar, J. Gheyselinck, A. Bolanos, M. D. Curtis and U. Grossniklaus (2009). "Intronic regulatory elements determine the divergent expression patterns of AGAMOUS-LIKE6 subfamily members in Arabidopsis." Plant J **59**(6): 987-1000

Schmidt-Nielsen, K. (1984). Scaling: Why Is Animal Size so Important? , Cambridge University Press, Cambridge.

Scott, W. G., M. Martick and Y. I. Chi (2009). "Structure and function of regulatory RNA elements: ribozymes that regulate gene expression." Biochim Biophys Acta **1789**(9-10): 634-641.

Segers, P., D. Georgakopoulos, M. Afanasyeva, H. C. Champion, D. P. Judge, H. D. Millar, P. Verdonck, D. A. Kass, N. Stergiopulos and N. Westerhof (2005). "Conductance catheter-based assessment of arterial input impedance, arterial function, and ventricular-vascular interaction in mice." Am J Physiol Heart Circ Physiol **288**(3): H1157-1164.

Schones, D. E., K. Cui, S. Cuddapah, T. Y. Roh, A. Barski, Z. Wang, G. Wei and K. Zhao (2008). "Dynamic regulation of nucleosome positioning in the human genome." Cell **132**(5): 887-898.

Schroder E, Magyar J, Burgess D, Andres D & Satin J (2007). Chronic verapamil treatment remodels ICa,L in mouse ventricle. *Am J Physiol Heart Circ Physiol* **292**, H1906-H1916.

Schroder F, Handrock R, Beuckelmann DJ, Hirt S, Hullin R, Priebe L, Schwinger RH, Weil J & Herzig S (1998). Increased availability and open probability of single L-type calcium channels from failing compared with nonfailing human ventricle. *Circulation* **98**, 969-76.

Scriven DR, Dan P & Moore ED (2000). Distribution of proteins implicated in excitation-contraction coupling in rat ventricular myocytes. *Biophys J* **79**, 2682-91.

Sean B. Carroll, Jennifer K. Grenier and S. D. Weatherbee (2001). From DNA to Diversity: Molecular Genetics and the Evolution of Animal, USA: Blackwell Science.

Sequeira-Mendes, J., R. Diaz-Uriarte, A. Apedaile, D. Huntley, N. Brockdorff and M. Gomez (2009). "Transcription initiation activity sets replication origin efficiency in mammalian cells." PLoS Genet **5**(4): e1000446.

Sham, J. S., S. N. Hatem and M. Morad (1995). "Species differences in the activity of the Na(+)-Ca2+ exchanger in mammalian cardiac myocytes." J Physiol **488 (Pt 3)**: 623-631.

Shapiro, M. D., M. E. Marks, C. L. Peichel, B. K. Blackman, K. S. Nereng, B. Jonsson, D. Schluter and D. M. Kingsley (2004). "Genetic and developmental basis of evolutionary pelvic reduction in threespine sticklebacks." Nature **428**(6984): 717-723.

Sharif, J., T. A. Endo, T. Toyoda and H. Koseki (2010). "Divergence of CpG island promoters: a consequence or cause of evolution?" Dev Growth Differ **52**(6): 545-554.

Shi, W., R. Wymore, H. Yu, J. Wu, R. T. Wymore, Z. Pan, R. B. Robinson, J. E. Dixon, D. McKinnon and I. S. Cohen (1999). "Distribution and prevalence of hyperpolarization-activated cation channel (HCN) mRNA expression in cardiac tissues." Circ Res **85**(1): e1-6.

Shi, W., R. S. Wymore, H. S. Wang, Z. Pan, I. S. Cohen, D. McKinnon and J. E. Dixon (1997). "Identification of two nervous system-specific members of the erg potassium channel gene family." J Neurosci **17**(24): 9423-9432.

Simonis, M., P. Klous, E. Splinter, Y. Moshkin, R. Willemsen, E. de Wit, B. van Steensel and W. de Laat (2006). "Nuclear organization of active and inactive chromatin domains uncovered by chromosome conformation capture-on-chip (4C)." Nat Genet **38**(11): 1348-1354.

Smale, S. T. and J. T. Kadonaga (2003). "The RNA polymerase II core promoter." Annu Rev Biochem **72**: 449-479.

Smith, A. N., M. L. Barth, T. L. McDowell, D. S. Moulin, H. N. Nuthall, M. A. Hollingsworth and A. Harris (1996). "A regulatory element in intron 1 of the cystic fibrosis transmembrane conductance regulator gene." J Biol Chem **271**(17): 9947-9954.

Spivakov, M., J. Akhtar, P. Kheradpour, K. Beal, C. Girardot, G. Koscielny, J. Herrero, M. Kellis, E. E. Furlong and E. Birney (2012). "Analysis of variation at transcription factor binding sites in Drosophila and humans." Genome Biol **13**(9): R49.

Sohal DS, Nghiem M, Crackower MA, Witt SA, Kimball TR, Tymitz KM, Penninger JM & Molkentin JD (2001). Temporally regulated and tissue-specific gene manipulations in the adult and embryonic heart using a tamoxifen-inducible Cre protein. *Circ Res* **89**, 20-5.

Stahl, W. R. (1967). "Scaling of respiratory variables in mammals." J Appl Physiol **22**(3): 453-460.

Stern, D. L. (2000). "Evolutionary developmental biology and the problem of variation." Evolution **54**(4): 1079-1091.

Stormo, G. D. (2000). "DNA binding sites: representation and discovery." Bioinformatics **16**(1): 16-23.

Striessnig, J. (1999). "Pharmacology, structure and function of cardiac L-type Ca(2+) channels." Cell Physiol Biochem **9**(4-5): 242-269.

Struhl, K. (2001). "Gene regulation. A paradigm for precision." Science **293**(5532): 1054-1055.

Su, Z., F. Li, K. W. Spitzer, A. Yao, M. Ritter and W. H. Barry (2003). "Comparison of sarcoplasmic reticulum Ca2+-ATPase function in human, dog, rabbit, and mouse ventricular myocytes." J Mol Cell Cardiol **35**(7): 761-767.

Sun, X. and H. S. Wang (2005). "Role of the transient outward current (Ito) in shaping canine ventricular action potential--a dynamic clamp study." J Physiol **564**(Pt 2): 411-419.

Suzuki, M. M., A. R. Kerr, D. De Sousa and A. Bird (2007). "CpG methylation is targeted to transcription units in an invertebrate genome." Genome Res **17**(5): 625-631.

Takahashi, M. and W. A. Catterall (1987). "Dihydropyridine-sensitive calcium channels in cardiac and skeletal muscle membranes: studies with antibodies against the alpha subunits." Biochemistry **26**(17): 5518-5526.

Takai, D. and P. A. Jones (2002). "Comprehensive analysis of CpG islands in human chromosomes 21 and 22." Proc Natl Acad Sci U S A **99**(6): 3740-3745.

Tang, Q. Q., M. S. Jiang and M. D. Lane (1997). "Repression of transcription mediated by dual elements in the CCAAT/enhancer binding protein alpha gene." Proc Natl Acad Sci U S A **94**(25): 13571-13575.

Tarn, W. Y. and J. A. Steitz (1997). "Pre-mRNA splicing: the discovery of a new spliceosome doubles the challenge." Trends Biochem Sci **22**(4): 132-137.

Tellez, J. O., H. Dobrzynski, I. D. Greener, G. M. Graham, E. Laing, H. Honjo, S. J. Hubbard, M. R. Boyett and R. Billeter (2006). "Differential expression of ion channel transcripts in atrial muscle and sinoatrial node in rabbit." Circ Res **99**(12): 1384-1393.

Takeshima, H., S. Yamashita, T. Shimazu, T. Niwa and T. Ushijima (2009). "The presence of RNA polymerase II, active or stalled, predicts epigenetic fate of promoter CpG islands." Genome Res **19**(11): 1974-1982.

Tarone, G. and G. Lembo (2003). "Molecular interplay between mechanical and humoral signalling in cardiac hypertrophy." Trends Mol Med **9**(9): 376-382.

Tazi, J. and A. Bird (1990). "Alternative chromatin structure at CpG islands." Cell **60**(6): 909-920.

Thomson, J. P., P. J. Skene, J. Selfridge, T. Clouaire, J. Guy, S. Webb, A. R. Kerr, A. Deaton, R. Andrews, K. D. James, D. J. Turner, R. Illingworth and A. Bird (2010). "CpG islands influence chromatin structure via the CpG-binding protein Cfp1." Nature **464**(7291): 1082-1086.

Tomaselli GF, Marban E (1999). Electrophysiological remodeling in hypertrophy and heart failure. *Cardiovasc Res* **42**, 270-83.

Tweedie, S., J. Charlton, V. Clark and A. Bird (1997). "Methylation of genomes and genes at the invertebrate-vertebrate boundary." Mol Cell Biol **17**(3): 1469-1475.

Tzingounis AV, Nicoll RA (2008). Contribution of KCNQ2 and KCNQ3 to the medium and slow afterhyperpolarization currents. *Proc Natl Acad Sci U S A* **105**, 19974-9.
Wagner, A (2007). *Robustness and Evolvability in Living Systems.* Princeton University Press, Princeton.

Valouev, A., S. M. Johnson, S. D. Boyd, C. L. Smith, A. Z. Fire and A. Sidow (2011). "Determinants of nucleosome organization in primary human cells." Nature **474**(7352): 516-520.

Vangheluwe, P., M. Schuermans, E. Zador, E. Waelkens, L. Raeymaekers and F. Wuytack (2005). "Sarcolipin and phospholamban mRNA and protein expression in cardiac and skeletal muscle of different species." Biochem J **389**(Pt 1): 151-159.

Varadi, G., P. Lory, D. Schultz, M. Varadi and A. Schwartz (1991). "Acceleration of activation and inactivation by the beta subunit of the skeletal muscle calcium channel." Nature **352**(6331): 159-162.

Veitia, R. A. and J. A. Birchler (2010). "Dominance and gene dosage balance in health and disease: why levels matter!" J Pathol **220**(2): 174-185.

Vernot, B., A. B. Stergachis, M. T. Maurano, J. Vierstra, S. Neph, R. E. Thurman, J. A. Stamatoyannopoulos and J. M. Akey (2012). "Personal and population genomics of human regulatory variation." Genome Res **22**(9): 1689-1697.

Vilar, J. M. and L. Saiz (2005). "DNA looping in gene regulation: from the assembly of macromolecular complexes to the control of transcriptional noise." Curr Opin Genet Dev **15**(2): 136-144.

Visel, A., E. M. Rubin and L. A. Pennacchio (2009). "Genomic views of distant-acting enhancers." Nature **461**(7261): 199-205.

Vornanen, M., A. Ryokkynen and A. Nurmi (2002). "Temperature-dependent expression of sarcolemmal K(+) currents in rainbow trout atrial and ventricular myocytes." Am J Physiol Regul Integr Comp Physiol **282**(4): R1191-1199.

Walsh, C. A. and E. C. Engle (2010). "Allelic diversity in human developmental neurogenetics: insights into biology and disease." Neuron **68**(2): 245-253.

Wang D, Papp AC, Binkley PF, Johnson JA & Sadee W (2006). Highly variable mRNA expression and splicing of L-type voltage-dependent calcium channel alpha subunit 1C in human heart tissues. *Pharmacogenet Genomics* **16**, 735-45.

Wang, L., Z. P. Feng and H. J. Duff (1999). "Glucocorticoid regulation of cardiac K+ currents and L-type Ca2+ current in neonatal mice." Circ Res **85**(2): 168-173.

Weinmann,Wang S, Ziman B, Bodi I, Rubio M, Zhou YY, D'Souza K, Bishopric NH, Schwartz A & Lakatta EG (2009). Dilated cardiomyopathy with increased SR Ca^{2+} loading preceded by a hypercontractile state and diastolic failure in the $_{1C}$TG mouse. *PLoS One* **4**, e4133.

Wang Z, Tristani-Firouzi M, Xu Q, Lin M, Keating MT & Sanguinetti MC (1999). Functional effects of mutations in KvLQT1 that cause long QT syndrome. *J Cardiovasc Electrophysiol* **10**, 817-26.

Wawersik, S. and R. (1992). "The basic RNA polymerase II transcriptional machinery." Gene Expr **2**(2): 81-91

L. Maas (2000). "Vertebrate eye development as modeled in Drosophila." Hum Mol Genet **9**(6): 917-925.

Weber, M., I. Hellmann, M. B. Stadler, L. Ramos, S. Paabo, M. Rebhan and D. Schubeler (2007). "Distribution, silencing potential and evolutionary impact of promoter DNA methylation in the human genome." Nat Genet **39**(4): 457-466.

Westerhof, N. and G. Elzinga (1991). "Normalized input impedance and arterial decay time over heart period are independent of animal size." Am J Physiol **261**(1 Pt 2): R126-133.

Whitfield, T. W., J. Wang, P. J. Collins, E. C. Partridge, S. F. Aldred, N. D. Trinklein, R. M. Myers and Z. Weng (2012). "Functional analysis of transcription factor binding sites in human promoters." Genome Biol **13**(9): R50.

White JA, McKinney BC, John MC, Powers PA, Kamp TJ & Murphy GG (2008). Conditional forebrain deletion of the L-type calcium channel Ca V 1.2 disrupts remote spatial memories in mice. *Learn Mem* **15**, 1-5.

Wierstra, I. (2008). "Sp1: emerging roles--beyond constitutive activation of TATA-less housekeeping genes." Biochem Biophys Res Commun **372**(1): 1-13.

Won, K. J., B. Ren and W. Wang (2010). "Genome-wide prediction of transcription factor binding sites using an integrated model." Genome Biol **11**(1): R7.

Wray, G. A. (2007). "The evolutionary significance of *cis*-regulatory mutations." Nat Rev Genet **8**(3): 206-216.

Wray, G. A., M. W. Hahn, E. Abouheif, J. P. Balhoff, M. Pizer, M. V. Rockman and L. A. Romano (2003). "The evolution of transcriptional regulation in eukaryotes." Mol Biol Evol **20**(9): 1377-1419.

Wu, H., B. Caffo, H. A. Jaffee, R. A. Irizarry and A. P. Feinberg (2010). "Redefining CpG islands using hidden Markov models." Biostatistics **11**(3): 499-514.

Wu, Q. and A. R. Krainer (1999). "AT-AC pre-mRNA splicing mechanisms and conservation of minor introns in voltage-gated ion channel genes." Mol Cell Biol **19**(5): 3225-3236H., A. C. D'Alessio, S. Ito, Z. Wang, K. Cui, K. Zhao, Y. E. Sun and Y. Zhang (2011). "Genome-wide analysis of 5-hydroxymethylcytosine distribution reveals its dual function in transcriptional regulation in mouse embryonic stem cells." Genes Dev **25**(7): 679-684.

Wu, H., A. C. D'Alessio, S. Ito, K. Xia, Z. Wang, K. Cui, K. Zhao, Y. E. Sun and Y. Zhang (2011). "Dual functions of Tet1 in transcriptional regulation in mouse embryonic stem cells." Nature **473**(7347): 389-393.

Wymore, R. S., G. A. Gintant, R. T. Wymore, J. E. Dixon, D. McKinnon and I. S. Cohen (1997). "Tissue and species distribution of mRNA for the IKr-like K+ channel, erg." Circ Res **80**(2): 261-268.

Xiong, H., I. Kovacs and Z. Zhang (2004). "Differential distribution of KChIPs mRNAs in adult mouse brain." Brain Res Mol Brain Res **128**(2): 103-111.

Yamaguchi, H., M. Hara, M. Strobeck, K. Fukasawa, A. Schwartz and G. Varadi (1998). "Multiple modulation pathways of calcium channel activity by a beta subunit. Direct evidence of beta subunit participation in membrane trafficking of the alpha1C subunit." J Biol Chem **273**(30): 19348-19356.

Xu M, Welling A, Paparisto S, Hofmann F & Klugbauer N (2003). Enhanced expression of L-type Cav1.3 calcium channels in murine embryonic hearts from Cav1.2-deficient mice. *J Biol Chem* **278**, 40837-41.

Yan, Q., R. Masson, Y. Ren, B. Rosati and D. McKinnon (2012). "Evolution of CpG island promoter function underlies changes in KChIP2 potassium channel subunit gene expression in mammalian heart." Proc Natl Acad Sci U S A **109**(5): 1601-1606.

Yin, L., H. Bien and E. Entcheva (2004). "Scaffold topography alters intracellular calcium dynamics in cultured cardiomyocyte networks." Am J Physiol Heart Circ Physiol **287**(3): H1276-1285.

Yokoyama, S. (2002). "Molecular evolution of color vision in vertebrates." Gene **300**(1-2): 69-78.

Yu, F. H., V. Yarov-Yarovoy, G. A. Gutman and W. A. Catterall (2005). "Overview of molecular relationships in the voltage-gated ion channel superfamily." Pharmacol Rev **57**(4): 387-395.

Zambelli, F., G. Pesole and G. Pavesi (2012). "Motif discovery and transcription factor binding sites before and after the next-generation sequencing era." Brief Bioinform.

Zhao, Z., G. Tavoosidana, M. Sjolinder, A. Gondor, P. Mariano, S. Wang, C. Kanduri, M. Lezcano, K. S. Sandhu, U. Singh, V. Pant, V. Tiwari, S. Kurukuti and R. Ohlsson (2006). "Circular chromosome conformation capture (4C) uncovers extensive networks of epigenetically regulated intra- and interchromosomal interactions." Nat Genet **38**(11): 1341-1347.

Zobel, C., Z.Yu FH, Mantegazza M, Westenbroek RE, Robbins CA, Kalume F, Burton KA, Spain WJ, McKnight GS, Scheuer T & Catterall WA (2006). Reduced sodium current in GABAergic interneurons in a mouse model of severe myoclonic epilepsy in infancy. *Nat Neurosci* **9**, 1142-9.

Zobel, C., Z. Kassiri, T. T. Nguyen, Y. Meng and P. H. Backx (2002). "Prevention of hypertrophy by overexpression of Kv4.2 in cultured neonatal cardiomyocytes." Circulation **106**(18): 2385-2391.